



HAL
open science

The Immunopathology of Primary and Metastatic tumors of the Liver

Héloïse Halse

► **To cite this version:**

Héloïse Halse. The Immunopathology of Primary and Metastatic tumors of the Liver. Immunology. Université Paris-Saclay, 2023. English. NNT : 2023UPASL126 . tel-04853265

HAL Id: tel-04853265

<https://theses.hal.science/tel-04853265v1>

Submitted on 22 Dec 2024

HAL is a multi-disciplinary open access archive for the deposit and dissemination of scientific research documents, whether they are published or not. The documents may come from teaching and research institutions in France or abroad, or from public or private research centers.

L'archive ouverte pluridisciplinaire **HAL**, est destinée au dépôt et à la diffusion de documents scientifiques de niveau recherche, publiés ou non, émanant des établissements d'enseignement et de recherche français ou étrangers, des laboratoires publics ou privés.

The Immunopathology of Primary and Metastatic tumors of the Liver

*Immuno-pathologie des tumeurs primitives
et métastatiques du foie*

Thèse de doctorat de l'université Paris-Saclay

École doctorale n° 582, Cancérologie : biologie – médecine – santé (CBMS)

Spécialité de doctorat : Science du Cancer

Graduate School : Life Sciences & Health. Référent: Faculté de médecine

Thèse préparée À Institut Imagine (Université Paris Cité),

Sous la direction de **Olivier HERMINE**, PUPH, L'encadrement de **Amélie BIGORGNE**, CR1, et le co-encadrement de **Aurélien MARABELLE**, PUPH,

Thèse soutenue à Paris-Saclay, le 27 novembre 2023, par

Héloïse HALSE

Composition du Jury

Membres du jury avec voix délibérative

Michel AROCK PUPH, Université Paris-Saclay	Président
Sophie CONCHON DR INSERM, CR2TI U1064, CHU de Nantes	Rapporteur et examinatrice
Eric ESPINOSA MCU, Professeur Assistant, Université Paul Sabatier Toulouse	Rapporteur et examinatrice
Cécile ALANIO Médecin, Directeur adjoint, Laboratoire d'Immunologie Clinique U932, Institut Curie	Examinatrice
Eric VIBERT PUPH, CHB Paul Brousse, Université Paris-Sud	Examineur

Table of Contents

Acknowledgements	5
List of Abbreviations	7
Introduction	14
General Background	14
Colorectal cancer Liver metastasis – Epidemiology and Clinical Landscape	15
Treatment	16
Primary Liver cancer - Epidemiology and Clinical Landscape	19
Hepatocellular carcinoma staging and treatment.....	20
Immunotherapies for HCC.....	21
The Liver architecture	24
The Tumor Immune Microenvironment of MSS CRC Liver metastases and its association with patient prognosis	31
Influence of molecular subtypes.....	34
The role of mast cells	34
The Tumor Immune Microenvironment of Primary Liver Tumors and its association with patient prognosis and response to immunotherapy	39
The immune microenvironment in HCC	39
Immunological correlates of response to Immunotherapy in HCC.....	40
Thesis Objectives	43
Chapter 1. Activation of liver mast cells potentiates anti-tumor immunity and improves patient prognosis in metastatic colorectal cancer	45
Introduction	48
Results	50
Liver metastatic CRC patient cohort	50
Tumor infiltration with mast cells is predictive of survival in KRAS wildtype metastatic CRC patients.....	50
Quantification and localization of intra-tumor mast cells in CRC liver metastases	52
TGFβ2 secretion negatively impacts tumor infiltrating mast cell expression of activating marker CD203c.....	54
CD203c expression on Mast cells positively correlates with CD8 ⁺ T cell activation and T effector phenotype.....	55
Mast cell FcεRI ^{high} CD203c ^{high} phenotype and production of Histamine is correlated with patient prognosis	56
Discussion	58
Materials and Methods	62
Annex	69
Figures	75
Tables	83

Supplementary Material.....	85
Chapter 2. Tumor infiltrating neutrophils are associated with decreased radiologic response and relapse-free survival in KRAS-wildtype patients with colorectal cancer liver metastasis.....	92
Introduction.....	93
Material and Methods	95
Results	102
Liver metastatic CRC patient cohort.....	102
Characterization of the liver immune microenvironment.....	102
Liver metastasis infiltration with neutrophils is associated with poor response to pre-operative therapy and decreased relapse-free survival in KRASwt metastatic CRC patients.	103
Neutrophil infiltration in KRASwt tumors is associated with an altered immune microenvironment mediated by a unique chemokine and cytokine gradient.....	106
Liver-infiltrating neutrophils in mCRC resemble PMN-MDSC based on membrane expression of LOX-1 and suppress T cell activation	109
T cells and mast cell phenotype are impacted by the unique chemokine and cytokine profile in KRASwt tumor with elevated neutrophil infiltration	111
Discussion	115
Supplementary Figures.....	119
Chapter 3. The immunopathological landscape of primary resected Hepatocellular carcinoma	123
Introduction.....	125
Materials and Methods.....	127
Secreted soluble cytokine, chemokine, and growth factor measurement.....	129
Results	133
Primary resected Hepatocellular Carcinoma patient cohort	133
Characterization of the liver immune microenvironment.....	133
The frequency of immune cell subsets in HCC are differentially enriched and define four distinct subgroups of patients.	134
Resident, activation, and exhaustive state of T cells are different across immune clusters	137
Different profiles of secreted soluble factors within HCC tumors.....	140
Enriched signaling pathways in #CD8, #CD4, #NK and #M-DC intra-tumor clusters in HCC	142
Differential Gene expression and enrichment pathway analysis between 'noninflamed', 'cytotoxic', and 'non-cytotoxic' patient subgroups identified by cytokine secretion.....	144
Discussion	145
Tables	150
Supplementary Figures.....	154
Discussion and Perspectives	160
General Discussion – Chapters 1 & 2.....	160
Future Directions – Chapters 1 & 2	165
General Discussion – Chapter 3.....	168

Future Directions – Chapter 3	170
Concluding Remarks	171
Bibliography	172

Acknowledgements

I extend my sincere gratitude to the esteemed members of the jury for evaluating my work and contributing their expertise. Your presence and insights are deeply appreciated.

The work over the last four years has not been achieved by myself alone; it was supported by many incredible individuals that have pulled me through to the end.

Foremost, I would like to thank my main supervisor Amélie Bigorgne, whose guidance and dedication shaped this remarkable project on liver metastases and liver cancer across Institut Imagine, Gustave Roussy and Paul Brousse Hospitals. Amélie has a big heart, and she has always been there for me. She is very driven and her passion for her translational research work is very inspiring. She has taught me so much, and I'm immensely grateful for the opportunity she has provided me.

I'm indebted to my thesis director, Olivier Hermine, who accepted to take me on in his lab at Institut Imagine. Your unwavering support, approachability and vast knowledge and insights provided crucial guidance to me along this challenging path. To have someone like you so committed to every member of the lab has made a significant difference, thank you.

I would also like to thank my recent co-supervisor Aurélien Marabelle, who stepped in this year to support me financially to help me complete my PhD. Thank you for your unending support and advice over the past four years, and for offering continued opportunities in the liver cancer project as part of your amazing team at Gustave Roussy next year.

To the vibrant community in U1163, including past and present members, colleagues, and fellow PhD students: Thank you for your unwavering support and camaraderie, even if we did not work at all on the same projects. You are truly wonderful.

Thank you to my dear colleagues in 215: Caro, Rachel, Mirjana, and Thiago. Thank you, Batoul, Camille, Coralie, Elisa, Eric, Marine, Margot, Michaël, Marie, Leïla, Lucile, Pascal, and Thierry. To my past and fellow PhD colleagues, THANK YOU and I wish you all the best in your future endeavors: Alice, Amira, Alexandre, Anne-Sophie, Bahia, Candice, Clotilde, Elia, Estelle, François, Haoua, Guillemette, Julien, Kitsada, Laura, Louise, Madeleine, Marc, Marion, Maryam, Milo, Nabiha, Sarah and Raphaël.

My heartfelt appreciation extends to the LRTI lab at Gustave Roussy, my second family. Even though I was a collaborator you have always made me feel so welcome and you have helped me so much. Without you, this project would not have been possible.

Thank you importantly to Delphine, Aminata, Séverine, Guillaume, and Marine who have helped me so much with sample processing and staining and the secretome analysis.

A special mention to Chifaou, who has been by my side every step of the way on the biological and clinical data collection.

Thank you, François-Xavier, for your help and advice as a fellow PhD student when I was starting out.

Thank you Mélodie, Edi and Naël, for your precious help in the last few months.

Elvire, thank you for being by my side inside and outside of work, I am so grateful to have you as my fellow PhD friend from the start.

Sandrine, thank you for always being there for me.

To past and present members: Diane, Masha, Lambros, Léa, Pauline, Romane, Thomas, and Visswa, thank you.

I'm indebted to all collaborators at Institut Imagine, Gustave Roussy and Paul Brousse:

Laetitia, Doris, Virginie, Karine, Nicolas, Peggy, and Jean-Yves from PETRA,

Marc and Thibault from Bioinformatics platform,

Jerome Cartry and Fanny Jaulin from Collective Invasion lab,

Eric Vibert, Léonie Bui, Rim Kalala, Catherine Guettier, Olivier Rosmorduc on the Liver cancer project,

Emilie-Fleur Gautier for the proteomics study,

Nicolas Goudin for training me on QuPath on the Imaris,

Nicolas Cagnard for help with RNAseq data.

To my dearest friends, all around the world, thank you for your never-ending support. I hope to have more time to see you all soon.

To my loving family in Australia, your unwavering love and encouragement have been my pillar of strength. I miss you all very much and look forward to being near you again.

To my family in the UK, I am eternally grateful to have you close.

À ma famille en France, à mes tantes, à ma marraine, je vous suis reconnaissante.

Lastly, to my husband, Fred, your unwavering love, and support brought us to France from Australia and fueled this endeavor. I am so lucky to have you by my side through it all. Here's to our next adventures together, wherever it may take us.

Merci infiniment.

List of Abbreviations

AdOVA = Adenoviral vector encoding the MHC I OVA-epitope
AFP = Alpha-feto protein
aHCC = Advanced Hepatocellular Carcinoma
ALBI = Albumin-Bilirubin
ALT = Alanine Transaminase
AP = Alkaline Phosphatase
ASH = Alcoholic Steatohepatitis
AST = Aspartate Aminotransferase
BRAF = V-Raf Murine Sarcoma Viral Oncogene Homolog B
BCLC = Barcelona Clinic Liver Cancer
BTLA = B and T lymphocyte attenuator
CAP = Controlled Attenuation parameter
CD = Cluster of Differentiation
CRC = Colorectal Cancer
CRCLM = Colorectal Cancer Liver Metastasis
CTL = Cytotoxic T Lymphocyte
CTLA-4 = Cytotoxic T Lymphocyte-Associated protein 4
CXCL = CXC chemokine ligand
DC = Dendritic cell
DFS = Disease-free Survival
dNLR = derived Neutrophil-to-Lymphocyte Ratio
EGFR = Epidermal Growth Factor Receptor
FasL = Fas-Ligand
FOLFIRI = Fluoropyrimidine with Irinotecan
FOLFIRINOX = Fluoropyrimidine with Irinotecan and Oxaliplatin
FOLFOX = Fluoropyrimidine with Oxaliplatin
GCSF = Granulocyte colony stimulating factor
GGT = Gamma-glutamyl Transferase
GITR = Glucocorticoid-induced TNFR-related protein
GZM = Granzyme
HBV = Hepatitis B Virus
HCC = Hepatocellular Carcinoma
HCV = Hepatitis C Virus
HIF1A = Hypoxia-inducible factor 1-alpha
HLA = Human leukocyte antigens
HR = Hazard Ratio
HSC = Hepatic Stellate cell
ICOS = Inducible costimulatory
ICOS-L = Inducible costimulatory-ligand
IDO = Indolamine 2,3-dioxygenase
IFN = Interferon
IHC = Immunohistochemistry

IL = Interleukin
KC = Kupffer cell
kPa = kilopascal
KRAS = Kirsten Rat Sarcoma Viral Oncogene Homolog
LAG3 = lymphocyte activation gene 3
LDH = Lactate Dehydrogenase
LOX-1 = Lectin-Like Oxidized Low Density Lipoprotein Receptor 1
LPS = Lipopolysaccharide
LSEC = Liver Sinusoidal Endothelial cell
MAIT = Mucosal-associated Invariant T cell
MDSC = Myeloid-derived suppressor cell
MHC = Major Histocompatibility Complex
mL = milliliter
MMR-d = Mismatch repair deficient
MMR-p = Mismatch repair proficient
MSI-H = Microsatellite Instability High
MSS = Microsatellite Stable
mut = mutated
NAFL = Non-alcoholic Fatty Liver
NAFLD = Non-alcoholic Fatty Liver Disease
NASH = Non-alcoholic Steatohepatitis
NK = Natural Killer
NKT = Natural Killer T
NLR = Neutrophil-to-Lymphocyte Ratio
NR = Not Reached
OS = Overall Survival
OSRR = Organ-specific Response Rate
ORR = Objective Response Rate
PD-1 = Programmed Death-1
pDC = Plasmacytoid Dendritic cell
PD-L1 = Programmed Death-Ligand 1
PFS = Progression-free Survival
PMN-MDSC = Polymorphonuclear-Myeloid-derived Suppressor cell
RAS = Rat Sarcoma virus
RFS = Relapse-free Survival
RPM = Revolutions per minute
SEMA3A = Semaphorin-3A
TACE = Trans-arterial Chemoembolization
Th = T-helper
TLR = Toll like receptor
TMB = Tumor Mutation Burden
TNF = Tumor Necrosis Factor
Treg = Regulatory T cell
Trm = Tissue resident-memory
VEGF-A = Vascular Endothelial Growth Factor-A
wt = wild-type

Titre : Immunopathologie des tumeurs primitives et métastatiques du foie

Mots clés : Métastase hépatique, Cancer Hépatocellulaire, Microenvironnement tumorale, Immunologie du Cancer, Biomarqueurs

Abstract : L'immunothérapie anti-cancéreuse est un traitement efficace chez certains patients, mais cela dépend de l'organe atteint. Les patients avec un cancer du foie primitif ou des métastases hépatiques d'un cancer colorectal (MHCCR) ont souvent des réponses limitées. Cela est lié à l'environnement immunitaire particulier du foie.

Dans cette étude, nous avons examiné l'impact des cellules immunitaires dans le MHCCR, en particulier les mastocytes et les neutrophiles, dans la survie. La présence accrue de mastocytes était liée à un meilleur pronostic, tandis que la présence de neutrophiles était associée à un mauvais pronostic.

De plus, chez les patients atteints d'un carcinome hépatocellulaire précoce, différents profils immunitaires ont été identifiés, ce qui pourrait aider à personnaliser le traitement.

En résumé, comprendre la réaction immunitaire dans le foie est essentiel pour améliorer l'efficacité de l'immunothérapie contre les tumeurs hépatiques, et cela pourrait conduire à de nouvelles cibles thérapeutiques pour améliorer la survie des patients.

Title: The Immunopathology of Primary and Metastatic Tumors to the Liver

Keywords: Liver metastasis, Liver Cancer, Tumor microenvironment, Cancer Immunologie, Biomarkers

Abstract: Anti-cancer immunotherapy can be highly effective for certain patients, but its success depends on the affected organ. Individuals with primary liver cancer or liver metastases from colorectal cancer often have limited responses to immunotherapy. This is largely due to the immune environment within the liver.

In this study, we examined how immune cells, particularly mast cells and neutrophils, impact outcomes in patients with colorectal cancer liver metastasis. We found that an increased presence of mast cells in tumors was associated with better outcomes for patients, while the presence of neutrophils was linked to a less favorable outcome.

Furthermore, in the case of early-stage liver cancer, we discovered that patients could be grouped into different immune profiles, which could help personalize treatment.

In summary, this study highlights the importance of understanding how the immune system reacts in the liver to enhance the effectiveness of immunotherapy for liver cancer and colorectal cancer. This information could also assist in identifying new therapeutic targets to improve treatments and patient survival in the future.

Abstract - Français

L'immunothérapie anti-cancéreuse, bien qu'elle donne des résultats exceptionnels chez certains patients, montre une efficacité variable en fonction de l'organe touché. Les patients atteints d'un cancer primitif du foie ou de métastases hépatiques d'un cancer colorectal ont souvent des réponses limitées à l'immunothérapie en raison de l'environnement immunitaire particulier du foie. Il est donc impératif d'améliorer notre compréhension du microenvironnement immunitaire au sein des tumeurs hépatiques. Ceci constitue le thème central de cette thèse.

La première partie de la thèse a évalué le microenvironnement immunitaire dans une cohorte prospective de N = 32 patients atteints d'un cancer colorectal avec métastases hépatiques (MHCCR). Dans cette étude, nous avons examiné comment certaines cellules immunitaires spécifiques, à savoir les mastocytes et les neutrophiles, influent sur les réponses au traitement et le pronostic. La présence accrue de mastocytes dans les tumeurs, notamment chez les patients de type KRAS sauvage, était associée à un pronostic amélioré. Elle était positivement corrélée à l'infiltration et à l'activation des lymphocytes T CD8⁺, mais inversement par rapport à la sécrétion de TGFβ2, aux cellules T régulatrices et à l'infiltration des neutrophiles. Les tumeurs riches en mastocytes montraient une sécrétion élevée d'histamine, suggérant une activation des mastocytes. In vitro, les lymphocytes exposés à des mastocytes préconditionnés dans les surnageants des tumeurs provenant de patients présentant un bon pronostic présentaient une expression intracellulaire élevée de l'IFN-gamma et du Granzyme B. Des corrélations positives entre les gènes spécifiques des mastocytes et des lymphocytes T ont également été observées dans un ensemble de données publiques d'expression génique de sujets atteints de MHCCR réséqués. En résumé, les mastocytes infiltrant les tumeurs pourraient favoriser l'immunité anticancéreuse dans le cas du MHCCR.

Nous avons ensuite exploré le rôle des neutrophiles infiltrant les tumeurs dans le MHCCR. Une infiltration élevée de neutrophiles, en particulier chez les patients de type KRAS sauvage, était associée à de moins bonnes réponses au traitement et à un pronostic moins favorable. La présence des neutrophiles était positivement corrélée à la sécrétion de CXCL8, TGFβ2 et TNF. Ils présentaient une expression élevée de LOX1 et leur présence était inversement corrélée à l'infiltration et à l'activation des lymphocytes T CD8⁺ et CD4⁺. Ces résultats suggèrent que les neutrophiles infiltrant les tumeurs peuvent entraver l'immunité anticancéreuse dans le MHCCR.

La dernière partie de la thèse était centrée sur l'environnement immunitaire dans le carcinome hépatocellulaire (CHC). Bien que l'immunothérapie ait profondément influencé la prise en charge du CHC, seuls 30% des patients présentent des réponses objectives. Nous avons analysé l'infiltrat immunitaire, la sécrétion de protéines et les transcriptomes tissulaires chez N=28 patients atteints d'un CHC à un stade précoce, n'ayant pas été préalablement traités et

ayant subi une résection chirurgicale curative. Malgré l'homogénéité clinique, nous avons identifié quatre groupes immunitaires distincts présentant différentes infiltrations de cellules T CD8⁺, T CD4⁺, NK et myéloïdes. Ces groupes présentaient des profils d'activation et d'épuisement parmi les lymphocytes et des profils transcriptomiques différents, offrant une meilleure compréhension pour la gestion des patients dans le contexte de l'immunothérapie péri opératoire du CHC.

En conclusion, cette thèse souligne l'importance de comprendre l'environnement immunitaire au sein du foie et son rôle dans l'immunité anticancéreuse et la survie dans le MHCCR et le CHC. Ces informations pourraient orienter de futures recherches visant à identifier des cibles thérapeutiques potentielles, améliorant ainsi le potentiel thérapeutique de l'immunothérapie et la survie des patients à l'avenir.

Abstract – English

While anti-cancer immunotherapy provides unprecedented results for some patients, its effectiveness varies depending on the organ affected. Patients with primary liver cancer and colorectal cancer liver metastasis often exhibit limited responses to immunotherapy. This points to the critical influence of the tissue microenvironment on treatment efficacy. The liver is an immunologically rich organ and contains a diversity of lymphoid and myeloid cells, which significantly shape how patients respond to treatment and their survival. It is therefore imperative to enhance our understanding of the immune microenvironment within primary liver and liver metastatic tumors and is the central focus of this thesis.

The first part of the thesis evaluated the immune microenvironment in a prospective cohort of N=32 colorectal cancer patients with liver metastasis (CRCLM). Despite improvements in treatment efficacy, response and survival after liver metastasis resection vary greatly. Furthermore, anti-tumor T cell responses in the liver are compromised. A less studied innate immune cell in the liver, the mast cell, bridges the gap between innate and adaptive immune responses. Their role in tumor immunity within liver metastasis is, however, unclear. We characterized mast cells in resected CRCLM using flow cytometry, secreted mediator quantification, and multiplex immunohistochemistry. Increased mast cell infiltration, particularly in KRAS wildtype patients, correlated with improved prognosis. Tumor-infiltrating mast cells correlated with CD8⁺T cell infiltration and activation but inversely with TGFβ₂ secretion, T-regulatory cells, and neutrophil infiltration. Mast cell-rich tumors exhibited elevated histamine secretion, indicating mast cell activation. In vitro, lymphocytes exposed to mast cells pre-conditioned within tumor supernatant from patients with good prognosis had elevated intracellular expression of IFN-gamma and Granzyme B. Positive correlations between mast cell and T cell-specific genes were also observed in a public gene expression dataset of resected CRCLM. In summary, these findings provide insight in the role of tumor-infiltrating mast cells, and that they may potentiate anti-tumor immunity in CRCLM.

We next explored the role of tumor-infiltrating neutrophils in CRCLM, as their impact on prognosis remains unclear. Elevated neutrophil infiltration was associated with poor response and decreased survival specifically in KRAS wildtype patients. Neutrophils were positively correlated with CXCL8, TNF, and TGFβ secretion and inversely correlated with CD8⁺T and CD4⁺T cell infiltration and activation. These results indicate that tumor-infiltrating neutrophils may hinder anti-tumor immunity in CRCLM.

The final part of the thesis centred on the immune landscape of early-stage hepatocellular carcinoma (HCC). Although immunotherapy has profoundly influenced HCC management, only 30% of patients show objective responses. We analysed the immune infiltrate, protein secretion and transcriptome from liver tissue of N=28 treatment-naïve, early-stage HCC patients who underwent curative surgical resection. Despite clinical homogeneity, we found four distinct immune clusters with variable CD8⁺T, CD4⁺T, NK, and Myeloid cell infiltration.

These clusters exhibited different activation and exhaustion profiles among lymphocytes correlated with cytokine and chemokine secretion and distinct transcriptomic profiles.

In conclusion, this thesis highlights the importance of understanding the immune microenvironment within the liver and its role in anti-tumor immunity and survival in CRCLM and HCC. These insights may guide further research to identify potential therapeutic targets, ultimately enhancing the therapeutic potential of immunotherapy and patient survival in the future.

Introduction

General Background

As the second largest organ in the human body, the liver plays vital roles in homeostasis, including metabolism regulation, protein synthesis and the removal of toxins and waste products. Its position and unique anatomy also contribute to its key role in barrier immunity against invading pathogens, while maintaining tolerance to the steady influx and exposure to harmless gut-derived microbial products and food-derived antigens. The liver is an immunologically rich organ that contains a diversity of lymphoid and myeloid cells, which regulate immune responses from tolerance to potent anti-viral and pathogen responses. However, the liver tends to favour hypo-responsiveness and induction of tolerance. As such, in the transplantation setting, the liver is unique, as it is the only organ for which immunosuppressive drug treatment can sometimes be stopped and long-term graft acceptance achieved in liver transplant recipients. Though beneficial in this context, this natural 'tolerogenicity' of the liver is detrimental in others, notably in primary liver cancer, and liver metastatic disease.

Clinically, primary liver cancer and liver metastases have specific immune suppressive consequences both locally and systemically and have long been associated with poor prognosis. In the context of checkpoint blockade therapy, the presence of liver metastasis is associated with worse objective response rates and survival compared to other sites of metastases across multiple histological subtypes. Furthermore, response rates to immunotherapy in primary liver and advanced liver cancer remains low. Nevertheless, the presence of anti-tumor immune cells in liver metastatic tumors and liver cancer are associated with improved prognosis as well as improved immunotherapy response, hinting that for some patients, anti-tumor immunity is present. However, for many patients, the immune response is either suppressed and/or excluded and negatively impacts prognosis. There is an unmet need for patients with primary liver cancer and non-liver derived metastatic disease; a better understanding of the biology of liver cancer and liver metastasis is needed, and how the

immune microenvironment specific to the liver influences anti-tumor immunity and patient prognosis, which is the focus of this thesis.

This introduction will initially outline the epidemiology and clinical landscape of colorectal cancer liver metastasis and primary liver cancer in the era of cancer immunotherapy. Next, we will describe immune cell populations residing in and recruited to the liver, elucidating their specific roles in normal liver physiology including the generation of immune tolerance. The immune contexture of colorectal cancer liver metastasis will then be presented, drawing insights from current literature regarding their respective impacts on patient prognosis. Lastly, we will provide an overview of the current understanding of the immune microenvironment in liver cancer, exploring its intricacies and heterogeneity concerning responses to immunotherapy treatment.

Colorectal cancer Liver metastasis – Epidemiology and Clinical Landscape

Colorectal cancer (CRC) is the third most diagnosed cancer, and stands as the second-leading cause of cancer-related deaths worldwide.¹ The incidence of colorectal cancer is increasing in developing countries, with a worrying increase in early-onset colorectal cancer affecting people younger than 50 years of age in developed countries.²⁻⁴ Both hereditary and environmental risk factors play a part in the development of colorectal cancer. Hereditary colorectal cancer can be categorized into non-polyposis, represented by Lynch syndrome, and polyposis syndromes. Lynch syndrome stems from dysfunction within the DNA mismatch repair pathway that is identified by molecular analysis of the deficiency of mismatch repair proteins (mismatch repair-deficient, MMR-d), commonly MLH-1, MLH-2, MSH-6 and PSM2. This leads to high-frequency microsatellite instability (MSI-H).⁵ However, MSI is also identified in approximately 15% of sporadic primary colorectal cancers.⁶ Other risk factors include inflammatory bowel disease and ulcerative colitis.⁷ Environmental and lifestyle factors associated with CRC risk include alcohol consumption, poor diet, obesity, physical inactivity, and type 2 diabetes.^{8,9}

Although prognosis is favorable for CRC patients diagnosed with early-stage disease, about 20% of CRC patients present with metastatic disease (mCRC) at distant sites, for which the five-year survival rate is substantially reduced.¹⁰ The most common site of CRC metastasis is the liver. Liver metastasis affects nearly 60% of patients diagnosed with mCRC.¹¹ Other metastatic sites in CRC include the lung, peritoneum, bone and brain.¹² Liver metastatic CRC is associated with poorer disease-specific and overall survival compared to non-liver metastatic CRC.¹²⁻¹⁴ Among patients who eventually pass away from the disease, 49% will have liver-dominant disease and 83% will have some liver involvement.¹⁴

Treatment

The primary treatment option for patients with mCRC is surgical resection, as it improves survival and in exceptional instances, can cure the disease.¹⁵⁻¹⁸ The addition of peri-operative therapy in the neo-adjuvant and/or adjuvant setting has also helped improve disease-free survival (DFS) for mCRC patients.¹⁹ Over the last two decades, survival rates for mCRC have improved due to various other factors. These include the use of biomarker-based selection for the application of more effective systemic therapies, resulting in a higher number of patients eligible for potentially curative surgical resection of liver metastasis.²⁰ Additionally, there has been an increased utilization of repeat surgical resections for cases of recurrence.²¹

The standard first line chemotherapy for mCRC typically includes a fluoropyrimidine (5-FU or capecitabine) in combination with irinotecan or oxaliplatin. Combining a fluoropyrimidine with oxaliplatin or irinotecan (FOLFOX or FOLFIRI) yields higher response rates, longer PFS and OS compared to using 5-FU alone.²² The combination of FOLFOX chemotherapy in the neoadjuvant setting with surgical resection improves resection margins and reduces relapse risk.^{19,23} Adjuvant chemotherapy also reduces risk of recurrence and improves survival.²⁴

Monoclonal antibodies like bevacizumab (anti-VEGF), cetuximab, and panitumumab (anti-EGFR) can also improve outcomes when added to first-line chemotherapy.²⁵⁻²⁸ The addition of bevacizumab to FOLFIRI also outperforms other combinations.²⁹ For the first-line treatment of mCRC, the current recommendations include doublet cytotoxic agent (FOLFOX or FOLFIRI), combined with targeted therapies (bevacizumab or cetuximab/panitumumab). In certain cases, the triplet FOLFIRI combined with bevacizumab may be considered as it has shown

superiority over FOLFIRI. See **Figure 1** of the ESMO guidelines for the treatment paradigm of mCRC.

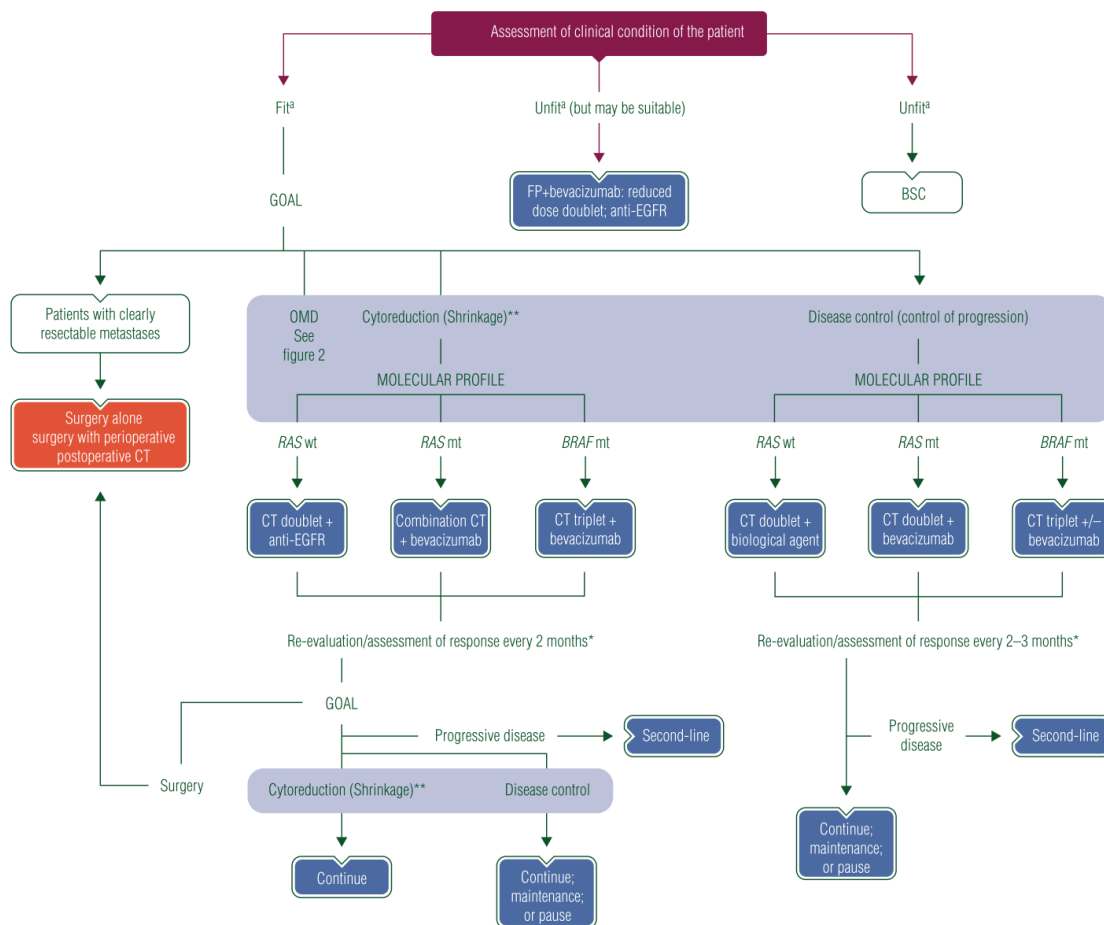


Figure 1. Treatment algorithm for mCRC.²⁰ BSC, best supportive care; CT, chemotherapy; EGFR, epidermal growth factor receptor; FP, fluoropyrimidine, mt, mutant; NED, no evidence of disease; OMD, oligometastatic disease; wt, wild type. ^aPatients assessed as fit or unfit according to medical condition not due to malignant disease. *After two re-evaluations, consider maintenance. ** (A) includes two subgroups: (1) those for whom intensive treatment is appropriate with the goal of cytoreduction (tumor shrinkage) and conversion to resectable disease; (2) those who need an intensive treatment, although they will never make it to resection, since they need a rapid reduction of tumor burden because of impending organ dysfunction, severe symptoms.²⁰

Current biomarker selection in mCRC relies on the following three main elements: MSI status, *RAS/BRAF* mutational status and primary CRC sidedness. These three biomarkers are all currently used for the routine application of preoperative systemic therapy to induce tumor reduction most effectively in mCRC. MSI is a condition characterized by the accumulation of insertions or deletions in repetitive DNA sequences called microsatellites within tumors. MSI tumors have a much higher mutational load (and thus potentially more neoantigens) than MSS

tumors and are associated with an activated, T cell-rich microenvironment balanced by elevated checkpoint marker expression.³⁰⁻³³ In mice, MSI-intermediate tumors do not respond to checkpoint blockade, but MSI-high tumors do, indicating that the neoantigen quantity is the driving force of immune checkpoint response in MSI-high tumors.³⁴ Recently, the KEYNOTE 177 trial analyzed the effect of Pembrolizumab (anti-PD-1) treatment to systemic chemotherapy on progression-free survival and overall survival in patients with newly diagnosed MSI-H or MMR-d mCRC.^{35,36} After median follow up of 44.5 months, median overall survival (OS) was not reached (NR) within the pembrolizumab group compared to chemotherapy group {(NR; 95% CI 49.2–NR) with pembrolizumab versus 36.7 months (27.6–NR) with chemotherapy (hazard ratio [HR] 0.74; 95% CI 0.53–1.03; p=0.036)}.³⁶ These promising findings have thus shifted the treatment paradigm in MMR-d/MSI-H patients, replacing chemotherapy with pembrolizumab in the 1st line setting.³⁷ Furthermore, the five-year follow up of previously treated MMR-d/MSI-H mCRC in Checkmate 142 clinical trial found durable clinical benefit in patients treated with combination Nivolumab and Ipilimumab after 1 or 2 lines of systemic chemotherapy treatment, supporting current treatment recommendations for patients with these tumors.³⁸⁻⁴⁰

Despite promising results in MMR-d/MSI-H mCRC, up to 95% of mCRC are mismatch-repair proficient/microsatellite stable (MMR-p/MSS).⁴¹ Patients with MMR-p/MSS mCRC treated with pembrolizumab showed 0% objective response rate compared with 40% in MMR-d/MSI-H mCRC.⁴¹ Roughly half of the patients in both cohorts had liver metastatic disease. The median PFS and OS in MMR-d mCRC was not reached in this study, whereas median PFS and OS in MMR-p/MSS mCRC was 2.2 and 5.0 months, respectively. Among patients with MMR-p/MSS tumors, the presence of *POLE* mutation in tumors has also been correlated with tumor mutation and elevated response to immunotherapy treatment.⁴² However, the prevalence of this mutation is also very low among MMR-p/MSS mCRC.

Recent single and multiple combination immunotherapy clinical trials have been tested in MSS patients, with clinical benefit largely observed in patients with non-liver metastases. Integrating clinical parameters including metastatic disease pattern in MSS metastatic colorectal cancer patients treated with PD-1 or PD-L1 inhibition showed that the presence of liver metastasis at the time of treatment initiation was the most significant factor associated with worse PFS in multivariate analysis {HR, 7.00 (95% CI, 3.18-15.42, $P < 0.001$)}.⁴³ Interestingly,

in patients without liver metastasis at the time of treatment but with a history of a liver lesion resection had lower PFS than patients without any history of liver involvement {PFS = 3.0 (IQR, 1.8-6.0) months versus PFS=5.5 (IQR, 2.0-11.5) months}.⁴³ Nevertheless, a significant benefit was observed in these patients compared to patients with liver metastasis, indicating that systemic immune suppression is relieved to an extent by liver tumor resection, and that these patients can derive a clinical benefit from immune checkpoint blockade.

In addition to MMR-d/MSI-H, mCRC are tested for mutations in *KRAS*, *NRAS*, and *BRAF*. For half of patients with *KRAS/NRAS/BRAF* wild-type tumors, monoclonal antibodies to the epithelial growth factor receptor (EGFR), in combination with chemotherapy can extend survival rates.⁴⁴⁻⁴⁶ Patients with *KRAS* or *NRAS* sequence variations, benefit instead from Vascular Endothelial Growth Factor-A (VEGF-A) monoclonal antibody as first-line treatment.⁴⁷ In addition to *KRAS/NRAS/BRAF* status, the response to EGFR inhibition is also associated with the specific location of the primary tumor in either the right or left colon.^{48,49} As a result, the practice guidelines suggest that anti-EGFR be used in combination with chemotherapy exclusively for metastatic CRC cases with wild-type *KRAS/NRAS/BRAF* and left-sided primary tumors.⁵⁰

Although five-year survival rates have improved after surgical resection of colorectal metastases the risk of recurrence is high (occurring in about 65% of patients) and mCRC remains incurable for more than 70% of patients.^{15,51,52} Patients who experience disease progression despite undergoing treatment with FOLFOX, FOLFIRI and biologic or targeted therapies are considered to have refractory disease. The application of Tyrosine Kinase Inhibitors Regorafenib and Tipiracil for these patients improved median OS by 1.4 and 1.8 month, respectively.^{53,54} At this point no other options of treatment are available that improve survival rates by 3 or more months in advanced refractory mCRC.⁵⁰

Primary Liver cancer - Epidemiology and Clinical Landscape

The incidence of Hepatocellular Carcinoma (HCC) is on the rise and is a major cause of cancer-related death in many countries, representing on average the third-leading cause of cancer-

related deaths worldwide.¹ The number of new cases and deaths from liver cancer is predicted to rise by more than 55% by 2040.⁵⁵ The incidence and mortality rates have dropped in some Asian countries such as Japan, China and South Korea but is on the rise in the West including the US, Australia and most parts of Europe.⁵⁶ These differences are most likely due to the different sets of risk factors for HCC. HCC is the most common type of liver cancer, accounting for over 75% of cases. 90% of HCC develop in the context of underlying chronic liver disease, accompanied by severe liver fibrosis and cirrhosis (severe scarring of the liver).⁵⁷ Leading risk factors for chronic liver disease and for HCC development include viral infection by hepatitis B (HBV) or C (HCV), alcohol-related toxicity (ASH), diabetes, or obesity-related non-alcoholic fatty liver disease (NAFLD). Alcohol is an independent risk factor for HCC in heavy drinkers. Excessive alcohol intake causes liver inflammation and damage (alcoholic steatohepatitis - ASH), that results in fibrosis and cirrhosis.⁵⁸ It also synergizes with other risk factors such as diabetes and HCV infection.⁵⁹ Chronic alcohol intake compromises the functional capacity of the liver by triggering steatosis, steatohepatitis, and cirrhosis. These sustained pathologic events subsequently participate in carcinogenic process. NAFLD is a spectrum of chronic liver disease characterized by fat accumulation and inflammation (steatosis, also called non-alcoholic fatty liver - NAFL), leading to hepatocyte injury (non-alcoholic steatohepatitis -NASH) and finally fibrosis/cirrhosis.⁶⁰ Although ASH and NAFLD share pathophysiologic processes in the development of fibrosis/cirrhosis, there is evidence of distinct alcohol-toxicity related mechanisms of tumorigenesis.⁵⁸ In some cases, HCC is caused by genetic haemochromatosis or alpha-1-antitrypsin deficiency. Although HBV and HCV are the most notable risk factors in Asia, as it accounts for a significant proportion of HCC cases, obesity, diabetes, and metabolic syndrome are becoming the fastest growing risk factor for HCC, particularly in the Western world.^{56,61,62}

Hepatocellular carcinoma staging and treatment

The treatment of HCC presents challenges as it occurs in patients with fibrosis/cirrhosis and with compromised liver function. Nevertheless, the management of HCC has significantly advanced in recent years, with treatments tailored to tumor stages, following the Barcelona Clinic Liver Cancer (BCLC) staging system (**Figure 2**).^{57,63} Briefly, it includes prognostic variables related to tumor status, liver function and health performance status, and is an evolving system as it updates treatment-dependent variables obtained from cohort studies and randomised

trials. Early-stage HCC patients are candidates for resection, transplantation, and local ablation, while those at intermediate and advanced stages are recommended for transarterial chemoembolization (TACE), or other systemic therapies, respectively.

Surgical resection and liver transplantation are the primary curative therapies for HCC. Non-cirrhotic HCC patients can achieve 5-year survival rates of approximately 70-80%. Specific scores such as albumin-bilirubin (ALBI) helps assess liver function and suitability for resection.⁶⁴ Recurrence of HCC following hepatic resection remains a significant challenge, with recurrence rates reaching up to 70% within 5 years, even in early-stage HCC.⁶⁵ This recurrence is categorized into two phases: early recurrence (within two years), typically caused by presence of microscopic vascular invasion, and serum alpha-fetoprotein (AFP) levels >32ng/mL, and late recurrence (after two years), which is caused by the development of new tumors in a predisposed microenvironment.⁶⁶

Immunotherapies for HCC

In HCC, immunotherapies are becoming the standard-of-care based on promising results from recent clinical trials, resulting in a shift in clinical management of HCC. The IMbrave150 clinical trial testing adjuvant atezolizumab (anti-PDL1) in combination with bevacizumab (anti-VEGF) in advanced HCC (aHCC) measured a 76.3% Disease control rate (partial response and stable disease) and 27.3% Objective response rate - ORR (complete or partial response) in patients, compared to 55.6% and 11.9% in patients treated with tyrosine kinase inhibitor sorafenib, respectively.⁶⁷

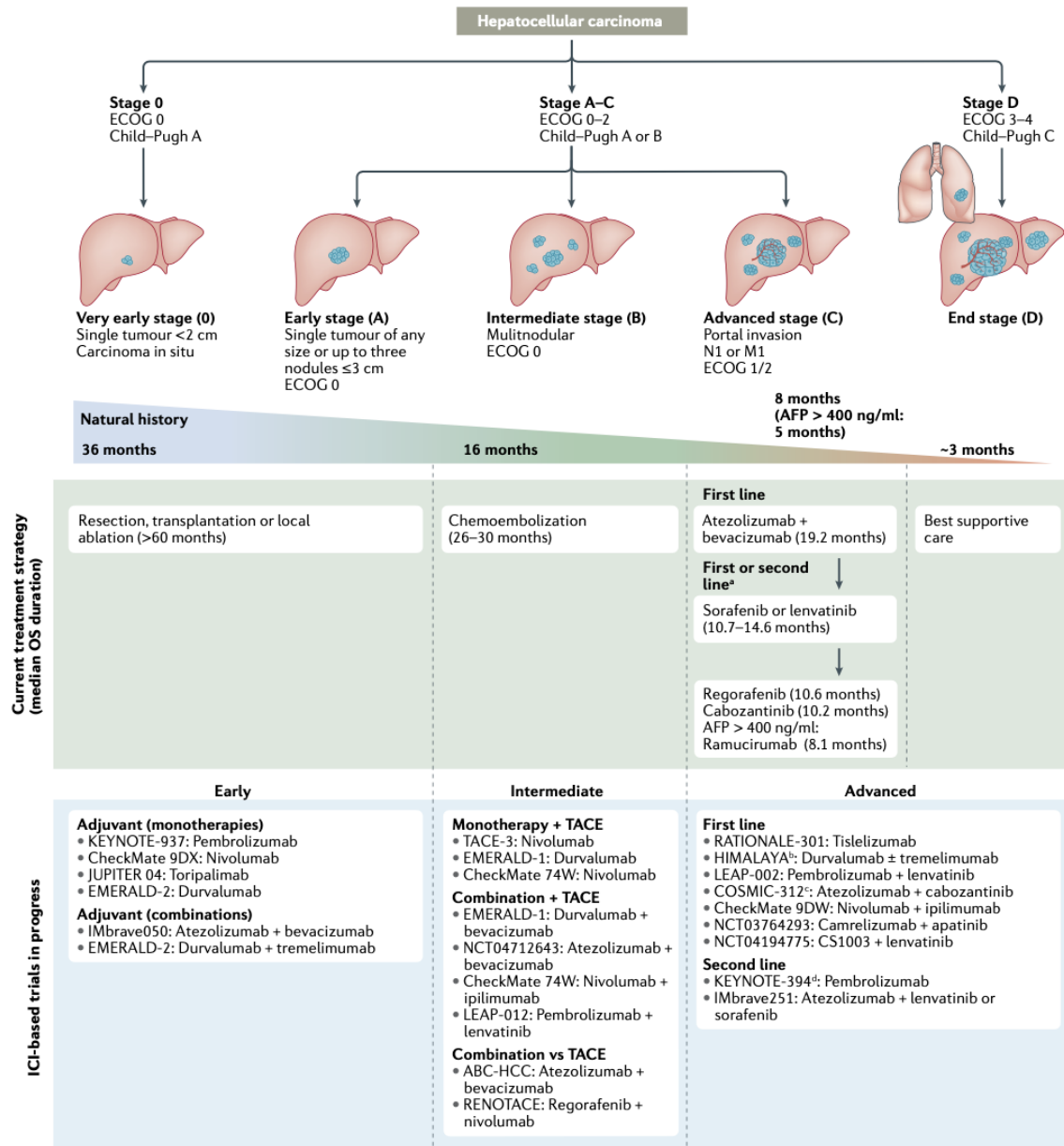


Figure 2. Treatment strategy in the management of HCC⁶⁸ The Barcelona Clinic Liver Cancer (BCLC) staging system consists of five stages depending on disease extension, liver function and performance status. Asymptomatic patients with low tumor burden and good liver function (BCLC 0/A) should be treated with local curative treatments (resection, ablation, or transplantation, depending on the presence of portal hypertension, number of nodules and liver function). Asymptomatic patients with multinodular disease and adequate liver function (BCLC B) should receive chemoembolization and patients with portal thrombosis or extrahepatic spread (BCLC C) should be treated with systemic therapies. Ongoing Immunotherapy-based trials in progress in all disease stages are depicted.

More recently, the STRIDE study testing Durvalumab (anti-PD-L1) plus Tremelimumab (anti-CTLA-4) showed superior OS relative to sorafenib {HR, 0.78 (95% CI, 0.65-0.93, $P < 0.0035$)} and ORRs of 20.1% compared with 5.1%.⁶⁹ These combinatory approaches more than doubled life

expectancy of aHCC, as opposed to monotherapy treatment with Nivolumab (anti-PD-1), which showed no improvement in OS relative to sorafenib {HR, 0.85 (95% CI, 0.72-1.02, $P=0.0752$)}.^{67,70} Currently, over 20 phase III clinical trials are ongoing, testing combination of anti-PD1 and bevacizumab across all stages of HCC.⁷¹

However, despite these advancements, there's a notable variation in patient responses. A retrospective study of 95 aHCC patients who received either single agent anti-PD-(L)1, anti-CTLA4, or a combination of the two compared organ-specific response rates (OSRR) and found heterogeneous responses among liver, lung, lymph node and abdominal tumors. The response rates were lowest in the liver (22.4%) and highest in the lung (41.2%).⁷² Patients with both evaluable hepatic and extrahepatic tumors at baseline had a better disease control rate within extrahepatic tumors as opposed to progressive disease in hepatic tumors. Intriguingly, patients with larger hepatic tumors had progressive disease at extrahepatic sites, whereas those with smaller liver tumors tended to show disease control. Another retrospective study of 261 aHCC patients treated with Nivolumab observed differences in OSRR. Specifically, intrahepatic tumors were the least responsive (10.1%), followed by lung (24.2%) and lymph node (37%) tumors.⁷³ Similarly, a separate retrospective study in patients with aHCC treated with immune checkpoint blockade found that patients with concurrent intra- and extra-hepatic tumors had the lowest ORR and worse OS.⁷⁴ Patients who demonstrated an intrahepatic lesion response to ICI was associated with improved OS and the use of ICI combinations were also associated with improved OS in the setting of aHCC. These findings need to be validated as they may be attributed to the inclusion of immune checkpoint monotherapy as well as combination treatments in these studies. The [NCT04862949](#) clinical trial is measuring OSRR in aHCC patients treated with combination atezolizumab and bevacizumab, to better dissect differences in the tissue-level responses and whether the treatment combination truly enhances intrahepatic responses to immune checkpoint blockade.

The promising results of immunotherapy trials in aHCC have supported phase I/II trials investigating peri-operative immunotherapy in early-stage HCC as both a downsizing and preventative strategy against tumor recurrence post surgical resection. A study exploring perioperative Nivolumab monotherapy and Nivolumab plus Ipilimumab combination therapy induced major pathological response in 30% of patients and 0% recurrence after 2-year follow

up, compared to 50% recurrence in patients without major pathological response.⁷⁵ The results are promising, and validation is needed in subsequent phase III randomized control studies to accelerate their approval for use in the early-stage setting.

Despite these advancements, the limited response of a small proportion of early-stage or aHCC patients to immunotherapy, and the almost negligible response in MSS mCRC liver metastatic patients, calls for further research into the cellular and immune constituents of the liver tissue. Understanding these elements and their influence on immune responses in the liver, under both normal physiological and pathological settings, could pave the way for more effective and tailored treatments across different stages and types of liver pathologies.

The Liver architecture

Understanding why primary liver tumors and metastatic tumors of the liver are less responsive to immune checkpoint blockade requires a thorough grasp of the liver architecture, its cellular and immune components, and how they dictate the delicate balance between immune responses that can destroy invading pathogens or cancerous cells versus those that foster tolerance, pivotal in both the normal and pathological settings. Here we will explore the roles of these components in physiological conditions, before delving into their impact in pathological contexts in the following sections.

The liver is structured around building blocks of hexagonal hepatic lobules (**Figure 3**) which house hepatocytes forming cellular plates between which are liver sinusoids, lined with fenestrated endothelial cells, called Liver sinusoidal endothelial cells (LSEC). The space of Disse between the hepatocytes and LSECs contains hepatic stellate cells (HSC), liver residential macrophages (Kupffer cells, KC) and dendritic cells (DC), along with a myriad of lymphocytic cell populations.

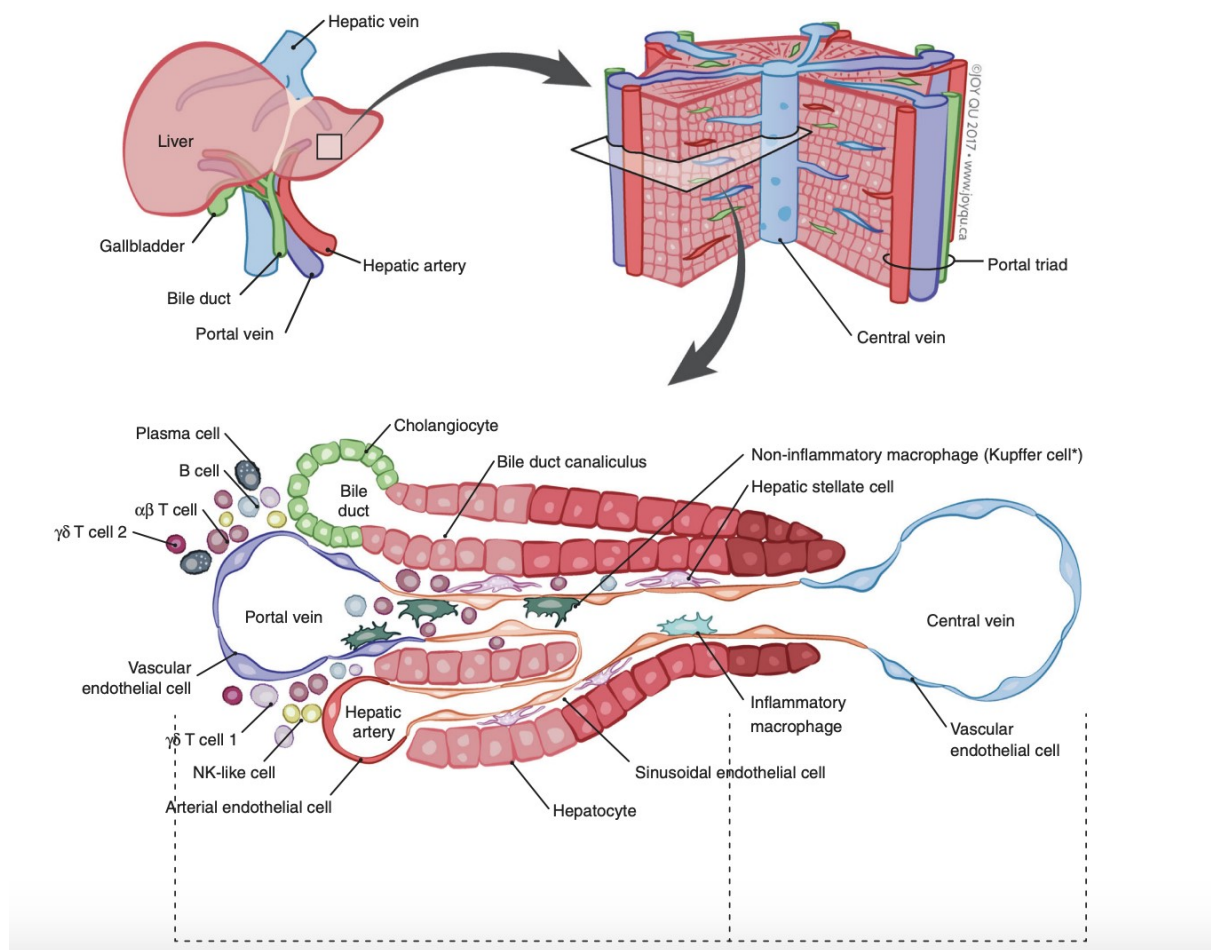


Figure 3. The liver immune microenvironment⁷⁶ Summary map of the human liver. The main “building block” of the liver is the hepatic lobule, which includes a portal triad, hepatocytes aligned between a capillary network, and a central vein. The portal triad is made up of the hepatic artery, the portal vein and the bile duct. Found between the liver sinusoids are parenchymal cells (hepatocytes) and non-parenchymal cells (endothelial cells, cholangiocytes, macrophages, hepatic stellate cells, and liver infiltrating lymphocytes- including B cells, $\alpha\beta$ and $\gamma\delta$, T cells, and NK cells). Non-inflammatory macrophages are labeled *Kupffer cells based

Unique to the liver, the portal vein provides 80% of the total blood supply, bringing to the liver constant influx of food, viral, and bacterial-derived products from the digestive system^{77,78}. Blood from the portal vein and hepatic artery flows through the sinusoids and drains into the central vein, allowing hepatocytes to regulate metabolism, synthesize proteins and remove toxins⁷⁹.

Hepatic cellular components are separated into two large entities: the hepatic parenchyma, which are the hepatocytes, making roughly 60% of the total cells, and the non-parenchymal cells, consisting of liver sinusoidal endothelium, hepatic stellate cells, residential myeloid and

residential and passenger lymphocytic cell populations which comprise up to 30% of the liver cell pool. Recently, single-cell RNA sequencing studies have provided a comprehensive overview of human liver cell subsets and their functions in normal liver physiology, and how together they create a unique niche that favours tolerance induction over immunity, which can be exploited by liver-tropic infections and metastatic disease.

Liver sinusoidal endothelial cells

Liver sinusoidal endothelial cells (LSEC) act as a physical barrier between liver tissue and the periphery, performing a vital role in the development of immune tolerance to exogenous antigens, including food-derived antigens⁸⁰⁻⁸². They achieve this by presenting antigens to CD8⁺T and CD4⁺T cells through MHC-I and MHC-II cross-presentation respectively, while inducing T cell tolerance through low expression of costimulatory molecules CD80/86 and engaging in PDL1-PD1 interaction⁸³⁻⁸⁶. They also control the activity of inflammatory Th1 and Th17 CD4⁺T cells by suppressing inflammatory cytokine secretion⁸⁷. Exposure of LSECs to IL-10 shifts their surface expression towards an inhibitory phenotype. Compared to other antigen presenting cells in the liver, LSECs are also more efficient at inducing peripheral-derived regulatory T cells through their efficient antigen presentation and co-secretion/tethering of TGF β to the cell membrane⁸⁸.

Hepatic stellate cells

Hepatic stellate cells (HSCs) store and metabolise Vitamin A (retinoic acid) and play a critical role in chronic liver diseases by secreting extracellular matrix proteins and matrix metalloproteinases when activated. Within the space of Disse, HSCs mediate T cell suppression by influencing the expression of inhibitory factors in dendritic cells (DCs) and by promoting the differentiation of regulatory T cells while inhibiting the activation of proinflammatory Th17 cells.⁸⁹⁻⁹³ In the transplant setting, HSCs have been shown to induce T cell apoptosis and skew T cell responses towards tolerance.^{89,94-97}

Kupffer cells

Kupffer cells (KCs) are liver resident macrophages that can induce immune tolerance. Single cell RNA sequencing in mouse and human liver have identified two distinct population of Kupffer cells with distinct functions under normal physiological or inflammatory settings^{76,98}.

In humans, two distinct populations of *CD68*+ macrophages are distinguished by MARCO expression and their location within the hepatic lobule ⁷⁶. Human *CD68*+*MARCO*+ cells are transcriptionally like liver-resident mouse KCs expressing *CD163*, *MRC1*, and *VSIG4*. In contrast *CD68*+*MARCO*- macrophages are transcriptionally like inflammatory macrophages, responding better to LPS and IFN γ stimulations than *MARCO*+ KCs. In mice, KCs are distinguished by *MRC1*(*CD206*), *CD107b* and *ESAM* expression ⁹⁸. *CD206*+ KCs are enriched with genes in the Ag processing, cross-presentation and IL-2 signaling pathways. Under steady state conditions, these cells are poor stimulators of intrahepatically primed CTLs. However, in the context of IL-2 inflammation, these KC are capable of efficient cross-presentation to T cells.

Kupffer cells induce immune tolerance in the liver under steady state by promoting the expansion of regulatory T cells (Tregs),^{99,100} and suppressing T cell proliferation and activation through lower MHC Class II and costimulatory molecules expression.¹⁰¹ Kupffer cells release IL-10 in response to physiological levels of LPS, acting in an autocrine fashion to downregulate the release of proinflammatory cytokines TNF α and IL-6.¹⁰² In the pathological and liver transplant setting, Kupffer cells upregulate IDO and FasL expression, inhibiting allogeneic T cell responses and inducing T cell apoptosis.^{103,104} However, in models of liver inflammation, tolerogenic signals of KCs are counteracted by high proportions of infiltrating inflammatory monocytes.⁹⁹ When TLR3 ligands are present in the liver, NK cell priming is also enhanced by Kupffer cells.¹⁰⁵

Dendritic cells

Dendritic cells (DCs) are involved in bridging innate and adaptive immunity. Liver DCs consist of distinct myeloid versus plasmacytoid cell (pDC) subpopulations. Liver DCs are less efficient at antigen uptake and processing compared to blood DCs and preferentially promote the generation of Tregs.¹⁰⁶ In a separate study, liver pDC were found to be more tolerogenic than pDC in other tissues ^{107,108}. In the context of liver transplantation, liver recipient dendritic cells acquire donor MHC molecules via cell-cell contact, leading to high expression of PD-L1 and IL-10 secretion, promoting liver transplantation tolerance.¹⁰⁹ Nevertheless, the balance of mature and non-mature DC populations can still impact acute liver transplant rejection in mice.¹¹⁰ *CD141*⁺ dendritic cells, capable of cross-presentation and induction of cytotoxic *CD8*⁺ T cell immunity, produce the highest levels of IFN- λ in the liver in response to TLR3

ligation¹¹¹. Decreased CD141⁺ DCs are associated with liver diseases including HCC and CRC liver metastasis, whereas plasmacytoid and myeloid DCs are increased^{111,112}. Plasmacytoid DCs are positively correlated with immunosuppressive IL-10 producing CD4⁺LAG3⁺ T cells in HCC and CRC liver metastasis via ICOS-ICOSL signaling¹¹³.

Mast cells

Residing along the liver sinusoids and portal tracts are liver mast cells. These cells of hematopoietic origin in the foetal liver and bone marrow, complete their differentiation and specification in peripheral tissues due to local microenvironmental factors¹¹⁴⁻¹¹⁷. The liver mast cells are mostly associated with the connective tissue, which is located close to the hepatic arteries, veins, and bile ducts of the portal tracts in the human liver. In the normal liver, mast cells accumulate in small numbers along the portal tract, becoming more abundant in cases of liver injury, including cholangiopathies, alcoholic liver injury, fatty liver disease, and allograft rejection.¹¹⁸ As they are an important source of pro-inflammatory mediators, they are implicated with liver inflammation and fibrosis, however their roles are controversial.¹¹⁸⁻¹²⁰

T cells

The liver is home to a large intrahepatic lymphocyte (IHL) population, including CD8⁺T cells, CD4⁺T cells, Tregs and Tissue-resident memory T cells (Trm).¹²¹ The liver's unique microenvironment can influence the balance between immune tolerance and immunity. Effective restimulation of liver-primed T cells often requires secondary activation within liver-draining lymph nodes,¹²² especially in the presence of high intrahepatic antigen load, as occurs in chronic HBV infections.¹²³⁻¹²⁵ In contrast, effective CTL responses can be generated within the liver in the presence of low antigen load.^{124,126} In the context of hepatotropic infections, a memory T cell pool established with vaccination cannot be recalled beyond a certain threshold of antigen expression in the liver, requiring inflammatory cytokines released by antigen presenting cells. Indeed, functional memory T cell responses to high intrahepatic antigen challenge can be restored with a previous and simultaneous activation of TLR9 signaling pathway during AdOVA vaccination in a transgenic mouse model.¹²⁷ In the event of liver transplantation, prolonged and persistent antigen stimulation of T cells coinciding with the lack of costimulatory molecules IL-2 and IFN γ eventually results in their exhaustion and unresponsiveness to antigens both locally and systemically within the same host.¹²⁸

Interestingly, these liver graft infiltrating cells can mount a response to reject skin allografts when transferred into secondary hosts, indicating the importance of microenvironment-regulated costimulatory versus coinhibitory signals, and the phenomenon known as 'split tolerance'. The systemic administration of IL-2 protects CD8⁺T cells from apoptosis and induces NK and NKT cell cytotoxicity, inducing acute liver graft rejection in mice.¹²⁹ A recent clinical trial testing low dose IL2 treatment in human liver transplant recipients failed to promote liver allograft tolerance.¹³⁰ Though circulating Tregs expanded in patients, they did not infiltrate the liver; instead, the treatment elicited a macrophage-driven IFN-gamma inflammatory transcriptional signature response in the liver and may have increased risk of rejection in this cohort.¹³⁰

In healthy liver, the CD4⁺/CD8⁺ ratio is in favour of CD8⁺T cells.¹²¹ However, in liver disease, preferential recruitment of CD4⁺T and Tregs occurs, skewing the ratio and thwarting CD8⁺ mediated cytotoxic response.^{131,132} Antigen specific regulatory T cells are key mediators of transplant tolerance.¹³³⁻¹³⁵ In a separate cohort of patients, a transient accumulation of Tregs within portal tracts associated with down-regulation of immune activation transcriptional signatures was observed in patients that became spontaneous operational tolerant after immunosuppression withdrawal.¹³⁶ In addition, operational tolerance has been induced in liver transplant patients infused with donor-derived *ex vivo*-generated Tregs in combination with splenectomy.¹³⁷

Tissue Resident Memory cells

The liver contains a substantial population of tissue-resident memory CD8 T cells, CD4 T cells and $\gamma\delta$ T-cells expressing liver-homing markers CD69, CD103^{+/+}, CXCR6, and CXCR3.¹³⁸⁻¹⁴¹ CD8⁺ Trm cells in the liver express high levels of IL-2, maintaining their survival and proliferation under homeostasis and antigen challenge. Constitutive TGF β signaling downregulates LFA-1 on liver Trm, which is required for adhesion within the hepatic sinusoids, differentiating its regulation from skin Trm.^{142,143}

Innate Lymphoid cells

The liver houses a large population of innate lymphoid cells including NK cells, invariant NKT cells, MAIT cells and $\gamma\delta$ T cells. These cells play a vital role in the rapid elimination of pathogens and viral products, contributing to immune surveillance in the liver.

Liver-resident NK cells are a pivotal component of the liver's innate immune response, constituting up to 40% of intrahepatic lymphocytes.¹⁴⁴ They represent a heterogeneous cell population, comprising 7 subsets within the human liver.¹⁴⁵ The unique liver microenvironment, characterized by higher levels of IL-10 and TGF β , influences the phenotype of these NK cells, rendering them hyporesponsive and tolerogenic in the liver tissue.^{146,147} Notably, CXCR6⁺ liver-resident NK cells express the inhibitory receptor NKG2A and are less responsive to target cell stimulation compared to peripheral blood counterparts.¹⁴⁸ NKG2A-expressing NK cells are known to play a crucial role in maintaining tolerance or exhaustion, particularly in the context of chronic viral infections. Additionally, liver NK cells negatively regulate vaccine-induced CD8 T cells against HBV through the upregulation of PD-L1, which could be reversed through PD-L1 blockade.¹⁴⁹

NKT cells constitute up to 15% of the intrahepatic lymphocytes. The cells are capable of TCR-mediated cytotoxicity and include Va24-JaQ TCR-bearing cells that recognize Ags presented by CD1d.¹⁵⁰ They are also enriched in $\gamma\delta$ T cells implicated in CD1c-restricted responses.¹⁵¹ Their functions and profiles are influenced by the liver microenvironment. NKT cells can produce various cytokines, including IFN γ , TNF α , IL-2 and IL-4. Importantly, these cells have the capacity to influence secondary adaptive immune responses based on their cytokine production.¹⁵² In humans, NKT cells express KIR and NKG2 receptors, important regulators of NKT cell activity mediated through interactions with MHC I on target cells.

Innate T cells such as MAIT and $\gamma\delta$ T cells, also play significant roles in the liver. MAIT cells are highly abundant in the human liver and can be activated by microbial antigens bound with MR1.¹⁵³ Several subsets of MAIT cells have been defined, most of which, if not all, are CD161^{high}IL17-secreting CD8⁺ T-cell subset.¹⁵⁴ MAIT cells are therefore often mixed with CD8⁺T cell subsets in flow cytometry staining of liver immune cells without CD161 staining. After being activated by microbial antigen bound with MR1, MAIT cells are licensed to kill targets by secreting IFN γ , granzyme, and perforin.¹⁵⁵

In summary, the liver's intricate immune network creates a unique niche favoring tolerance induction over immunity. The liver's specialized immune microenvironment has implications for both physiological liver functions and various pathological conditions, influencing the balance between immune responses that eliminate pathogens or cancer cells and those that foster immune tolerance.

The Tumor Immune Microenvironment of MSS CRC Liver metastases and its association with patient prognosis

Though tumor cells potentially reach the vasculature of all organs through the circulatory system, colorectal cancer preferentially metastasizes to the liver.¹² Several reasons include anatomical and mechanical factors, including the livers' anatomical position and reception of 80% of its blood supply from the digestive tract, but also the mechanical factors such as regulated blood flow and expression of adhesion molecules that can facilitate the initial step of adhesion and extravasation into the tissue.¹⁵⁶ The ability of extravasated cancer cells to survive and establish themselves once within the liver, is further facilitated not only by survival and growth factors but also the tolerogenic nature or 'bias' of the immune cells within the liver.¹⁵⁷ The collaboration between the cancer cells and the tissue-immune microenvironment of the liver reprograms both metastasizing tumor cells and the tissue-immune microenvironment, leading to an organ-specific phenotype.¹⁵⁸

Compared to primary colorectal cancer, and even other metastatic sites, T cell excluded tumors are common in CRC liver metastasis, with decreased tumor infiltration of T cells, and elevated accumulation of myeloid suppressor cell subsets either at the margin or within the tumor.^{159,160,161} Nevertheless, it has become strikingly apparent in the last decade the important role of the immune response in CRC tumors and CRC liver metastasis. Initially described in primary CRC, the assessment of CD3⁺T cell infiltrate at both the central tumor (CT) and invasive margin (IM), increased the prediction of DFS and OS.¹⁶² Since this study, the "Immunoscore" has predicted the clinical outcome also in patients with mCRC in liver metastatic tissue.^{163,164} Importantly, the predictive role of T cells infiltration in mCRC may be associated with the

application of neoadjuvant chemotherapy, as studies in resected tumors from patients without neoadjuvant chemotherapy treatment did not demonstrate a prognostic benefit of T cell infiltration.¹⁶⁴ In humans, T cell numbers are significantly increased in surgically resected specimens of CRC liver metastatic patients treated with neoadjuvant chemotherapy and are independently associated with improved disease-free survival.^{164,165} Also, PD-L1 expression is significantly increased in liver biopsies from patients with mCRC after FOLFOX accompanied by an increase in CD8⁺T cell infiltration.¹⁶⁶ Resected RAS wildtype mCRC tumors are more infiltrated with CD3⁺, CD8⁺ and CD45RO⁺ cells following chemotherapy in combination with anti-EGFR treatment in lesions with pre-existing immune infiltrate.¹⁶⁴ In mice, certain chemotherapy combinations including Fluorouracil and Oxaliplatin can induce immunogenic cell death, associated with T cell infiltration into tumors and improved anti-tumor immunity.¹⁶⁶⁻¹⁶⁸ Cetuximab (an anti-EGFR antibody) can also induce antibody-dependent cell-mediated cytotoxicity.¹⁶⁹

Variable levels of T cell infiltration in MMR-p mCRC liver metastasis following response to chemotherapy could reflect expanded tumor-specific clones in a subset of patients. Resected mCRC liver metastases from 85 patients enrolled in the Oslo-CoMet trial (NCT01516710) compared TCR repertoire sequencing in patients who had received neoadjuvant chemotherapy (NACT) or not. A short time interval (<9.5 Weeks) between NACT completion and tumor resection was strongly associated with high intra-tumoral T cell densities compared to long-interval and untreated patients, suggesting a transient increase in intra-tumoral T cells after NACT.¹⁷⁰ Additionally, the increase in T cell infiltration was associated with TCR clonal expansion of the cells, suggesting chemotherapy could drive T cell clonal expansion in this setting.¹⁷¹ However, the effect may be transient due to multiple pathways of resistance (intrinsic or acquired) within the liver immune microenvironment, and these effects need further exploration.

Indeed, a large proportion of mCRC patients with liver metastasis are unable to generate sufficient T cell infiltrates despite neoadjuvant chemotherapy treatment and at an increased risk of relapse. Additionally, a detailed study of over 600 cases of liver metastatic CRC unveiled variations in the level of T cell and B cell infiltration among different liver metastases from the same patient.¹⁶⁴ These disparities in immune cell infiltration partially stem from distinct genetic

evolutionary patterns within these metastatic lesions, driven, in part, by the proliferation of immune-escaped clones with a low mutation burden.¹⁷² Also, the resistance could be intrinsic, and that immunogenic cell death was not triggered by the chemotherapy treatment, or the resistance was acquired through modulation of the tumor immune microenvironment by the recruitment of immunosuppressive cell subsets that hampered the infiltration and expansion of tumor-antigen specific T cells.

Recent studies in mCRC have prioritized to further our understanding of the molecular, biologic, and cellular mechanisms of resistance to chemotherapy in MSS mCRC. Resident as well as recruited immune cells in the liver are known to play major roles in the escape from immune control and tumor outgrowth in colorectal cancer liver metastasis.^{157,173,174} Pre-clinical models have ascribed impaired cytotoxicity of CD8⁺ T cells in CRC liver metastasis to the loss of antigen-specific T cells through apoptosis induction, as well as poor co-stimulation, mediated by liver myeloid cells and Tregs^{173,174} In humans, activated and proliferating intra-tumor Tregs restrain anti-tumor immunity in CRC liver metastasis and high numbers of Tregs relative to CD8 T cells are associated with poor OS.^{175,176} Research from other studies has highlighted the significant contribution of non-immune cellular types in the tumor microenvironment, specifically cancer-associated fibroblasts, to the advancement of metastasis and resistance to drugs in mCRC.¹⁷⁷ These cells not only facilitate tumor expansion but also exert influence over immune responses in the CRC tumor microenvironment, thereby fostering mechanisms of immune evasion.¹⁷⁸ Studies by single-cell RNA sequencing in human resected CRC liver metastasis have highlighted the heterogeneity and reprogramming of myeloid cells within the tumor microenvironment in chemotherapy-treated patients with different levels of radiologic response.^{179,180} Patients with stable disease/progressive disease (SD/PD) to chemotherapy had increased infiltration in Neutrophils, *SPP1*⁺ macrophages and *MRC1*⁺*CCL18*⁺ macrophages and decreased cytotoxic immune cells. In contrast, the opposite was observed in partial response (PR) tumors, with decreased *SPP1*⁺ macrophages and upregulate cytotoxic T cells in tumors and adjacent liver and PBMCs. The results show intra-tumor immune balance is reprogrammed in treated tumors as compared to untreated tumors, providing evidence to the notion that “chemo-immunosensitization” occurs, either favorably or unfavorably.¹⁷⁹

Influence of molecular subtypes

RAS mutations have a significant impact on the immune microenvironment in liver metastasis. The Kirsten rat sarcoma viral oncogene homolog (KRAS) proto-oncogene is the most commonly altered gene in CRC.¹⁸¹ KRAS mutations in CRC liver metastasis are associated with worse DFS and OS after surgical resection.¹⁸² Emerging studies have highlighted the relationship of KRAS-mutated cancer and tumor microenvironment components, mainly with T cells. The recent study of Immunoscore in resected CRC liver metastasis noted in general that tumors harboring KRAS mutations were less infiltrated with T cells and B cells but did not express elevated levels of immune checkpoints PD1, PDL1 or CTLA4.¹⁶⁴ Another recent study noted in surgically resected mCRC an association between RAS mutation and decreased MHC Class I expression on the tumor cells.¹⁸³ In vitro, lactic acid derived from KRAS mutant tumor cells sensitized tumor-specific CD8⁺ T cells to activation induced cell death via NFκB.¹⁸⁴ In advanced CRC, KRAS mutation represses interferon regulatory factor 2 (IRF2), which increases myeloid-derived suppressor cell (MDSC) recruitment and immune suppression.¹⁸⁵ Furthermore, other researchers have noted increased accumulation at the tumor margin of CD66b⁺ neutrophils compared to wild-type tumors in resected liver metastases.¹⁸⁶ In summary, these reports establish possible links between KRAS signaling, T cell infiltration and immunosuppression, leading to poor outcomes for these patients.

The role of mast cells

Mast cells are innate immune cells that reside in barrier site organs, notably, the liver, intestine, colon, skin, and lung. In the liver, mast cells reside along the liver portal tracts within the liver stroma. Mast cells are considered as 'sentinel' cells, with a capacity to respond to a plethora of danger signals to trigger different immunologic responses.¹⁸⁷ **Figure 4** demonstrates the variety of surface receptors that can be expressed by human mast cells and illustrates how these cells are activated by a diverse range of stimuli.¹⁸⁸ Mast cells have common features across different tissue sites including a conserved elevated expression of C-Kit (CD117), important in their development and survival. Mast cells upregulate FcεRI and Fcγ receptors in response to maturation signals and antigen stimulus. Upon activation through IgE or Non-IgE stimuli, mast cells produce a spectrum of proinflammatory pre-formed mediators (including cytoplasmic granules, vasoactive amines, proteases, proteoglycans and some cytokines and

growth factors). In situations of prolonged activation, they undertake de-novo synthesis of prostaglandins, growth factors, cytokines, and chemokines in situations of prolonged activation.¹⁸⁹ Their distinct immunoregulatory roles, highly dependent on environmental factors, enable mast cells to initiate a broad spectrum of responses. These responses are mediated through direct interactions with other cells or by its secretory functions.¹⁸⁹ While mast cells have been notorious for their association with detrimental roles in pathologies like allergies and asthma, they also play vital immunoregulatory roles, bridging the gap between innate and adaptive immunity.¹⁹⁰ Recent findings have unveiled mast cells' intricate information-processing capabilities, enabling them to translate various incoming warning signals into specific and diverse response programs dependent on the type of tissue and the signal encountered.^{191,192}

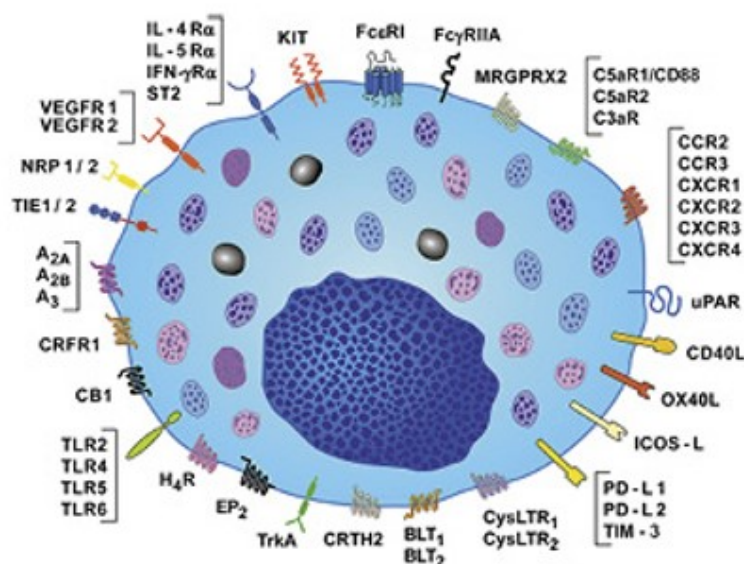


Figure 4 Surface receptors expressed by human mast cells.¹⁸⁷ Human mast cells express the high-affinity receptor for IgE (FcεRI) and FcγRIIA, and their cross-linking induces the release of proinflammatory and immunomodulatory mediators. All mast cells display the KIT receptor (CD117), which is activated by stem cell factor (SCF), whereas only certain types of mast cells (e.g., skin and synovial) express the MAS-related G protein-coupled receptor-X2 (MRGPRX2) activated by neuropeptides (e.g., substance P), opioids, and cationic drugs. Mast cells express receptors for various cytokines (IL-4Rα, IL-5Rα, IFN-γRα, and ST2), vascular endothelial growth factors (VEGFR1 and VEGFR2), neuropilin-1 (NRP1) and neuropilin-2 (NRP2), and angiopoietins (ANGPTs) (TIE1 and TIE2). These cells also display adenosine receptors (A_{2A}, A_{2B}, and A₃), corticotropin-releasing factor receptor type 1 (CRFR1), cannabinoid receptor 1 (CB1), toll-like receptor (TLR)2, TLR4, TLR5, TLR6, histamine H₄ receptor (H₄R), prostaglandin E₂ receptor (EP₂), NGF receptor (TrkA), PGD₂ receptor (CRTH₂), 2 leukotriene B₄ receptors (BLT₁ and BLT₂), and 2 receptors for cysteinyl leukotrienes (CysLTR₁ and CysLTR₂). Mast cells express receptors for anaphylatoxins (C5aR1/CD88, C5aR2, and C3aR), several receptors for CC and CXC chemokines, and the high-affinity urokinase plasminogen activator receptor (uPAR). These cells also express coreceptors for T cell activation CD40 ligand (CD40L), TNF superfamily member 4 (OX40L),

inducible costimulator ligand (ICOS-L), programmed cell death ligands (PD-L1 and PD-L2), and T cell immunoglobulin and mucin domain-containing protein 3 (TIM-3). Not shown in this figure are the inhibitory receptors CD300a, Siglec-8, Siglec-9, and CD200R expressed by human mast cells.¹⁸⁷

Mast cells have distinct origins during different stages of development: they arise from erythro-myeloid progenitors (EMP) in the fetal liver during embryogenesis and from haematopoietic stem cells (HSCs) in the bone marrow.¹¹⁴ Recent evidence from mouse studies demonstrates that late-EMP derived mast cells dominate connective tissues, while HSC-derived mast cells predominate in mucosal tissues including the colon and lung.¹¹⁶ In humans, distinguishing features between “connective tissue-like” (CTMC) and “mucosal-like” (MMC) mast cells include the expression of specific proteases, tryptase and chymase.¹⁹³ CTMCs, located around venules and nerve endings in connective tissues, primarily contain chymase, carboxypeptidase, and tryptase. On the other hand, MMCs, found inside epithelial of the intestine/colon and respiratory mucosa, produce only tryptase. Other differences in these subtypes of mast cells are that CTMCs are long-lived cells capable of self-renewal, whereas MMCs originate from HSCs and are replenished regularly.¹¹⁴ A recent proteomics assessment of mast cells in connective and mucosal tissue identified CD203c expression levels highest on CTMCs.¹⁹⁴ CD203c expression is also a marker of mast cell activation and can control chronic stimulation of mast cells.¹⁹⁵ It is a more stable marker of mast cell activation than CD63.¹⁹⁶

Historically, mast cells were the first immune cell subtype recorded to infiltrate cancerous tissue and are considered an important component of the tumor microenvironment.¹⁹⁷ Because of their phenotypic heterogeneity and diverse roles in different environments, the role of mast cells in patient survival has been controversial in many cancer types, including CRC liver metastasis.¹⁹⁷ Based on their phenotypic diversity and high plasticity, the role of mast cells in tumors is highly context dependent, on secreted factors as well as other cell subtypes within the tumor microenvironment. On the one hand, chemo-attractants from tumor cells such as SCF, IL33, VEGF, TGF β , and CXCL12 can attract mast cells and drive the production and secretion of pro-angiogenic and immune suppressive mediators, while other signals such as TLR agonists or IgE/IgG antibodies can promote mast cell activation to drive the recruitment and activation of T cells and dendritic cells.¹⁹⁸

Activated mast cells play a significant role in recruiting and activating various immune cells within the tumor microenvironment.¹⁹⁸ A summary of the main mechanisms is presented in **Figure 5**. Mast cells can contribute to local immune suppression through the recruitment of MDSCs and neutrophils through CCL2 and CXCL1/2 secretion.^{199,200} Histamine release from mast cells can also control myeloid cell differentiation to suppress their function. In histamine deficient mice, increased inflammation associated carcinogenesis occurred with a coinciding increase of immature granulocytic MDSCs.²⁰¹ Mast cell histamine can also inhibit Tregs, whereas Tregs can inhibit mast cell degranulation and enhance IL-6 secretion.²⁰² In certain contexts, mast cells can skew Treg differentiation towards a Th17 proinflammatory cell subtype, that can have either tumor-promoting, or tumor-inhibitory effects.^{203,204} Secreted mediators from mast cells such as CCL5 and CXCL10 can participate in T cell recruitment to tumor sites.²⁰⁵ Mast cell histamine can also enhance T cell and NK cell function as well as dendritic cell migration and maturation.^{206,207}

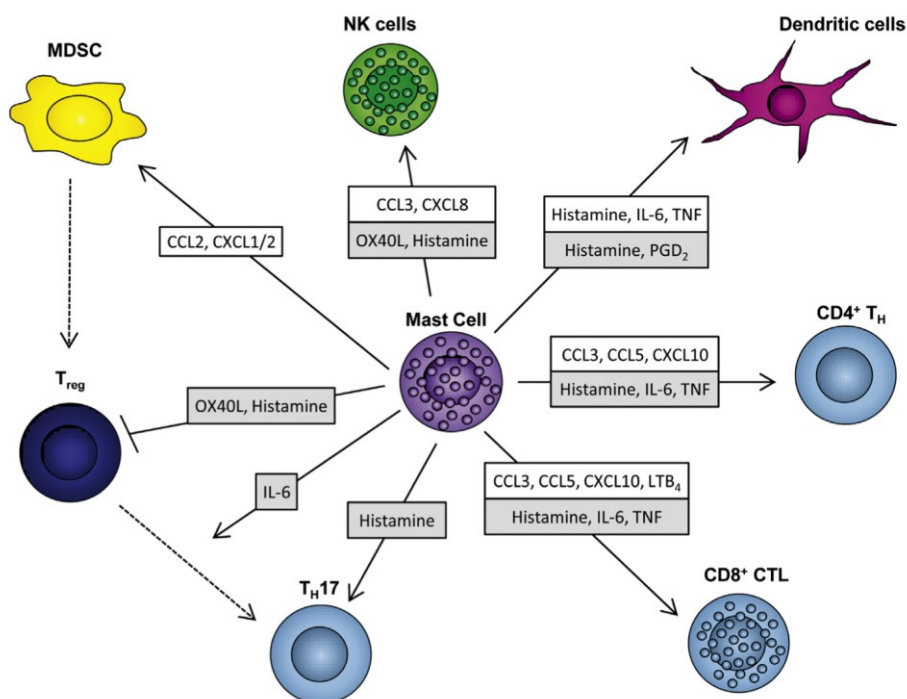


Figure 5. Major mechanisms by which mast cells may modulate anti-tumor immunity¹⁹⁸ Mast cells can modulate anti-tumor immunity through the release of granule-associated and de novo synthesized mediators that induce the mobilization of immune cells (white boxes) and their activation and differentiation (grey boxes). Mast cells can contribute to the immune suppressive tumor microenvironment via mobilization of and interaction with MDSC and Tregs. With appropriate activation, mast cells may also enhance anti-tumor responses via the recruitment of NK cells, T cells and DC subsets via their interactions with these cells to enhance their activation. In turn, cells recruited to tumor sites via mast cells can then modulate mast cell activity.¹⁹⁸

So far, the assessment of mast cells to identify their localization and prognostic role in colorectal cancer liver metastasis has relied on the use of single immunohistochemistry staining of mast cells with CD117, Tryptase and Chymase. Gulubova *et al*²⁰⁸ performed a structural examination of Tryptase- and Chymase- positive mast cells in livers containing metastases from gastrointestinal cancers. This study is the first to examine tryptase- and chymase- positive mast cells in liver metastasis. In normal livers, there were equal proportions of Tryptase⁺ and Tryptase⁺/Chymase⁺ Mast cells, whereas their numbers increased in liver tissue surrounding and within CRC liver metastatic tissues, largely by Tryptase⁺/Chymase⁺ subset. These cells appeared degranulated and were increased particularly in 'highly-differentiated' (i.e., Associated with improved prognosis) CRC tumors than in 'poorly differentiated' tumors. They hypothesized therefore that low-grade differentiated metastases had an exhausted immunologic response that correlated with a connective tissue stroma containing fewer mast cells. Later studies described peritumoral Tryptase⁺ mast cells in liver metastases having an unfavorable impact on patient OS.²⁰⁹ Conversely, other studies have shown the presence of peritumoral Tryptase⁺ or CD117⁺ mast cells are correlated with increased OS, and the presence of intra-tumoral CD117⁺ mast cells in association with CD3⁺T cells is correlated with increased DFS.^{165,210} Unfortunately, the staining by Tryptase, Chymase or CD117 do not permit us to know whether the mast cells are properly activated or not in CRC liver metastases. Furthermore, their different roles according to the micro-localization of the cells suggest that the contribution of mast cells can also vary according to their micro-localization.

These results suggest that the assessment of mast cells by their numbers and without an association with other immune cell subsets infiltrating the tumors does not provide insight into how they interact with the cells within the tumor microenvironment to influence the immune profile and prognosis of mCRC. In addition, no study has assessed their functions according to the *RAS/BRAF* mutation status of patients. Therefore, a better knowledge of their activation as well as the secreted factors within the tumor microenvironment that could be regulating their activity could help improve our understanding on the actual role of mast cells in modulating the tumor immune microenvironment in mCRC liver metastasis and how this could influence patient prognosis.

The Tumor Immune Microenvironment of Primary Liver Tumors and its association with patient prognosis and response to immunotherapy

The immune microenvironment in HCC

The immune landscape of HCC is shaped by intricate interplay of innate and adaptive immune systems.²¹¹ The immune microenvironment within the liver is primarily immunosuppressive and fosters tolerogenic niche as mentioned in the previous section. Key immunosuppressive players in HCC encompass Kupffer cells, monocyte-derived macrophages, regulatory T cells (Tregs) and Granulocytic myeloid-derived suppressor cells (gMDSCs).^{211,212} Regulatory DCs, CD8⁺PD1⁺ cells (in the context of NASH) and neutrophils also contribute to immune dysfunction.^{113,213,214} Regulatory DCs in HCC also are highly immunosuppressive through production of high levels of IL-10.²¹⁵ In contrast, certain immune components drive antitumor immune responses and effective cancer cell clearance. CD8⁺ T cells play an important role, in particular, tissue-resident memory CD8⁺T cells and more recently, a cytotoxic role of MAIT cells against HCC has been appreciated.²¹⁶ However, tumor antigen specific T cells are rarely detected in HCC patients. Also, antigens capable of inducing antitumor immunity in HCC may originate from various sources, such as tumor-associated antigens, viral peptides or neoantigens derived from driver genes or passenger mutations. However, unlike some cancer types, the tumor mutational burden does not correlate with immune infiltration, possibly due to disruptions in antigen presenting machinery and copy-number alterations affecting antigen presentation.^{217,218}

HCC is a heterogeneous disease developing from chronic liver inflammation, oxidative stress, and deregulation of cell signaling pathways caused by pathologies including chronic viral hepatitis infections (HBV/HCV), alcoholic (ASH) and non-alcoholic fatty liver diseases (NASH-NAFLD).⁷¹ The progression of HBV/HCV related HCC, ASH-HCC, and NAFLD-HCC are inherently tied with deregulated immune responses. In chronic-HBV/HCV derived HCC, aberrant immune responses that fail to clear hepatotropic viruses promote tumorigenesis. In the context of NASH-NAFLD, chronic inflammation induced by fat accumulation activates 'auto-aggressive' CD8⁺ PD1⁺ T cells and NKT cells that cause chronic tissue damage.²¹⁹⁻²²¹ Therefore, the assessment of distinct aetiologies of HCC is important to identify potential mechanisms for potential immunotherapeutic intervention. For example, chronic HBV

infection results in immune alterations that create a tolerogenic environment, including the elevation of inhibitory immune checkpoint proteins, and highly suppressive PD-1 positive Tregs.²²² However, the presence of viral-specific T cells are important markers of prognosis in these patients. Non-viral HCC such as ASH and NASH, however, exhibit a distinct landscape. Metabolic activation of 'auto-aggressive' CD8⁺ T cells and NKT cells induces necro-inflammation in NASH-induced HCC.^{220,221} Neutrophils also compromise immune responses in NASH-induced HCC, and their reprogramming through CXCR2 blockade increased recruitment of cross-presenting dendritic cells together with cytotoxic CD8⁺ T cells in a mouse model of NASH-HCC.²¹³ In the context of ASH, alcohol increases gut permeability, allowing immunomodulatory microbiota-derived molecules to suppress hepatic immune responses. Cytokines such as IL-1 and IL-17 play roles in the pathogenesis of alcohol-induced HCC. Dysbiosis of the gut microbiota is observed in various stages of chronic liver disease, including HCC, and it may affect HCC growth by promoting HCC development, contributing to HCC growth, and modulating hepatic immunity. Antibiotic treatment can prevent HCC development in preclinical studies, suggesting the potential for combining immunotherapies with antibiotics in clinical trials for HCC patients.⁶⁸

Immunological correlates of response to Immunotherapy in HCC

The etiology of HCC contributes to the heterogeneity of responses to immunotherapy, as a meta-analysis of 8 trials including 3739 patients revealed that the efficacy of immune checkpoint therapy was significantly greater in patients with viral related than non-viral related HCC.²²³ Advanced technologies including CyTOF and single cell RNA sequencing have described elevated CD8⁺ T cell infiltration and enrichment of CD103⁺ tissue resident memory (TRM) cells expressing PD1⁺ in HBV-related HCC.^{224,225} CD103⁺CD8⁺ TRM cells in HCC were identified as functionally competent cells associated with improved PFS in patients treated with anti-PD1, compared with exhausted non-TRM CD8⁺ T cells expressing high levels of PD1, CTLA4 and LAG3.²²⁶ Exhausted non-TRM CD8⁺ T cells were negatively correlated with earlier disease stages and positively correlated with non-alcoholic steatohepatitis (NASH) - derived HCCs.²²⁶ Thus, TRM and non-TRM CD8⁺ T cells possessing divergent properties are prevalent in HCC and are important cellular biomarkers of response.

Recent studies have leveraged results from different clinical trials to determine correlates of response to different immunotherapies and their various combinations at the molecular and cellular level.^{75,227-229} Monotherapy anti-PD1 treatment has demonstrated its efficacy specifically in resectable HCC patients harboring elevated immune infiltration in their tumors.^{75,230} In the study by Kaseb *et al.*, gene expression analysis showed that higher infiltration of T cells at baseline was required for response to anti-PD1 monotherapy but was not required for combination (anti-PD1 and anti-CTLA4).⁷⁵ It is possible that blocking CTLA4 lead to favorable immunological changes in the tumor environment, by suppressing Tregs for example, that potentiated response to anti-PD1. Using a deconvolution approach on RNA-sequencing data in aHCC, elevated infiltration of immunosuppressive Regulatory T cells (Tregs) was negatively associated with response to anti-PD1 monotherapy treatment in the first-line as well as second- and third-line setting, indicating the important role for Tregs in relapsing/recurring HCC patients.²²⁸ Another study showed HCC patients with elevated Treg and myeloid cells signature and angiogenesis marker *KDR* (VEGFR2) benefited from combination treatment Atezolizumab (anti-PDL1) and Bevacizumab (anti-VEGF) compared to Atezolizumab alone.²²⁷ In a separate study, patients with resistance to anti-PD1 therapy were not a homogenous subgroup but represented three subgroups of patients, 'T cell enriched,' 'Angiogenesis' and 'Cell-cycle' subgroups.²³¹ Among T-cell enriched 'non-responders' to anti-PD1, a recent study has identified clonal expansion of PD1^{high}CD39^{positive} 'terminally-exhausted' CD8 T cells and Tregs.²²⁹ The heterogeneity of patients un-responsive to immunotherapy in HCC highlights how different molecular, proteomic and cellular components distinguish these patients and that strategic combinations must be applied, according to the particular immune escape signature.

Comprehensive immune classification of HCC using a transcriptomics deconvolution approach identified that 30-35% of HCC tumors are characterized by immune signatures of infiltration and inflammation, and response signatures to immunotherapy.^{217,218} The immune class was further divided into three distinct microenvironment states in the form of 'active' (enrichment in interferon signaling, overexpression of genes related to adaptive immunity and favourable prognosis), 'immune-like' (presence of CTNBN1 mutations with interferon signaling and immune activation), and 'immune exhausted' (high TGF β signaling, T cell exhaustion and immunosuppressive components). The inflamed class signature was enriched in patients with

HCC responding to anti PD1/PD-L1 antibodies.²²⁸ The non-inflamed class comprising the 65% remaining HCC is divided into two subclasses: 'intermediate class' consisting of enrichment in TP53 mutations, and deletions in genes related to IFN signaling or antigen presentation, and 'excluded class' associated with *CTNNB1* mutations and immune desertification.

Another study has demonstrated the largely heterogenous nature within poorly infiltrated and 'immune-excluded' tumors in HCC based on molecular features such as CRP production, EpCAM-positivity, and LPS response signatures, highlighting its complexity and the proposition for more adapted treatment strategies for 'immune-excluded' subgroup (Job S et al., to be submitted).

Thesis Objectives

METASTATIC COLORECTAL LIVER METASTASIS

The immune microenvironment within mCRC liver metastasis is a critical determinant of chemotherapy response and patient prognosis. While advances in the field have pointed to the positive impact of T cells and the detrimental impact of certain cell types, such as myeloid cells and Tregs, the role of mast cells remains elusive. Mast cells play important immunoregulatory functions and can orchestrate immune responses to either promote or inhibit tumor growth. However, the activation, recruitment, and interaction of mast cells within the tumor microenvironment of mCRC has not been comprehensively studied, leaving a gap in our understanding of their role.

The primary objective of the first part of the thesis is to comprehensively characterize the immune landscape within resected mCRC liver tumors with the aim to identify immune markers associated with patient prognosis and to identify the pivotal role played by mast cells in this context. This will be achieved with the following approaches:

1. Employing 18-color flow cytometry to evaluate the immune infiltrate as well as mast cell quantity and activation within extra-tumoral, marginal and intra-tumoral regions of resected mCRC liver metastases.
2. Identifying secreted factors that modulate mast cell activation and migration
3. Investigating mast cell interactions with other cell types in the tumor microenvironment using multiplex immunohistochemistry.

PRIMARY HEPATOCELLULAR CARCINOMA

The immune microenvironment in HCC is complex, influenced by both the underlying etiology and the dynamic interplay between immunosuppressive and antitumor immune components. This complexity leads to significant immune microenvironment heterogeneity within HCC, posing challenges in the context of immunotherapy treatment, as only a limited subset of patients responds favorably.

Therefore, there is an essential need to identify specific and distinct immune profiles in HCC through a comprehensive characterization of the tumor immune microenvironment using a multi-Omics approach.

The main objective of the second part of the thesis is to perform a comprehensive assessment of the immune profiles in primary HCC encompassing the following methodologies:

1. Utilizing Flow cytometry to phenotype major immune cell subtypes in extra-tumoral, marginal and intra-tumoral regions of freshly resected liver tumors.
2. Measuring secreted factors that can influence immune cell subtypes and their activation or exhaustion status.
3. Conducting transcriptomics analysis on paired FFPE tissue to explore the associations between HCC immune profiles and critical signaling pathways.

Chapter 1. Activation of liver mast cells potentiates anti-tumor immunity and improves patient prognosis in metastatic colorectal cancer

This chapter is in the manuscript format in preparation for submission to Science Translational Medicine

Activation of liver mast cells potentiates anti-tumor immunity and improves prognosis in metastatic colorectal cancer

Héloïse Halse^{1,2}, Chifaou-Mohamed-Djalim^{2,3}, Delphine Bredel², Severine Mouraud², Guillaume Escriou², Laetitia Bordelet⁴, Aminata Drame², Marine Andrade², Rachel Rignault, Mirjana Weimershaus¹, Marc Rassy¹, Kitsada Kangboonruang¹, Maximiliano Gelli⁵, Michel Ducreux⁵, Peggy Dartigues^{4,6}, Jean-Yves Scoazec^{4,6}, Thiago Trovati Maciel¹, Aurélien Marabelle^{2,3}, Olivier Hermine¹ and Amélie E. Bigorgne^{1,2} *

1 Laboratory of Cellular and Molecular Mechanisms of Haematological Disorders and Therapeutical Implications, Label "Ligue Contre le Cancer", Imagine Institute, Inserm U1163, Université Paris Cité; Paris, France"

2 Institut national de la santé et de la recherche médicale (INSERM) U1015, Laboratoire de Recherche Translationnelle en Immunothérapie (LRTI), Gustave Roussy ; Villejuif, France.

3 Gustave Roussy, Département d'Innovation Thérapeutique et d'Essais Précoces (DITEP), F-94805, Villejuif, France.

4 Experimental and Translational Pathology Platform (PETRA), Gustave Roussy; Villejuif, France

5 Department of Visceral and Digestive Surgery, Gustave Roussy; Villejuif, France

6 Department of Pathology, Gustave Roussy; Villejuif, France

*Corresponding Author

KEYWORDS

Mast cells, liver metastasis, colorectal cancer, CD8⁺T cell, anti-tumor immunity

Abstract

The presence of liver metastasis is strongly associated with poor progression-free survival and overall survival across multiple cancers including colorectal cancer. Immune cells in the liver are known to play a major role in the induction of tolerance in colorectal cancer liver metastasis. Rare innate immune cells such as mast cells, have been observed both at the tumor margin and intra-tumor zones of liver tumors but their role remains controversial. In freshly resected liver metastasis samples from CRC patients, we characterized mast cell phenotype using flow cytometry, quantification of secreted factors, and *in-situ* tissue heterogeneity by multiplex immunohistochemistry. We observed that an elevated mast cell infiltration in CRC liver metastasis is associated with improved patient prognosis, specifically in KRAS wildtype patients. Mast cell expression of activation marker CD203c and histamine secretion, a specific marker of mast cell degranulation, was elevated in tumors with high infiltration of mast cells. Mast cells infiltration was correlated with an elevated ratio between CD8⁺T cells and regulatory T cells. Furthermore, activated mast cells positively correlated with CD8⁺T cell infiltration and activation. *In situ*, mast cell-CD8⁺ cell interactions were increased. In contrast, intra-tumor mast cell activation was inversely correlated with regulatory T cell infiltration and TGFβ2 secretion. *In vitro*, pre-conditioned mast cells from patients with good prognosis increased intracellular expression of IFN-gamma and Granzyme B in lymphocytes. In summary, tumor-infiltrating mast cells may potentiate anti-tumor immunity in CRC liver metastasis through co-stimulation of T cells. Histamine secretion, as a marker of mast cells activation, constitutes a potential biomarker to stratify patients with KRAS wildtype metastatic CRC for complementary treatment approaches.

Introduction

Colorectal cancer (CRC) is the third most diagnosed cancer and the second cause of cancer mortality worldwide.¹ The liver is the most frequent site of metastasis in metastatic colorectal cancer (mCRC) and a major cause of mortality in mCRC patients compared to other metastatic sites such as the lung.¹² The presence of liver metastasis has been strongly associated with poor progression-free survival and overall survival, and is associated to poor responses to immune checkpoint blockade across multiple cancer subtypes, including colorectal cancer.^{41,232–234} Interestingly, patients treated with prior liver metastasis resection respond better to immunotherapy, corroborating the notion that immune tolerance of the liver tumor is the critical variable associated with patient prognosis in microsatellite stable mCRC.⁴³ Thus, surgical liver metastasis resection, along with improved efficacy of systemic therapies have greatly improved clinical outcome for some patients with mCRC in the last two decades.^{235–238} Individual patient responses to treatments and survival following surgical resection remains, however, highly variable.²³⁹ This implies the need for consideration of additional prognostic factors, including a more specific characterization of the tumor immune microenvironment and its role within liver metastatic CRC to define best therapeutic strategies for patients.

The metastatic cascade of colorectal cancer is a complex process and closely tied with a co-evolutionary immune response.¹⁷² Resident as well as recruited immune cells in the liver are known to play major roles in the induction of tolerance in colorectal cancer liver metastasis.^{157,174,240} Nevertheless, the immune system plays a crucial role in the survival of patients with CRC liver metastasis based on the survival benefit of patients with liver tumors harboring elevated T cell density localized at the periphery and within the tumor at the time of surgical resection.^{131,241} However, most patients fail to generate effective intra-tumoral T cell infiltrates in liver metastases when compared to their primary tumors or with other metastatic sites.^{161,233,242} Furthermore, cytotoxic responses of CD8⁺T cells are impaired in CRC liver metastasis.^{243,244} Pre-clinical models have ascribed impaired cytotoxicity of CD8⁺T cells in CRC liver metastasis to the loss of antigen-specific T cells through apoptosis induction, as well as poor co-stimulation, mediated by liver myeloid cells and Tregs.^{173,174} In humans, activated and proliferating intra-tumor Tregs restrain anti-tumor immunity in CRC liver metastasis and high numbers of Tregs

relative to CD8⁺T cells are associated with poor overall survival.^{175,176} Studies by single-cell RNA sequencing in human resected CRC liver metastasis have highlighted the heterogeneity and reprogramming of myeloid cells within the tumor microenvironment in chemotherapy-treated patients with different levels of radiologic response.^{179,180} Other studies have observed a vital role of non-immune cell components of the tumor microenvironment, such as cancer-associated fibroblasts, in metastasis progression and drug resistance in mCRC.¹⁷⁷ In addition to promoting tumor growth, these cells modulate immune function within the tumor microenvironment of CRC.¹⁷⁸

Rarer innate immune cells, such as mast cells, have been observed in both tumor margin and intra-tumor zones of liver tumors in mCRC.^{165,209,210} Mast cells are residential cells in barrier tissue sites such as the liver, intestine, colon, lung and skin. Arising from erythro-myeloid progenitors in the fetal liver and hematopoietic stem cells in the bone marrow, they mature in peripheral tissues under influence of tissue-specific factors.^{114,116} Across organs, mast cells show a conserved expression of high levels of C-kit (CD117) and upregulate FcεRI and Fcγ receptors in response to antigen stimulus. Upon activation through IgE or non-IgE stimuli, mast cells can release pro- or anti-inflammatory pre-formed cytoplasmic granules, as well as undertake *de-novo* synthesis of mediators such as prostaglandins, growth factors, cytokines and chemokines.²⁴⁵ Their immunoregulatory roles are highly dependent on environmental factors and these cells are capable of a broad spectrum of responses, mediated through cell interactions or by their secretory functions.¹⁸⁹

Due to their phenotypic heterogeneity and varying functions across tissues, the impact of mast cells on patient survival has been controversial in many cancer types including CRC liver metastasis, and their specific role remains to be elucidated.¹⁹⁷ In CRC liver metastases, all studies have so far based their analysis on immunohistochemistry staining of CD117 and Tryptase. One study described peritumoral Tryptase⁺ mast cells in liver metastases having a deleterious impact on overall survival.²⁰⁹ Conversely, the presence of peritumoral Tryptase⁺ or CD117⁺ mast cells has been correlated with increased overall survival, and the presence of intra-tumoral CD117⁺ mast cells correlated with increased disease-free survival.^{165,210} Although intra-tumoral mast cells are associated with concomitant increased lymphocyte infiltration in patients, their role on lymphocyte function and patient prognosis remains poorly understood due to their high plasticity within the tumor microenvironment. Due to their poorly

characterized phenotype, quantification of mast cells does not permit a direct association with a particular function. These findings suggest that achieving a more precise characterization of mast cells requires a more comprehensive approach.

In this study, our objective was to characterize mast cell phenotypic and histologic heterogeneity within surgically resected CRC liver metastases using flow cytometry, secreted mediator quantification, and multiplex immunohistochemistry, to better define their potential role as a predictive biomarker of patient prognosis. We identified that mast cell infiltration in liver metastasis is associated with improved patient prognosis in patients with metastatic CRC, and this survival benefit is specific for KRAS wildtype (wt) patients. Intra-tumor mast cells portray an activated phenotype and infiltrate the liver given a gradient toward metastatic CRC tumor cells. Their activation is positively correlated with liver tumor infiltration and activation of CD8⁺T cells, and inversely correlated with Regulatory T cells. Similar correlations between mast-cell and T cell specific genes were observed in a publicly available gene expression dataset of 27 CRC liver metastatic patients treated with chemotherapy, supporting the notion that a mast cell-T cell crosstalk could potentiate anti-tumor immunity in KRAS-wildtype CRC liver metastasis.

Results

Liver metastatic CRC patient cohort

Thirty-two patients with MSS metastatic colorectal cancer were included in the study (17 women and 15 men; median age 60 years). Patient demographics and tumor characteristics are described in Table 1. All patients had Microsatellite Stable CRC. KRAS was mutated in 38% of patients. Most patients (84%) were diagnosed with synchronous metastatic disease and were treated with preoperative systemic chemotherapy prior to complete resection of liver metastases. Half of the patients had a partial response to preoperative chemotherapy according to RECIST 1.1 guidelines. Following surgical resection, Kaplan-Meier analysis demonstrated a median relapse-free survival (RFS) for all patients of 289 days (9.5 months), with many relapses occurring in the liver and/or lung in this cohort.

Tumor infiltration with mast cells is predictive of survival in KRAS wildtype metastatic CRC patients

To characterize the immune cell landscape in CRC liver metastases, 18-color flow cytometry was performed in dissociated paired intra-tumoral, marginal and extra-tumoral tissue for most patients (n=27), and only in intra-tumoral tissue for few patients (n=5). A multiparametric flow cytometry panel was designed to assess the frequency and distribution of mast cells, monocytes/macrophages, dendritic cells, and lymphocytes (including CD8 T, CD4 T, regulatory T, NK and NKT cells), to gain a comprehensive view of the liver immune microenvironment. The gating strategy is described in Supplementary Fig 1A. Compared with paired marginal and extra-tumoral tissue samples, CRC liver metastases were infiltrated with a higher percentage of T cells, including CD4⁺T and Regulatory T cells, increased Monocytes/Macrophages and a decreased infiltration of dendritic cells and NK cells (Supplementary Fig 1B).

The impact of the infiltration of immune cell subpopulations on relapse-free survival (RFS) was analyzed in liver metastases using the optimal cut-off ratio determined by ROC analysis for each immune cell type. Among all immune cells which were analyzed in the tumor, RFS was specifically increased in patients with ‘High intra-tumor infiltration’ of mast cells (CD117^{high}FcεRI⁺) (**Fig 2A**). In contrast, the frequency of intra-tumor lymphocytes (CD8⁺T, CD4⁺T, Tregs and NK, NKT cells) or monocytes/macrophages and dendritic cell subpopulations did not significantly affect RFS (**Fig 2A and Supplementary Fig 2A**), although there was a clear trend for an association between CD8⁺T and CD4⁺T cells infiltration and improved RFS (**Fig 2A**). High intra-tumor mast cell infiltration was specific to the tumor site, and no significant differences in mast cell frequencies in the extra-tumor or margin tissue was observed (Supplementary Fig 2B).

The Kirsten rat sarcoma (KRAS) proto-oncogene is the most frequently mutated gene in CRC and is associated with worse prognosis and resistance to anti-epidermal growth factor receptor (EGFR) inhibitors.^{20,183} Considering this, we compared RFS between KRAS wild type (wt) and KRAS mutated (mut) patients (**Fig 2B, top panel**). As expected, we found a significant difference in RFS between the two subgroups of patients. We first explored whether KRAS mutation impacted immune cell infiltration, including mast cells, lymphocytes, and myeloid cell subsets, and found no statistically significant differences between groups (Supplementary Fig 2C). We then compared the impact of mast cell infiltration and patient RFS according to KRAS mutation (**Fig 2B, bottom panel**). All KRAS mut

patients except one had low intra-tumor infiltration of mast cells. In contrast, in KRAS wt patients, tumor infiltration with mast cells permitted the discrimination between two groups: one group with ‘High intra-tumor infiltration’ of mast cells ($\geq 0.15\%$ infiltration) who had better RFS than the other group with ‘Low intra-tumor infiltration’ of mast cells ($\leq 0.08\%$ infiltration). The prognostic value of elevated tumor infiltration of mast cells was independent of other intra-tumor immune cell subsets, although there was a clear trend for increased CD8⁺T cells and decreased infiltration of regulatory T cells (**Fig 2C**). A known prognostic marker of survival in multiple cancer types including metastatic CRC is the ratio between CD8⁺T cells and regulatory T cells.¹⁷⁵ This ratio was positively correlated with mast cell infiltration in tumors (**Fig 2D**), and suggests an improved immune response correlated with mast cell infiltration.

Mast cell tumor infiltration was increased in KRAS wt patients treated with preoperative systemic chemotherapy, (**Fig 2E, left panel**) but was independent of the type of treatment received including Oxaliplatin or anti-EGFR (**Fig 2E, right panel**). Though it is a known marker of increased tumor aggressiveness and spread, we did not find significant differences in liver lesion number or size in our cohort dependent on mast cell infiltration (**Fig 2F**). Nevertheless, elevated mast cells were inversely correlated with progressive disease/stable disease to treatment, indicating a potential anti-tumor role of these cells in KRAS wildtype metastatic CRC (**Fig 2G**). To document the hepatic function of our cohort of metastatic CRC patients, we collected blood levels of liver transaminases (ALT, AST, and GGT) and a biomarker of tumor burden and metabolism (LDH). LDH might also be elevated in liver cytolysis and is considered as a biomarker of poor prognosis in patients with liver metastasis across multiple cancer subtypes.²⁴⁶ The infiltration of metastatic CRC with mast cells was not correlated to elevated levels of liver enzymes ALT, AST or GGT, but was inversely correlated with systemic levels of LDH (**Fig 2H**).

Quantification and localization of intra-tumor mast cells in CRC liver metastases

We performed *in situ* quantification of mast cells in paired FFPE resected liver tumor sections in patients with high mast cell infiltration (‘good prognosis’) and low mast cell infiltration (‘poor

prognosis'). Several publications have shown that mast cells can have a direct cytotoxic activity against tumor cells through antibody-dependent degranulation synapses that triggers the cells to release anti-tumor mediators.^{247,248} We therefore wanted to measure the migration of mast cells towards the tumor cells, and whether there were direct mast cells and tumor cell interactions *in situ* in patients with good versus poor prognosis (**Fig 3A**).

Within the tumor stroma of patients with poor prognosis, mast cells were few and dispersed within the stromal infiltrate (**Fig 3A, left panel**). Conversely, mast cells were preferentially localized with a dense stromal infiltrate in proximity of Cytokeratin (CK)-positive cancer cells in patients with good prognosis (**Fig 3A, right panel**). We then quantified mast cell density in distance intervals starting at 200 μ m from CK⁺ tumor cells and measured increased mast cells in proximity of CK⁺ tumor cells in patients with good prognosis (**Fig 3B**). We did not observe KI67⁺ mast cells, indicating that the increased number of mast cells was not associated with an increased local proliferation, but rather an active recruitment of the mastocytes or their precursors within the tumor space. In favor of this hypothesis, the quantification of mast cells in the margin and within the tumor was significantly increased from extra-tumor tissue in patients with good prognosis (**Fig 3C**). However, we rarely observed direct mast cell contact with CK⁺ tumor cells and hypothesized that mast cells would more likely be associated with regulating the immune response within the tumor microenvironment than directly regulating the tumor cells proliferation and/or survival.

We compared mast cell infiltration and spatial distribution with that of cells with known anti-tumor cytotoxicity (CD8⁺ T cells) versus immunosuppressive cell subtype (FOXP3⁺ Tregs). Several studies have investigated the interactions between mast cells and CD8⁺ T cells to demonstrate the positive role of mast cells in orchestrating immunity against pathogens, viruses and tumors.^{249–251} In contrast, Tregs are known to have a direct inhibitory role on Mast cells through OX40-OX40L interaction.²⁵² However, as mast cells are highly sensitive to different inflammatory signals, they can also inhibit the suppressive function of Tregs.^{202,204} Quantification of CD8⁺T cell infiltration and FOXP3⁺ Tregs infiltration in patients with good versus poor prognosis revealed that the infiltration of FOXP3⁺ Tregs was the predominant cell type inversely correlated with mast cell infiltration (**Fig 3D**). Though there were no significant differences between CD8⁺ T cell numbers (Supplementary Fig 3A), the ratio of CD8⁺ T cells

to FOXP3⁺ Tregs was significantly increased in patients with good prognosis, and strongly correlated with mast cell infiltration in tumors (**Fig 3E**).

We quantified the number of CD117⁺ mast cell - FOXP3⁺ Treg cell interactions in the tumor tissue sections to determine whether a direct inhibitory effect of tumor infiltrating Tregs was responsible for the inverse phenotype we observed (Supplementary Fig 3B). We counted very few interactions between these two cell subtypes (<1 interaction per mm²) relative to their respective densities (range 20-100 cells/mm²) across patient subgroups. Thus, the inverse relationship between mast cells and Tregs infiltrating CRC liver metastasis is independent of a direct cell crosstalk and is more likely dependent on secreted factors within the tumor microenvironment.

Based on reports of the positive role of mast cells in orchestrating immunity against tumors and a colocation between mast cells and T cells,²⁵³ we quantified the number of CD117⁺ mast cell – CD8⁺T cell interactions in the tumor tissue. Indeed, we observed increased cell-cell interactions between CD117⁺ mast cells and CD8⁺ T cells in patients with good prognosis (**Fig 3F**). Conversely, patients with poor prognoses displayed increased FOXP3-CD8 T cell interactions indicating a direct immunosuppressive role of Tregs on CD8⁺ T cells in the absence of mast cell infiltration. These results suggest a positive association between tumor infiltrating mast cells and CD8⁺ T cells within mCRC liver metastasis of patients with good prognosis.

TGFβ2 secretion negatively impacts tumor infiltrating mast cell expression of activating marker CD203c

To identify which factor may mediate mast cell infiltration and their immunomodulatory function within CRC liver metastasis, we analyzed by electrochemiluminescence the production of different cytokines and growth factors involved in mast cell differentiation and activation. Among all analytes quantified only the secretion of TGF-beta 2 (TGFβ2) and TNF were significantly increased in the tumor stroma of patients with low infiltration of mast cells and poor prognosis (**Fig 4A**). Since TGFβ is known to inhibit mast cell maturation and activation,²⁵⁴ we investigated the correlation with mast cell expression of CD203c and FcεRI. CD203c is an activation-linked surface antigen on mast cells upregulated in response to IgE receptor (FcεRI) cross-linking.¹⁹⁵ We assessed the expression of these

markers by taking their relative fluorescence intensity (RFI) on intra-tumor mast cells compared to extra-tumor mast cells. We found that TGFβ2 was inversely correlated with CD203c RFI on mast cells, but not with FcεRI (**Fig 4B**). We also observed an inverse correlation between TNF and CD203c expression on mast cells, however, this did not reach significance (Supplementary Fig 4A).

No studies exist on the effects of TGFβ2 *in vitro* on the expression of costimulatory and coinhibitory molecules on mast cells. We therefore tested the impact of recombinant human TGFβ2 on peripheral-blood derived mast cells for 5 days and measured by flow cytometry the modulation of expression. We observed that 5 days of co-culture of human PB-derived mast cells with 100ng/mL of TGFβ2 induced moderate downregulation of CD203c (**Fig 4C**). Furthermore, MHC Class I expression along with CD80/86 expression was moderately decreased (**Fig 4D**). The modulation of CD80/86 might indicate poorer co-stimulation by mast cells of CD8 T cells through antigen presentation.

We assessed whether TGFβ2 was produced by tumor cells by measuring the same analytes from 4 patient-derived CRC liver metastasis organoids with known KRASwt and KRASmut status (Supplementary Fig 4B). The levels of TGFβ2 were significantly decreased in ex vivo generated organoids compared to tissue storage solution from resected tumors. Furthermore, the organoids were generated from patient tumor biopsies with end-stage disease (poor prognosis). Thus, TGFβ2 may more likely be secreted by other cell types within the tumor microenvironment and does not originate from the tumor cells. In the liver, hepatic stellate cells are recruited and activated through various modulators secreted by malignant cells to become a source of CAFs and are an important source of TGFβ in liver pathologies.^{255,256} We stained for CAFs in paired FFPE tissue sections using Fibroblast Activation Protein (FAP) antibody and quantified the percentage of FAP⁺ fibroblasts within the tumor stroma (Supplementary Fig 4C & 4D). Though there was a tendency for increased FAP⁺ tissue in patients with poor prognosis, the difference was not statistically significant.

CD203c expression on Mast cells positively correlates with CD8⁺T cell activation and T effector phenotype

We evaluated the relationship between mast cell CD203c expression and CD8⁺ T cells and Tregs. Notably, there was a strong correlation between CD203c expression on mast cells and CD8⁺ T cell infiltration (**Fig 5A**). In contrast, the correlation displayed an opposite pattern between CD203c

expression on mast cells and Tregs. We assessed the activation as well as memory phenotype of CD8⁺ T cells infiltrating the liver (**Fig 5B and Supplementary Fig 5A & 5B**). CD8⁺ T cells displayed elevated CD69 activation marker expression (**Fig 5B**, top panel). Concerning the memory phenotype, patients with good prognoses demonstrated an increased frequency of “T effector memory RA” (TEMRA) cells (**Fig 5B**, bottom panel). These cells were also positively correlated with CD203c expression on mast cells (Supplementary Fig 5C). T effector memory RA cells are antigen-experienced cells, and exhibit potent cytotoxic capabilities through granzyme and perforin production.^{257–259} Prior in vitro studies have identified that mast cells can promote effector T cell recruitment via secreted factors, and T cell activation through MHC-I dependent antigen cross-presentation^{249,250}. We therefore aimed to evaluate the costimulatory potential of pre-conditioned mast cells derived from peripheral blood, treated with tissue storage solution from patients with good versus poor prognosis, on autologous pre-activated lymphocytes (**Fig 5C**). Notably, autologous lymphocytes co-cultured with conditioned mast cells from patients with good prognosis had elevated intracellular expression of granzyme b and IFN-gamma (**Fig 5D**). This finding supports the notion that mast cells within the tumor microenvironment of CRC liver metastatic patients with good prognoses likely fulfill a costimulatory role, either through a secretory or cell-mediated contact mechanism to potentiate immune responses.

Mast cell FcεRI^{high}CD203c^{high} phenotype and production of Histamine is correlated with patient prognosis

Our initial assessment of elevated Mast cell infiltration in KRAS wt patients with good prognosis was correlated with an elevated CD8⁺T:Treg ratio (**Fig 2D**). Next, we observed that mast cell expression of CD203c was correlated with CD8⁺ T cell infiltration and effector phenotype. This suggests that a modulation in the phenotype of mast cells along with their enhanced infiltration may play an important role in the regulation of anti-tumor immune responses.

We evaluated the membrane expression of the IgE receptor ‘FcεRI’ and Ecto-nucleotide pyrophosphatase/phosphodiesterase ‘CD203c’ on the surface of mast cells (**Fig 6A, left panel**). For comparative purposes, we calculated the relative fluorescence intensity (RFI) for each marker between intra-tumor mast cells and paired extra-tumor mast cells for each patient. Interestingly, mast cells infiltrating tumors with good prognosis had higher RFI of CD203c and FcεRI, suggesting an alteration

in the behavior or traits of these cells in patients with good versus poor prognosis (**Fig 6A, right panel**). Importantly, this phenotype was found to be independent of KRAS mutation status, affirming its dependence on the microenvironment rather than tumor biology (Supplementary Fig 6A).

Both higher RFI of FcεRI and CD203c on mast cells were correlated with improved relapse-free survival through Kaplan Meier Analysis (**Fig 6B**). Moreover, when subjected to ROC curve analysis, the Intra-tumor/Extra-tumor CD203c expression on mast cells emerged as a more powerful predictor of RFS in patients compared to FcεRI expression alone (**Fig 6B, right panel**).

To evaluate whether FcεRI and CD203c expression on mast cells correlated with functional difference in their degranulation, we quantified histamine secretion levels in extra-tumor, margin, and intra-tumor tissue storage solution. Strikingly, patients with high FcεRI and CD203c expression on mast cells had significantly elevated histamine levels within the tumor, compared to patients with poor prognosis (**Fig 6C**). In contrast, no discernible differences in Histamine levels were observed between patients in the margin or extra tumor tissue storage solutions. Histamine secretion in tissue is a specific marker of mast cells, although it can also be released by basophils under chronic inflammatory conditions such as during chronic allergic responses. We therefore checked in our cohort whether there was a significant difference between basophil frequency in liver tumors using CD203c⁺FcεRI⁺CD117⁻ phenotype (Supplementary Fig 6B). We did not observe a significant difference in basophils in the groups of patients. Furthermore, the occurrence of allergic reactions to medications in the time preceding the operation was rare and not specific to the group of patients with high intra-tumor mast cell infiltration in our cohort (Supplementary Fig 6C). We measured the impact of elevated histamine on survival in our patient cohort. Using the optimal cut off ratio determined by ROC analysis we found a positive trend between elevated histamine secretion and improved RFS (**Fig 6D**). Therefore, though Histamine is correlated with mast cells FcεRI^{high}CD203c^{high} phenotype, it may not be the only secreted factor associated with improved RFS.

Histamine is a biogenic amine that has pleiotropic effects on the immune system.²⁶⁰ Unsupervised clustering of histamine secretion with major lymphocyte subsets showed clustering of a subgroup of patients with both high intra-tumoral histamine and high CD8 T cells infiltration in our cohort (**Fig 6E**).

We performed a Pearson correlation matrix analysis of cell-type-specific genes using TPM values in a separate public dataset of bulk RNA sequencing of surgically resected liver metastasis (GSE207194) (Fig 6F). Unsupervised clustering revealed a main cluster with T cell (*CD3D*, *CD8A*, *GZMA*) and mast cell associated genes, including Histamine (*HDC*, *TPSAB1*, *MS4A2*, *CPA3*), forming the predominant cell types. Due to the association between intra-tumor histamine levels, elevated CD203c expression on mast cells, and their clear association with prognosis, we propose that mast cells may be a key modulator of immune responses in KRAS wildtype CRC liver metastasis.

Discussion

In this study we comprehensively characterized the immune microenvironment of surgically resected CRC liver metastases. We demonstrate in a prospective cohort of mCRC patients that tumor-infiltrating mast cells were associated with improved relapse-free survival after surgical resection of liver metastasis. These findings align with earlier retrospective studies on CRC liver metastatic patients treated with preoperative chemotherapy.^{165,210}

For the first time, we identify that this protective role of mast cells is specific to patients with KRAS wildtype tumors. In these patients, elevated tumor infiltrating mast cells correlate with improved radiologic response before resection, indicating a potential anti-tumor role of these cells. Despite no observed difference in mast cell infiltration based on the type of pre-operative treatment received in KRAS wildtype patients, both Fluorouracil and Oxaliplatin chemotherapies induce immunogenic cell death, linked to T cell infiltration, clonal expansion, and improved anti tumor immunity.^{167,168,170,171} Moreover, the anti-EGFR agent Cetuximab enhances T cell infiltration and antibody-dependent cell-mediated cytotoxicity.¹⁶⁹ Therefore, it is possible that in responding tumors to treatment the infiltration of mast cells may be closely tied with enhanced T cell infiltration and function. Transient conditions such as these could be exploited by combining these agents with immunotherapy in a timely manner to sustain long-term anti-tumor immunity. Recent results from the CAVE-I and CAVE-II clinical trials testing Cetuximab in combination with anti-PDL1 have shown survival benefits in KRAS wt patients undergoing rechallenge therapy.²⁶¹ Considering the role of mast cells in predicting prolonged relapse-

free survival in KRAS wt patients, it will be of interest to determine what drives mast cell infiltration in tumors of patients with improved prognosis, and to assess whether the presence of tumor-infiltrating mast cells in future clinical trials testing chemo-immunotherapy combinations are associated with improved response rates and survival in these patients.

Tumor infiltration in KRAS wildtype metastatic CRC was inversely correlated with systemic levels of LDH. LDH is a known biomarker of poor prognosis in patients with liver metastasis across multiple cancer subtypes.²⁴⁶ In addition, recent evidence suggests that elevated levels of LDH might be independent of tumor burden and can reflect impaired anti-tumor immunity due to the direct immunosuppressive effects of LDH on tumor-infiltrating immune cells.²⁶² Furthermore, the metabolic by-product of LDH, lactate, has been shown to inhibit mast cell function in different models *in vitro* and *in vivo*.²⁶³⁻²⁶⁵

Spatial analysis of tumor infiltrating mast cells in paired FFPE tissue from patients with improved relapse-free survival revealed mast cells migrating toward CK⁺ tumor cells. Additionally, positive mast cell infiltration is inversely correlated with FOXP3⁺ Treg cell infiltration. In the pre-clinical setting, Tregs negatively regulate local and systemic immune response through trogocytosis of costimulatory molecules on antigen-presenting cells in liver metastasis.²⁴⁰ Tregs have also been found to directly inhibit mast cell degranulation through OX40-OX40L interaction.²⁵² However, multiplex staining of CD117, CD8, and FOXP3 in paired FFPE tissue revealed negligible mast cell-Treg interactions, with no disparity between patients with good or poor prognosis. Thus, the inverse correlation between Tregs and mast cells may more likely involve secreted factors affecting their respective infiltration in the tumor microenvironment.

We noted a strong correlation between CD203c expression on mast cells and CD8⁺T cell infiltration. Through multiplex immunohistochemistry, we found patients with improved prognosis had more CD117 - CD8⁺T cell interactions, suggesting a potential costimulatory role of mast cells. Lymphocytes co cultured with autologous conditioned mast cells exposed to tumor tissue solution from patients with good prognosis exhibited elevated intracellular expression of granzyme b as well as IFN-gamma, supporting this notion. Previous studies have demonstrated the capacity of mast cells to promote effector T cell activation through MHC-I dependent antigen cross-presentation,²⁵⁰ and proliferation

through OX40L-OX40 interaction.²⁶⁶ Mast cells can also be induced to secrete histamine upon cell contact with activated T cells,²⁶⁷ and activated CD8 T cells can upregulate the expression of MHC-I and 41BB on mast cells.²⁵⁰ Therefore, the modulation of both mast cells and T cells can be bidirectional, and the mechanism implicated in this crosstalk within the liver needs further investigation. The role of mast cells is multifaceted, and the small number of interactions does not rule out other costimulatory roles of mast cells mediated through secretion of additional costimulatory molecules.

The TGF β signaling pathway is an important driver of metastasis, immune evasion, and chemotherapy/targeted therapy resistance in various cancers, including colorectal cancer liver metastasis.¹⁷⁸ In mice with established liver metastasis, TGF β blockade increased tumor susceptibility and improved anti-PD-L1 response.¹⁷⁸ We discovered TGF β 2 as a potential mediator of mast cell inhibition in patients with poor prognosis. TGF β 2, alongside TGF β 1 and TGF β 3, potently inhibit mast cell maturation and effector functions in the presence of activating factors IL3 and SCF.²⁵⁴ No difference existed in IL3 and SCF secretion in our cohort, therefore elevated TGF β 2 likely represses IL3 and SCF's activating potential in patients with low mast cell infiltration and poor prognosis. In vitro, TGF β 2 negatively impacted CD203c expression in blood-derived mast cells. The expression of CD80/86 and MHC class I was also negatively impacted, demonstrating a potential negative effect of TGF β on mast cell phenotype and function. In liver tumors, CAFs are recruited and activated by tumor cells and are a major source of TGF β .^{255,256} TGF β directly induces hepatic fibrosis through JAK/STAT3 and SMAD pathways in coordination.²⁶⁸ The JAK2 inhibitor Pacritinib shows promise in liver fibrosis treatment by its inhibition of TGF β .²⁶⁹ Pacritinib could therefore benefit liver metastatic patients with heightened TGF β signaling. However, the assessment of Pacritinib on rescuing mast cell infiltration and function in patient liver tumors remains to be elucidated.

There have been recent reports on the heterogeneity of mast cells in tumors that display opposing roles in tumor progression.²⁵³ We confirmed a positive association between mast cell infiltration and elevated Fc ϵ RI and CD203c expression, both activation-associated markers in mast cells. CD203c (ENPP3) belongs to the family of ecto-nucleotide pyrophosphatase/phosphodiesterase.²⁷⁰ It cleaves phosphodiester and phosphosulfate bonds of molecules, including deoxynucleotides, NAD, and nucleotide sugars.²⁷¹ It is an activation-linked surface antigen on Mast cells upregulated in response to

IgE receptor cross-linking.¹⁹⁵ CD203c regulates ATP-dependent activation of mast cells and prevents chronic allergic responses.²⁷² It is a more stable marker of activation on mast cells compared to other degranulation associated markers such as CD63.^{196,273} Histamine levels were higher in tumors with mast cells expressing high levels of CD203c and FcεRI. In a separate public dataset of surgically resected CRC liver metastasis, Histamine Decarboxylase (*HDC*) gene expression was strongly correlated with mast cell-associated genes (*TPSAB1*, *MS4A2*, *CPA3*) as well as T cell-associated genes (*CD3D*, *CD8A*, *GZMA*).

Histamine is a biogenic amine that has pleiotropic effects on the immune system.²⁶⁰ Its effects are mediated through four different receptors, H1-H4, which are expressed on a variety of innate and adaptive immune cell subtypes. The expression profiles of these receptors vary between cell subtypes, and as a result the effects of Histamine on T cell cytokine secretion are diverse.²⁷⁴ For example, histamine signaling through H1R can enhance IFN-gamma secretion, and signaling through H1R on Tregs can also suppress their function.²⁰² In models of skin inflammation, histamine acts through H1R on dendritic cells and promotes the priming of effector IFNγ⁺CD8⁺ T cells.²⁷⁵ Another important effect of Histamine is protection of effector T cells against myeloid cell-derived reactive oxygen species, which can restore their function and activation within the tumor microenvironment.^{276,277} In patients with Acute Myeloid Leukemia, Histamine & low-dose IL2 subcutaneous immunotherapy also demonstrated positive effects on increasing the frequencies of T effector memory RA (TemRA) CD8⁺T cells associated with significant survival benefit.²⁷⁸

Histamine's overall impact on the immune response varies based on receptor profiles on different immune cell subtypes in tumor tissue, making its immunomodulatory effects context-dependent. Importantly, chronic allergic response-related Histamine negatively affects antitumor immunity and immunotherapy in mouse models of breast cancer and melanoma.²⁷⁹ However, studies are controversial with regards to epidemiological findings.²⁸⁰ In addition, Li et al.'s study showed cancer cells mainly produced Histamine to recruit H1R-expressing myeloid cells. Furthermore, elevated histamine levels were detected systemically in non-responding patients to immunotherapy. In our cohort, histamine secretion was tumor zone-specific, and absent in extra-tumor liver tissue in patients with high intra-tumor mast cells. This suggests that there was no systemic elevation of histamine, and that the activation

of mast cells was tumor-specific. There was no association between allergic response to medications and the presence of mast cells in liver tumors of these patients, and none of the patients had pre-existing chronic allergies.

Limiting factors of this study include the small cohort size due to few tissue samples available for obtaining enough mast cells to characterize *ex vivo*. In addition, the immune phenotyping of immune cells was performed in one resected lesion, and most patients had at least two resected lesions. Due to the heterogeneous nature of the disease, mast cell infiltration in one lesion may not represent its infiltration into other lesions from the same patient and so caution should be taken in the interpretation of these results. The mechanism of activated mast cells on T cell stimulation and antitumor immunity will need to be further investigated and validated in larger cohorts. Furthermore, the higher frequency of mast cells associated with improved RFS was specific to patients with KRAS wt status, emphasizing the necessity to study the role of mast cells specifically in patients with KRAS wt status undergoing similar pre-operative treatments.

In conclusion, analyzing the phenotype of mast cells and their association with tumor infiltrating lymphocytes *in situ* shed light on a rare cell subset with important implications in the development of anti-tumor immunity in liver metastasis. Despite improved survival of patients thanks to surgical resection, identifying relapse-prone patients who may require combination treatment approaches is crucial. The expression of CD203c on mast cells and histamine secretion could potentially be used to stratify patients for complementary treatment approaches, including TGF β blockade or immunotherapy treatment, and further reduce relapse risk.

Materials and Methods

Study Design

Resected intra-tumor, margin and extra-tumor liver tissue were prospectively collected from patients treated with surgical resection of colorectal cancer liver metastasis in the pathology department at Gustave Roussy Hospital from June 2019 to September 2022. (**Fig 1**). The resected tissue was initially stored in a tissue storage solution overnight at 4°C. This solution was harvested for downstream analysis

of secreted protein by the respective tissue. The resected tissue was then processed by mechanical and enzymatic dissociation for downstream flow cytometry analysis. For some patients, paired formalin-fixed paraffin embedded tissue of surgically resected liver tissue was also collected for multiplex immunohistochemistry staining.

Patient samples

Patient information and sample collection was authorized by the Ministry of Higher Education and Research (DC-2021-4572), and in respect of the reference methodology MR-004 of the French data protection authority (CNIL). Inclusion criteria included patients undergoing complete liver metastasis resection from colorectal cancer for curative intent, along with availability of clinical, biological and follow-up data post surgical resection. The median follow-up was 8 months (range 1 – 32 months). Previous data obtained on RFS were confirmed by the measure of radiologic response of target lesions to pre-operative treatment, according to RECIST 1.1 guidelines.²⁸¹ Relapse-free survival was defined as the interval from the date of surgical resection to the date of relapse of metastasis to the liver or within extrahepatic sites including lung, peritoneum, or lymph nodes. Patients presenting with other co-occurring cancers or suffering an unknown cause of death post-surgery were excluded from the study.

Peripheral Blood Samples

Results from peripheral blood tests performed preoperatively were obtained to record liver enzymes Alkaline Phosphatase (AP), Alanine Transaminase (ALT), Aspartate Aminotransferase (AST), and gamma-glutamyl transferase (GGT). Lactate Dehydrogenase (LDH) levels were also recorded.

Preparation of intra-tumor, margin, and extra-tumor liver tissue storage solution for secreted soluble factor measurement

Resected intra-tumor, margin and extra-tumor liver tissue storage solution was prepared by storing immediately each respective tissue in 3-5 milliliters of Tissue Storage Solution (Miltenyi Biotec, DE) at 4°C. Following 18-hour to 48-hour storage, the supernatant was harvested by centrifugation at 1800RPM for 10 minutes and stored in aliquots at -80°C.

Tumor dissociation and flow cytometry staining

Fresh samples of resected intra-tumor and when possible, at the margin and extra-tumor liver tissue were collected for tissue dissociation and flow cytometry staining. Intra-tumor, Margin and Extra-tumor

liver tissue were weighed and cut into small fragments of 1-2mm in diameter using a sterile scalpel blade and petri dish. Tissue fragments were transferred to a C-tube (Miltenyi Biotec, DE) and 5-10mL of enzyme digestion mixture consisting of RPMI 1640 medium (Gibco, MT), 50 U/mL Collagenase IV, 30 U/mL DNase I and 280 U/mL Hyaluronidase (Merck, DE) was added. The tubes were placed on to the GentleMACS dissociator (Miltenyi Biotec, DE) and subjected to mechanical and enzymatic dissociation using the program TDK_1 (incubation for 1 hour at 37°C). Following this, the dissociated tissue mixture was filtered using 70um sterile filter and the cell suspension was washed 1x in 50mL of sterile Phosphate-buffered saline (PBS) followed by a second wash in cold sterile PBS with 2% Bovine Serum Albumin and 2mM EDTA. CD45⁺ cells were counted after staining a 50µl aliquot of the cell suspension with anti-CD45 FITC (BD Biosciences, NJ) and 50µl of Precision Count Beads (BioLegend, CA).

Mast cell and Myeloid cell panel (MMC). Following the counting step, a minimum of 100,000 CD45⁺ cells were stained using flow cytometry antibodies (BD Biosciences, NJ) and Zombie Aqua Fixable Viability Dye (BioLegend, CA) listed in Annex Table 1 at the dilutions indicated in final volume of 100µl of buffer (PBS with 2% Bovine Serum Albumin and 2mM EDTA) at 4°C for 30 minutes. After staining, the cells were washed twice in buffer before acquisition.

T cell polarization and activation panel. When possible, a further 50,000-100,000 CD45⁺ cells were stained using flow cytometry antibodies and Zombie Aqua Fixable Viability Dye listed in Annex Table 2 at the dilutions indicated and in a final volume of 100µl of buffer (PBS with 2% Bovine Serum Albumin and 2mM EDTA) at 4°C for 30 minutes. After staining, the cells were washed twice in buffer before acquisition.

All events were acquired on the BD FORTESSA X-20 cytometer equipped with BD FACSDiva software (BD Biosciences, NJ), and data were analyzed using FlowJo software (Tree Star, OR).

Secreted soluble factor and secreted Histamine measurement

Soluble factors secreted by Intra-tumor, Margin and Extra-tumor liver tissue were measured in tissue storage solution using Mesoscale Discovery biomarker electrochemiluminescence detection assay kits according to the manufacturer's instructions (MSD, MA).

Secreted Histamine was measured in Intra-tumor, Margin and Extra-tumor liver tissue storage solution using the Histamine HTRF (Homogeneous Time Resolved Fluorescence) Dynamic kit according to the manufacturer's protocol (CisBio, FR).

Multiplex Immunohistochemistry staining and image analysis

Formalin-fixed and paraffin-embedded (FFPE) tissue from resected colorectal cancer liver metastasis and adjacent non-tumor liver were used for histological assessment of CD117⁺ Mast cell localization within the tumor microenvironment, their distance to proliferating and non-proliferating tumor cells stained with KI67 and Cytokeratin, respectively, and their association with tumor infiltrating immune cells including CD8⁺ T cells, and FOXP3⁺ Tregs. A separate stain for Cancer Associated Fibroblasts using FAP⁺ was also performed. Serial sections of 4µm thickness were used for multiplex chromogenic staining using the automated DISCOVERY ULTRA system (Roche, CH). An initial Antigen retrieval step was performed with CC1 buffer for 64 minutes at 95°C. Peroxidase Blocking was performed after the primary antibody incubation using Discovery Inhibitor (Roche, CH). Denaturation/Stripping was performed with CC2 buffer at 100°C. Primary and secondary antibodies used, denaturation/stripping buffers, antigen retrieval buffers and counterstains are detailed in Annex Table 4. Hematoxylin Eosin and Saffron stain (HES) was performed on the first serial section. The images were scanned using the Olympus VS120 microscope (Olympus, JP) at 40X magnification resolution and analyzed using QuPath (v.4.02).

Analysis of CD117⁺ Mast cells and their localization within the tumor stroma. Images were loaded into QuPath and Pixel Classifier was trained using RTrees Classification at High Resolution on two regions of interest: (CK⁺ tumor, CK⁻ stroma). The tumor area was traced manually, and the Pixel Classifier applied to generate tumor and stroma annotations. Within the stroma annotation cell detection was performed using Hematoxylin Optical Density at 0.05 threshold and cell expansion of 2µm. An Object Classifier was trained using RTrees Classification on training points identifying CD117⁺ Mast cells and applied to the cells detected within the stroma region. The annotated CD117⁺ Mast cells were quantified between 0-50µm to the tumor annotation at 25µm intervals and between 50µm-200µm at 50µm intervals as demonstrated in Figure 3C.

Quantification of CD117⁺ Mast cells, CD8⁺ T cell and FOXP3⁺ Treg infiltrate and their interactions in intra-tumor, margin, and extra-tumor liver tissue zones.

Cell detection was performed using Hematoxylin Optical Density at 0.05 threshold and cell expansion of 2 μ m in Intra-tumor, margin and extra-tumor tissue annotations. An Object Classifier was trained using RTrees Classification on training points identifying CD117⁺ Mast cells, FOXP3⁺ Tregs and CD8⁺ T cells and applied to the cells detected within each annotation. Quantification was measured as the average number of cells per mm² from 3 annotations per zone, and within areas of highest infiltration. Interactions between Mast cells and CD8⁺ T cell and FOXP3⁺ Tregs was performed manually for the same annotations as above and the average number of interactions per mm² recorded.

Quantification of FAP⁺ Cancer Associated Fibroblasts in the tumor stroma. Images were loaded into QuPath and the Pixel Classifier was trained on FAP-DAB stain using RTrees Classification at High Resolution and Gaussian/Structure Tensor coherence as selected features. The pixel classifier was applied to 3 annotations of tumor stroma representative of the FAP⁺ staining within the tumor tissue per patient. FAP⁺ was then quantified as the area of FAP⁺ classification in mm² divided by the total area of each annotation in mm².

Isolation of PBMC and CD34⁺ progenitors from peripheral cytopheresis blood samples

Peripheral Cytopheresis blood sample was collected from a healthy donor. The cytopheresis blood sample was diluted 2X in Phosphate buffered saline. Density gradient separation was performed using FICOLL (Merck, DE) at 2000RPM, 30mins, room temperature, acceleration 1; deceleration 0. The mononuclear layer was collected, washed with PBS, and washed a second time with cold PBS, 2% FCS and 1mM EDTA before proceeding with isolation of CD34 progenitors using anti-CD34 magnetic beads according to the manufacturers' protocol (Miltenyi Biotec, DE). The remaining PBMCs were frozen in DMSO 10% FCS 90% for 4 weeks before thawing 96 hours prior to the coculture experiment.

In vitro differentiation of Mast cells from CD34⁺ progenitor cells

Immediately after magnetic isolation of CD34 progenitor cells, the cells were counted and plated at 500,000 cells per mL in Mast cell culture medium in a 6 well plate at 37°C, 5% CO₂. Mast cell culture medium was made up with the following constituents: IMDM (Gibco), 15% BIT (Gibco), 1%

Penicillin/Streptomycin, 1% Glutamine, 1% Sodium Pyruvate, 1% Vitamins, 1% Insulin-Transferrin-Selenium, 2% Non-Essential Amino Acids. To the medium 100ng/mL recombinant human SCF, 50ng/mL recombinant human IL-6 and 1ng/mL recombinant human IL-3 (Miltenyi Biotec) were added. Following the first week of differentiation, IL-3 was no longer added to the culture medium. During the first week of differentiation cells were counted every 2-3 days and maintained at 500,000 cells per mL concentration to promote cell expansion. Medium was replaced entirely after 1.5 weeks of culture and replaced once weekly. Cells were spun gently at 1200 RPM for 5 minutes each time that medium was replaced. After 4 weeks of culture mast cell purity was measured with anti-CD117 and anti-FcεRI and viability dye Sytox Blue (Thermofisher Scientific, MA). After three weeks the mast cells were maintained at 800,000 cells/mL. Once mast cell purity had reached 90% at 4.5 weeks the cells were prepared for chemotaxis and coculture experiments.

Phenotyping of mast cells exposed to recombinant TGFβ2

Differentiated Mast cells were counted and plated at 100,000 cells per well in triplicate in a 96-well plate with 200μl of Mast cell medium or with medium consisting of 100ng/mL of recombinant human TGFβ2. The cells were left for 5 days at 37°C, following which the cells were stained for cell surface expression of activation marker CD203-BV421 (NP4D6), MHC-Class I-APCCy7 (W6/32), MHC-Class II-PECy7 (G46-6), costimulatory ligands CD80/86-BB515 (L307.4/2331 FUN1), 41BB-L-BUV395 (C65-485), ICOSL-BB700 (2D3/B7-H2), OX40L-BV711 (IK-1), and co-inhibitory ligand PDL1-PECF594 (2AE-2E3). Cells were stained for viability using the Zombie Aqua Fixable Viability dye (BioLegend, CA) at a 1:1000 final dilution. Cells were stained for 30 minutes at 4°C in the dark and washed twice with FACS buffer (1XPBS + 2%FCS) before acquisition on the Fortessa x-20 (BD Biosciences, NJ).

Mast cell and autologous peripheral blood lymphocyte coculture

Autologous PBMCs were thawed 96 hours before the co-culture experiment. After thawing, the cells were plated in RPMI 1640 medium, 10% Fetal Bovine Serum, 1% Penicillin/Streptomycin, 1% Glutamate and 30μM β-mercaptoethanol at 1 million cells per mL and left overnight at 37°C, 5%CO₂ in 6-well plates. 24 hours later, the lymphocytes in suspension were counted wash and plated at 500,000

cells per mL into a 48-well plate. The cells were stimulated with OKT3 (1ug/mL) and CD28.2 (1ug/mL) (eBioscience, CA) with recombinant human IL2 10 IU/mL and left for 72 hours at 37°C, 5%CO₂.

At the 72-hour timepoint, differentiated Mast cells were counted and plated at 200,000 cells per well in a 96-well plate with 200µl of patient intra-tumor and extra-tumor tissue 'supernatant' at a concentration of 1mg/mL of total protein, and left overnight (18 hours) at 37°C, 5% CO₂.

At the 90-hour timepoint, the pre-activated autologous lymphocytes were counted and plated in duplicate at 50,000 cells per well per condition in a 96-well plate. The pre-conditioned Mast cells were added at a 1:1 ratio to each well of lymphocytes and left overnight (18 hours) at 37°C, 5% CO₂.

After 18 hours, one well per condition was stained with membrane stain to assess T cell phenotype. The other well was treated with PMA (5ng/mL) + Ionomycin (125ng/mL) in the presence of protein transport inhibitors Brefeldin A and Golgi Stop (BD Biosciences, NJ) for 4 hours to perform intracellular staining of cytokines.

Phenotype stain. 50,000 cells were stained using the following monoclonal antibodies: CD3-BUV395 (UCHT1), CD4-BUV496 (SK3), CD8-APCH7 (SK1), CD25-BV786 (M-A251), (Beckton Dickinson, NJ); CD69-BV711 (FN50), and PD1-PE (EH12) (BioLegend, CA). Cells were stained for viability using the Zombie Aqua Fixable Viability dye (BioLegend, CA) at a 1:2000 final dilution. Cells were stained for 30 minutes at 4°C in the dark and washed twice with FACS buffer (1XPBS + 2%FCS) before acquisition on the Fortessa x-20 (BD Biosciences, NJ).

Intracellular stain. 50,000 cells were stained using the following monoclonal antibodies: CD3-BUV395 (UCHT1), CD25-BV786 (M-A251), PD1-FITC (EH12) and Zombie Aqua Fixable Viability dye (BioLegend, CA) at a 1:2000 final dilution for 30 minutes before washing cells twice with FACS buffer. The cells were resuspended in 100µl of Perm buffer (eBioscience), incubated for 45 minutes at 4°C in the dark before washing twice with Perm Wash Buffer (eBioscience). Cells were then stained with a mixture of antibodies (BD Biosciences, NJ) to mark intracellular factors: Granzyme B-PECF594 (GB11), IFNγ-BV421 (4S.B3), and TNF-BV650 (Mab11) for 20 minutes at 4°C in the dark before washing twice in Perm Wash buffer. The final cell pellets were resuspended in 1XPBS and stored at 4°C until acquisition on the Fortessa x-20.

Bioinformatic analysis

Pearson correlation matrix of cell-type specific genes^{282,283} was tested using TPM values from bulk RNA-seq data in 27 liver metastases retrieved from Gene Expression Omnibus (GEO) GSE207194. The correlation matrix was subjected to unsupervised hierarchical clustering (Euclidean distance measurement and average linkage clustering). Each colored square within the figure illustrates the correlation between two genes for all patients, red illustrating positive correlation, white no correlation and blue negative correlation. The package ‘pheatmap’ was used for graphics and ‘cor’ was used for correlation analysis through R software.

Statistical analysis

Differences between two groups was analyzed using Mann Whitney U test, and Kruskal-Wallis test when differences between more than two groups were assessed. Correlations between parameters were assessed using Spearman correlation test.

Optimal cut-point values for intra-tumor liver tissue immune infiltrates, CD203c and FcεRI expression, and Histamine levels to discriminate patients with good versus poor Relapse-free survival was determined using the package cutpointr in R studio. The sensitivity and specificity of each variable was visualized using plot.ROC in R studio.

Relapse-free survival outcomes were estimated using the Kaplan-Meier method, stratifying patients according to the optimal cut-point value determined per continuous variable tested, or stratified according to mutation status, and compared using the Log-rank Mantel-Cox test. Relapse-free survival (RFS) was defined as the period from liver metastasis resection to the date of disease relapse in the liver or in extrahepatic sites.

Statistical tests were performed using Prism 9 software and R studio version 2022.12.0. All tests were 2 sided, with $P < 0.05$ considered as statistically significant.

Annex

Table 1. Flow Cytometry Reagents - Mast cell Myeloid Cell Panel			
Reagent	Clone	Reference	Dilution
BD Horizon™ BUV395	HI30	563791	1/50
Mouse anti-human CD45		RRID:AB_2869519	

BD Optibuild™ BUV496 Mouse anti-human CD14	MoP9	741200 RRID:AB_2870760	1/40
BD Optibuild™ BUV737 Mouse anti-human HLADR	G46-6	748339 RRID:AB_2872758	1/50
BD Horizon™ BUV805 Mouse anti-human CD4	SK3	612888 RRID:AB_2870177	1/50
BD Horizon™ BV421 Mouse anti-human CD203c	NP4D6	563296 RRID:AB_2738124	1/50
BD Horizon™ BV510 Mouse anti-human CD19	SJ25C1	562947 RRID:AB_2737914	1/50
BD Horizon™ BV605 Mouse anti-human CD39	A1	567691	1/100
BD Horizon™ BV650 Mouse anti-human CD3	SP34-2	563916 RRID:AB_2738486	1/50
BD Horizon™ BV711 Mouse anti-human CD11c	B-ly6	563130 RRID:AB_2738019	1/50
BD Optibuild™ BV786 Mouse anti-human CD11b	D12	742642 RRID:AB_2740935	1/50
BD Horizon™ BB515 Mouse anti-human CD117	104D2	565172 RRID:AB_2739091	1/100
BD Optibuild™ BB700 Mouse anti-human CD16b	CLB-gran11.5	745773 RRID:AB_2743234	1/50
BD Horizon™ PECy7 Mouse anti-human CD56	B159	557747 RRID:AB_396853	1/50
BD Horizon™ PE Mouse anti-human FcεR1a	AER-37	566607 RRID:AB_2744475	1/50
BD Horizon™ PE-CF594 Mouse anti-human CD15	HI98	562463 RRID:AB_2737619	1/200
BD Pharmingen™ AF647 Mouse anti-human CD163	GHI/61	562669 RRID:AB_2737710	1/50

BD Horizon™ APC-R700 Mouse anti-human CD25	2A3	565106 RRID:AB_2744339	1/50
BD Pharmingen™ APC-H7 Mouse anti-human CD8	SK1	560179 RRID:AB_1645481	1/50
Zombie Aqua™ Fixable Viability kit	BioLegend®	423102	1/1000

Table 2. Flow Cytometry Reagents – T cell Polarization Panel

Reagent	Clone	Reference	Dilution
BD Horizon™ BUV805 Mouse anti-human CD45	HI30	612891 RRID : AB_2870179	1/50
BD Horizon™ BUV395 Mouse anti-human CD3	UCHT1	563548 RRID: AB_2744387	1/50
BD Horizon™ BUV496 Mouse anti-human CD4	SK3	569179	1/50
BD Pharmingen™ APCH7 Mouse anti-human CD8	SK1	560179	1/50
BD OptiBuild™ BUV737 Mouse anti-human ICOS	DX29	749665 RRID: AB_2873929	1/25
BD Horizon™ BV605 Mouse anti-human CD103	Ber-ACT8	569162	1/50
BD Horizon™ BB700 Mouse anti-human CD56	B159	566574	1/50
BD Horizon™ PE-Cy7 Mouse anti-human CXCR3	1C6	560831 RRID: AB_2033944	1/50
BD Horizon™ APC-R700 Mouse anti-human CCR6	11A9	565173 RRID: AB_2739092	1/50
BD Pharmingen™ FITC Mouse anti-human CD39	TU66	561444 RRID: AB_10896292	1/50

BD Horizon™ PECF594 Mouse anti-human CD25	M-A251	562403 RRID: AB_11151919	1/50
BD Horizon™ BV786 Mouse anti-human CD45RA	HI100	563870 RRID: AB_2728469	1/50
BioLegend® BV711 Mouse anti-human CD69	FN50	310944 RRID: AB_2566466	1/50
BioLegend® Pacific Blue™ Mouse anti-human CCR7	G043H7	353210 RRID: AB_10918984	1/50
BioLegend® PE Mouse anti-human PD1	EH12.2H7	329906 RRID: AB_940483	1/25
BioLegend® APC Mouse anti-human PDL1	29E-2A3	329708 RRID: AB_940360	1/25
Zombie Aqua™ Fixable Viability kit	BioLegend®	423102	1/1000

Table 3. Multiplex Immunohistochemistry

Antibody	Source	Reference	Clone	Dilution	Diluent	Incubation time (min)	Incubation temp	Antigen Retrieval	Denaturation/ Stripping	Secondary
CD117	Dako	A4502	Poly	1/400	Zytopmed	20	RT	CC1	/	Anti-Rabbit HQ; Anti-HO HRP
KI67	Dako	M7240	MIB-1	1/100	Zytopmed	60	RT	/	CC2	UltraMap anti-Rabbit HRP
CK	DBS	Mob190.05	AE1-AE3	1/40	Zytopmed	60	RT	/	CC2	UltraMap anti-Mouse HRP
CD8	Roche	0593724800 1	SP57	Ready-to-Use	/	28	36	/	CC2	OmniMap anti-Rabbit HRP
FOXP3	Abcam	Ab99963	SP97	1/100	Zytopmed	60	36	/	CC2	UltraMap anti-Rabbit HRP
FAP alpha	R&D Systems	AF3715	Poly	1/40	Zytopmed	60	37	/	/	Anti-Sheep HRP 1/50

Table 4. Tissue Culture Reagents	
Reagent	Source/Reference
Ficoll®-Paque Plus	Merck GE17-1440-02
IMDM (Iscove's Modified Dulbecco Medium)	Gibco™ 12440046
BIT 9500 Serum Substitute	STEMCELL™ Technologies 17189951
Insulin-Transferrin-Selenium (100X)	Gibco™ 41400045
Penicillin-Streptomycin (10,000 U/mL)	Gibco™ 15140122
GlutaMAX™ Supplement (100X)	Gibco™ 35050061
Sodium Pyruvate (100mM)	Gibco™ 11360070
MEM Non-Essential Amino Acids (100X)	Gibco™ 11140050
MEM Vitamin Solution (100X)	Gibco™ 11120052
Human SCF, premium grade	Miltenyi Biotec 130-096-695
Human IL-6, premium grade	Miltenyi Biotec 130-093-932
Human IL-3, premium grade	Miltenyi Biotec 130-095-070
Human TGF-β2, research grade	Miltenyi Biotec 130-123-657

Figures

Fig. 1

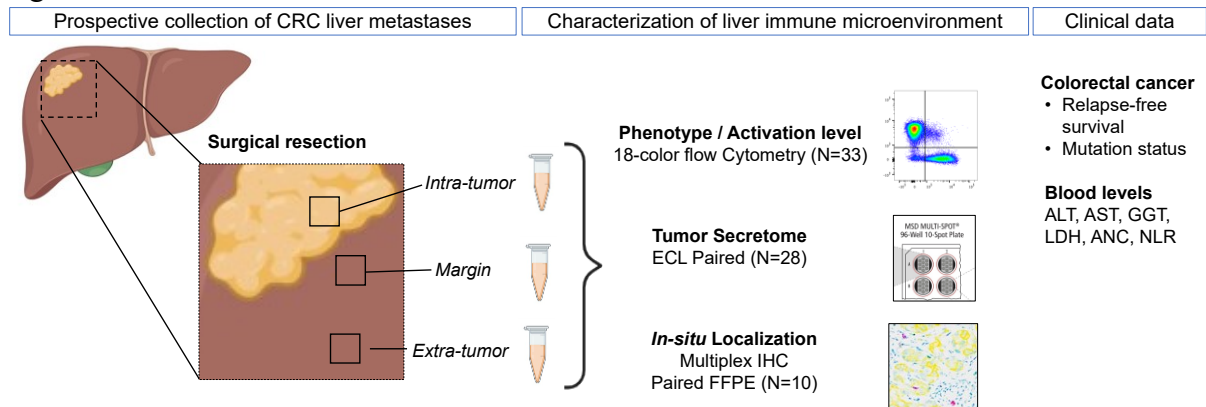


Figure 1: Prospective collection of surgical resections of liver metastases from colorectal cancer patients and characterization of the liver immune microenvironment.

Fresh samples from patients undergoing curative resection for liver metastasis (N=32) were prospectively collected. Intra-tumor, margin and extra-tumor tissue were collected and analyzed separately for the characterization of the immune microenvironment by (i) 18-color flow cytometry phenotyping and assessments of activation levels of liver-infiltrating immune cells, (ii) electrochemiluminescence measurement of the secretion of proteins by the resected tissue and (iii) multiplex immunohistochemistry staining for spatial profiling and quantification of cell-cell interactions. Available clinical data were accessible (as listed in Table 1) as well as blood biomarkers of liver function (ALT, AST, GGT and LDH).

Fig.2

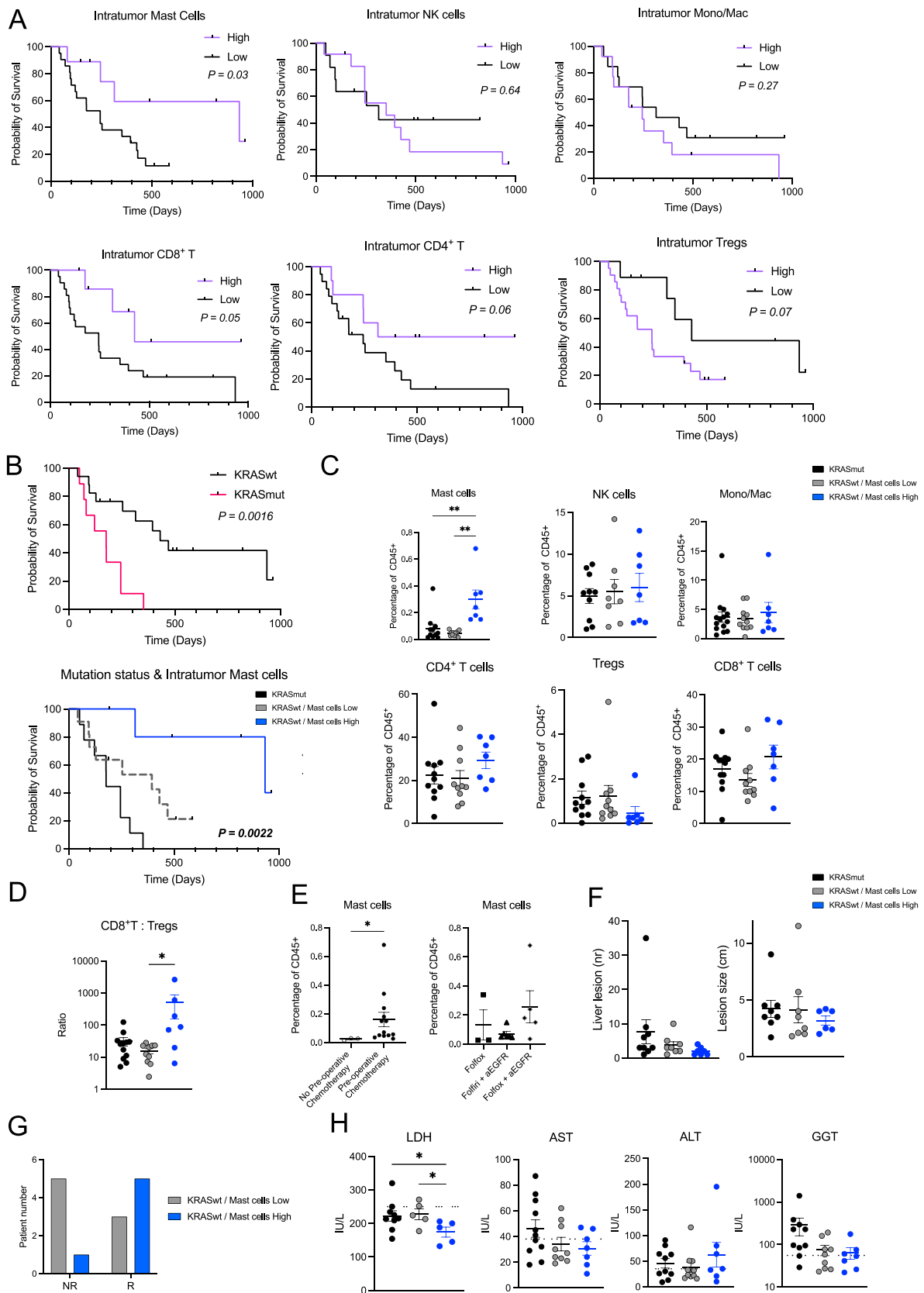


Figure 2: Liver metastases infiltration with mast cells is beneficial and correlates with increased survival in KRAS wildtype metastatic CRC patients

A/ Relapse-free survival, stratified by the intra-tumor infiltration analyzed by flow cytometry, of mast cells (CD117^{high}FcεRI⁺), NK cells (CD3⁻CD56⁺), monocyte/macrophages (CD11b⁺CD14⁺), and lymphocytes (CD8⁺T cells, CD4⁺T cells, Tregs (CD25^{high}CD39⁺) (Kaplan-Meier curve analysis, Log-rank Mantel Cox test). **B/** Relapse-free survival, stratified by KRAS mutation status (*top panel*) and intra-tumor infiltration with mast cells (*bottom panel*) (Kaplan-Meier curve analysis, Log-rank Mantel Cox test). **C&D/** Quantification of intra-tumor infiltration with CD8⁺T cells, CD4⁺T cells, Tregs, NK cells, mono/macrophages, and mast cells in patients with high or low mast cells, stratified by KRAS mutation (Kruskal-Wallis test, *, $P < 0.05$; **, $P < 0.01$; ***, $P < 0.001$). **E/** Quantification of intra-tumor infiltration with mast cells in KRAS wt patients treated without (open circle) or with (closed circle) preoperative chemotherapy (*left panel*); and stratification according to combination preoperative treatment received (*right panel*). **F/** Quantification of the number and size of liver metastases. The number of metastatic lesions was counted in the liver and the diameter of largest lesions was measured in patients with 'Low intra-tumor mast cells' versus 'High intra-tumor mast cells'. **G/** Response of target lesions to pre-operative treatment in KRAS wt patients. NR (Non-responders) refers to patients with stable disease or progressive disease; and R (Responders) refers to Partial Response, according to RECIST 1.1 guidelines (Eisenhauer EA EJC 2009) in KRAS wt patients with high versus low intra-tumor mast cells (N= 14, Chi-squared test). **H/** Circulating biomarkers of liver function (ALT, AST, GGT) and systemic inflammation (LDH) in patients with 'Low intra-tumor mast cells' versus 'High intra-tumor mast cells'.

Fig. 3

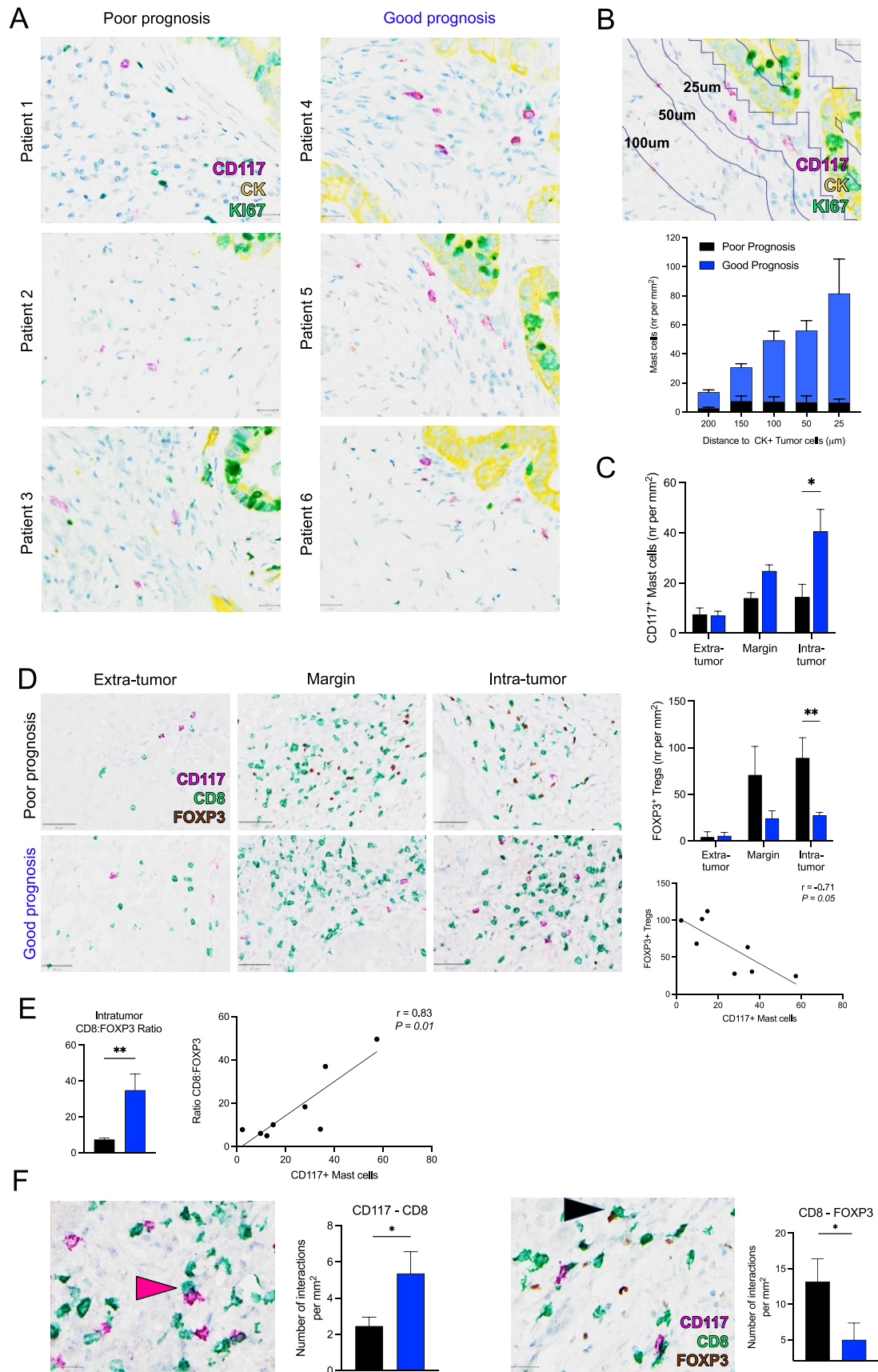


Figure 3. Spatial distribution of intra-tumor mast cells and Tregs in CRC liver metastases

A/ Multiplex immunohistochemistry staining of mast cells and tumor cells. Paired FFPE intra-tumor tissue sections from resected patients were stained for mast cells (CD117, pink), and proliferating (Ki67, green) cancer cells (Cytokeratin, yellow). Nuclei were counterstained with hematoxylin. Representative images of multiplex IHC from tumor stroma tissue from N=3 patients with poor vs. good prognosis (40X magnification). **B/** Quantification of mast cells (CD117 staining) in proximity with tumor cells (CK staining) within the intra-tumor stroma in patients with poor vs. good prognosis. The distance to the nearest CK⁺ tumor cells was expressed as the density of cells per mm². (Kruskal-Wallis test; *, $P < 0.05$). **C/** Quantification of mast cells (CD117 staining) in extra-tumor, margin and intra-tumor FFPE tissue in patients with poor vs. good prognosis (Kruskal-Wallis test; *, $P < 0.05$). **D/** Multiplex Immunohistochemistry staining of mast cell (CD117, pink), CD8⁺ T cell (CD8, green), and FOXP3⁺ Treg (FOXP3, brown) infiltration in liver metastases. Representative images of immune infiltrate in extra-tumor, margin and intra-tumor paired FFPE samples from patients with poor vs. good prognosis (40X magnification) (*left panel*); quantification of FOXP3 staining in patients with poor vs. good prognosis (Mann-Whitney U test, *, $P < 0.05$) (*right panel*). **E/** Ratio of CD8⁺/FOXP3⁺ cell density within intra-tumor paired FFPE tissue from patients with poor vs. good prognosis (Mann-Whitney U test, *, $P < 0.05$) (*left panel*). Spearman correlation between FOXP3⁺ Tregs and mast cells in intra-tumor FFPE tissue (*middle panel*); and between CD8⁺/FOXP3 ratio and mast cells in intra-tumor FFPE tissue (*right panel*). **F/** In-situ localization of mast cell, CD8⁺ T cell and Treg in CRC liver metastases. Representative images of multiplex immunohistochemistry on paired FFPE tumor tissue showing CD117⁺ mast cells and CD8⁺T cell interaction (*pink arrow*), and CD8⁺T cells and FOXP3⁺ Tregs interaction (*black arrow*) (40X magnification). The average number of interactions per surface unit was quantified in regions of highest CD8⁺T cell and mast cell infiltration (Mann-Whitney test, *, $P < 0.05$).

Fig. 4

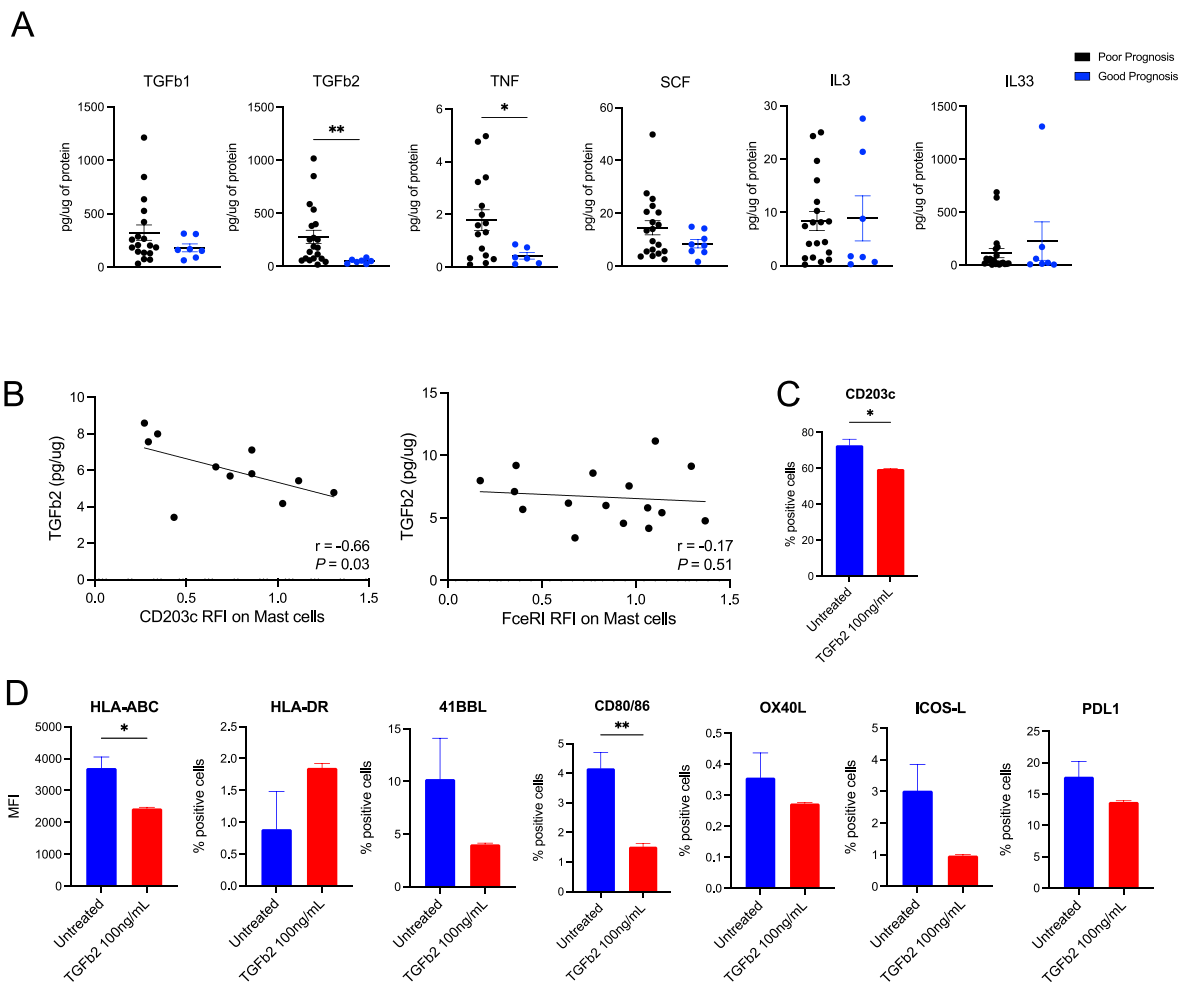


Figure 4. TGFβ2 secretion is correlated with high mast cells infiltration in the tumor, their activation and MHC-I expression

A/ Comparison of secreted factors in tumor tissue storage solution in patients with ‘Low intra-tumor mast cells’ versus ‘High intra-tumor mast cells’, represented as the ratio to total protein (*right panel*) (Mann Whitney U test; *, $P < 0.05$; **, $P < 0.01$). **B/** Spearman correlation test between secreted TGFβ2 and CD203c and FcεRI expression on mast cells in resected CRC liver metastases. **C/** In vitro stimulation of peripheral blood-derived mast cells by TGFβ2, measured by CD203c membrane expression (N=3 experimental replicates per group). **D/** Effect of TGFβ2 on peripheral blood-derived mast cells MHC Class I and MHC Class II, costimulatory 41BBL, CD80/86, OX40-L, ICOS-L, and co-inhibitory PDL1 expression (N=3 experimental replicates per group).

Fig. 5

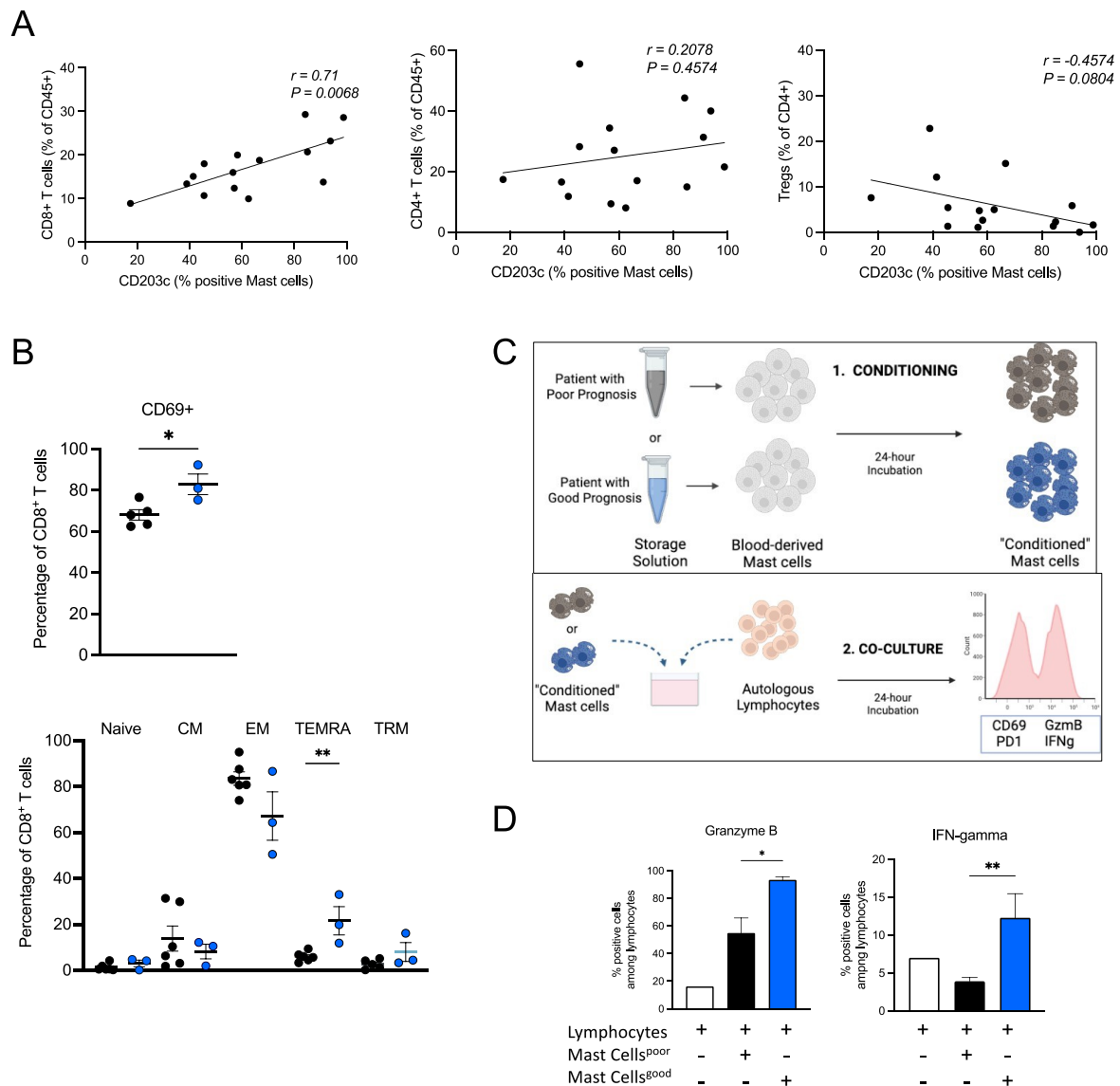


Figure 5. Patients with good prognosis show increased cell interactions between mast cells and activated CD8⁺T cells in tumors

A/ Spearman correlation test between CD203c expression on intra-tumor mast cells and intra-tumor CD8⁺ T cells, CD4⁺T and Tregs. **B/** Flow cytometry quantification of CD8⁺T cell subpopulations and activation markers on tumor infiltrating CD8⁺T cells. CD69 expression on tumor-infiltrating CD8⁺T cells in patients with poor vs. good prognosis (Unpaired t-test, **, $P < 0.01$) (*top panel*). Percentage of naive (CD45RA⁺CCR7⁺), central memory (CD45RA⁻CCR7⁺), effector memory (CD45RA⁻CCR7⁻), terminally differentiated ‘TEMRA’ (CD45RA⁺CCR7⁻) and resident memory (CD103⁺CD69⁺) cells among CD8⁺T cells in poor vs. good prognosis (N=8 patients, Unpaired t-test, *, $P < 0.05$) (*bottom panel*). **C/** Impact of mast cells on T cell activation experiment design. Peripheral blood-derived mast cells were conditioned overnight in tumor tissue storage solution from patients with poor vs. good prognosis. Pre-conditioned mast cells were then added at a 1:1 ratio to autologous pre-activated lymphocytes. After 24 hours, lymphocytes were stained to assess T cell activation phenotype and intracellular cytokine expression. **D/** Intracellular expression of Granzyme B and IFN-gamma in

autologous lymphocytes cultured alone or co-cultured with conditioned mast cells from patients with good vs. poor prognosis.

Fig. 6

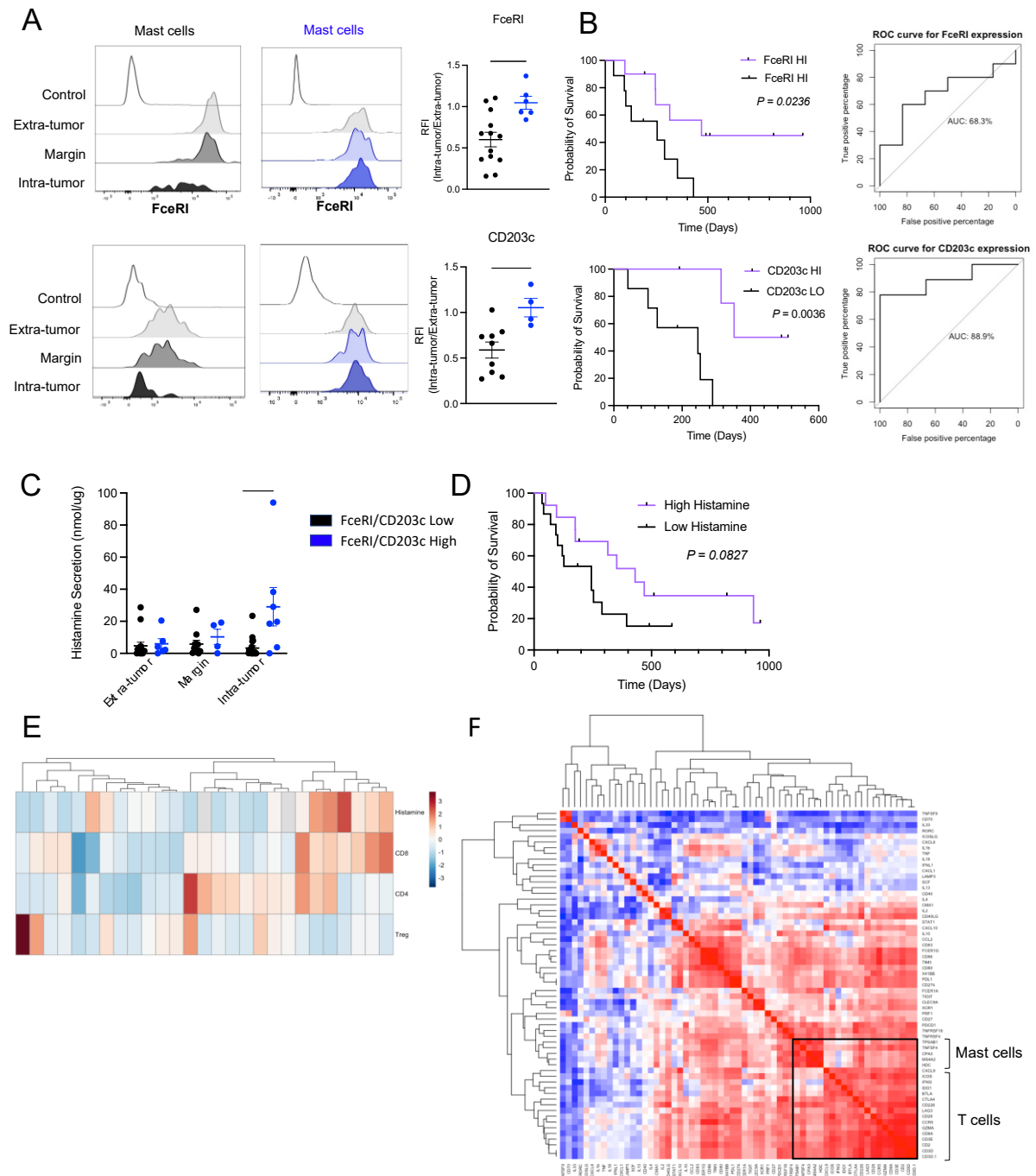


Figure 6. Mast cell activation and histamine is associated with improved relapse-free survival
A/ Flow cytometry analysis of membrane expression of FcεRI and CD203c in 1 patient with ‘Low intra-tumor mast cells’ (black) and in 1 patient with ‘High intra-tumor’ mast cell infiltration (blue) (*left panel*). Quantification of FcεRI and CD203c, represented as the fold-ratio of FcεRI expression in intra-tumor/extra-tumor tissue (Mann-Whitney test) (*right panel*). **B/** Impact of FcεRI and CD203c expression on patient relapse-free survival (Log-rank Mantel-Cox test) (*left panel*). ROC curve analysis of intra-tumor/extra-tumor FcεRI and CD203c expression on mast cells for predicting Relapse-free survival in patients (*right panel*). **C/** Secretion of histamine by tumor, margin, and extra-tumor tissue,

measured in tissue storage solution from patients with ‘Low intra-tumor mast cells’ versus ‘High intra-tumor mast cells’ (*left panel*, Mann-Whitney U test *, $P < 0.05$). **D/** Impact of histamine secretion on patient relapse-free survival. Kaplan-Meier analysis for Relapse-free survival, stratified by High versus Low intra-tumor histamine secretion (*right panel*) (Log-rank Mantel-Cox test). **E/** Unsupervised clustering of histamine and lymphocytic subsets in resected CRC liver metastases. **F/** Pearson correlation matrix of cell type specific genes using normalized gene expression values derived from public dataset GSE207194 of chemotherapy-treated and resected colorectal cancer liver metastases (N=27 patients)

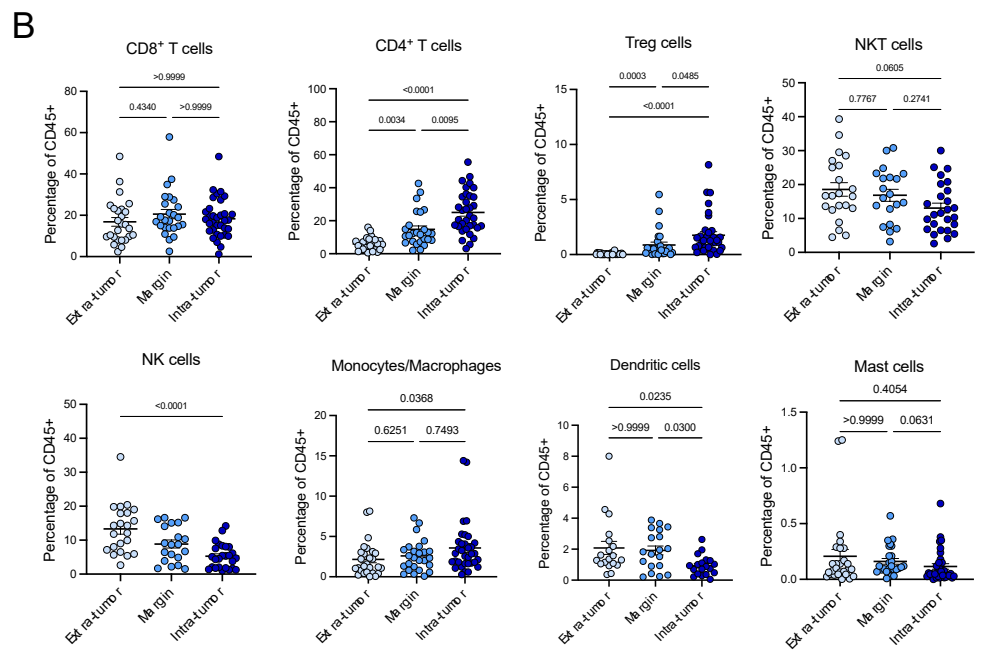
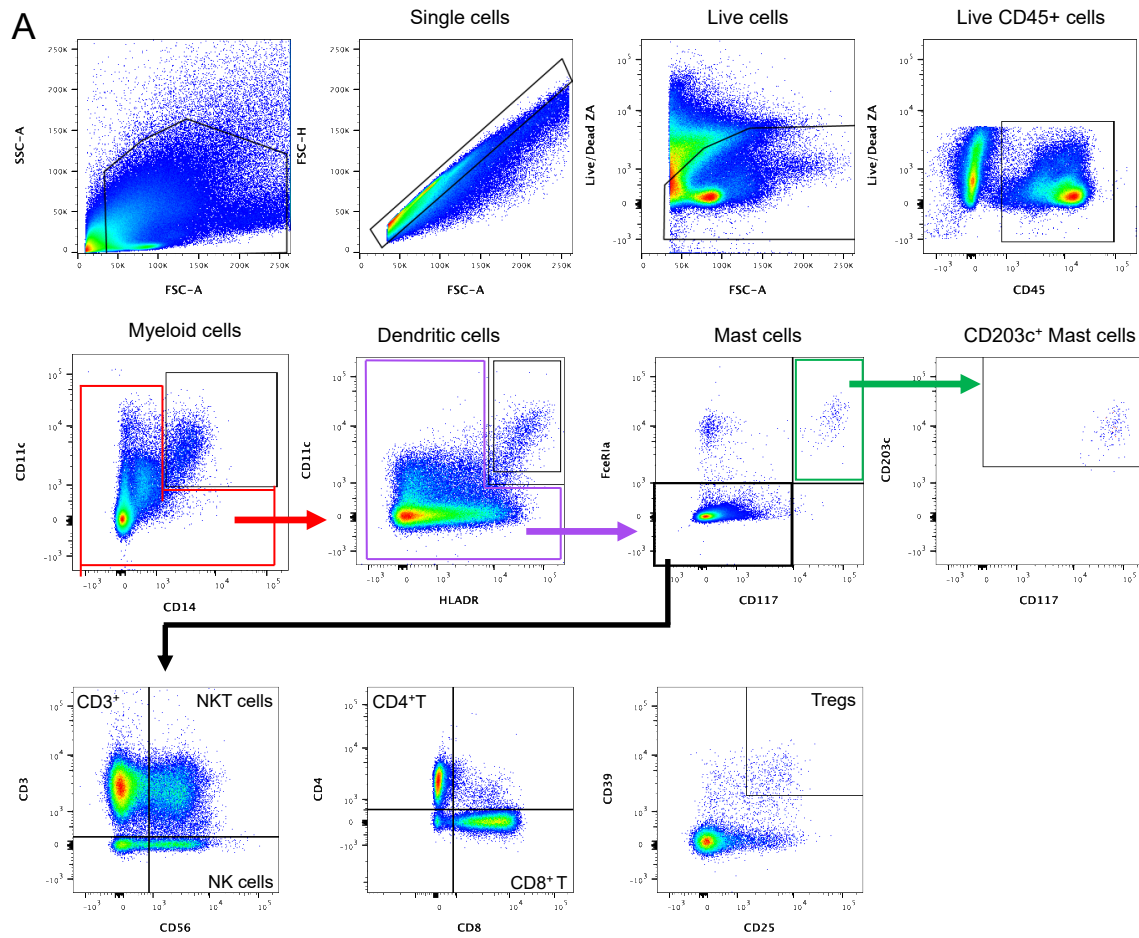
Tables

Table 1. Patients’ demographic and clinical characteristics

Characteristic	Patients (n=32)
Median Age (range)	60 (37-79)
Sex - no. (%)	
Female	17 (53%)
Male	15 (47%)
Median Body Mass Index (range)	26 (16-39)
Mutation status - no. (%)	
KRAS	12 (38%)
TP53	5 (16%)
NRAS	1 (3%)
NA	2 (6%)
Primary Tumor sidedness - no. (%)	
Rectum	8 (25%)
Left Colon	17 (53%)
Right Colon	5 (16%)
Transverse	2 (6%)
Metastasis Diagnosis - no. (%)	
Synchronous	27 (84%)
Metachronous	5 (16%)
Median liver lesion number - no. (range)	2 (1-35)
Median liver lesion diameter cm. (range)	3.5 (0.9-11.5)
Presence of Extrahepatic metastasis	8 (25%)
Blood values - median U/L (range)	
ALT	33 (13-195)
AST	34 (17-119)
GGT	83 (23-1404)
LDH	213 (145-320)
Preoperative systemic chemotherapy - no. (%)	
Chemotherapy	9 (28%)
Folfini/Folfox/Folfinirox + aEGFR	12 (38%)
Folfox/Folfinirox + aVEGF	7 (22%)
None	4 (13%)
Treatment Line setting - no. (%)	
1st line	23 (72%)
2nd line	9 (28%)
Radiologic Response - no. (%)	
Partial Response	15 (54%)
Stable Disease	10 (36%)
Progressive Disease	3 (10%)
Site of Disease Relapse Post Surgery	
Liver	14 (44%)
Lung	12 (38%)
Lymph Node	5 (16%)
Peritoneum	3 (9%)

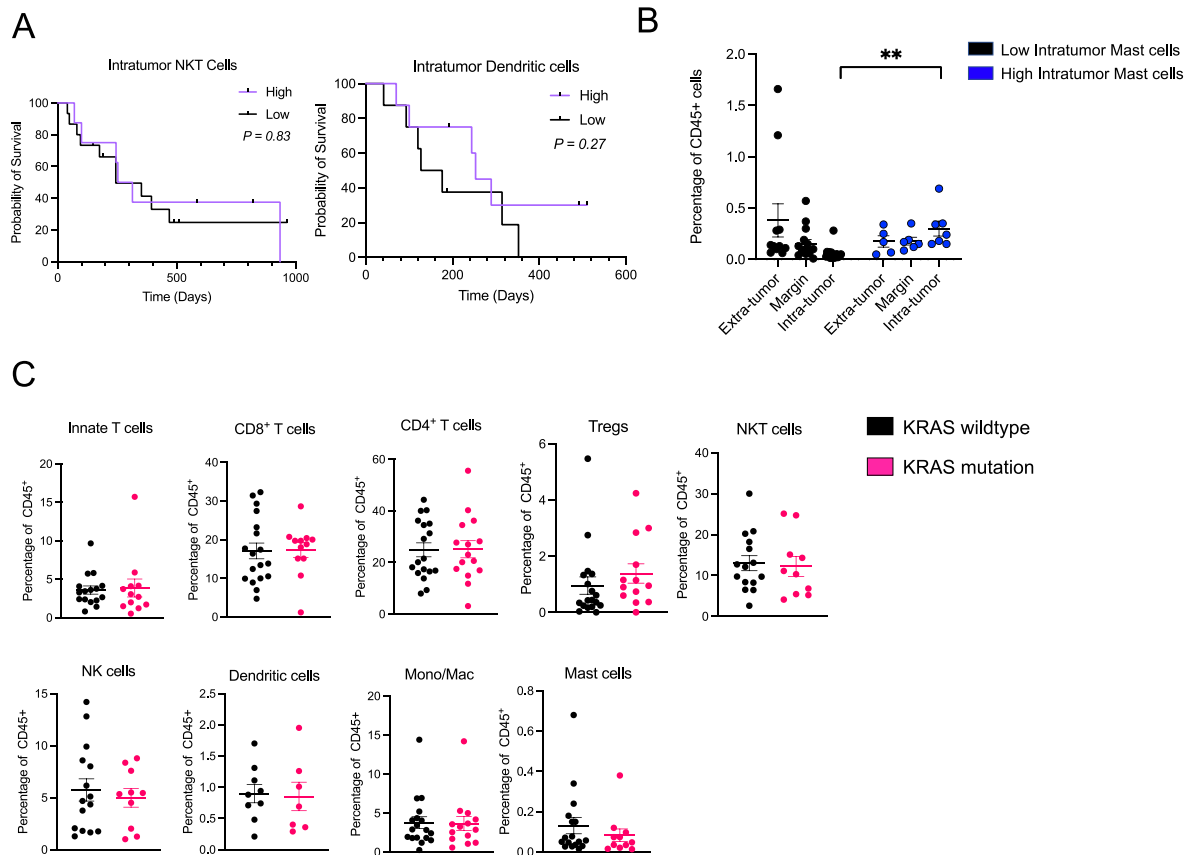
Supplementary Material

Supp. Fig. 1



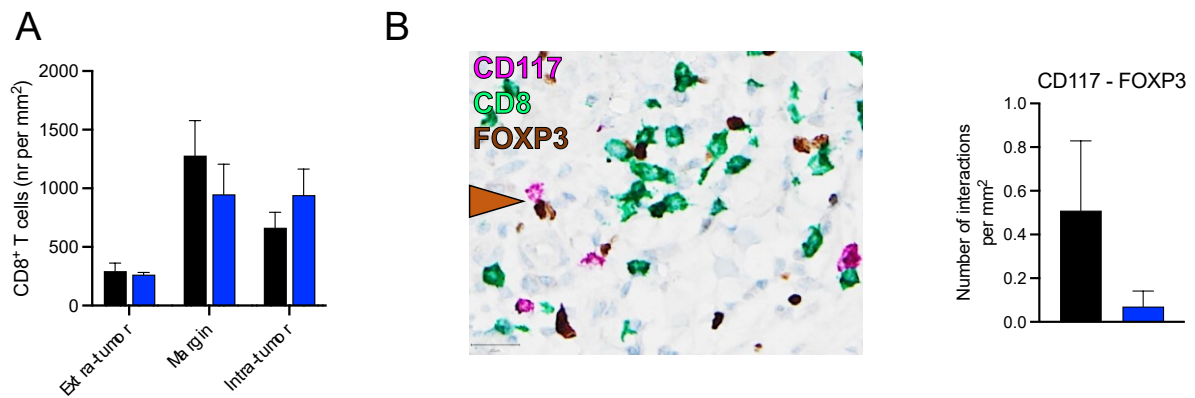
Supplementary Figure 1. A/ Flow Cytometry Panel Gating Strategy The flow cytometry panel gating strategy is depicted and includes the following cell populations and markers used to identify them in order from left to right: Myeloid cells (CD11b⁺CD14⁺), Dendritic cells (CD14⁻CD11c^{high}HLADR⁺), and Mast cells (CD117^{high}FcεRI⁺). Total T cells (CD3⁺CD56⁻), NK cells (CD3⁻CD56⁺), CD8⁺T cells (CD3⁺CD56⁻CD8⁺), CD4⁺T cells (CD3⁺CD56⁻CD4⁺), and Tregs (CD4⁺CD25^{high}CD39⁺). **B/** Percentage of immune cell subsets among CD45⁺ cells from paired samples of extra-tumor, margin, and intra-tumor tissue from n=32 CRC liver metastatic patients (Kruskal-Wallis test, *, $P < 0.05$; **, $P < 0.01$; ***, $P < 0.001$).

Supp. Fig. 2



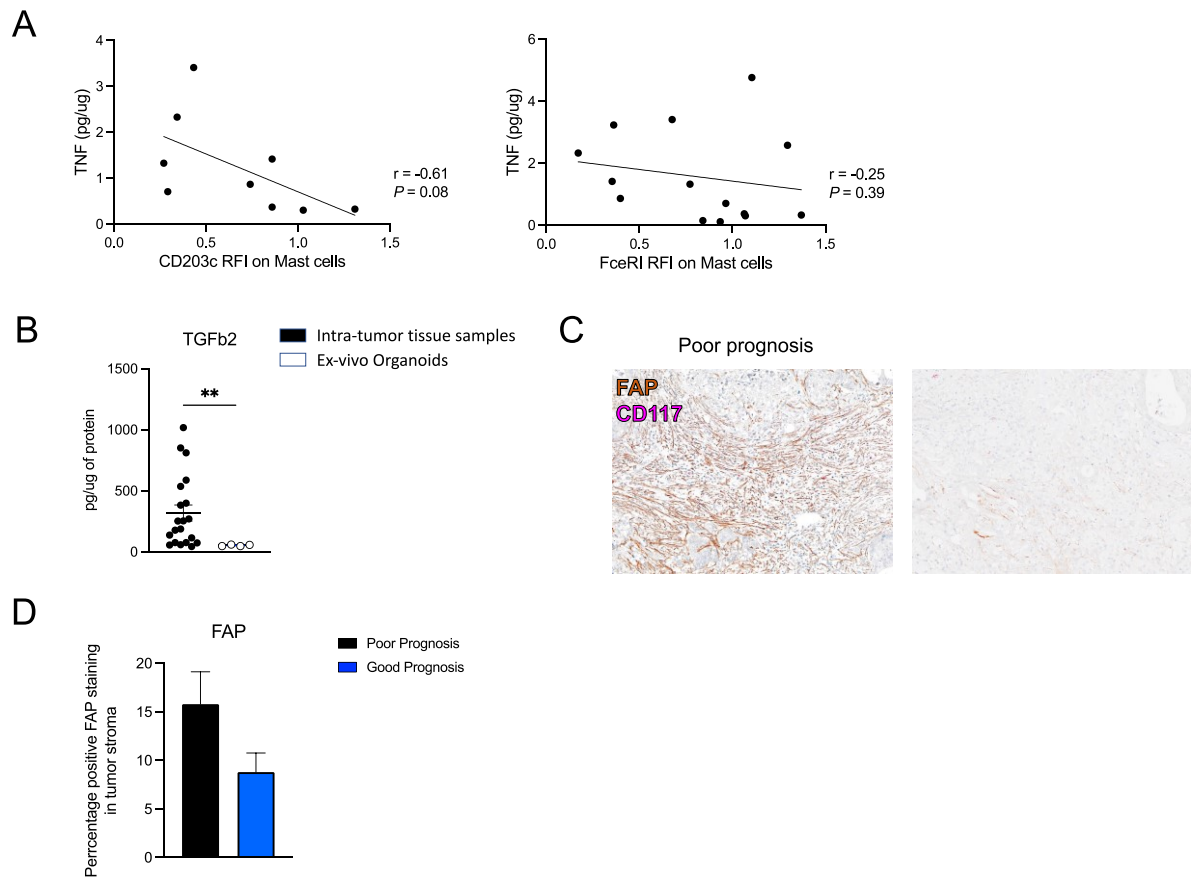
Supplementary Figure 2 Mast cell infiltration in liver and radiologic response to preoperative therapy **A/** Relapse-free survival, stratified by the intra-tumor infiltration analyzed by flow cytometry, of NKT cells ($CD3^+CD56^+$) and dendritic cells ($CD14^{neg}HLADR^+CD11c^+$) (Kaplan-Meier curve analysis, Log-rank Mantel Cox test). **B/** Flow cytometry analysis of Mast cell infiltration in metastatic liver. Cell frequency was measured in extra-tumor, margin, and intra-tumor resected tissue in patients with low versus high mast cells intra-tumor infiltration (Mann-Whitney test, **, $P < 0.01$). **C/** Quantification of intra-tumor infiltration of lymphocytes ($CD8^+$ T cells, $CD4^+$ T cells, Tregs, NKT, and NK cells), dendritic cells, mono/macrophages, and mast cells in patients stratified by KRAS mutation (Mann-Whitney test).

Supp. Fig. 3



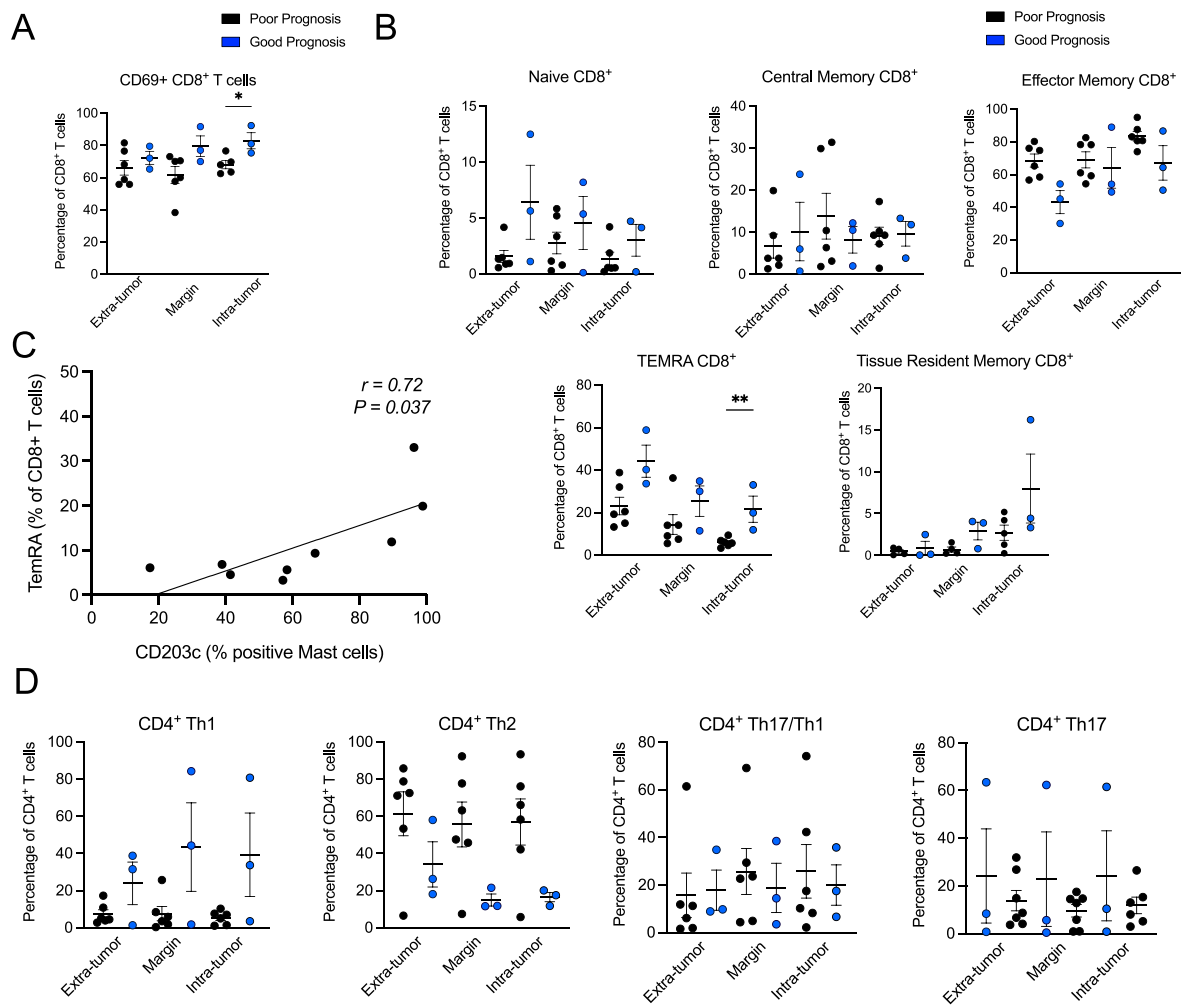
Supplementary Figure 3 Spatial assessment of CD8⁺T cell infiltration and FOXP3⁺ Tregs interaction with CD117⁺ mast cells **A/** Quantification of CD8⁺ staining in paired FFPE tissue from patients with poor vs. good prognosis (Mann-Whitney U test). **B/** In-situ localization of mast cell and Treg in CRC liver metastases (*left panel*). Representative images of multiplex immunohistochemistry on paired FFPE tumor tissue showing CD117⁺ mast cells (pink) and FOXP3⁺ Tregs (brown) interaction (*black arrow*) (40X magnification). Quantification of cell interactions in patients with poor vs. good prognosis (*right panel*). The average number of interactions per surface unit was quantified in regions of highest Treg cell infiltration (Mann-Whitney test, *, P < 0.05).

Supp Fig. 4



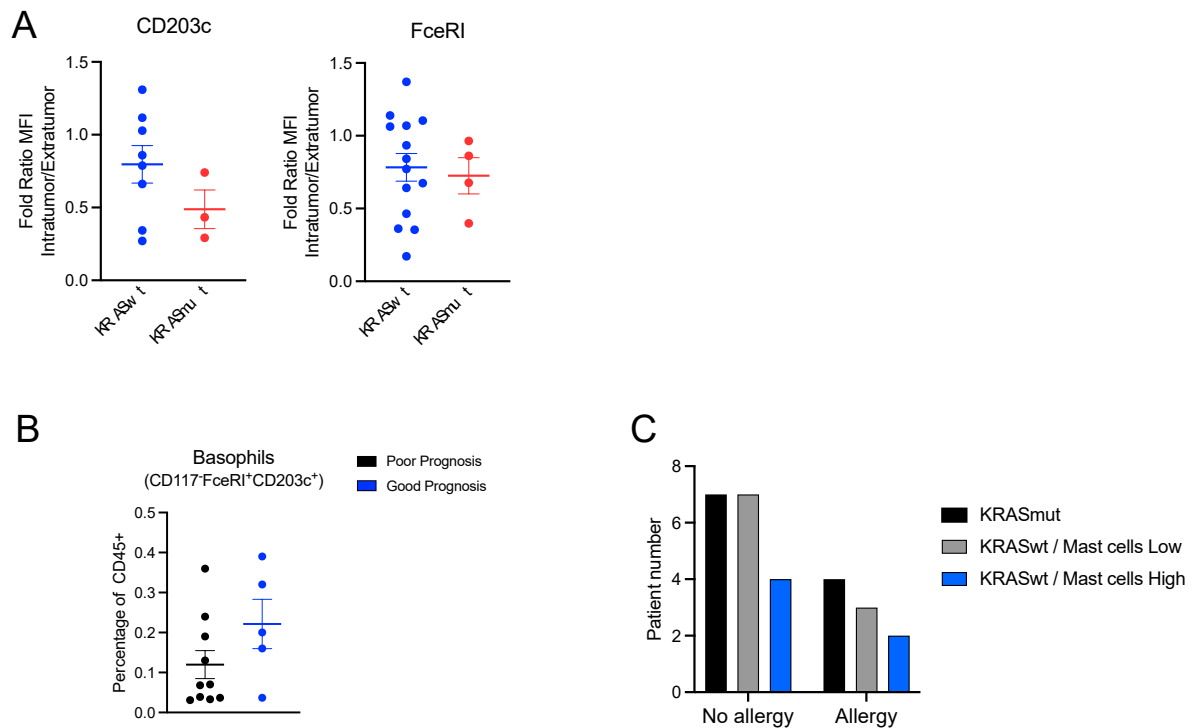
Supplementary Figure 4. TGFβ₂ secretion may originate from FAP⁺ cells in the tumor microenvironment **A/** Spearman correlation test between secreted TNF, and CD203c and FcεRI expression on mast cells in resected CRC liver metastases. **B/** Concentration of TGFβ₂ secreted by resected intra-tumor tissue compared with concentration secreted by ex-vivo cultivated Liver metastasis organoids (Mann-Whitney test, **, $P < 0.01$). **C/** Multiplex Immunohistochemistry analysis of Mast cell CD117 (pink), and FAP⁺ Fibroblasts (brown) infiltrate in colorectal cancer liver metastasis paraffin sections. Representative images of multiplex at 40X magnification from tumor tissue depict FAP⁺ fibers present within the tumor stroma in each patient subgroup. **D/** Quantification of FAP⁺ cells by measurement of positively stained area of FAP⁺ within the tumor stroma in patients (Mann-Whitney test).

Supp. Fig. 5



Supplementary Figure 5. Patients with good prognosis have increased frequency of T effector memory RA 'TemRA' CD8⁺T cells that are positively correlated with mast cell expression of activation marker CD203c A/ Percentage of CD69 expression among CD8⁺ T cells from paired samples of extra-tumor, margin and intra-tumor tissue from n=8 patients with poor vs. good prognosis (Unpaired t-test; *, P < 0.05). B/ Percentage of naive (CD45RA⁺CCR7⁺), central memory (CD45RA⁻CCR7⁺), effector memory (CD45RA⁻CCR7⁻), T effector cells memory RA 'TemRA' (CD45RA⁺CCR7⁻) and tissue resident memory (CD69⁺CD103⁺) cells among CD8⁺ T cells from paired samples of extra-tumor, margin, and intra-tumor tissue from n=8 patients with poor vs. good prognosis (Unpaired t-test; **, P < 0.01). C/ Spearman correlation between intra-tumor T effector memory RA 'TemRA' and CD203c expression on mast cells. D/ Percentage of Th1 (CCR6⁻CXCR3⁺), Th2 (CCR6⁻CXCR3⁻), Th17/Th1 (CCR6⁺CXCR3⁺) and Th17 (CCR6⁺CXCR3⁻) among CD4⁺ T cells from paired samples of extra-tumor, margin, and intra-tumor tissue from n=8 patients with poor vs. good prognosis.

Supp. Fig. 6



Supplementary Figure 6. Mast cell activation in tumors **A/** Comparison of relative expression of activation-associated markers CD203c and FcεRI on intra-tumor mast cells according to mutation profile. **B/** Percentage of intra-tumor Basophils (CD117⁺FcεRI⁺CD203c⁺) among CD45⁺ cells from patients with poor vs. good prognosis. **C/** The number of patients experiencing allergic response to medications or non-specific allergies prior to surgical resection of liver tumor compared according to mutation status and mast cell infiltration.

Chapter 2. Tumor infiltrating neutrophils are associated with decreased radiologic response and relapse-free survival in KRAS-wildtype patients with colorectal cancer liver metastasis

Héloïse Halse^{1,2}, Chifaou-Mohamed-Djalim^{2,3}, Delphine Bredel², Severine Mouraud², Guillaume Escriou², Aminata Drame², Marine Andrade², Rachel Rignault, Mirjana Weimershaus, Maximiliano Gelli⁵, Michel Ducreux⁵, Peggy Dartigues^{4,6}, Jean-Yves Scoazec^{4,6}, Thiago Trovati Maciel¹, Aurélien Marabelle^{2,3}, Olivier Hermine¹ and Amélie E. Bigorgne^{1,2}

1 Laboratory of Translational Immunotherapy Research (LRTI) INSERM U1015, Gustave Roussy; Villejuif, France

2 Laboratory of Cellular and Molecular Mechanisms of Haematological Disorders and Therapeutical Implications, Label "Ligue Contre le Cancer", Imagine Institute, Inserm U1163, Université Paris Cité; Paris, France

3 Drug Development Department (DITEP), Gustave Roussy; Villejuif, France

4 Department of Visceral and Digestive Surgery, Gustave Roussy; Villejuif, France

KEYWORDS

Neutrophils, Colorectal cancer liver metastasis, inflammation

Introduction

The liver is the most frequent site of metastasis in metastatic colorectal cancer (mCRC) and is associated with significant morbidity and mortality.^{12,13} While advances in treatment, including combination pre-operative chemotherapy and surgical resection, have greatly improved survival rates, the risk of relapse is high, with the 5-year survival rate in mCRC liver metastatic remaining below 50%.^{15,21}

Cancer cells often exploit the body's physiological inflammatory and innate immune responses to indirectly support tumor growth, progression, and metastasis.^{284,285} This inflammatory microenvironment, characterized by various cytokines, chemokines, and growth factors, significantly contribute to the growth, invasiveness, and metastatic potential of cancer cells. Neutrophils play an active role in this process and are closely linked to chronic inflammation and the inflammatory microenvironment associated with cancer progression.²⁸⁶ Neutrophils play a pivotal role in the metastatic cascade of different cancer subtypes to the liver, including colorectal cancer, from premetastatic niche formation to tumor cell invasion, extravasation, and eventual tumor outgrowth in the liver.²⁸⁷⁻²⁹⁰

Systemic markers such as the absolute neutrophil count (ANC), the neutrophil-to-lymphocyte ratio (NLR) and derived neutrophil-lymphocyte ratio (dNLR), have highlighted the prognostic significance of neutrophils in mCRC patients.²⁹¹⁻²⁹⁵ Elevated NLR has been associated with reduced response to chemo-immunotherapy combination treatment like those in the recent CAVE (Cetuximab plus Avelumab (anti-PDL1)) trial in KRAS wildtype patients with refractory mCRC.²⁹⁶ The systemic mobilization of neutrophils and myeloid derived suppressor cells (MDSC) is hypothesized to mirror the intra-tumor immune microenvironment and is associated with a diminished anti-tumor immune response found within tumors. However, these biological markers have not yet been routinely compared with the intra-tumoral immune profiles or secreted inflammatory mediators of surgically resected liver metastases in patients, and so the impact of intra-tumoral neutrophils on relapse-free survival in colorectal cancer liver metastasis patients remains uncertain.

In this prospective study, we characterized the immune profiles of surgically resected mCRC liver metastases using flow cytometry and secreted inflammatory mediator quantification, to explore the prognostic role of liver-infiltrating neutrophils in mCRC patient prognosis. Our findings reveal that neutrophil infiltration in liver metastasis negatively affects patient prognosis, particularly KRAS wild-type patients. Furthermore, we observe a positive correlation between liver-infiltrating neutrophils and blood ANC. These liver-infiltrating neutrophils prominently express the PMN-MDSC marker LOX1 and are positively correlated with elevated intra-tumor secretion of inflammatory mediators including CXCL8, TGF β 2 and TNF, which exhibit an inverse relationship with T cell and mast cell infiltration and activation. Given the protective roles of T cells and mast cells in KRASwt mCRC prognosis, our results underscore the negative impact of neutrophils on anti-tumor immune responses in mCRC, emphasizing their potential as therapeutic target to improve anti-tumor immune responses in mCRC and patient prognosis.

Material and Methods

Patient samples

Resected colorectal cancer liver metastatic tissue was collected prospectively from surgically treated patients from the pathology department at Gustave Roussy Hospital from June 2019 to September 2022. Patient information and sample collection was authorized by the Ministry of Higher Education and Research (DC-2021-4572), and in respect of the reference methodology MR-004 of the French data protection authority (CNIL). Inclusion criteria included patients undergoing complete liver metastasis resection from colorectal cancer for curative intent, along with availability of clinical, biological and follow-up data post surgical resection. The median follow-up was 8 months (range 1 – 32 months). Previous data obtained on RFS were confirmed by the measure of radiologic response of target lesions to pre-operative treatment, according to RECIST 1.1 guidelines.³⁶ Relapse-free survival was defined as the interval from the date of surgical resection to the date of relapse of metastasis to the liver or within extrahepatic sites including lung, peritoneum, or lymph nodes. Patients presenting with other co-occurring cancers or suffering an unknown cause of death post-surgery were excluded from the study.

Peripheral Blood Samples

Results from peripheral blood tests performed preoperatively were obtained to record liver enzymes Alkaline Phosphatase (AP), Alanine Transaminase (ALT), Aspartate Aminotransferase (AST), and gamma-glutamyl transferase (GGT). Lactate Dehydrogenase (LDH) levels were also recorded. LDH is a biomarker reflecting tumor burden and metabolic status and a known marker of prognosis in patients with liver metastasis. The timing from last chemotherapy injection and peripheral blood test was considered and white blood cell counts (Neutrophils and Lymphocytes), the ratio of Neutrophil-to-lymphocyte (NLR), and derived Neutrophil-to-lymphocyte ratio (dNLR) only recorded from 4 weeks after last chemotherapy injection.

Preparation of intra-tumor, margin, and extra-tumor liver tissue storage solution for secreted soluble factor measurement

Resected intra-tumor, margin and extra-tumor liver tissue storage solution was prepared by storing immediately each respective tissue in 3-5 milliliters of Tissue Storage Solution (Miltenyi Biotec, DE) at 4°C. Following 18-hour to 48-hour storage, the supernatant was harvested by centrifugation at 1800RPM for 10 minutes and stored in aliquots at -80°C.

Tumor dissociation and flow cytometry staining

Fresh samples of resected intra-tumor and when possible, at the margin and extra-tumor liver tissue were collected for tissue dissociation and flow cytometry staining. Intra-tumor, margin and extra-tumor liver tissue were weighed and cut into small fragments of 1-2mm in diameter using a sterile scalpel blade and petri dish. Tissue fragments were transferred to a C-tube (Miltenyi Biotec, DE) and 5-10mL of enzyme digestion mixture consisting of RPMI 1640 medium (Gibco, MT), 50 U/mL Collagenase IV, 30 U/mL DNase I and 280 U/mL Hyaluronidase (Merck, DE) was added. The tubes were placed on to the GentleMACS dissociator (Miltenyi Biotec, DE) and subjected to mechanical and enzymatic dissociation using the program TDK_1 (incubation for 1 hour at 37°C). Following this, the dissociated tissue mixture was filtered using 70um sterile filter and the cell suspension was washed 1x in 50mL of sterile Phosphate-buffered saline (PBS) followed by a second wash in cold sterile PBS with 2% Bovine Serum Albumin and 2mM EDTA. CD45⁺ cells were counted after staining a 50µl aliquot of the cell suspension with anti-CD45 FITC (BD Biosciences, NJ) and 50µl of Precision Count Beads (BioLegend, CA).

Mast cell and Myeloid cell panel (MMC). Following the counting step, a minimum of 100,000 CD45⁺ cells were stained using flow cytometry antibodies (BD Biosciences, NJ) and Zombie Aqua Fixable Viability Dye (BioLegend, CA) listed in Annex Table 1 at the dilutions indicated in final volume of 100µl of buffer (PBS with 2% Bovine Serum Albumin and 2mM EDTA) at 4°C for 30 minutes. After staining, the cells were washed twice in buffer before acquisition.

T cell polarization and activation panel. When possible, a further 50,000-100,000 CD45⁺ cells were stained using flow cytometry antibodies and Zombie Aqua Fixable Viability Dye listed in Annex Table 2 at the dilutions indicated and in a final volume of 100µl of buffer (PBS with 2% Bovine Serum Albumin and 2mM EDTA) at 4°C for 30 minutes. After staining, the cells were washed twice in buffer before acquisition.

All events were acquired on the BD FORTESSA X-20 cytometer equipped with BD FACSDiva software (BD Biosciences, NJ), and data were analyzed using FlowJo software (Tree Star, OR).

Staining of paired blood sample for neutrophil phenotyping

200µl of whole blood was used for flow cytometry staining. The blood sample was washed once with 1mL of PBS and 2% BSA to remove serum. The blood was stained for 30 minutes with flow cytometry antibodies and Zombie Aqua Fixable Viability Dye listed in Annex Table 3

at the dilutions indicated at 4°C for 30 minutes. After staining, the cells were washed twice in buffer (PBS with 2% Bovine Serum Albumin and 2mM EDTA) before BD FACS lyse for 3 minutes to remove red blood cells. Briefly, 2mL of BD FACS lyse was added to the blood and pipetted a few times to ensure even mixing. Tube shaken every minute in the dark. The cells were then spun down and resuspended in FACS buffer for acquisition.

Secreted Soluble Factor and secreted Histamine measurement

Soluble factors secreted by intra-tumor, margin and extra-tumor liver tissue were measured in tissue storage solution using Mesoscale Discovery biomarker electrochemiluminescence detection assay kits according to the manufacturer's instructions (MSD, MA).

Secreted Histamine was measured in intra-tumor, margin and extra-tumor liver tissue 'supernatant' using the Histamine HTRF (Homogeneous Time Resolved Fluorescence) Dynamic kit according to the manufacturer's protocol (CisBio, FR).

Cell sorting neutrophils and T cells from extra-tumor liver sample of a patient with decreased RFS

After tissue dissociations, wash, and counting steps, extra cells (1.7 million) were stained for 30 minutes on ice for cell sorting of neutrophils and T cells with the following antibodies: CD3 PE, CD19 BV510, CD56 BV510, CD11b BV786, CD14 BUV496, CD16 BV711, CD45 HI30 BUV805, and Zombie Aqua. The staining buffer contained cold 1XPBS with 15% Human AB Serum (to maintain cell viability) and 20mM EDTA (to prevent granulocyte clumping and activation). After the staining and 2 wash steps, the cells were sorted on the BD influx (BD Bioscience). The cells were sorted into fresh staining buffer and left for one hour on ice after sorting to prevent activation. After the resting period, the cells were washed once with cold sorting buffer and resuspended in RPMI medium with 10% Human AB serum. 10,000 T cells were plated per well and 50,000 neutrophils. The cells were stimulated with 50U/mL and 50ng/mL of PMA for at least 30 minutes. At 30 minutes and 20-hours, the supernatant was collected and stored at -80°C for downstream analysis of secreted factors. At the 20-hour timepoint, the cells were stained for the following: CD3 BUV396, CD4 BUV496, CD8 APCH7, CD45 BUV805, CD39 PECF594, CD25 APCR700, PD1 PE, PDL1 APC, CD69 BV421, CD11B BV786, CD16 BV711, CD10 FITC.

Statistical analysis

Differences between two groups was analyzed using Mann Whitney U test, and Kruskal-Wallis test when differences between more than two groups were assessed. Correlations between parameters were assessed using Spearman correlation test.

Optimal cut-point values for intra-tumor liver tissue immune infiltrates, to discriminate patients with good versus poor Relapse-free survival was determined using the package cutpointr in R studio.

Relapse-free survival outcomes were estimated using the Kaplan-Meier method, stratifying patients according to the optimal cut-point value determined per continuous variable tested, or stratified according to mutation status, and compared using the Log-rank Mantel-Cox test. Relapse-free survival (RFS) was defined as the period from liver metastasis resection to the date of disease relapse in the liver or in extrahepatic sites.

Statistical tests were performed using Prism 9 software and R studio version 2022.12.0. All tests were 2 sided, with $P < 0.05$ considered as statistically significant.

Annex

Reagent	Clone	Reference	Dilution
BD Horizon™ BUV395 Mouse anti-human CD45	HI30	563791 RRID:AB_2869519	1/50
BD Optibuild™ BUV496 Mouse anti-human CD14	MoP9	741200 RRID:AB_2870760	1/40
BD Optibuild™ BUV737 Mouse anti-human HLADR	G46-6	748339 RRID:AB_2872758	1/50
BD Horizon™ BUV805 Mouse anti-human CD4	SK3	612888 RRID:AB_2870177	1/50
BD Horizon™ BV421 Mouse anti-human CD203c	NP4D6	563296 RRID:AB_2738124	1/50

BD Horizon™ BV510 Mouse anti-human CD19	SJ25C1	562947 RRID:AB_2737914	1/50
BD Horizon™ BV605 Mouse anti-human CD39	A1	567691	1/100
BD Horizon™ BV650 Mouse anti-human CD3	SP34-2	563916 RRID:AB_2738486	1/50
BD Horizon™ BV711 Mouse anti-human CD11c	B-ly6	563130 RRID:AB_2738019	1/50
BD Optibuild™ BV786 Mouse anti-human CD11b	D12	742642 RRID:AB_2740935	1/50
BD Horizon™ BB515 Mouse anti-human CD117	104D2	565172 RRID:AB_2739091	1/100
BD Optibuild™ BB700 Mouse anti-human CD16b	CLB-gran11.5	745773 RRID:AB_2743234	1/50
BD Horizon™ PECy7 Mouse anti-human CD56	B159	557747 RRID:AB_396853	1/50
BD Horizon™ PE Mouse anti-human FcεR1a	AER-37	566607 RRID:AB_2744475	1/50
BD Horizon™ PE-CF594 Mouse anti-human CD15	HI98	562463 RRID:AB_2737619	1/200
BD Pharmingen™ AF647 Mouse anti-human CD163	GHI/61	562669 RRID:AB_2737710	1/50
BD Horizon™ APC-R700 Mouse anti-human CD25	2A3	565106 RRID:AB_2744339	1/50
BD Pharmingen™ APC- H7 Mouse anti-human CD8	SK1	560179 RRID:AB_1645481	1/50

Zombie Aqua™ Fixable Viability kit	BioLegend®	423102	1/1000
------------------------------------	------------	--------	--------

Reagent	Clone	Reference	Dilution
BD Horizon™ BUV805 Mouse anti-human CD45	HI30	612891 RRID : AB_2870179	1/50
BD Horizon™ BUV395 Mouse anti-human CD3	UCHT1	563548 RRID: AB_2744387	1/50
BD Horizon™ BUV496 Mouse anti-human CD4	SK3	569179	1/50
BD Pharmingen™ APCH7 Mouse anti-human CD8	SK1	560179	1/50
BD OptiBuild™ BUV737 Mouse anti-human ICOS	DX29	749665 RRID: AB_2873929	1/25
BD Horizon™ BV605 Mouse anti-human CD103	Ber-ACT8	569162	1/50
BD Horizon™ BB700 Mouse anti-human CD56	B159	566574	1/50
BD Horizon™ PE-Cy7 Mouse anti-human CXCR3	1C6	560831 RRID: AB_2033944	1/50
BD Horizon™ APC-R700 Mouse anti-human CCR6	11A9	565173 RRID: AB_2739092	1/50
BD Pharmingen™ FITC Mouse anti-human CD39	TU66	561444 RRID: AB_10896292	1/50
BD Horizon™ PECF594 Mouse anti-human CD25	M-A251	562403 RRID: AB_11151919	1/50
BD Horizon™ BV786 Mouse anti-human CD45RA	HI100	563870 RRID: AB_2728469	1/50
BioLegend® BV711 Mouse anti-human CD69	FN50	310944 RRID: AB_2566466	1/50
BioLegend® Pacific Blue™ Mouse anti-human CCR7	G043H7	353210 RRID: AB_10918984	1/50
BioLegend® PE Mouse anti-human PD1	EH12.2H7	329906 RRID: AB_940483	1/25
BioLegend® APC Mouse anti-human PDL1	29E-2A3	329708 RRID: AB_940360	1/25

Zombie Aqua™ Fixable Viability kit	BioLegend®	423102	1/1000
------------------------------------	------------	--------	--------

Table 3. Flow Cytometry Reagents – Neutrophil Panel

Reagent	Clone	Reference	Dilution
BD Horizon™ BUV805 Mouse anti-human CD45	HI30	612891 RRID : AB_2870179	1/50
BD Horizon™ BV510 Mouse anti-human CD3	UCHT1	563109	1/50
BD Horizon™ BV510 Mouse anti-human CD56	NCAM16.2	563041	1/50
BD Horizon™ BV510 Mouse anti-human CD19	SJ25C1	562947	1/50
BD Optibuild™ BV786 Mouse anti-human CD11b	D12	742642 RRID:AB_2740935	1/50
BD Optibuild™ BUV496 Mouse anti-human CD14	MoP9	741200 RRID:AB_2870760	1/40
BioLegend® BV711 Mouse anti-human CD16	3G8	302044	1/50
BD Pharmingen™ APC-Cy7 Mouse anti-human HLADR	G46-6	561358	1/50
BD Horizon™ BV605 Mouse anti-human CD38	HB-7	562666	1/50
BioLegend® PE mouse anti-human LOX1	15C4	358604	1/50
BioLegend® FITC mouse anti-human CD10	HI10a		1/50
BD Horizon™ BV650 Mouse anti-human CD117	104D2	563859	1/50
Biolegend® PerCPCy5.5 Mouse anti-human CD33	WM53	303414	1/50
Biolegend® Pacific Blue™ Mouse anti-human CXCR2	5E8	320724	1/25
Biolegend® PE-Cy7 Mouse anti-human CXCR4	12G5	306508	1/25
Zombie Aqua™ Fixable Viability kit	BioLegend®	423102	1/1000

Results

Liver metastatic CRC patient cohort

Thirty-two patients with MSS metastatic colorectal cancer and known *KRAS/BRAF* mutation status were included in the study (17 women and 15 men; median age 60 years). Patient demographics and tumor characteristics are described in **Table 1**. *KRAS* was mutated in 38% of patients. >90% of *KRAS* wildtype patients had left-sided primary colorectal cancer. Most patients (84%) were diagnosed with synchronous metastatic disease and were treated with preoperative systemic chemotherapy prior to complete resection of liver metastases. Half of the patients had a partial response to preoperative chemotherapy according to RECIST 1.1 guidelines. Following surgical resection, Kaplan-Meier analysis demonstrated a median relapse-free survival (RFS) for all patients of 289 days (9.5 months), with many relapses occurring in the liver and/or lung in this cohort.

Characterization of the liver immune microenvironment

Resected intra-tumor, margin and extra-tumor liver tissue were prospectively collected from patients treated with surgical resection of CRC liver metastasis (**Fig 1**). Each resected tissue was initially stored in a tissue storage solution overnight at 4°C. This solution was then harvested for downstream analysis of secreted cytokines and chemokines by the respective tissue. The resected tissue was then processed by mechanical and enzymatic dissociation for downstream flow cytometry analysis. A multiparametric flow cytometry panel was designed to assess the frequency and distribution of neutrophils, monocytes/macrophages, mast cells, dendritic cells, and lymphocytes (including CD8 T, CD4 T, regulatory T cells (Tregs), NK, and NKT cells) to gain a comprehensive view of the liver immune microenvironment. The gating strategy is described in Supplementary Figure 1.

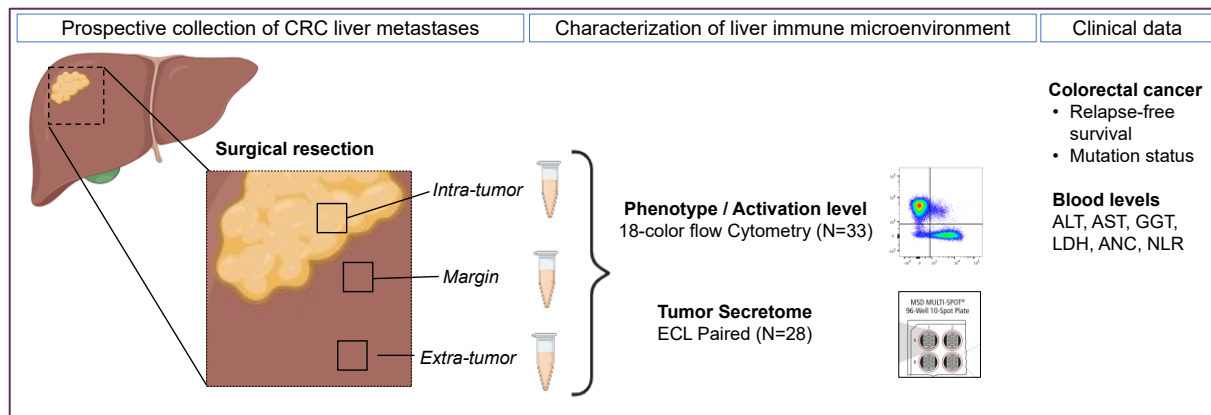


Figure 1: Prospective collection and study of the immune micro-environment in surgically resected CRC liver metastasis Fresh samples of resected liver tissue (intra-tumor, margin, and extra-tumor) from 28 patients undergoing curative resection for CRC liver metastasis were prospectively collected. Characterization of the immune microenvironment was undertaken by (i) 18-color flow cytometry analysis of liver-infiltrating lymphocytes and myeloid cell populations, and (ii), Electrochemiluminescence measurement of secreted proteins by the resected tissue. These variables were then correlated with clinical data including radiologic response and relapse-free survival, and biological data including systemic markers of inflammation.

Liver metastasis infiltration with neutrophils is associated with poor response to pre-operative therapy and decreased relapse-free survival in KRASwt metastatic CRC patients.

The KRAS proto-oncogene is the most frequently mutated gene in CRC associated with worse prognosis and resistance to chemotherapy.^{182,297,298} We therefore compared RFS between KRAS wildtype and KRAS mutation status. As expected, we found a significant difference in RFS between KRASwt and KRASmut patients (**Fig 2A**).

Then the impact of the infiltration of neutrophils and other immune cell subpopulations on relapse-free survival (RFS) was analyzed. Among all immune cells RFS was specifically decreased in patients with 'High' intra-tumor infiltration of neutrophils (**Fig 2B**). In contrast, tumor infiltration with T cells and mast cells was correlated with prolonged relapse-free survival (Supplementary Fig 2A). High infiltration of neutrophils in CRC liver metastasis was not associated with differences in liver lesion number or size but was correlated with elevated systemic levels of LDH and neutrophil counts in the blood (**Fig 2C and Supplementary Fig 2B**).

In previous studies, increased neutrophils at the margin and decreased infiltration of T cells in KRASmut tumors have been observed based on immunohistochemistry staining.^{163,186,299} To evaluate whether this finding was not a confounding factor we compared the infiltration of

neutrophils between the two subgroups of patients. We found no significant difference in the frequency of neutrophils infiltrating KRASwt or KRASmut tumors suggesting that neutrophils infiltration was independent of mutational status (**Fig 2D**). We then compared the impact of neutrophils and KRAS mutation on patient RFS (**Fig 2E**). Interestingly, we found that elevated tumor infiltration of neutrophils was significantly associated with decreased RFS specifically in KRASwt patients and did not influence the poor outcome of patients with KRASmut tumors. In this cohort, KRASwt patients were treated with either chemotherapy or chemotherapy combination with anti-EGFR (cetuximab or panitumumab). We therefore wanted to test whether there was an influence of treatment received and intra-tumor infiltration of neutrophils. Overall, we found no significant impact of pre-operative therapy on neutrophil frequency in tumors (**Fig 2F & Supplementary Fig 2C**). Instead, we observed a significant impact of tumor infiltration by neutrophils and radiologic response to pre-operative treatment in KRASwt patients (**Fig 2F**). We also tested whether there were other mutations in the subgroup of KRASwt patients that may influence neutrophil infiltration and response. None of the patients in the KRASwt subgroup harbored *BRAF* mutations, known to be associated with resistance to chemotherapy treatment.³⁰⁰⁻³⁰² There are conflicting reports as to improved sensitivity or resistance to cetuximab in patients with inactivating *TP53* mutations.³⁰³⁻³⁰⁵ Among KRASwt subgroup 44% patients with high neutrophils and 22% of patients with low neutrophils harbored *TP53* mutations, but because of the small cohort size, this difference was not significant (Fisher's exact test). In summary, elevated neutrophil infiltration within KRASwt tumors, is associated with treatment resistance and decreased RFS.

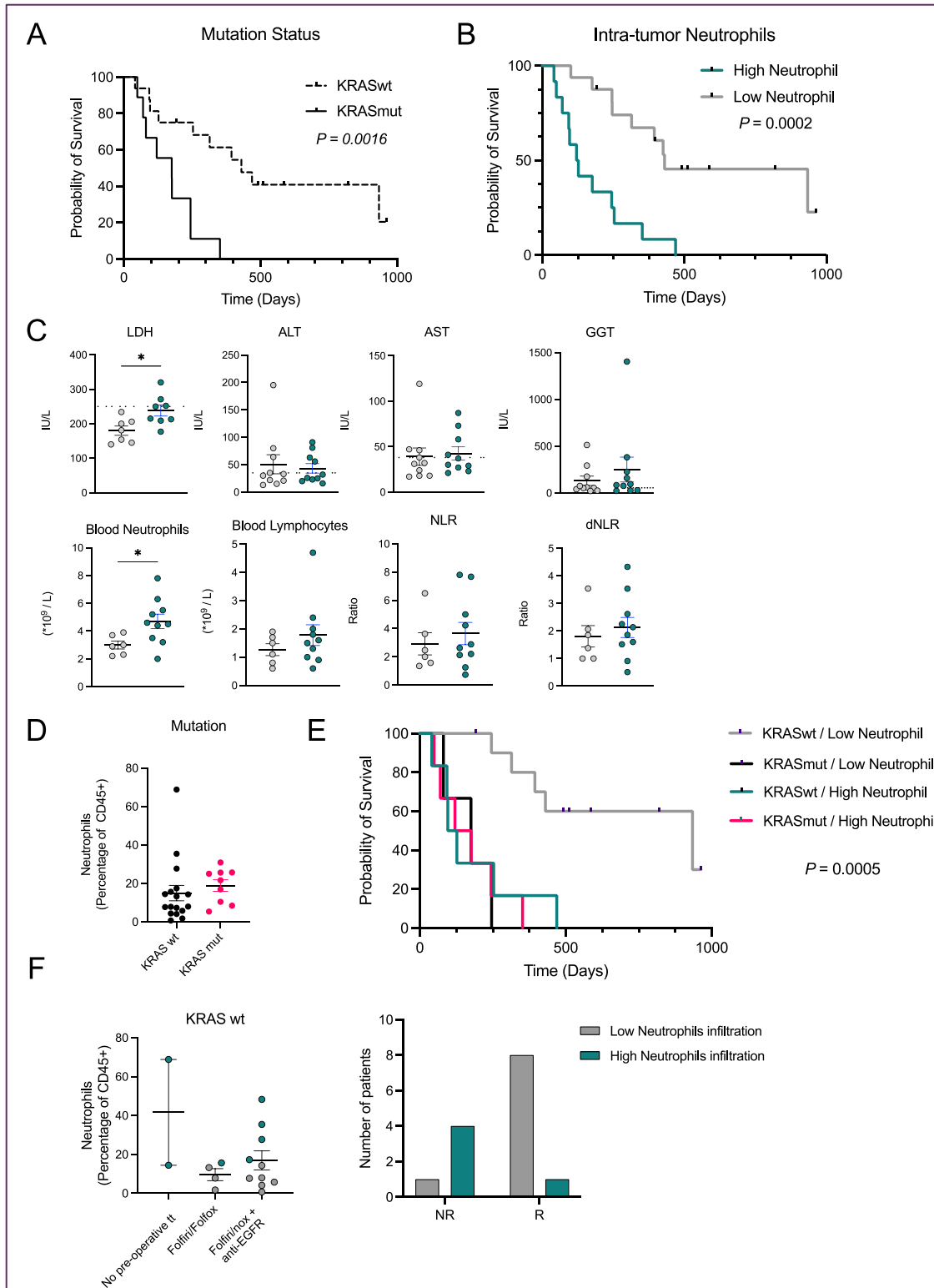


Figure 2: Liver metastases infiltration with Neutrophils is associated with poor response to preoperative chemotherapy and decreased relapse-free survival in CRC liver metastatic patients. They specifically impact relapse-free survival in KRASwt patients. **A/** Kaplan-Meier curve for Relapse-free survival, stratified by KRAS mutation status (Log-Rank test). **B/** Kaplan-Meier curves for Relapse-free survival, stratified by High or Low intra-tumor frequency of Neutrophils (CD14⁺CD11B⁺CD15⁺CD16b⁺) (Log-Rank test). **C/** Circulating biomarkers of systemic inflammation (LDH) and liver function (ALT, AST, GGT) in patients with 'Low intra-tumor neutrophils' versus

'High intra-tumor neutrophils'.(top panel) **C/** Circulating blood counts for neutrophils, lymphocytes, NLR and dNLR in patients with 'Low intra-tumor neutrophils' versus 'High intra-tumor neutrophils' (Bottom panel). **D/** intra-tumor neutrophil infiltration according to KRAS mutation status. **E/** Kaplan-Meier curve for Relapse-free survival, stratified by KRAS mutation status and neutrophil infiltration. (Log-Rank test) **F/** Quantification of intra-tumor infiltration with neutrophils in KRAS wt patients treated without or with preoperative chemotherapy (left panel); and Response of target lesions to pre-operative treatment in KRAS wt patients. NR (Non-responders) refers to patients with stable disease or progressive disease; and R (Responders) refers to Partial Response, according to RECIST 1.1 guidelines (Eisenhauer EA EJC 2009) in KRAS wt patients with high versus low intra-tumor mast cells (N= 14, Chi-squared test).

Neutrophil infiltration in KRASwt tumors is associated with an altered immune microenvironment mediated by a unique chemokine and cytokine gradient.

The specific increase of neutrophils in KRASwt tumors with poor prognosis was associated with decreased infiltration of CD4⁺T, CD8⁺T and mast cells (**Fig 3A**). Tumor infiltration of neutrophils was negatively correlated with both CD8⁺T cell and CD4⁺T cells in KRASwt patients (Supplementary Fig 3A). There was a trend for negative correlation between neutrophils and mast cell infiltration (Supplementary Fig 3A). This may indicate a direct negative impact of neutrophils on T cell infiltration in CRC liver metastasis. Although total T cell infiltration was associated with increased relapse-free survival we did not find a positive correlation between circulating lymphocytes and intra-tumor infiltration of total T cells (Supplementary Fig 3B). Therefore, the negative impact of tumor infiltration with neutrophils on T cells may take place more specifically in and around the liver tumors rather than systemically.

Based on the striking impact of neutrophils on patient outcome in KRASwt patients, we focused our analysis on this subgroup of patients. We measured and compared the infiltration of neutrophils in the extra-tumor, margin, and intra-tumor tissue in KRASwt patients with low neutrophil infiltration ('good prognosis') and high neutrophil infiltration ('poor prognosis'). The level of neutrophils infiltration was consistently elevated in all areas of liver tissue including the extra-tumor in patients with poor prognosis (**Fig 3B**). This finding correlates with our primary observation that the level of tumor infiltration with neutrophils was correlated to systemic levels of blood neutrophils, implying a systemic mobilization of neutrophils in these patients (Supplementary Fig 2B & 3B). However, the difference remained most significant at

the margin and within the tumor tissue, suggesting local mediators influencing their enhanced recruitment towards tumors in KRASwt patients with poor prognosis.

To measure what may be influencing neutrophil migration towards the tumors of KRASwt patients with poor prognosis, we quantified by electrochemiluminescence the secretion of different chemokines and cytokines associated with chronic inflammation, angiogenesis, and neutrophil chemotaxis within surgically resected liver tumor tissue storage solution. KRASwt patients with poor prognosis secreted elevated levels of the potent chemokine CXCL8, and cytokines TNF and TGF β 2 (**Fig 3D**). All three proteins were positively correlated with intra-tumor frequency of neutrophils (**Fig 3E**). We found no differences in other chemokines and/or cytokines involved in neutrophil chemotaxis, survival, and activation, which included IL1a, IL1b, CXCL1, VEGF and GCSF. We observed the same differences at the margin but not in the extra-tumor tissue (Supplementary Fig 3C). We also assessed whether these proteins and others were different in KRASmut tumors with high neutrophils infiltration and found no differences. However, we found tendencies for elevated TNF and GCSF. This may indicate a different mode of neutrophil recruitment within KRASmut tumors (Supplementary Fig 3D).

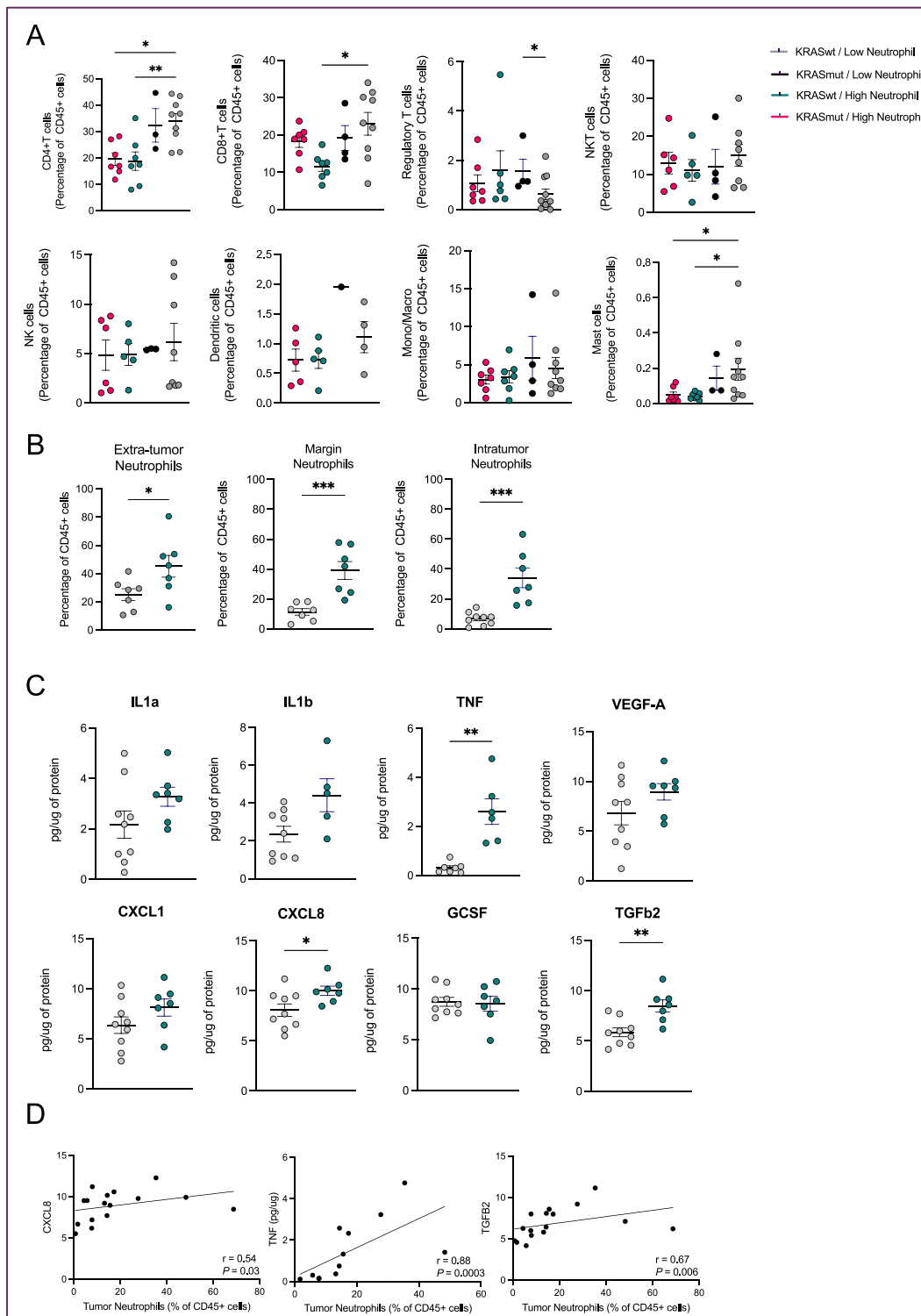


Figure 3. Neutrophil infiltration associated with altered immune microenvironment, mediated by a unique chemokine and cytokine gradient. A/ Quantification of intra-tumor infiltration with CD8⁺T cells, CD4⁺T cells, Tregs, NKT cells, NK cells, Dendritic cells, mono/macrophages, and mast cells discriminates in KRAS wt patients with high vs low neutrophils. The data presented constitutes analyses performed on N=28 patients (Kruskal-Wallis test, *, $P < 0.05$; **, $P < 0.01$; ***, $P < 0.001$). **B/** Comparison in the quantification of neutrophils in extra-tumor, margin, and intra-tumor tissue between patients with low neutrophils and good prognosis (grey circles), versus patients with high neutrophils and poor prognosis (green circles) (Mann-Whitney test, *, $P < 0.05$; **, $P < 0.01$; ***, $P < 0.001$).

C/ Comparison in the quantification of secreted inflammatory chemokines and cytokines in resected intra-tumor tissue between patients with low neutrophils and good prognosis (*grey circles*), versus patients with high neutrophils and poor prognosis (*green circles*) (Mann-Whitney test, *, $P < 0.05$; **, $P < 0.01$; ***, $P < 0.001$). **D/** Spearman correlation test between secreted CXCL8, TNF, and TGF β 2 and Tumor Neutrophils infiltration in resected colorectal cancer liver metastases.

We assessed the secretion of these proteins in 2 KRAS WT patient-derived CRC liver metastasis organoids (Supplementary Fig 3E). The level of CXCL8 secretion was similar, whereas the secretion of TGF β 2 and TNF were decreased in ex vivo generated organoids compared to tissue storage solution in patients with elevated neutrophil infiltration. Therefore, unlike CXCL8, TNF and TGF β 2 could derive from other cell types within the tumor microenvironment and not directly from the tumor cells. Furthermore, the organoids were generated from patient tumor biopsies with end-stage disease (poor prognosis).

Liver-infiltrating neutrophils in mCRC resemble PMN-MDSC based on membrane expression of LOX-1 and suppress T cell activation

Cytokines including CXCL8, TGF β and TNF have been reported to play a role in steering neutrophils toward a pro-tumoral phenotype. Pro-tumoral neutrophils, also known as N2 neutrophils or polymorphonuclear-Myeloid-derived Suppressor cells (PMN-MDSC), represent a population of neutrophils that fail to complete their regular differentiation process. However, it has been noted that these cells may also originate from their mature counterparts and are skewed towards different phenotypes determined by the inflammatory profiles within the tumor microenvironment.³⁰⁶

Recently, diminished expression of CD16 on circulating neutrophils in colorectal cancer patients was closely related to poor prognosis.³⁰⁷ Closer analysis of these cells revealed that the neutrophils had also diminished CD15 expression, an immature phenotype, and were particularly immunosuppressive on autologous T cells in co-culture experiments. We assessed the expression of surface markers on tumor infiltrating neutrophils compared to extra tumor neutrophils by taking the fold ratio of the mean fluorescence intensity of CD11B, CD15 and CD16b expression on the cells (Relative Fluorescence Intensity – RFI) (**Fig 4A**). There was no significant difference in the RFI of these markers between patients with good versus poor prognosis, although a decreasing trend in the RFI of CD15 was detected in patients with poor

prognosis. Because the decrease in CD15 is associated with decrease in neutrophil maturation, this prompted us to measure CD10 expression on the neutrophils to test their maturation. For N=3 of the patients we were able to stain a paired blood sample from the day of liver resection. We observed that CD10 expression was variable from the blood to the extra-tumor liver, after which the levels did not change from the extra-tumor to the intra-tumor (**Fig 4B**). For 3 out of 4 patients, the proportion of CD10⁺ neutrophils were larger than 80%. These findings suggest that most neutrophils infiltrating the liver tumors in this cohort are 'mature' cells.

Recent research has introduced lectin-type oxidized LDL receptor-1 (LOX-1) as a distinct surface marker of PMN-MDSC in cancer patients with strong immunosuppressive properties.³⁰⁸ Previous studies in liver cancer have identified these cells as having potent immunosuppressive properties against T cells, through elevated ROS and Arginase production.³⁰⁹ For 4 patients, we had enough cells to study the expression of LOX-1 on neutrophils in CRC liver metastases, and for 2 of these patients we were able to stain matching blood sample to observe whether these cells were differentiating in the liver or already present in the circulation. In all patients, extra-tumor, margin, and intra-tumor neutrophils were positive for the PMN-MDSC specific marker LOX-1 (**Fig 4C**). Interestingly, for the patients which we had paired blood samples, we also observed LOX-1 expression on circulating neutrophil in these patients. The expression of LOX1 further intensified once the neutrophils entered the liver tissue. Importantly, regardless of prognosis, LOX-1 was expressed on most neutrophils, although slightly less in the patients with good prognosis. Thus, the negative impact of LOX-1 positive neutrophils is related not to the type of neutrophil but to their quantity and function once near and within the tumor.

We were able to sort from one progressive disease and oxaliplatin resistant patient's extra-tumor liver sample liver-infiltrating T cells and neutrophils and place them in coculture overnight in the presence of IL-2 and PMA (**Fig 4D**). Indeed, the liver neutrophils negatively impacted T cell activation in the presence of IL-2 and PMA, indicating an immune suppressive role of the cells.

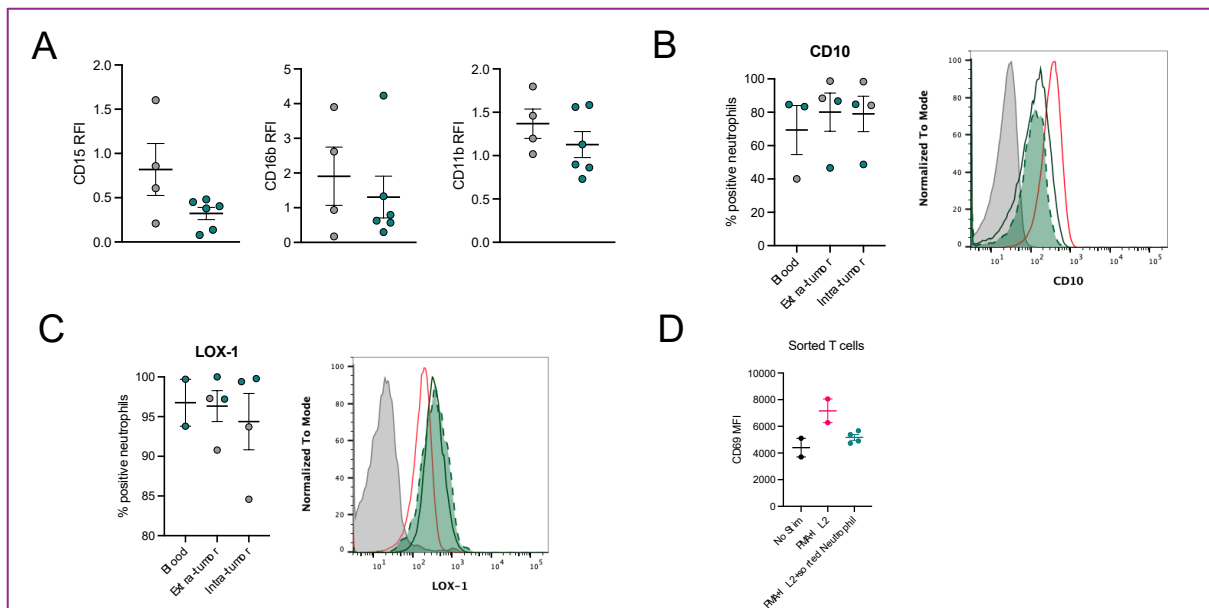


Figure 4. Liver-infiltrating neutrophils in KRASwt patients with poor prognosis have decreased expression of CD15 and resemble PMN-MDSC based on membrane expression of LOX-1 and suppress T cell activation.

A/ Quantification of CD15, CD16b and CD11b on Neutrophils in tumor, represented as the fold-ratio of expression on neutrophils in intra-tumor/extra-tumor tissue. Comparison between patients with good prognosis/low neutrophils (*grey circles*) and patients with high neutrophils/poor prognosis (*green circles*) (Mann-Whitney test). **B/** Quantification of CD10 positive neutrophils in the blood, extra-tumor and intra-tumor tissue. Each dot represents a patient sample and colored according to prognosis (*green=poor prognosis; grey = good prognosis*). Histogram of CD10 expression from N=1 patient with poor prognosis. Unstained (*grey*), blood neutrophils (*red*), extra-tumor neutrophils (*green line*) and intra-tumor neutrophils (*green dotted line-filled*) **C/** Quantification of LOX-1 positive neutrophils in the blood, extra-tumor and intra-tumor tissue. Each dot represents a patient sample and colored according to prognosis (*green=poor prognosis; grey = good prognosis*). Unstained (*grey*), blood neutrophils (*red*), extra-tumor neutrophils (*green line*) and intra-tumor neutrophils (*green dotted line-filled*). **D/** CD69 mean fluorescence intensity on sorted unstimulated T cells (*black*), stimulated T cells (*pink*), and stimulated T cells in the presence of sorted neutrophils from extra-tumor liver tissue from N=1 patient resistant to pre-operative chemotherapy treatment.

T cells and mast cell phenotype are impacted by the unique chemokine and cytokine profile in KRASwt tumor with elevated neutrophil infiltration

Within KRASwt tumors from patients with high neutrophils and decreased RFS, we also observed a diminished infiltration of CD4⁺T, CD8⁺T and mast cells (**Fig 5A**). Furthermore, we observed a trend toward decreased expression of activation marker CD69, on CD8⁺T and CD4⁺T cells, and a decrease in the activation marker CD203c on mast cells (**Fig 5B**). We also observed a trend toward increased PD1 expression, a marker of T cell exhaustion, and decreased ICOS expression, a marker of co-stimulation, on CD8⁺T cells (**Fig 5C**).

We tested the correlation between the cytokines TGF β 2, TNF and CXCL8 on T cell infiltration and mast cell activation. Notably, the cytokines TGF β 2 and TNF were both inversely correlated with both CD4⁺T and CD8⁺T cell infiltration, and mast cell activation (**Fig 5D & 5E**). In the previous chapter we identified that mast cell activation and histamine secretion may be associated with increased T cell infiltration, activation and improved RFS in KRASwt CRC liver metastasis. The activation of mast cells is largely dependent on microenvironment factors, and we identified that TGF β 2 may be key in negatively impacting mast cell activation. It is possible that T cells infiltration is also impacted directly by tumor microenvironment derived cytokines, including TGF β 2 and TNF, as previous studies in mice have demonstrated the blocking of either TGF β or TNF can improve anti-tumor immunity and response to immunotherapy.^{178,310}

To test the prognostic value of both T cells and mast cells on KRASwt patient Relapse-free survival using Kaplan-Meier analysis, we separated patients based on high and low infiltration of Neutrophils and Mast cells (**Fig 6A**) or based on high and low infiltration of Neutrophils and T cells (**Fig 6B**). We observed that either Mast cells or T cells positively impacted RFS in patients with low neutrophils infiltration. The lack of either mast cells or T cells in patients with low neutrophils infiltration negatively impacted RFS. We decided to compare the level of secreted factors TNF, TGF β 2 and Histamine in the three subgroups of patients to test which factor was clearly associated with neutrophil infiltration, versus T cell infiltration (**Fig 6C**). Interestingly, TGF β 2 levels were highest in tumors with high neutrophils, but did not decrease completely in tumors with low neutrophils and low T cells, possibly indicating an immunosuppressive effect on T cells in the absence of neutrophils infiltration. In contrast, TNF secretion appeared to impact neutrophil infiltration but did not rescue T cell infiltration when it was depleted. Strikingly, although mast cell infiltration was slightly increased in patient tumors with low neutrophils/low T cells, the main factor associated with high T cell infiltration in Neutrophil- 'low' tumors was histamine secretion by the mast cells (**Fig 6D**). Therefore, this data suggests that, while elevated neutrophil infiltration is highly detrimental to patient RFS for KRAS wt patients with mCRC, their absence does not always lead to elevated T cell or mast cell infiltration/activation, and this may be due principally to TGF β 2. However, the application of molecules blocking both TNF and TGF β 2 would be most effective for rescuing anti-tumor immunity in KRAS wt mCRC patients.

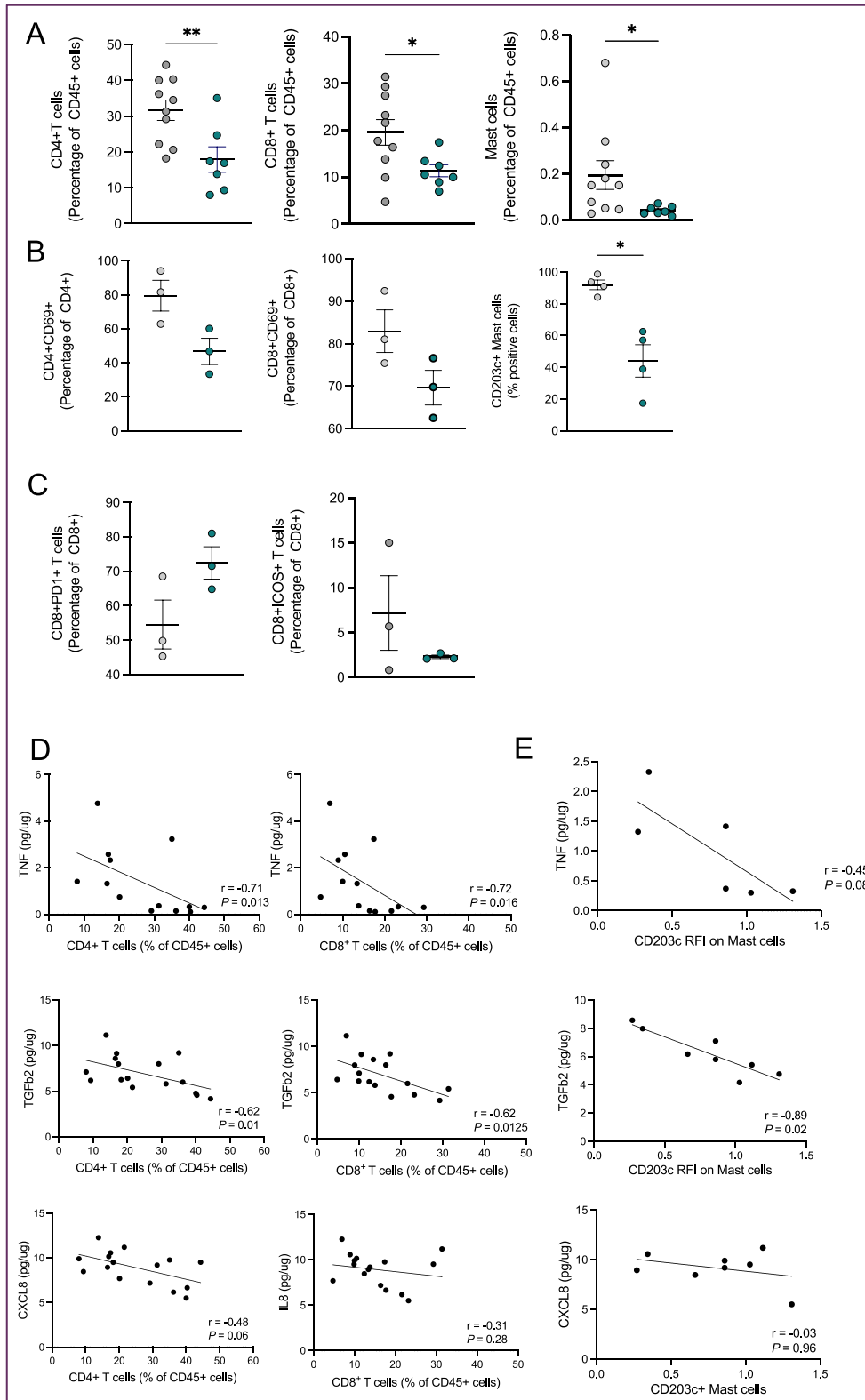


Figure 5 T cells and mast cell phenotype are impacted by the unique chemokine and cytokine profile in KRASwt tumor with elevated neutrophil infiltration. A/ Comparison in the quantification of CD4⁺T, CD8⁺T and mast cells in resected intra-tumor tissue between patients with low neutrophils and good prognosis (*grey circles*), versus patients with high neutrophils and poor prognosis (*green circles*) (Mann-Whitney test, *, $P < 0.05$). **B/** Comparison in the expression of activation marker CD69 on CD4⁺T and CD8⁺T cells, and activation marker CD203c

on mast cells in resected intra-tumor tissue between patients with low neutrophils and good prognosis (*grey circles*), versus patients with high neutrophils and poor prognosis (*green circles*) (Mann-Whitney test, *, $P < 0.05$). **C/** Comparison in the expression of exhaustion marker PD1 and co-stimulation marker ICOS on CD8⁺T cells in resected intra-tumor tissue between patients with low neutrophils and good prognosis (*grey circles*), versus patients with high neutrophils and poor prognosis (*green circles*) (Mann-Whitney test) **D/** Spearman correlation test between secreted CXCL8, TNF, and TGFβ2 and CD4⁺T and CD8⁺T cell infiltration in resected colorectal cancer liver metastases. **E/** Spearman correlation test between secreted CXCL8, TNF, and TGFβ2 and CD203c expression on infiltrating mast cells in resected colorectal cancer liver metastases.

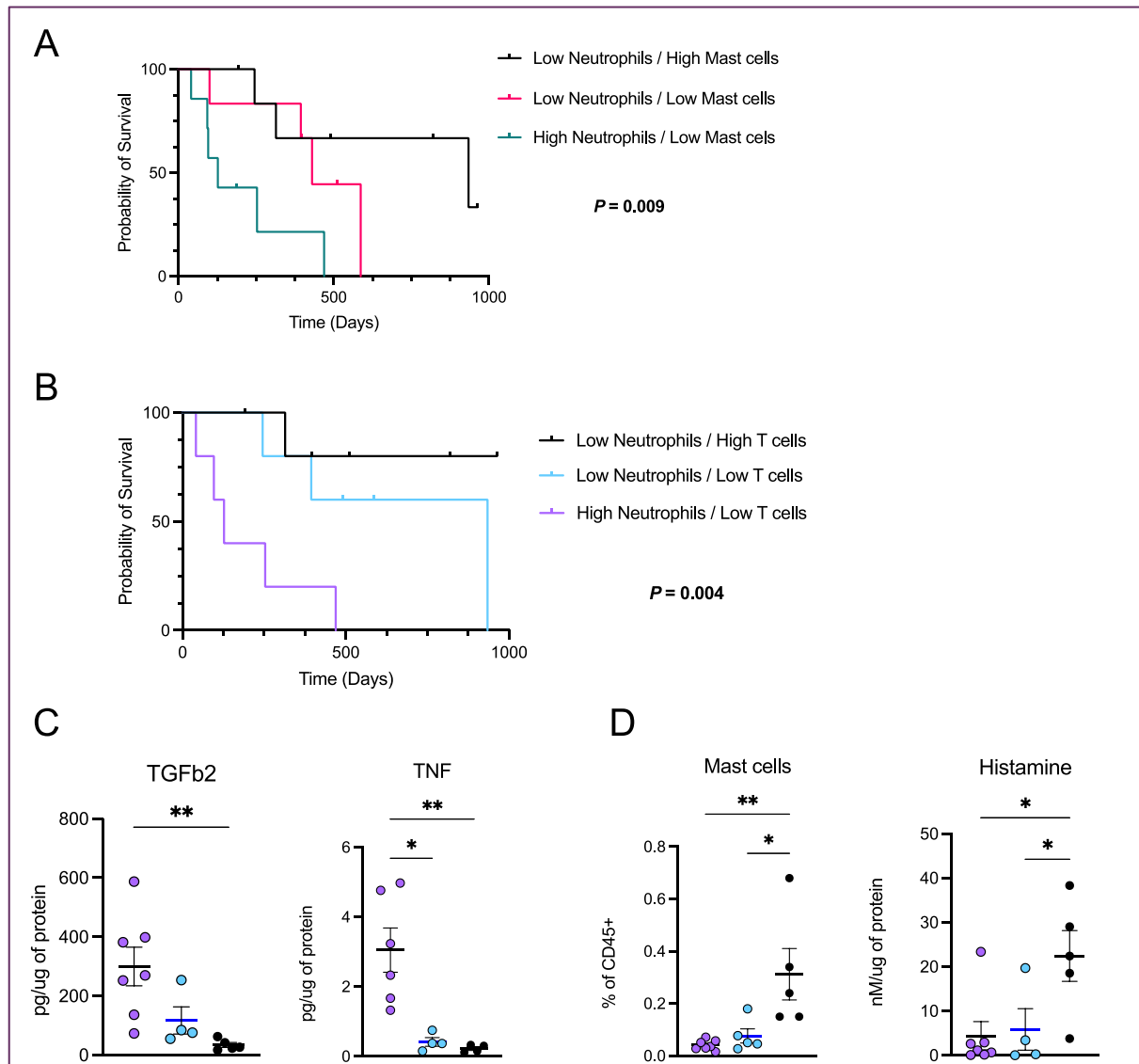


Figure 6 Low neutrophils infiltration in addition to decreased TGFβ2 levels are the limiting factors for elevated mast cell and T cell infiltration and increased RFS. A/ Kaplan-Meier curve for Relapse-free survival, stratified by Neutrophil and Mast cell infiltration in KRAS WT patients (Log-Rank test). **B/** Kaplan-Meier curves for Relapse-free survival, stratified by Neutrophil and T cell infiltration in KRAS WT patients (Log-Rank test). **C/** Intra-tumor secretion of TGFβ2 and TNF in KRAS wt tumors stratified by Neutrophil and T cell infiltration (Kruskal-Wallis

test). **D/** Intra-tumor Mast cell frequency and Histamine secretion in KRAS wt tumors stratified by Neutrophil and T cell infiltration (Kruskal-Wallis test).

Discussion

In this prospective study of mCRC patients undergoing elective surgery for liver metastases, elevated tumor infiltration of neutrophils was associated with decreased relapse-free survival after surgical resection of liver metastasis. For the first time, we demonstrate that this detrimental role of neutrophils is specific to patients with KRASwt mCRC. In these patients, elevated tumor infiltrating neutrophils was correlated with decreased radiologic response before resection, and positively correlated with systemic absolute neutrophil counts (ANC) in the blood. Previous reports have also highlighted the detrimental impact of elevated systemic ANC and survival in CRC and mCRC patients.^{293,311} We also measured variable infiltration of neutrophils in KRASmut tumors, but it did not significantly impact survival in this subgroup. This may be attributed to other immune escape mechanisms at play in KRASmut tumors. Neutrophils infiltrating KRASwt tumors were negatively correlated with CD4⁺T and CD8⁺T cell as well as mast cell infiltration. Notably, both T cell and mast cell infiltration in mCRC were associated with increased RFS in this cohort. These findings corroborate results from previous retrospective studies that relied on immunohistochemistry staining and quantification of T cells and mast cells infiltration in resected mCRC.^{165,210} Neutrophil infiltration in liver tumors was neither impacted by the treatment received prior to surgical resection, nor by the presence of *TP53* mutations among KRASwt patients. These results demonstrate that the infiltration of neutrophils in KRASwt metastatic tumors may more likely reflect an innate or adaptive resistance mechanism of the tumor cells regardless of treatment type, with consequences including diminished immune mediated anti-tumor responses and increased relapse-risk.

The increase in neutrophil infiltration in KRASwt tumors with poor prognosis was also significant at the margin and even within extra-tumor tissue, indicating a systemic mobilization of neutrophils in these patients. Chronic inflammation is implicated in the pathogenesis of cancer, and cancer-related inflammation is considered one of the hallmarks of cancer.^{284,312} Inflammatory cytokines and chemokines from cancer cells are responsible for the mobilization of neutrophils and other MDSC systemically, which promotes tumor progression and metastasis development in distant sites.²⁸⁶ We tested multiple chemokines and cytokines

involved in tumor-related inflammatory response and identified elevated secretion of CXCL8, TGFβ2 and TNF in KRASwt tumors with high neutrophil infiltration and poor prognosis. All three proteins were positively correlated with neutrophil infiltration and inversely correlated with T cell infiltration, while TGFβ2 was inversely correlated with mast cell activation. Of the three, TNF was the most striking because of no overlap between the patient subgroups.

CXCL8, TGFβ2 and TNF secretion have all been reported to play tumor-promoting roles in colorectal cancer, including primary malignancy formation, chemotherapy resistance and metastatic progression.^{178,313–317} These mediators released during CRC progression are also established chemoattractants of neutrophils, linked to their recruitment and modulating their function within the tumor microenvironment to promote immune evasion and liver metastatic spread of CRC.^{287,288,318,319} The Immune suppressing roles of neutrophils within the tumor microenvironment are multiple. Studies in pre-clinical models have demonstrated tumor-derived CXCL8 to elicit the extrusion of neutrophil extracellular traps (NETs), which, in turn favors metastatic tumor seeding in the liver.^{288,320} Furthermore, NETs extruded from neutrophils coat tumor cells, ultimately obstructing infiltration and contact from cytotoxic CD8⁺T cells and NK cells.³²¹ Other studies have reported that TGFβ, including TGFβ2 is responsible for promoting the generation of neutrophils with pro-tumor function, and TGFβ blockade can divert neutrophils towards an antitumor phenotype and improve anti-tumor immune responses.^{287,322–324} Furthermore, elevated TGFβ2 in the tumor microenvironment of CRC is a primary mechanism of immune evasion promoting T cell exclusion in orthotopically transplanted tumors.^{178,287} In liver tumors, cancer-associated fibroblasts (CAFs) are also a major source of TGFβ and promotes the recruitment of pro-tumorigenic neutrophils, leading to a positive feedback loop for TGFβ production.^{255,256,325} During chronic inflammation, elevated levels of TNF is involved in the enhanced recruitment of PMN-MDSC, blocking their natural differentiation and enhancing their immune suppressive functions.^{326,327} As well as modulating neutrophil function, tumor-associated neutrophils express TNF and induce apoptosis of non-activated CD8 T cells.³²⁸ More recently, CXCL1 and TNF production from PMN-MDSCs has been shown to orchestrate therapeutic resistance through CAFs activation and promote liver metastasis in a mouse model of pancreatic ductal adenocarcinoma.^{329,330} TNFR2 blockade with Etanercept reduced CAF inflammation and enhanced chemosensitivity. Importantly, TNF production in PMN-MDSCs was dependent on CXCR2-MAPK signaling, and CXCR2 blockade

was sufficient to activate T cells within the TME in this model. In summary, these studies highlight the various mechanisms through which tumor-infiltrating neutrophils (or PMN-MDSC) can promote tumor progression and block anti-tumor immunity via the mediators, CXCL8, TGF β and TNF. The question remains whether one serves as the key driver of the others or if they all work in tandem to facilitate tumor immune escape within mCRC.

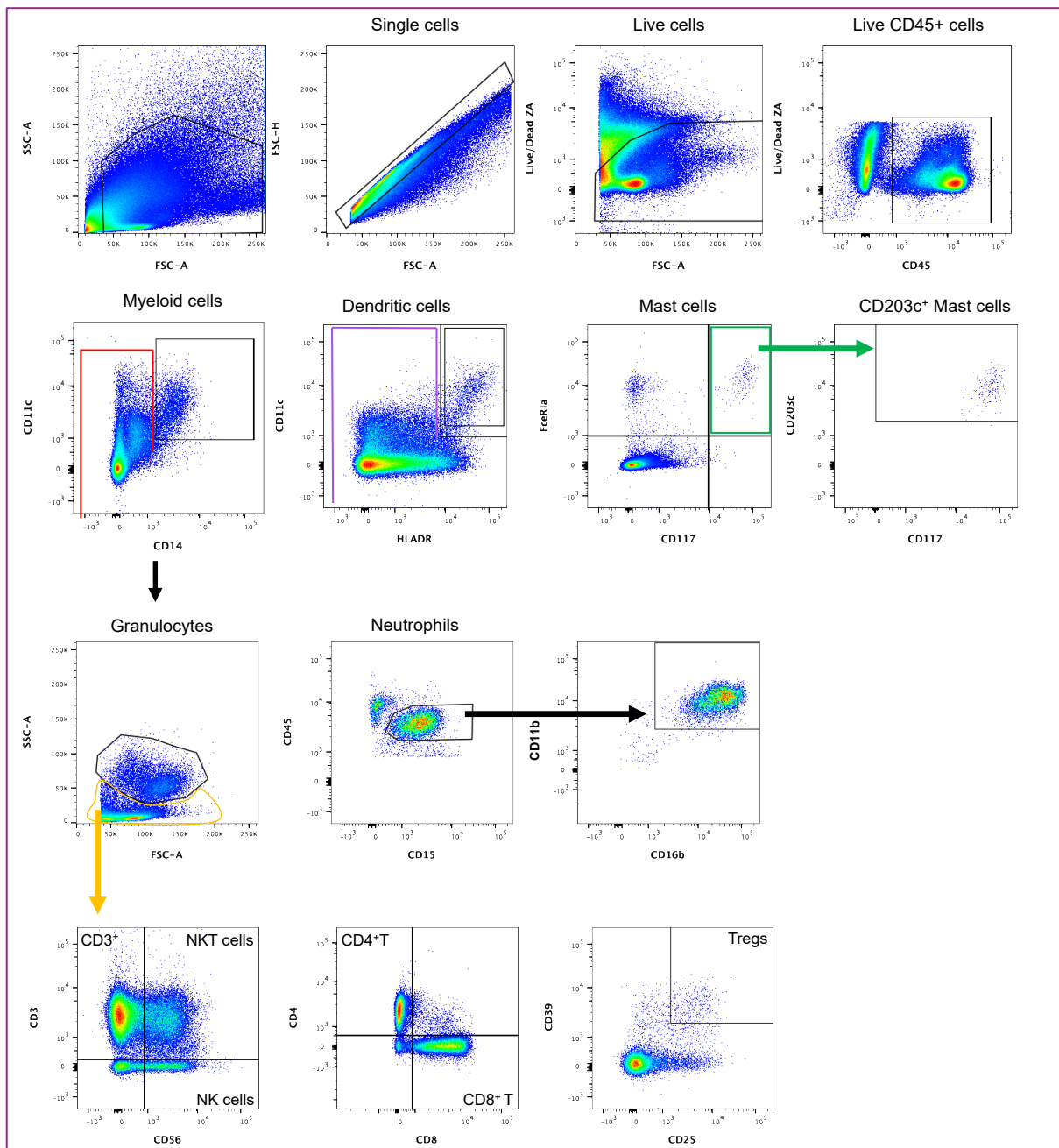
Subdividing patients in subgroups based on neutrophil and T cell infiltration gave us some insight into which was the major factor associated with neutrophils infiltration, which was largely driven by TNF. Secondly, tumors with low neutrophils did not always facilitate T cell infiltration. A subgroup of patients with low neutrophils and low T cells maintained slightly elevated levels of TGF β 2 despite having decreased levels of TNF in the tumors. This suggests that the blocking of only TNF signaling may not restore effective intra-tumoral T cell infiltration or mast cell function and relies on the blocking of both TNF and TGF β 2 signaling pathways.

There are several limitations to the current study. We cannot rule out the role of other gene amplifications which may have occurred in KRASwt mCRC patient tumors resistant to pre-operative therapy, which was beyond the scope of this prospective study. Also, we are uncertain whether neutrophils directly inhibit T cells or if their effects are mediated indirectly through various cytokines and other unidentified cells within the TME of mCRC. Moreover, the precise mediator (CXCL8, TGF β , TNF, or all three) of enhanced mobilization and infiltration of neutrophils in KRASwt mCRC patients remains to be elucidated, as well as the direct source of these mediators, which could be cancer cells, but also could originate from stromal cells including endothelial cells, CAFs and liver-resident macrophages. Understanding which downstream molecules are activated and shared between CXCL8, TGF β and TNF signaling pathways and in which cell type will also guide the optimal mode and target of treatment, which remains unclear and requires further investigation.

In summary, our findings suggest that neutrophils play a negative role in KRASwt mCRC and are associated with poor response to pre-operative therapy and increased relapse-risk post surgical resection. With further validation in external cohorts, these patients could potentially be identified by elevated systemic neutrophils or quantification of elevated secretion of CXCL8, TGF β 2 and TNF by resected tumors. The precise function and mode of recruitment of

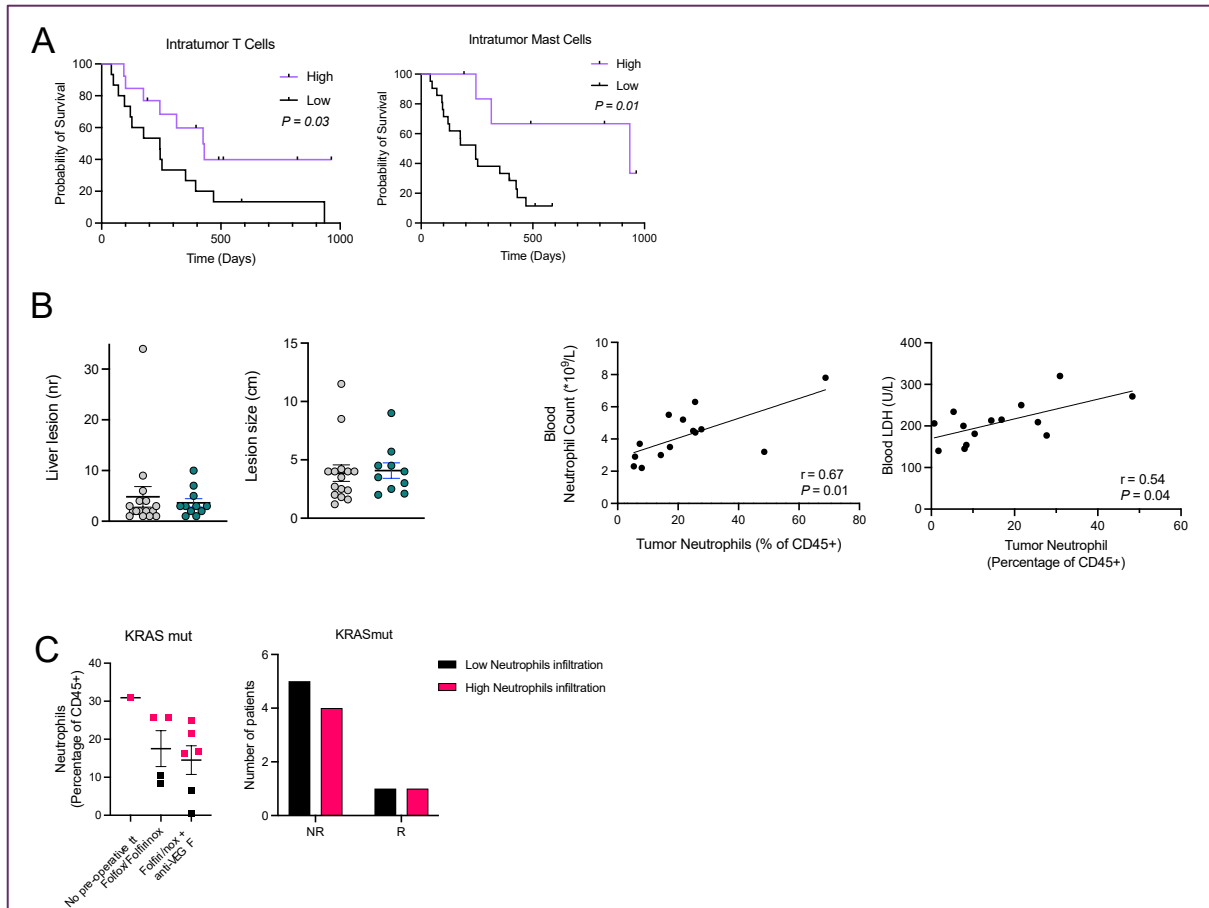
neutrophils in KRASwt mCRC patients remains to be elucidated, necessitating a deeper understanding of the exact mechanisms involved and potential interventions. These insights may lead to novel targeted treatment strategies for KRASwt mCRC patients with poor RFS that could enhance the prospects for patients with mCRC in the future.

Supplementary Figures

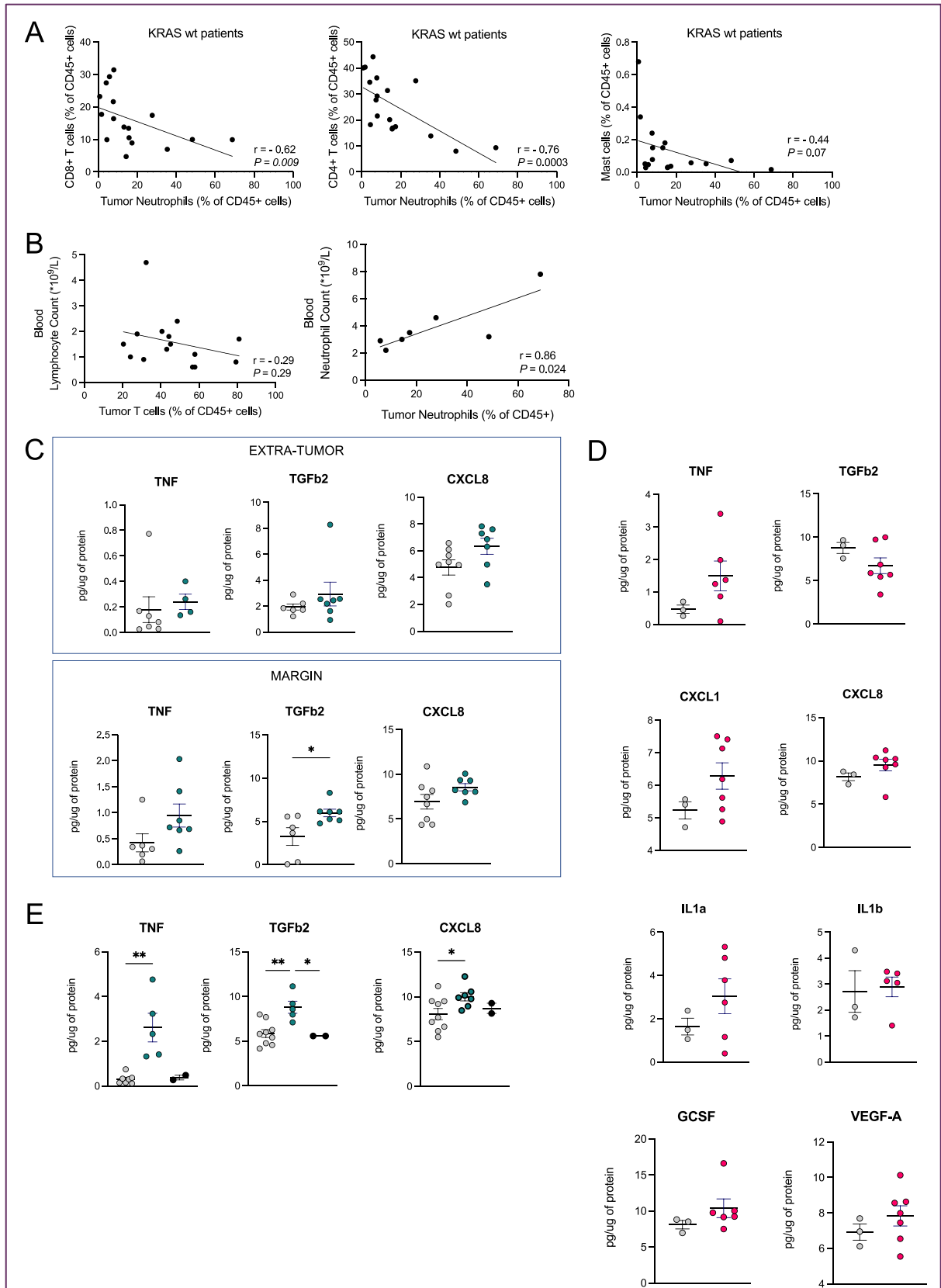


Supplementary Figure 1. Flow Cytometry Panel Gating Strategy

Depiction of gating strategy for 18-color flow cytometry panel is depicted and includes the following cell populations in order: Myeloid cells ($CD11c^+CD14^+$), Dendritic cells ($CD14^-CD11c^{high}HLADR^+$), and Mast cells ($CD117^{high}FceRI^+$), including CD203c expression on mast cells; Neutrophils ($CD11b^+CD14^-CD45^{low}CD15^+CD16b^+$), total T cells ($CD3^+CD56^-$), NK cells ($CD3^-CD56^+$), NKT cells ($CD3^+CD56^+$), CD8+T cells, CD4+T cells, and Tregs ($CD25^{high}CD39^+$).



Supplementary Figure 2. A/ Kaplan-Meier curves for Relapse-free survival, stratified by High or Low intra-tumor frequency of T cells (*left panel*) and stratified by High or Low intra-tumor frequency of mast cells (*right panel*) is depicted. (Log-Rank test) **B/** Quantification of the number and size of liver metastase (*left panel*). The number of metastatic lesions was counted in the liver and the diameter of largest lesions was measured in mCRC patients with 'low intra-tumor neutrophils' (grey circles) versus 'High intra-tumor neutrophils' (green circles); 'Spearman correlation test between Blood Absolute Neutrophil Count (ANC) and Blood LDH levels and Tumor Neutrophils (*right panel*). **C/** Quantification of intra-tumor infiltration with neutrophils in KRAS mut patients treated without or with preoperative chemotherapy (*left panel*); and Response of target lesions to pre-operative treatment in KRAS mut patients. NR (Non-responders) refers to patients with stable disease or progressive disease; and R (Responders) refers to Partial Response, according to RECIST 1.1 guidelines (Eisenhauer EA EJC 2009) in KRAS wt patients with high versus low intra-tumor mast cells (N= 11, Chi-squared test).



Supplementary Figure 3. A/ Spearman correlation test between Tumor CD8⁺T, CD4⁺T, mast cells and Tumor Neutrophils infiltration in resected colorectal cancer liver metastases from KRAS wt patients. **B/** Spearman correlation test between Blood Lymphocyte count and Tumor T cells (*left panel*), and Blood ANC and Tumor Neutrophils (*right panel*) in KRASwt patients. **C/** Comparison in the quantification of secreted inflammatory

chemokines and cytokines in resected extra-tumor tissue (*top panel*) and margin tissue (*bottom panel*) between patients with low neutrophils and good prognosis (*grey circles*), versus patients with high neutrophils and poor prognosis (*green circles*) in KRASwt patients (Mann-Whitney test, *, $P < 0.05$; **, $P < 0.01$; ***, $P < 0.001$). **D/** Comparison in the quantification of secreted inflammatory chemokines and cytokines in resected intra-tumor tissue between patients with low neutrophils (*grey circles*), versus patients with high neutrophils (*pink circles*) in KRASmut patients with poor prognosis (Mann-Whitney test). **E/** Comparison in the quantification of secreted TNF, TGF β 2 and CXCL8 in resected tumor tissue in patients with low neutrophils (*grey circles*), high neutrophils (*green circles*), and tumor organoids supernatant derived from N=2 mCRC KRASwt patients (Kruskal-Wallis test, *, $P < 0.05$; **, $P < 0.01$).

Chapter 3. The immunopathological landscape of primary resected Hepatocellular carcinoma

Héloïse Halse^{1,2}, Chifaou-Mohamed-Djalim^{2,3}, Léonie Bui⁴, Margot Tissandier¹, Delphine Bredel², Severine Mouraud², Aminata Drame², Guillaume Escriou², Marine Andrade², Rim Kalala⁴, Catherine Guettier⁵, Eric Vibert⁴, Mélodie Bonvalet², Amélie Bigorgne^{1,2}, and Aurélien Marabelle^{2,3}

1 Laboratory of Translational Immunotherapy Research (LRTI) INSERM U1015, Gustave Roussy, Villejuif

2 Laboratory of cellular and molecular mechanisms of haematological disorders and therapeutic implications INSERM U1163, IMAGINE Institute, Paris

3 Drug Development Department (DITEP), Gustave Roussy, Villejuif

4 Depart of Visceral and Digestive Surgery, Hepato-biliary Centre, Paul Brousse Hospital, Villejuif

5 Department of Pathology, Kremlin Bicêtre Hospital, Paris

ACKNOWLEDGEMENTS:

Pathologists at Kremlin Bicêtre who provided FFPE tissue

Funding: MSD Avenir

KEYWORDS:

Primary Liver Cancer, immune microenvironment, anti-tumor immunity, Immunotherapy

Introduction

Hepatocellular carcinoma (HCC) is the most common form of liver cancer and is the third leading cause of cancer-related death worldwide.¹ While surgical resection is the mainstay treatment for primary HCC leading to improved survival rates, the risk of recurrence is high.^{331,332} Recent advances in the application of immunotherapies targeting cytotoxic T lymphocyte-associated antigen-4 (CTLA-4), programmed death-1 (PD-1), and programmed death ligand-1 (PD-L1), have profoundly modified the standard of care of HCC.^{67,69} Clinical trials testing peri-operative immunotherapy in resectable HCC are currently ongoing and show promise in patients that display a major objective response to treatment.^{75,230} However, only 20-30% of patient show objective response rates in both early-stage and advanced HCC setting. Therefore, a better understanding of the immunopathologic contexture of primary HCC is needed to improve patient stratification and responses.

The immune microenvironment of HCC plays a crucial role in tumor development and progression.^{221,333,334} Leading risk factors include chronic hepatitis B (HBV) or hepatitis C (HCV) infections, alcohol-related toxicity (ASH) and nonalcoholic fatty liver disease (NAFLD).^{335,336} In chronic-HBV/HCV derived HCC, aberrant immune responses that fail to clear hepatotropic viruses promote tumorigenesis.^{224,337-339} In alcoholic liver disease (ASH), increased macrophage infiltration and reduction in liver CD8⁺T cells, exacerbates liver fibrosis, cirrhosis and promotes cancer growth.³⁴⁰ In the context of NAFLD, chronic inflammation induced by fat accumulation activates 'auto-aggressive' T cells that cause chronic tissue damage and promote cancer growth.²¹⁹⁻²²¹

Recent reports on whole exome, transcriptome, and single cell RNA sequencing have proposed new classifications of HCC subtypes which could explain the heterogeneity of HCC responses to immune checkpoint blockade.^{217,218,341,342} Other studies have leveraged results from different clinical trials to determine correlates of response to different immunotherapies and their various combinations at the molecular and cellular level.^{75,227-229} Monotherapy anti-PD1 treatment has demonstrated its efficacy specifically in resectable HCC patients harboring elevated immune infiltration in their tumors.^{75,230} Using a deconvolution approach on RNA-sequencing data in advanced HCC, elevated infiltration of immunosuppressive Regulatory T cells (Tregs) was negatively associated with response to anti-PD1 monotherapy treatment.²²⁸ Another study showed HCC patients with elevated Treg signature, myeloid cells signature and

angiogenesis marker *KDR* (VEGFR2) benefited from combination treatment Atezolizumab (anti-PDL1) and Bevacizumab (anti-VEGF) compared to Atezolizumab alone.²²⁷ In a separate study, patients with resistance to anti-PD1 therapy were not a homogenous subgroup but represented three subgroups of patients, 'T cell enriched,' 'Angiogenesis' and 'Cell-cycle' subgroups.²³¹ Among T-cell enriched 'non-responders' to anti-PD1, a recent study has identified clonal expansion of PD1^{high}CD39^{positive} 'terminally-exhausted' CD8 T cells and Tregs.²²⁹ Another study has demonstrated the largely heterogenous nature within poorly infiltrated and 'immune-excluded' tumors in HCC, highlighting its complexity and proposing more adapted treatment strategies for each subgroup (Job S et al., submitted). Overall, these studies highlight the heterogenous nature of each responsive and non-responsive immune profiles in HCC dependent on the type of immunotherapy treatment received.

Based on the largely molecular focus of these studies, and because of the relevant overlap in gene expression between several immune cell types, gene expressions may not necessarily correlate with the expression of membrane or extracellular proteins targeted by anti-checkpoint antibodies. We therefore wanted to perform a characterization of immune profiles specifically in early-stage, non-treated HCC, at both the protein (cell surface and extracellular) and transcriptomic level. Our overarching objective is to find clear distinctive immune phenotypes with specific molecular signatures that could be used in routine diagnostic and prognostic assessment in the clinic for improved HCC patient management.

In this chapter, we present our preliminary findings in a prospective cohort of N=28 primary resected HCC patients in collaboration with the Hepatobiliary center at Paul Brousse Hospital.

Materials and Methods

Patient samples

Resected primary liver cancer (intra-tumor and margin) and non-cancerous (extra-tumor) liver tissue was collected prospectively from N=28 surgically treated patients from the pathology department at the Hepatobiliary Center in Paul Brousse Hospital from October 2020 to March 2023. Patient information and sample collection was authorized by the Ministry of Higher Education and Research (DC-2021-4572), and in respect of the reference methodology MR-004 of the French data protection authority (CNIL). Inclusion criteria comprised of (i) patients having not received pre-operative therapy for liver cancer, (ii) complete surgical resection of primary liver cancer for curative intent, and (iii) the availability of clinical, biological and follow-up data post surgical resection. Relapse-free survival was defined as the interval from the date of surgical resection to the date of relapse of metastasis to the liver or within extrahepatic sites.

Tumor staging of patient HCC was performed using the AJCC T classification, and Barcelona Clinic Liver Cancer Staging.⁶³

Liver function score using the Albumin-Bilirubin (ALBI) grade was calculated with the following formula: $(\log_{10} \text{bilirubin (umol/L)} \times 0.66) + (\text{albumin (g/L)} \times -0.0852)$.³⁴³

Liver fibrosis and Liver steatosis measurements were collected from Vibration-Controlled Transient Elastography (FibroScan-Echosens, Paris, France) measurements of Liver stiffness measurement in kPa and Controlled Attenuation parameter (CAP) in dB/m, respectively.

Peripheral Blood Samples

Results from peripheral blood tests performed preoperatively were obtained to record liver enzymes Alkaline Phosphatase (AP), Alanine Transaminase (ALT), Aspartate Aminotransferase (AST), gamma-glutamyl transferase (GGT) and Lactate Dehydrogenase (LDH), liver proteins Albumin and Bilirubin for ALBI grade measurement. Other measurements included tumor marker Alpha-fetoprotein (AFP), and systemic markers of inflammation C-reactive protein (CRP), Neutrophil-lymphocyte ratio (NLR) and derived Neutrophil-leucocyte ratio (dNLR).

Histology

Resected intra-tumor, margin and extra-tumor liver tissue were fixed in 10% buffered formalin and embedded in paraffin. Sections were stained with H&E. Histopathologic evaluation was

assessed by certified pathologist (C.G) and included AJCC scoring, satellite nodules, microvascular invasion, and liver fibrosis scores.

Sample preparation for RNA-sequencing and Whole Exome Sequencing

Intra-tumor, margin and extra-tumor tissue areas were drawn out by certified pathologist (C.G) and 10-15 FFPE tissue sections of 10 μ m thickness were prepared (H.H) in Eppendorf tubes for downstream RNA-sequencing and Whole exome sequencing analysis of each tissue zone by BGI Genomics.

Preparation of intra-tumor, margin, and extra-tumor liver tissue storage solution for secreted soluble factor measurement

Resected intra-tumor, margin and extra-tumor liver tissue solution was prepared by storing immediately each respective tissue in 3-5 milliliters of physiologic solution at 4°C. Following 4-hour storage, the supernatant was harvested by centrifugation at 1800RPM for 10 minutes and stored in aliquots at -80°C, and the tissue was stored overnight at 4°C in tissue storage solution before dissociation.

Tumor dissociation and flow cytometry staining

Fresh samples of intra-tumor, margin and extra-tumor liver tissue were weighed and cut into small fragments of 1-2mm in diameter using a sterile scalpel blade and petri dish. Tissue fragments were transferred to a C-tube (Miltenyi Biotec, DE) and 5-10mL of enzyme digestion mixture consisting of RPMI 1640 medium (Gibco, MT), 50 U/mL Collagenase IV, 30 U/mL DNase I and 280 U/mL Hyaluronidase (Merck, DE) was added. The tubes were placed on to the GentleMACS dissociator (Miltenyi Biotec, DE) and subjected to mechanical and enzymatic dissociation using the program TDK_1 (incubation for 1 hour at 37°C). The dissociated tissue mixture was then filtered using a 70 μ m sterile filter and the cell suspension washed 1x in 50mL of sterile Phosphate-buffered saline (PBS) followed by a second wash in cold sterile PBS with 2% Bovine Serum Albumin and 2mM EDTA (staining buffer) and final resuspension in 2mL of staining buffer.

An initial phenotyping and counting step were performed. A 50 μ l aliquot of the cell suspension was stained for 20 minutes at 4°C with anti-CD45 FITC (BD Biosciences, NJ), anti-CD3 BUV395 (BD Biosciences, NJ), anti-CD56 AF647 (BD Biosciences, NJ), and anti-CD19-PECF594 (BD Biosciences, NJ). The cells were washed with 1mL of cold staining buffer and resuspended in

50 μ l of Precision Count Beads (BioLegend, CA). 5ul of 7AAD solution (Miltenyi Biotec, DE) was added to the suspension, the cells vortexed and immediately acquired on the BD FORTESSA X-20.

Following the counting step, a minimum of 100,000 CD45⁺ cells were stained with 5ul of FcR block (BioLegend, CA) for 10 minutes, after which the cells were stained using flow cytometry antibodies listed in Annex Table 1 and Zombie Aqua Fixable Viability Dye (BioLegend, CA) at the dilutions indicated in final volume of 100 μ l of cold staining buffer at 4°C for 30 minutes. After staining, the cells were washed twice in staining buffer. Following the wash step the cells were fixed and permeabilised with eBioscience™ Intracellular Fixation and Permeabilization Buffer Set following the instruction manual. After this step, the cells were stained intracellularly for FOXP3 at 4°C for 30 minutes. After staining, the cells were washed twice in permeabilization wash buffer and resuspended in PBS for acquisition.

For N=10 samples with higher numbers of CD45⁺ cells, a further 100,000 CD45⁺ cells were stained with 5ul of FcR block (BioLegend, CA) for 10 minutes, after which the cells were stained using flow cytometry antibodies listed in Annex Table 2 and Zombie Aqua Fixable Viability Dye (BioLegend, CA) at the dilutions indicated in final volume of 100 μ l of cold staining buffer at 4°C for 30 minutes. These antibodies were specific for monocytes/macrophages, dendritic cells, and granulocytes including neutrophils. After staining, the cells were washed twice in staining buffer. Following the wash step the cells were fixed and permeabilised with eBioscience™ Intracellular Fixation and Permeabilization Buffer Set following the instruction manual. After this step, the cells were stained intracellularly for CD68 and CD163 at 4°C for 30 minutes. After staining, the cells were washed twice in permeabilization wash buffer and resuspended in PBS for acquisition.

All events were acquired on the BD FORTESSA X-20 cytometer equipped with BD FACSDiva software (BD Biosciences, NJ), and data were analyzed using FlowJo software (Tree Star, OR). For unsupervised analysis of cell phenotypes, Euclidean distance and hclust method were applied with Pheatmap package in R.

Secreted soluble cytokine, chemokine, and growth factor measurement

Soluble cytokines, chemokines and growth factors secreted by intra-tumor, margin and extra-tumor liver tissue were measured in physiologic solution using Mesoscale Discovery biomarker

electrochemiluminescence detection assay kits according to the manufacturer’s instructions (MSD, MA).

For unsupervised analysis of cytokine secretion, Euclidean distance and Average clustering method were applied with Pheatmap package in R.

Bioinformatics analysis

Normalised read-count values from bulk RNA-seq data in 26 HCC tumors was retrieved from Dr. Tom Data Visualisation tool (BGI Genomics) for Gene Set Enrichment Analysis (GSEA) for enriched pathways and gene signatures using the MSigDB gene set database.

Differential expression analysis was performed within the Dr. Tom Data Visualisation tool (BGI Genomics) with DESeq2, selecting differentially expressed genes with minimum fold change of 1.3 and adjusted p-value and Q-value <0.05.

Statistical analysis

Differences between two groups was analyzed using Wilcox t-test, and Kruskal-Wallis test when differences between more than two groups were assessed. Correlations between parameters were assessed using Spearman correlation test.

Statistical tests were performed using Prism 9 software and R studio version 2022.12.0.

All tests were 2 sided, with $P < 0.05$ considered as statistically significant.

Annex

Reagent	Clone	Reference	Dilution
BD Horizon™ BUV805 Mouse anti-human CD45	HI30	612891 RRID: AB_2870179	1/50
BD Horizon™ BUV496 Mouse anti-human CD4	SK3	612936	1/50
BD Horizon™ BUV396 Mouse anti-human CD3	UCHT1	563546 RRID: AB_2744387	1/50
BD Horizon™ BUV650 Mouse anti-human CD56	HCD25	564057 RRID: AB_2738568	1/50
BioLegend® BV711 Mouse anti-human CD69	FN50	310944 RRID: AB_2566466	1/30
BD Optibuild™ BV786 Mouse anti-human CD11b	ICRF44	742642 RRID: AB_2740935	1/50

BD Pharmingen™ APC-H7 Mouse anti-human CD8	SK1	560179 RRID: AB_1645481	1/50
BioLegend® AF700 Mouse anti-human HLA-ABC	W6/32	311438 RRID: AB_2566306	1/50
BioLegend® PC7 Mouse anti-human CD25	BC96	302612 RRID: AB_314282	1/50
BD Pharmingen™ PE Mouse anti-human CD14	M0P9	562691 RRID: AB_2737725	1/50
BD Pharmingen™ PerCPCy5.5 Mouse anti-human HLA-DR	G46-6	552764 RRID: AB_394453	1/50
eBiosciences® APC Mouse anti-human FOXP3	PCH101	17-4776-42 RRID: AB_1603280	1/30
Zombie Aqua™ Fixable Viability kit	BioLegend®	423102	1/1000

Table 2. Flow Cytometry Reagents – Myeloid/Granulocytes Panel			
Reagent	Clone	Reference	Dilution
BD Horizon™ BUV805 Mouse anti-human CD45	HI30	612891 RRID: AB_2870179	1/50
BD Horizon™ BUV395 Mouse anti-human CD3	UCHT1	563548 RRID: AB_2744387	1/50
BD OptiBuild™ BUV737 Mouse anti-human FceR1a	AER-37	749338 RRID: AB_2873712	1/50
BD Horizon™ BUV496 Mouse anti-human CD16	3G8	612944 RRID: AB_2870224	1/50
BioLegend® Pacific Blue™ Mouse anti-human CXCR2	5E8	320724 RRID: AB_2800843	1/50
BD Horizon™ BV605 Mouse anti-human CD117	104D2	562687 RRID: AB_2737721	1/50
BioLegend® BV650 Mouse anti-human PDL1	29E.2A3	329740 RRID: AB_2629614	1/50
BD Horizon™ BV711 Mouse anti-human CD33	WM53	563171 RRID: AB_2738045	1/50
BD OptiBuild™ BV786 Mouse anti-human CD11B	ICRF44	740965 RRID: AB_2740590	1/50
BD Pharmingen™ APC-H7 Mouse anti-human HLA-DR	G46-6	561358 RRID: AB_10611876	1/50
BD Horizon™ PECF594 Mouse anti-human CD15	W6D3	562372 RRID: AB_11153311	1/50

BD Pharmingen™ PE Mouse anti-human CD14	MOP9	562691 RRID: AB_2837725	1/50
BioLegend® PE-Cy7 Mouse anti-human CD11c	3.9	301608 RRID: AB_389351	1/50
BioLegend® APC Mouse anti-human CD68	Y1/82A	333810 RRID: AB_2275735	1/50
BD Pharmingen™ FITC Mouse anti-human CD163	GHI/61	563697 RRID: AB_2738379	1/50
Zombie Aqua™ Fixable Viability kit	BioLegend®	423102	1/1000

Results

Primary resected Hepatocellular Carcinoma patient cohort

28 patients with primary resected Hepatocellular Carcinoma (HCC) were included in the study (2 women and 26 men; median age 72 years). Patient demographics and tumor characteristics are described in **Table 1**. Most patients (64%) were diagnosed with early-stage (BCLC stage A) HCC and had good liver function as measured by the ALBI test. AJCC staging was divided mostly between T1b and T2 stages. T1b represents a single tumor lesion of more than 2cm and no microvascular invasion; T2 represents a single tumor lesion of more than 2cm with microvascular invasion or more than one lesion less than 5cm. For the most part (70%), T2 stage patients in this cohort had a single tumor lesion with intra-tumor microvascular invasion. The median follow-up was 14.5 months (range 1 – 30 months). Following surgical resection, only 5 patients (18%) suffered relapse and therefore a median survival time was not defined for this study. 80% of relapses occurred in the liver.

Characterization of the liver immune microenvironment

Resected intra-tumor, margin and extra-tumor liver tissue were prospectively collected from patients treated with surgical resection of primary HCC (**Fig 1**). Each resected tissue was initially stored in physiologic solution for 4 hours. This solution was then harvested for downstream analysis of secreted soluble factors (i.e. cytokines, chemokines and growth factors) by the respective tissue. The resected tissue was then processed by mechanical and enzymatic dissociation for downstream flow cytometry analysis. A multiparametric flow cytometry panel was designed to assess the frequency and distribution of lymphocytes (including CD8 T, CD4 T, regulatory T cells (Tregs), NK, and NKT cells), and myeloid cells (including Monocytes/Macrophages/Dendritic cells, and Neutrophils) to gain a comprehensive view of the liver immune microenvironment. The gating strategy is described in **Supp. Figure 1**. For N=10 patients with sufficient CD45⁺ leucocyte cell infiltration, an additional panel characterizing myeloid cell subsets, dendritic cells and neutrophils was also performed. The gating strategy for this panel is described in **Supp. Figure 2**. Monocytes/Macrophage/Dendritic cells were identified as CD11B⁺HLADR⁺ cells and were strongly correlated with CD68⁺CD163⁺ double-positive macrophages (**Supp. Fig 3A**). Furthermore, their frequencies were similar in paired samples. This cell profile also positively correlated with CD68⁺ single-positive macrophages as well as CD14⁻CD11C⁺HLADR⁺ dendritic cells. Neutrophils were identified as CD11B⁺HLADR⁻ cells and were strongly correlated with

Neutrophils identified in the myeloid panel as CD45^{low}CD15⁺CD16b⁺ cells (see Supp Figure 2 for the gating strategy of myeloid cells).

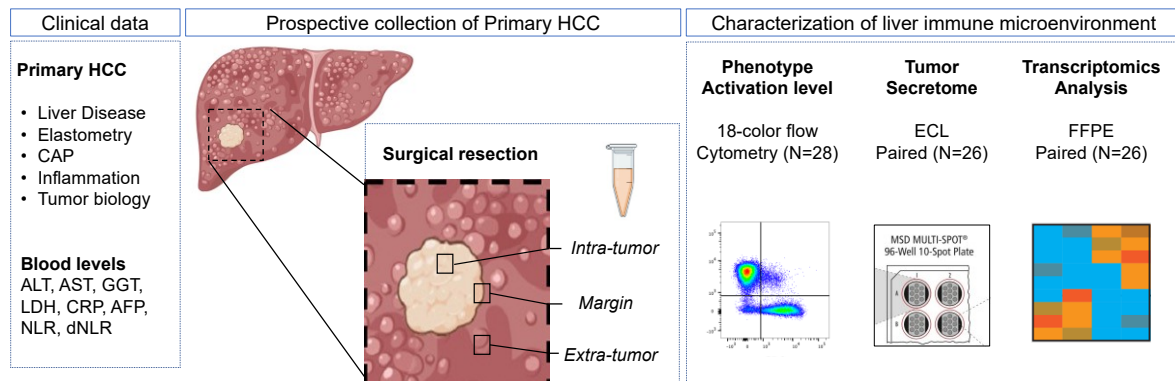


Figure 1: Prospective study of the immune microenvironment in surgically resected primary liver cancer Fresh samples of resected tumor from 28 patients undergoing curative resection for primary liver cancer were prospectively collected, and when possible, at the margin and in extra-tumor liver tissue. Characterization of the immune microenvironment was undertaken by (i) 18-color flow cytometry analysis of liver-infiltrating lymphocytes and myeloid cell populations, (ii) Electrochemiluminescence measurement of secreted protein, and (iii) transcriptomics analysis.

The frequency of immune cell subsets in HCC are differentially enriched and define four distinct subgroups of patients.

Comparative analyses were performed between intra-tumor, margin and extra-tumor samples obtained from HCC patients treated with surgical resection (**Fig 2A & 2B**). The frequency of CD4⁺ T cells, Tregs and Monocytes/Macrophage/Dendritic cells (CD11B⁺HLADR⁺ cells) were significantly higher compared to the extra-tumor immune infiltrate. Among innate lymphoid cells, the frequency of NKT cells were significantly lower in the tumor compared to the peritumor and extra-tumor infiltrate. The frequencies of Neutrophils (CD11B⁺HLADR⁻ cells), CD8⁺ T cells, Innate T (CD4⁻CD8⁻) cells and NK cells did not differ. The profiles of each immune cell subtype showed high variability across patients, indicating differential enrichment of cell subsets. Therefore, unsupervised hierarchical clustering was applied to determine distinct immune subclasses within the HCC tumors (**Fig 2C**). With this method, four immune subclasses were identified, #CD8, #CD4, #NK and #M-DC cell clusters. Each cluster was named by the dominant immune cell subset enriched within the respective cluster (**Fig 2D**). The #CD4 cluster was predominantly patients with Alcoholic Steatohepatitis etiology (70%) and AJCC T2 stage tumors ($P = 0.01$, chi-squared test). The #CD8 cluster had a higher percentage of CD45⁺ cells infiltration compared with #NK and #M-DC clusters (**Supp Fig 4**), while the #CD4 cluster had a more variable level of CD45⁺ cell infiltration. Systemic levels of AFP in patients within the #CD8 and #CD4 clusters were significantly increased compared to patients within the #NK

cluster. However, AFP levels for only four patients were elevated (above normal limit of 10ug/L) and we do not know if the differences in AFP levels below the normal upper limit of 10ug/L are also clinically significant. We did not find other biological or clinical markers that were significantly associated with the immune subclasses (**Supp. Fig 4**). This can in part be explained by the fact that most systemic tumor inflammation markers (LDH, NLR and dNLR) were below the normal upper limit level. Therefore, the immune subclasses in this cohort were more likely influenced by the respective liver immune and tumor microenvironment within each subtype.

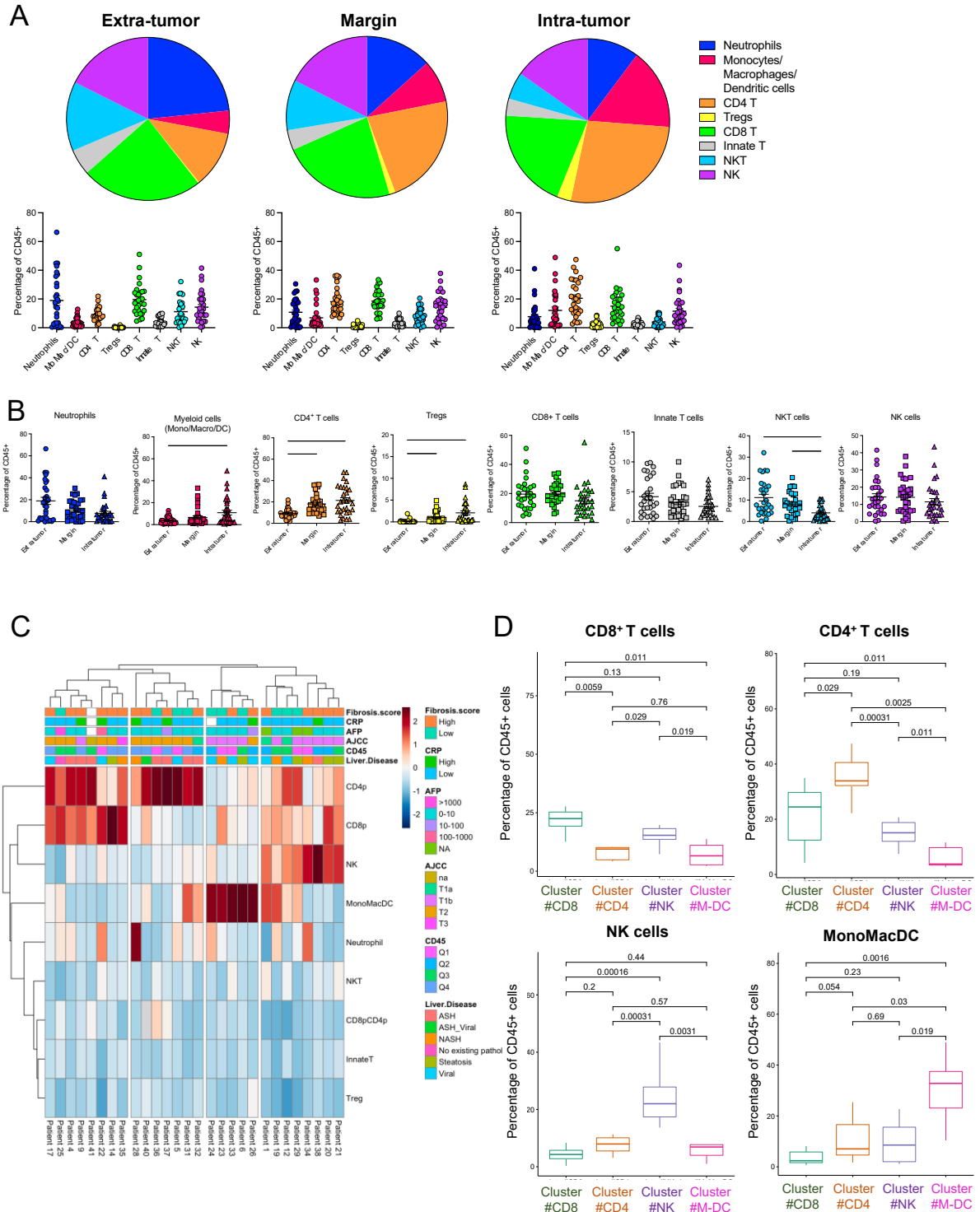


Figure 2: Tumor immune infiltration of lymphocytes, neutrophils and myeloid cells in primary resected HCC **A/** The mean frequency among CD45⁺ cells of Neutrophils (CD11B⁺HLADR^{neg}), Monocytes/Macrophages/Dendritic cells (CD11B⁺HLADR^{pos}), CD4⁺T cells, Tregs, CD8⁺T cells, Innate T cells, NKT cells, and NK cells are depicted as pie charts in extra-tumor, margin and intra-tumor liver tissue (*top panel*) and depicted per patient (*bottom panel*). Each dot represents an individual sample. **B/** Dot plots showing the frequency of cells in **A** in extra-tumor, margin and intra-tumor tissue (*, P < 0.05; **, P < 0.01; ***, P < 0.001Kruskal-Wallis test). **C/** Unsupervised clustering of major tumor-infiltrating immune cell subsets distinguishes patients into 4 subgroups, from left to right, Cluster#CD8, Cluster#CD4, Cluster#NK and Cluster#M-DC (myeloid and dendritic cell) cluster. **D/** The frequency of Intra-tumor CD8⁺T cells, CD4⁺T cells, NK cells, and Monocytes/Macrophages/Dendritic cells

(MonoMacDC) among CD45⁺ cells are presented across patients and compared between intra-tumor clusters from **C** (Wilcox test).

Unsupervised hierarchical clustering was also applied on immune cell frequencies at the margin and extra-tumor zones to determine whether there were direct associations with intra-tumor immune clusters (**Supp Fig 5A-C**). We observed that the intra-tumor #CD8 and #CD4 clusters were associated with elevated CD8 and CD4 T cell infiltration at the tumor margin (**Supp Fig 5A**). The intra-tumor #NK cluster was associated with elevated NK cell infiltration at both margin and extra-tumor liver tissue (**Supp Fig 5A-C**). Interestingly, liver fibrosis, graded in the extra-tumor liver tissue, was associated with elevated CD8 and NK cells, whereas patients with low fibrosis had elevated neutrophils within extra-tumor liver tissue.

Resident, activation, and exhaustive state of T cells are different across immune clusters

CD69 and PD1 expression on lymphocyte subsets infiltrating HCC was assessed to characterize the resident/activation phenotype and functional state, respectively (**Fig 3A**). The mean fraction of PD1 expression on CD69^{pos} and CD69^{neg} subsets of CD8⁺T cells, CD4⁺T cells and NK cells across the intra-tumor immune clusters (#CD8, #CD4, #NK, and #M-DC) were compared. Overall, the #M-DC cluster contained the lowest fraction of CD69^{pos}CD8⁺T cells, and these cells poorly expressed PD1. This may indicate poor activation and recruitment of CD8⁺T cells within the tumor (**Fig 3B**). CD69 expression on CD8⁺T cells are identified as tissue-resident memory cells in the liver.^{138,139} They are functionally competent cells associated with improved PFS in HCC patients treated with anti-PD1.²²⁶ However, the frequency of this subset of cells was highly variable in the #CD8 cluster. This implies that the patients within the #CD8 cluster contain may contain two subgroups according to CD69^{pos}PD1^{pos} CD8⁺T cells.

The #CD4 cluster was characterized by the strongest infiltration of CD69^{pos} CD4⁺T cells that expressed high levels CD69 and PD1 (**Fig 3A & 3C**). Previous studies have demonstrated CD69^{pos} CD4⁺T cells are resident T cells of the liver and possess strong cytotoxic properties.¹⁴⁰ However, their high expression of PD1 suggests that the cells may be chronically stimulated and therefore exhausted within the #CD4 cluster. A previous study has reported the hyporesponsiveness of CD4⁺ T cells infiltrating HCC although not all cells are functionally impaired.³⁴⁴ The #CD4 cluster also demonstrated an increased infiltration Tregs and of PD1-positive Tregs compared the #NK cluster, underlining an immunosuppressive nature specific

to the #CD4 cluster, despite its high infiltration of lymphocytes. We compared the ratio between the frequency of PD1^{pos}CD69^{pos}CD8⁺T cells and PD1⁺ Tregs between clusters and observed that this ratio was lowest in the #CD4 cluster compared to either the #CD8 and #NK clusters (**Fig 3E**).

Regarding the NK cells residency phenotype, relatively equal proportions of tumor-infiltrating NK cells were CD69^{pos} and CD69^{neg} across the clusters (**Fig 3A**). CD69 is known to be expressed on resident NK cells of the liver.³⁴⁵ Liver-resident NK cells have an immature phenotype and expressing high levels of CD56 and produce fewer cytotoxic mediators than non-resident NK cells. Therefore, the main difference in the NK cluster was the increased frequency of both resident and non-resident NK cells infiltrating the tumor.

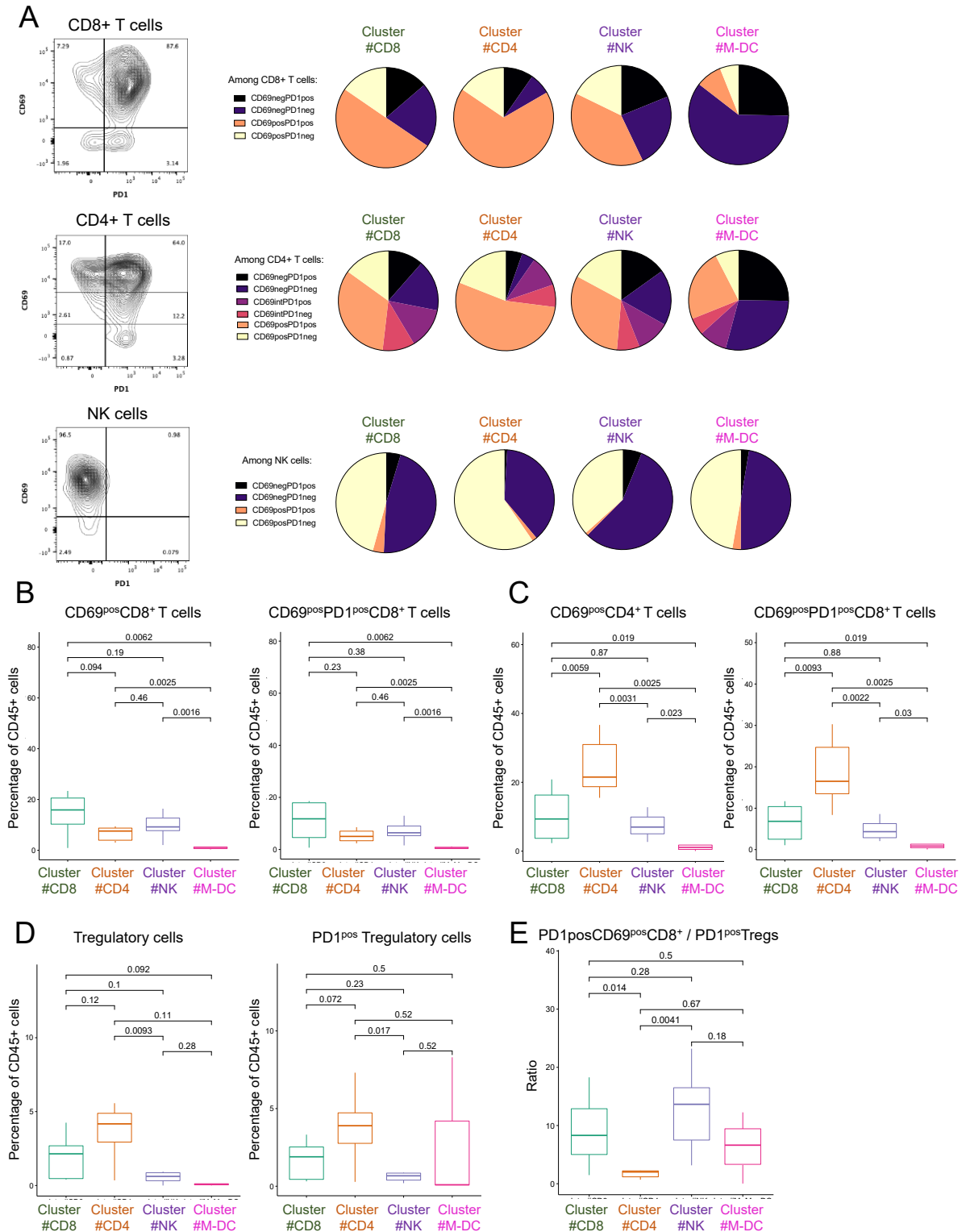


Figure 3. Intra-tumor profiles of T cell activation and exhaustion are distinct across intra-tumor clusters **A/** Contour plot of CD69 and PD1 expression on CD8⁺ T cells, CD4⁺ T cells and NK cells (*left panel*); pie charts reflecting the mean fraction of PD1 expression on CD69^{pos} and CD69^{neg} subsets of CD8⁺ T cells, CD4⁺ T cells and NK cells across the intra-tumor immune clusters (#CD8, #CD4, #NK, and #M-DC). **B/** The frequency of CD69^{pos} CD8⁺ T cells and PD1^{pos}CD69^{pos} CD8⁺ T cells compared across resected HCC immune clusters (wilcox t-test). **C/** The frequency of CD69^{high} CD4⁺ T cells and PD1^{pos}CD69^{high} CD4⁺ T cells compared across resected HCC immune clusters (wilcox t-test). **D/** The frequency of T-regulatory cells and PD1^{pos} T-regulatory cells compared across resected HCC immune

clusters (wilcox t-test). **E/** The ratio between PD1^{pos}CD69^{pos} CD8⁺ T cells and PD1^{pos} T-regulatory cells compared across resected HCC immune clusters (wilcox t-test).

Different profiles of secreted soluble factors within HCC tumors

Secreted chemokines, cytokines and growth factors were quantified within the intra-tumor physiologic storage solution to measure differences in inflammatory profiles across patients. Unsupervised hierarchical clustering was performed on the normalized values to the total secreted protein to compare tissue samples (**Fig 4A**). This clustering permitted us to see three subgroups of patients emerge, although there was no precise distinction between the intra-tumor immune clusters identified by flow cytometry, particularly for the #CD4, #CD8 and #NK clusters. The left subgroup contained all patients identified within the #M-DC cluster and some patients from the #NK cluster (**Fig 4B**). Apart from MIF, SCF, and VEGFD this subgroup secreted lower levels of all other detected cytokines and chemokines and was called 'non-inflammatory'. Macrophage migration inhibitory factor (MIF) has been recently reported as an important regulator in the promotion of tumor metastasis and invasion as well as tumor-associated macrophage infiltration in HCC and represents a promising therapeutic target.³⁴⁶ The second, middle subgroup contained a mixture of patients from the #CD4, #CD8 and #NK cluster and secreted high levels of multiple cytokines and chemokines notably Perforin, Granzyme B, CXCL10, CCL17 and VEGF-A and was called 'cytotoxic' (**Fig 4C**). These chemokines and cytokines were comparatively less expressed in the third subgroup, which also contained a mixture of patients from the #CD4, #CD8 and #NK clusters and was therefore called 'non-cytotoxic'. This subgroup secreted elevated levels of pro-inflammatory cytokine IL18 and less of its natural inhibitor IL18 Binding Protein (IL18BP) compared to the 'cytotoxic' group (**Fig 4D**). We checked for differences in PD1 expression on lymphocytes between the 'cytotoxic' and 'non-cytotoxic' subgroups based on the secretory profile and observed a higher frequency of PD1 expression on CD4⁺ T cells and Tregs in the 'cytotoxic' subgroup (**Fig 4E**). There was a trend towards increased PD1⁺ CD8⁺ T cells although this difference was not statistically significant. Therefore, the 'cytotoxic' subgroup contains a mixture of patients from #CD8, #CD4 and #NK clusters and may represent patients with an activated but exhausted signature, with immunosuppressive mechanisms driven by the enhanced activation of Tregs and/or through VEGF-A mediated immunosuppression.

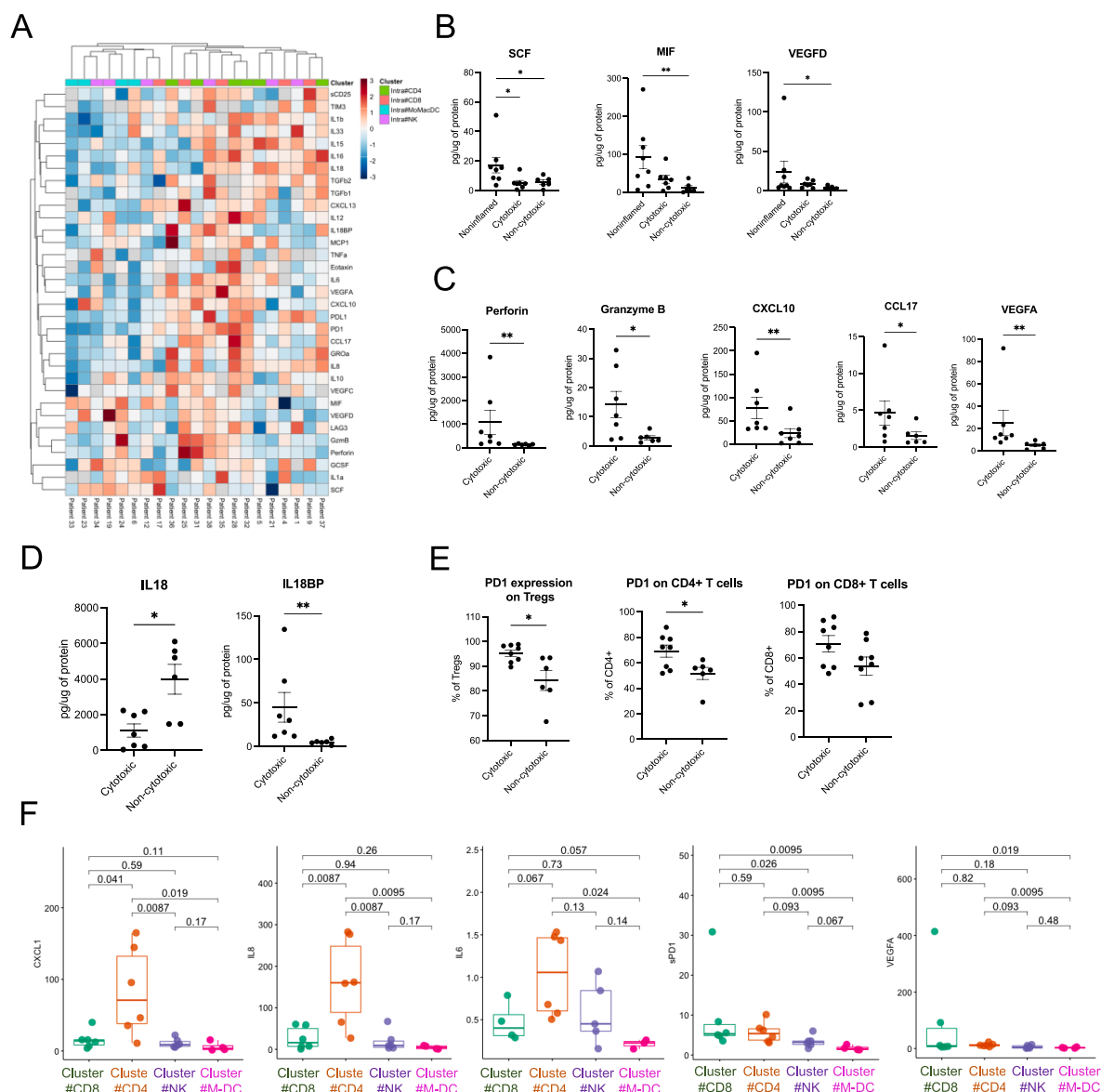


Figure 4: Distinct secretory profiles correlated with HCC tumor immune clusters **A/** Unsupervised clustering of the secreted factors in HCC **B/** Box plots showing the quantity of CXCL1, IL-6 and IL-8 secretion in HCC tumors between intra-tumor immune clusters (Wilcox t-test). **C/** Box plots showing the quantity of sPD1, sPD-L1 and VEGF-A secretion in HCC tumors between intra-tumor immune clusters (Wilcox t-test). **D/** Box plots showing the quantity of MIF and VEGF-D secretion in HCC tumors intra-tumor immune clusters (Wilcox t-test).

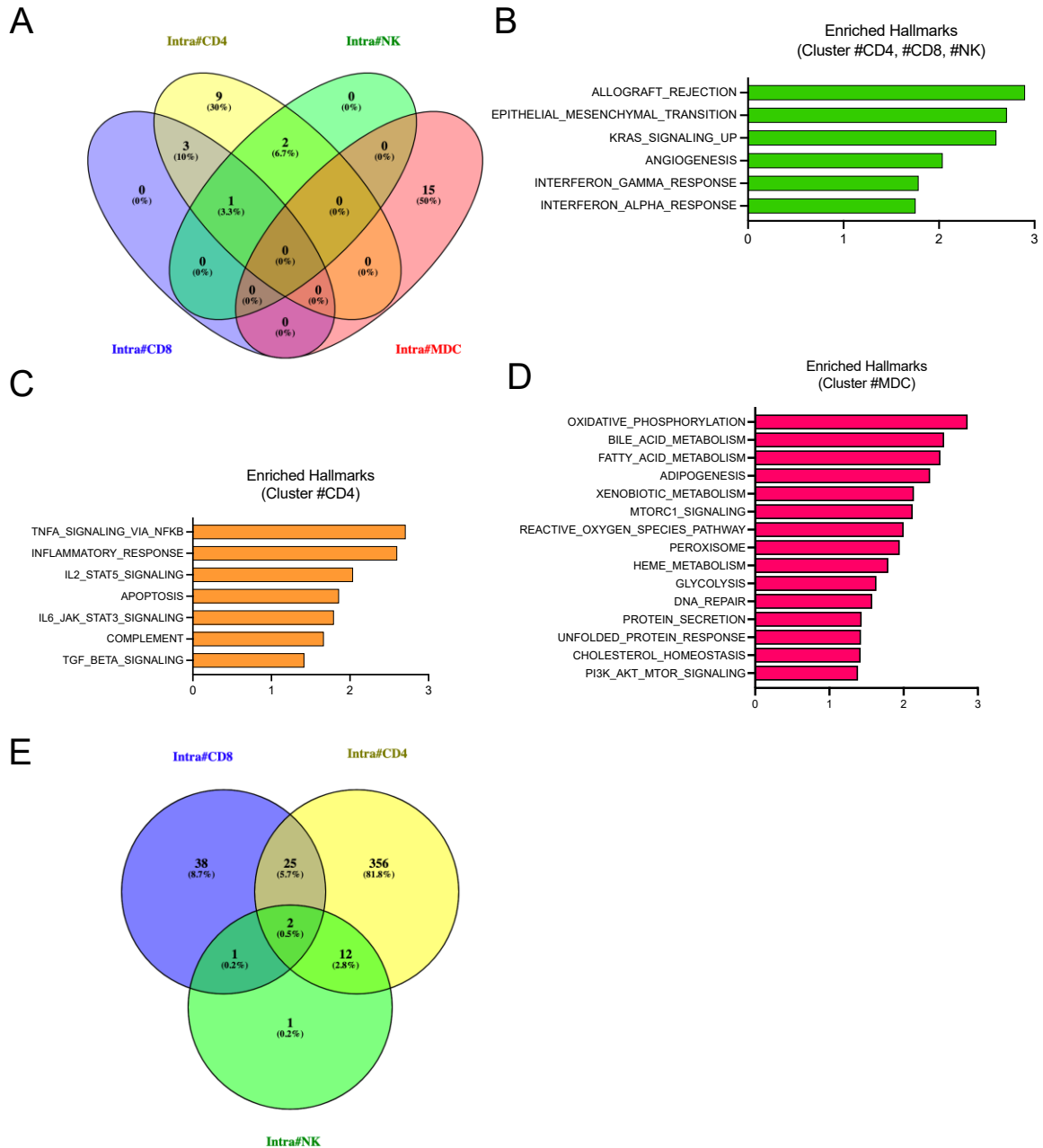
We also undertook a supervised analysis between clusters to determine whether there were distinctive differences between intra-tumor immune clusters in secreted cytokines (**Fig 4F**). We found that CXCL1 and IL-8 secretion was significantly increased in patients within the #CD4 cluster, although this was driven largely by 4/6 patients. CXCL1 is known to be involved in hepatic stellate cell activation, fibrogenesis and angiogenesis in the liver.³⁴⁷⁻³⁴⁹ The fibrotic response in HCC has known immunosuppressive effects on immune cells in chronic liver disease and liver cancer. Elevated IL-8 secretion may also be associated with a more aggressive

tumor type in this subset of patients. Soluble PD1 and VEGF secretion was increased in both #CD8 and #CD4 cluster compared to the #MDC cluster. Soluble PD1 is likely derived from activated T cells and has been shown to be indicative of response to immunotherapy. However, considering the elevated secretion of VEGF-A in the #CD8 cluster and particularly of CXCL1 and IL-8 in the #CD4 cluster imply different mechanisms which may drive immune escape in these two patient subgroups.

Enriched signaling pathways in #CD8, #CD4, #NK and #M-DC intra-tumor clusters in HCC

Molecular characterization using Gene Set Enrichment analysis (GSEA) was undertaken to identify enriched Hallmark pathways within each intra-tumor cluster. Enrichment was reported for pathways with a P-value and False Discovery Rate (FDR)-value below 0.05. Hallmark GSEA identified that the #CD8, #CD4 and #NK clusters commonly shared Allograft rejection pathway. The allograft rejection pathway consists of genes upregulated during transplant rejection. Commonly enriched genes in the three clusters are listed in **Table 2**. The #CD4 and #NK clusters shared innate immunity pathways and #CD4 and #CD8 clusters shared Epithelial mesenchymal Transition and Angiogenesis pathways (**Fig 5B**). Uniquely enriched pathways in the #CD4 cluster included TNF signaling, Inflammatory response, IL6-JAK-Stat3, IL2-Stat5, complement and TGF β signaling pathways (**Fig 5C**). In contrast, multiple metabolic pathways including Oxidative phosphorylation, Bile acid, Fatty acid, Xenobiotic and Heme metabolism pathways were enriched in the #M-DC cluster (**Fig 5D**).

We also performed GSEA to identify enriched biological processes within each lymphocyte clusters to gain further insight on immune activation and immune escape pathways (**Fig 5E**). Altogether, the #CD4 #CD8 and #NK cluster shared 2 commonly enriched pathways, T cell selection and NK cell mediated immunity. Common pathways shared between #CD8 and #CD4 clusters were multiple pathways in the adaptive immune response, whereas common pathways shared between #CD4 and #NK cluster were cytotoxicity regulation and lymphocyte immunity, and between #CD8 and #NK cluster natural killer cell mediated cytotoxicity (**Table 3**).



We turned to unique pathways within each cluster for hypothetical immune escape mechanisms (**Table 4**). Multiple pathways including myeloid dendritic cell and dendritic cells chemotaxis, but also tolerance induction and negative regulation of immune responses were associated with the #CD4 cluster. In addition, collagen biosynthesis and activation as well as TGF β , VEGF and IL-6 production pathways were also enriched. These preliminary results demonstrate that the inflammatory microenvironment of patients in the #CD4 cluster contains both immunostimulatory and immunosuppressive pathways constituting a subgroup of patients for which a combination treatment strategy may be more impactful than anti-PD1 monotherapy.

Unique to the #CD8 cluster included several pathways in nerve development, neuropeptide signaling and norepinephrine secretion and production. Commonly enriched genes in these signaling pathways included SEMA3A, ADRA2C, OXTR, STX1A, and LRIG2. Among these SEMA3A is a known prognostic markers of worse prognosis in liver cancer associated with liver cancer tumor growth and progression.³⁵⁰ Adrenergic receptors including ADRAC2 are known to be involved in liver fibrosis pathology and their blockade can improve liver permeability.³⁵¹

Differential Gene expression and enrichment pathway analysis between 'noninflamed', 'cytotoxic', and 'non-cytotoxic' patient subgroups identified by cytokine secretion

Unsupervised clustering with the intra-tumor secreted cytokines permitted us to distinguish non-inflamed, cytotoxic, and non-cytotoxic patient subgroups within the lymphocyte-enriched tumors. We therefore wanted to test whether these differences would be also reflected in the RNAseq data from these patients and if we could identify enriched pathways involved in immune activation versus immune escape.

463 genes were upregulated in the 'cytotoxic' subgroup and 302 genes were upregulated in the 'non-cytotoxic' subgroup compared to the 'non-inflamed' patients' subgroup (**Table 5 & 6**). 305 genes were uniquely upregulated in the cytotoxic subgroup versus 144 in the 'non-cytotoxic' subgroup. Among those unique to the 'cytotoxic' subgroup included immune checkpoints BTLA, CTLA4, PD1, IL4I1, CD73, and GITR. Other genes related to immune activation included GZMA, CD80, CD8A, CD2 and HLA-DOB. Genes upregulated uniquely in the 'non-cytotoxic' subgroup included SEMA3A, CXCL1 and HIF1A among others. However, enrichment pathway analysis did not draw clear differences based on the differentially expressed genes in each subgroup.

Discussion

The diversity of tumor immune microenvironments within HCC partly contributes to the heterogeneity of responses to immunotherapy treatment in the current clinical setting. Low levels of objective response rates from phase I/II clinical trials in early-stage HCC warrants the investigation of immune microenvironment subtypes in early-stage HCC. In this preliminary study, we identified four intra-tumor immune clusters in early-stage HCC using flow cytometry: one myeloid-enriched cluster (#M-DC), and three lymphocyte-enriched clusters (#CD8, #CD4 and #NK). The lymphocyte clusters had shared enrichment for CD69^{pos}CD8⁺PD1⁺ T cell infiltration, while the #M-DC cluster was poorly infiltrated with this cell subset. The #CD4 cluster was strongly enriched for CD69^{pos}PD1⁺CD4⁺ T cells. Both cell types may represent infiltration in part by resident-memory cells based on their expression of CD69. However, recent studies have described CD103⁺ expression among PD1⁺ CD8⁺ T cells as an important marker of functional tumor reactive cells within HCC tumor microenvironment in the response to immune checkpoint blockade.²²⁶ Other markers of resident memory CD8⁺ T cells in the liver include CXCR3 and CXCR6 expression.³⁵² CXCR6 has been recently identified as a marker of tumor-reactive T cells in HCC and associated with response to immune checkpoint blockade.^{353,354} However, CXCR6 expression on PD1^{hi} CD8⁺ T cells in the liver is also associated with auto-aggressivity and increased incidence of NASH-HCC in mice.^{219,221} Therefore, consideration for both disease etiology as well as exhaustion levels must be taken into consideration in the assessment for appropriate cellular biomarkers of immunotherapy response, particularly in HCC. For 18/28 patients, we have included flow cytometry antibodies for CXCR6 and CD103 surface markers to identify residency phenotypes across the lymphocyte subsets. For this preliminary study, we preferred to perform clustering on the major immune cell subsets shared across the entire cohort to keep the maximum number of included patients and to assess the feasibility of discriminating patients according to the relative proportions of cells. Nevertheless, the inclusion of CXCR6 and CD103 residency markers on lymphoid subsets remains vital to discriminate the quality of immune response over the quantity and how they correlate with each other, as well as with secreted proteins and corresponding transcriptome.

Unsupervised analysis of cytokine secretion demonstrated another level of complexity, as it did not permit us to find clear distinctions between the #CD8, #CD4 and #NK lymphocyte

clusters. Instead, patients from #CD8, #CD4 and #NK clusters were mixed and distinguished by the level of cytotoxic molecules Granzyme B and Perforin, and cytokines CXCL10, CCL17 and VEGFA, demonstrating that the description of subgroups solely based on the prevalence of a particular cell type may not be sensitive enough. Patients within the 'cytotoxic' subgroup displayed increased PD1 expression on intra-tumor CD4⁺ T cells and Tregs. Therefore, tumor infiltrating T cells within the 'cytotoxic' subgroup of patients may be chronically activated and exhausted compared to the cells within the 'non-cytotoxic' subgroup. Indeed, uniquely upregulated genes within patients from the 'cytotoxic' subgroup included checkpoint molecules BTLA, CTLA4, PD1, IL4I1, CD73, and GITR. However, we do not know whether the cytotoxic group contains more tumor-reactive T cells or not, as recent studies in HCC patients treated with immunotherapy have demonstrated not all 'T cell-enriched' tumors respond to anti-PD1 immunotherapy, caused by a clonal expansion of PD1^{high}CD39^{positive} 'terminally-exhausted' CD8 T cells in non-responders.²²⁹ Furthermore, in responders, clonally expanded PD1⁺ effector-like CD8⁺ T cells appeared to originate from 'progenitor-exhausted' CD8⁺ T cells in pretreatment biopsies.²²⁹ Furthermore, these cells were in proximity with CXCL13⁺ T-helper cells and mature regulatory dendritic cells, implying the need to consider a pre-existing co-stimulatory source within the tumor microenvironment prior to PD-1 monotherapy treatment as well as consideration for the level of T cell exhaustion.²²⁹ Progenitor stem-like cells have been identified in HCC tumors as PD1-intermediate expressing cells and associated with improved survival.³⁵⁵ In this preliminary study, PD1 expression levels was not discriminated by the intensity of staining per sample. Although it would need validation, the level of PD1 expression could also be included among CD8⁺ T cells to discriminate the quality of the cell subtypes within immune clusters over the quantity.

We identified potential secreted factors associated with immune escape, including elevated VEGF-A secretion in the 'cytotoxic' subgroup of patients and MIF in the 'non-inflamed' subgroup. Furthermore, supervised analysis showed that specific to the #CD4 cluster was elevated CXCL1 and IL-8, as well as VEGF-A secretion in both #CD8 and #CD4 clusters. VEGF is a potent immunomodulatory molecule, inducing Treg proliferation, increasing PD1 expression on T cells, inhibiting dendritic cell maturation, and driving the accumulation of immunosuppressive cell types, such as MDSCs.³⁵⁶⁻³⁶⁰ The #CD4 cluster was also significantly associated with T2 stage tumors. A previous study comparing immune profiles in HCC across

tumor stages noted that immune evasion peaks at T2 stage of HCC, with increasing frequencies of Tregs and exhausted T cells, and decreasing frequencies of activated CD8⁺ and NK cells.³³³ Progressive evolution of immune responses in HCC also coincided with tumor progression, including transcriptomic upregulation of Wnt signaling pathway in T2 HCC. This signaling pathway is known to promote immune escape and resistance to immune checkpoint blockade in HCC.^{361,362} A separate study of immunogenomic classification of HCC demonstrated that highly infiltrated 'inflamed' HCC has three components: immune active, immune-like and immune exhausted components.²¹⁸ The immune-like subclass was enriched for Wnt-Beta catenin signaling pathway, whereas the immune-exhausted subclass was enriched for Wnt/TGF β signaling. We observed enrichment for TGF β signaling pathway specifically in the #CD4 cluster. TGF β regulates cancer associated fibroblast activation, angiogenesis, metastasis and also suppresses anti tumor immune responses through T cell exhaustion and exclusion.^{363,364}

Limitations of this preliminary study include the small cohort and lack of clinical follow-up data to correlate the immune profiles to patient prognosis such as recurrence-free survival. In addition, while flow cytometry can permit the evaluation of the main cell subsets within tumors, we do not have an appreciation for the specific myeloid and dendritic cell subtypes for most patients. At this point, N=10 patients have been stained for the additional panel on myeloid cells which is not sufficient yet for comparison between the #CD8, #CD4, #NK and #MDC clusters. Also, it should be noted that the myeloid panel is applied to tumor samples with sufficient CD45⁺ cells to apply two panels, and we do not know if we are biased because of our assessment of myeloid cells within tumors that are more 'highly' infiltrated.

Multiple oncogenic pathways can influence the immune profile in HCC. Resistance to immunotherapy involves the perturbation of neoantigen expression, processing, or presentation, as well as induction of T cell dysfunction through the recruitment of immunosuppressive cell subsets or alternative immunosuppressive molecules.³⁶⁵ Some driver mutations may also inherently resist immunotherapy. Specifically in HCC, changes in several oncogenic pathways such as Wnt/Beta-catenin, PI3K and TGF β can impact T cell recruitment and function.^{217,361,366-370} We have conducted gene set enrichment analysis to gain an overview of molecular pathways that are common or unique to various intra-tumor immune clusters

and the cytotoxic and non-cytotoxic subgroups. However, considering the intricate nature of cell phenotypes and inflammatory signals for each patient, it would be more appropriate to employ single-sample GSEA or Gene Set Variation Analysis (GSVA) for patient subgrouping based on immune infiltration and signaling pathways. Moreover, we find it relevant to utilize published signatures specific to innate and adaptive immune pathways, and fibroblast activation, sourced from liver pathologies and HCC datasets for a more precise stratification. Furthermore, we will utilize signatures from the Hoshida and Chiang classifications which categorize and classify different molecular subtypes of HCC, associated with different clinical outcomes.^{371,372}

In addition, Whole Exome Sequencing (WES) has also been performed on paired intra-tumor and extra-tumor samples from patients included in this study, of which the data has not yet been analyzed. This data will be used in part for the quantification of neoantigens, somatic copy number mutations, copy number alterations and TCR repertoire analysis.³⁷³ Copy number alterations can lead to loss of genes involved in antigen presentation in HCC and may be involved in immune exclusion or lack of tumor recognition by adaptive immune system.^{218,374} The molecular subgroups identified by single sample GSEA in parallel with WES analysis, could then be correlated to the flow cytometry and cytokine secretion profiles. This will ultimately permit us to identify the immune escape phenotype they converge towards. These subgroups could then be validated in external cohorts of HCC patients undergoing immunotherapy treatment at Gustave Roussy Hospital, with the goal of predicting response to different combination treatment approaches. However, we acknowledge that the use of transcriptomic data analysis though more exhaustive may not be suitable for routine clinical practice. Nonetheless, the use of flow cytometry and cytokine secretion holds the promise to be standardized and optimized with a rapid turnover in the application of improved HCC patient management in the advent of immunotherapy treatment.

We also have flow cytometry, cytokines secretion and transcriptomics data from the margin of the resected HCC tumors. Our results showed interesting correlations between intra-tumor HCC clusters with margin and extra-tumor clusters. These tissues and cytokine secretion will provide insight into other immunosuppressive mechanisms that may influence the

microenvironment adjacent to the tumor, and whether these signatures are complementary or more impactful in deciphering the immune profile of HCC tumors.

A further 20 patients are expected to be recruited and this could be an opportunity to apply more rigorous phenotyping for immune checkpoints to identify the exhaustive nature as well as functional assays to test the cytotoxic capacity of lymphocytes according to which cluster they belong.

Tables

Table 1. Patients' demographic and clinical characteristics

Characteristic	Patients (n=28)
Median Age (range)	72 (41-86)
Sex - no. (%)	
Female	2 (7%)
Male	26 (93%)
Median Body Mass Index (range)	26 (22-35)
BCLC stage - no. (%)	
0	2 (7%)
A	18 (64%)
B	2 (7%)
C	1 (4%)
NA	4 (14%)
AJCC - no. (%)	
T1a	3 (11%)
T1b	11 (39%)
T2	13 (46%)
NA	1 (4%)
Satellite Nodules - no. (%)	
No	19 (68%)
Yes	6 (21%)
Missing	3 (11%)
Microvascular Invasion - no. (%)	
No	21 (75%)
Yes	6 (21%)
Missing	1 (4%)
Positive Margins - no. (%)	
No	21 (75%)
Yes	6 (21%)
Liver Disease - no. (%)	
Viral	9 (32%)
Steatosis	4 (14%)
Alcoholic Steatosis (ASH)	9 (32%)
Non-alcoholic Steatohepatitis (NASH)	6 (21%)
No Liver Disease	1 (4%)
Fibrosis Score - no. (%)	
F1/F2	8 (29%)
F3/F4	17 (61%)
NA	3 (11%)
Elastometry (kPa) - median (range)	8.0 (3.7 - 23.2)
CAP (kPa) - median (range)	310 (201-351)
Blood values - median U/L (range)	
ALT	29 (7-143)
AST	31 (19-69)
GGT	43 (13-556)
LDH	187 (140-284)
Albumin - median g/L (range)	41 (30-49)
Bilirubin - median umol/L (range)	9 (4-17)
AFP levels	
< 10 ng/mL	23 (82%)
10 - 100 ng/mL	2 (7%)
100 - 1000 ng/mL	1 (4%)
> 1000 ng/mL	1 (4%)
Missing	1 (4%)
CRP (mg/L) - median (range)	2 (0.2-19.7)
NLR - median (range)	2.3 (0.9-6.1)
dNLR - median (range)	1.6 (0.6-3.1)
Local Recurrence post-surgery - no. (%)	5 (18%)

Table 2. Common and uniquely enriched genes in Allograft Rejection Pathway

Shared #CD8/#CD4/#NK	Shared #CD8/#CD4	Shared #NK/#CD8	Shared #NK/#CD4	Unique #CD8	Unique #CD4	Unique #NK
CD96	ABI1	GCNT1	IGSF6	ACHE	TLR6	STAB1
CXCL13	ELF4	APBB1	CCR1	TGFB2	NLRP3	ICOSLG
GLMN	HLA-DOB	IL11	F2	CCND2	EREG	IKKBK
MAP4K1	IFNG	IL12A	FCGR2B	CD7	FGR	IRF7
CCR5	IL7	IL12RB1	IRF8	CARTPT	FLNA	MBL2
CTSS	IRF4	PRF1	IFNAR2	SOCS5	HCLS1	MTIF2
ETS1	LCK	CCL5	IL2RA		HIF1A	NOS2
F2R	LTB	TAP1	IL4R		HLA-DMB	TAP2
FYB1	NPM1	TLR3	IL13		HLA-DOA	ST8SIA4
GBP2	PRKCG	TRAF2	IL16		HLA-DQA1	CD40
SIT1	RPS9	ZAP70	ITGB2		ICAM1	
CXCR3	CCL19		JAK2		IL1B	
GZMA	TNF		LCP2		IL2	
HLA-G	CCR2		CCL2		ITK	
FASLG	UBE2D1		SPI1		LY75	
IL2RB	RIPK2		WARS1		LYN	
IL6	CD3E		WAS		MMP9	
IL18	CD40LG		EIF3D		CFP	
INHBA			CD247		SRGN	
INHBB			CD86		BCAT1	
ITGAL					CCL7	
CXCL9					CCL22	
NCF4					STAT4	
TRAT1					TLR2	
CRTAM					TPD52	
PSMB10					DEGS1	
PTPN6					EIF3J	
PTPRC					IL18RAP	
RPS19					BCL10	
CCL4					CD4	
CCL11						
CCL13						
STAT1						
TGFB1						
THY1						
TIMP1						
TLR1						
CAPG						
DYRK3						
CCND3						
CD2						
CD3D						
CD3G						
CD8A						
CD8B						
CD28						
CD80						
LY86						
CD79A						
HDAC9						

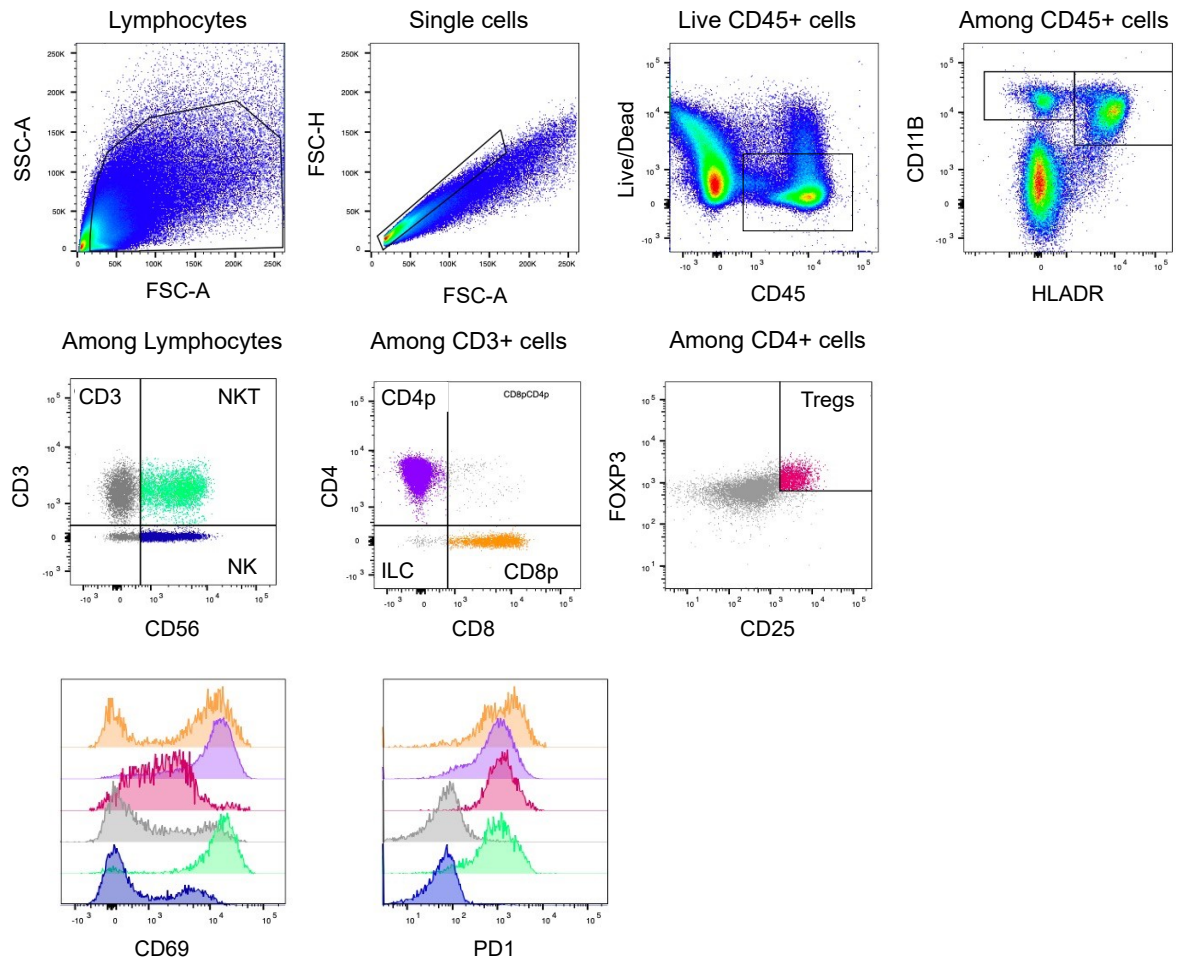
Table 3. Commonly enriched Biological Processes in #CD8, #CD4 and #NK clusters in HCC

Shared #CD8/#CD4/#NK	Shared #CD8/#CD4	Shared #NK/#CD8	Shared #NK/#CD4
REGULATION_OF_NATURAL_KILLER_CELL_MEDIATED_IMMUNITY	REGULATION_OF_PLATELET_AGGREGATION	POSITIVE_REGULATION_OF_NATURAL_KILLER_CELL_MEDIATED_IMMUNITY	REGULATION_OF_LEUKOCYTE_MEDIATED_IMMUNITY
	REGULATION_OF_HOMOTYPIC_CELL_CELL_ADHESION		NEGATIVE_REGULATION_OF_CELL_KILLING
	POSITIVE_REGULATION_OF_RHO_PROTEIN_SIGNAL_TRANSDUCTION		REGULATION_OF_T_CELL_MEDIATED_IMMUNITY
	ALPHA_BETA_T_CELL_DIFFERENTIATION		NEGATIVE_REGULATION_OF_LEUKOCYTE_MEDIATED_CYTOTOXICITY
	MONOCYTE_CHEMOTAXIS		NEGATIVE_REGULATION_OF_ANTIGEN_RECEPTOR_MEDIATED_SIGNALING_PATHWAY
	CD4_POSITIVE_ALPHA_BETA_T_CELL_DIFFERENTIATION		POSITIVE_REGULATION_OF_IMMUNE_EFFECTOR_PROCESS
	NEGATIVE_REGULATION_OF_LYMPHOCYTE_ACTIVATION		REGULATION_OF_CELL_KILLING
	NEGATIVE_REGULATION_OF_STRIATED_MUSCLE_CELL_DIFFERENTIATION		REGULATION_OF_LYMPHOCYTE_MEDIATED_IMMUNITY
	CHONDROCYTE_DIFFERENTIATION		REGULATION_OF_LEUKOCYTE_MEDIATED_CYTOTOXICITY
	REGULATION_OF_PLATELET_ACTIVATION		POSITIVE_REGULATION_OF_LEUKOCYTE_MEDIATED_IMMUNITY
	NEGATIVE_REGULATION_OF_CELL_CELL_ADHESION		NEGATIVE_REGULATION_OF_NATURAL_KILLER_CELL_MEDIATED_IMMUNITY
	CARDIAC_VENTRICLE_MORPHOGENESIS		REGULATION_OF_T_CELL_MEDIATED_CYTOTOXICITY
	B_CELL_PROLIFERATION		
	NEGATIVE_REGULATION_OF_CELL_ACTIVATION		
	ALPHA_BETA_T_CELL_ACTIVATION		
	REGULATION_OF_T_CELL_DIFFERENTIATION		
	REGULATION_OF_ALPHA_BETA_T_CELL_ACTIVATION		
	REGULATION_OF_CELL_CELL_ADHESION		
	T_CELL_DIFFERENTIATION		
	REGULATION_OF_CD4_POSITIVE_ALPHA_BETA_T_CELL_DIFFERENTIATION		
	NEGATIVE_REGULATION_OF_LEUKOCYTE_PROLIFERATION		
	POSITIVE_REGULATION_OF_INTERLEUKIN_17_PRODUCTION		
	EOSINOPHIL_CHEMOTAXIS		
	REGULATION_OF_LYMPHOCYTE_DIFFERENTIATION		
	REGULATION_OF_B_CELL_ACTIVATION		

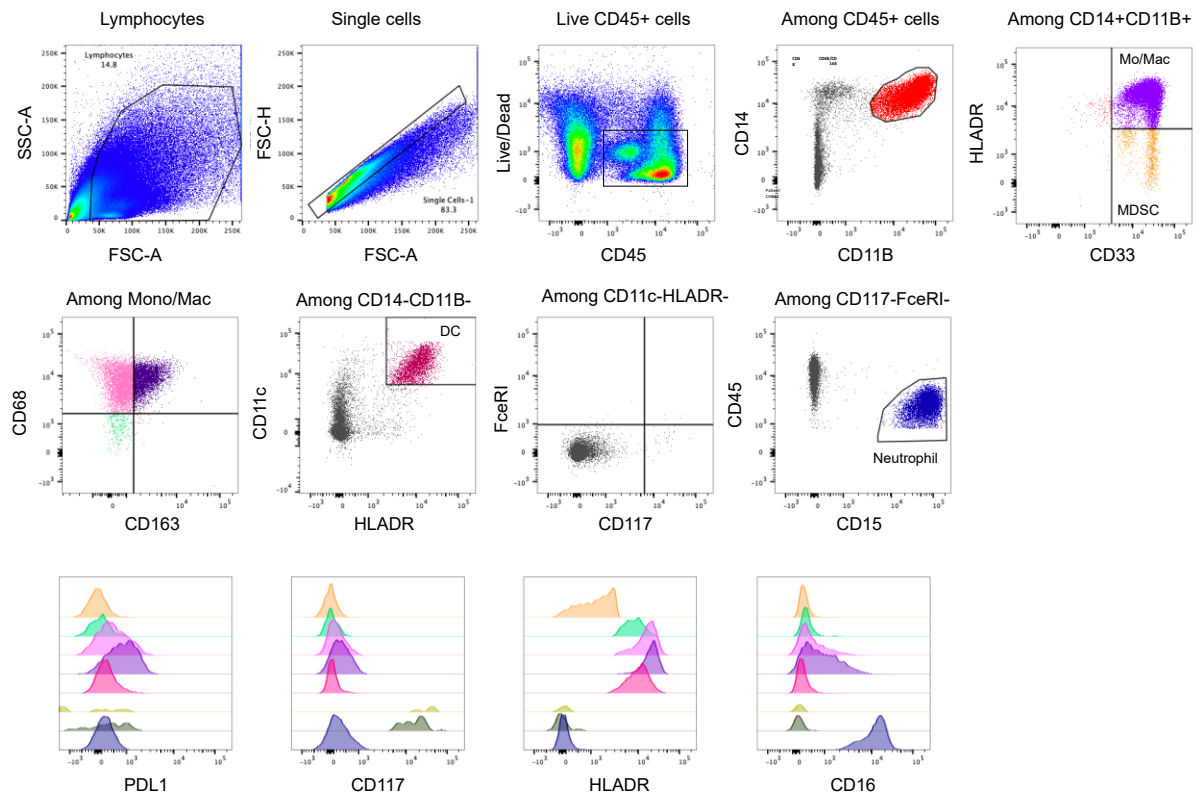
Table 4. Uniquely enriched Biological Processes in #CD8, #CD4 and #NK clusters in HCC

Unique #CD8	Unique #CD4	Unique #NK
HOMOPHILIC_CELL_ADHESION_VIA_PLASMA_MEMBRANE_ADHESION	MYELOID_DENDRITIC_CELL_ACTIVATION	POSITIVE_REGULATION_OF_NATURAL_KILLER_CELL_MEDIATED_CYTOTOXICITY
CELL_CELL_ADHESION_VIA_PLASMA_MEMBRANE_ADHESION	DENDRITIC_CELL_MIGRATION	
REGULATION_OF_KIDNEY_DEVELOPMENT	NITRIC_OXIDE_SYNTHASE_BIOSYNTHETIC_PROCESS	
CELL_FATE_COMMITMENT	DENDRITIC_CELL_CHEMOTAXIS	
CRANIAL_NERVE_DEVELOPMENT	DENDRITIC_CELL_DIFFERENTIATION	
APPENDAGE_MORPHOGENESIS	LEUKOCYTE_CELL_CELL_ADHESION	
NERVE_DEVELOPMENT	MYELOID_DENDRITIC_CELL_DIFFERENTIATION	
SENSORY_ORGAN_MORPHOGENESIS	POSITIVE_REGULATION_OF_INTERLEUKIN_2_PRODUCTION	
REGIONALIZATION	INTERLEUKIN_2_PRODUCTION	
CALCIUM_DEPENDENT_CELL_CELL_ADHESION_VIA_PLASMA	MONONUCLEAR_CELL_MIGRATION	
INNER_EAR_MORPHOGENESIS	POSITIVE_REGULATION_OF_CELL_CELL_ADHESION	
RENAL_VESICLE_DEVELOPMENT	POSITIVE_REGULATION_OF_INTERLEUKIN_4_PRODUCTION	
PROXIMAL_DISTAL_PATTERN_FORMATION	REGULATION_OF_LYMPHOCYTE_ACTIVATION	
SENSORY_PERCEPTION_OF_BITTER_TASTE	POSITIVE_REGULATION_OF_LEUKOCYTE_CELL_CELL_ADHESION	
NEPHRON_MORPHOGENESIS	POSITIVE_REGULATION_OF_CELL_ACTIVATION	
REGULATION_OF_BRANCHING_INVOLVED_IN_URETERIC_BUD	MONONUCLEAR_CELL_DIFFERENTIATION	
DIENCEPHALON_DEVELOPMENT	REGULATION_OF_B_CELL_PROLIFERATION	
APPENDAGE_DEVELOPMENT	LEUKOCYTE_DIFFERENTIATION	
PATTERN_SPECIFICATION_PROCESS	B_CELL_ACTIVATION	
EYE_MORPHOGENESIS	POSITIVE_REGULATION_OF_NITRIC_OXIDE_SYNTHASE_BIOSYNTHETIC_PROCESS	
DORSAL_VENTRAL_PATTERN_FORMATION	REGULATION_OF_LEUKOCYTE_PROLIFERATION	
PITUITARY_GLAND_DEVELOPMENT	REGULATION_OF_ADAPTIVE_IMMUNE_RESPONSE	
NOREPINEPHRINE_SECRETION	INTERLEUKIN_1_PRODUCTION	
SYNAPSE_ASSEMBLY	INTERLEUKIN_4_PRODUCTION	
REGULATION_OF_NEURAL_PRECURSOR_CELL_PROLIFERATION	LEUKOCYTE_PROLIFERATION	
NEGATIVE_REGULATION_OF_AMINE_TRANSPORT	ADAPTIVE_IMMUNE_RESPONSE	
KIDNEY_MORPHOGENESIS	INTERLEUKIN_1_BETA_PRODUCTION	
HETEROCHROMATIN_ORGANIZATION	REGULATION_OF_MACROPHAGE_ACTIVATION	
NEGATIVE_REGULATION_OF_MUSCLE_CELL_DIFFERENTIATION	NEGATIVE_REGULATION_OF_B_CELL_ACTIVATION	
NEUROPEPTIDE_SIGNALING_PATHWAY	EXTERNAL_ENCAPSULATING_STRUCTURE_ORGANIZATION	
MOTOR_NEURON_AXON_GUIDANCE	VASCULAR_ENDOTHELIAL_GROWTH_FACTOR_PRODUCTION	
EAR_MORPHOGENESIS	REGULATION_OF_T_CELL_ACTIVATION	
CRANIAL_NERVE_MORPHOGENESIS	T_CELL_ACTIVATION	
SKELETAL_SYSTEM_MORPHOGENESIS	B_CELL_HOMEOSTASIS	
EMBRYONIC_APPENDAGE_MORPHOGENESIS	CELL_ADHESION_MEDIATED_BY_INTEGRIN	
DNA_REPLICATION_DEPENDENT_NUCLEOSOME_ORGANIZATION	NEGATIVE_REGULATION_OF_B_CELL_PROLIFERATION	
EMBRYONIC_ORGAN_MORPHOGENESIS	T_CELL_PROLIFERATION	
FOREBRAIN_REGIONALIZATION	POSITIVE_REGULATION_OF_ALPHA_BETA_T_CELL_ACTIVATION	
	REGULATION_OF_CD4_POSITIVE_ALPHA_BETA_T_CELL_ACTIVATION	
	REGULATION_OF_LEUKOCYTE_DIFFERENTIATION	
	POSITIVE_REGULATION_OF_MONONUCLEAR_CELL_MIGRATION	
	RESPONSE_TO_CHEMOKINE	
	B_CELL_RECEPTOR_SIGNALING_PATHWAY	
	POSITIVE_REGULATION_OF_VASCULAR_ENDOTHELIAL_GROWTH_FACTOR_PRODUCTION	
	CELL_CHEMOTAXIS	
	REGULATION_OF_ANTIGEN_RECEPTOR_MEDIATED_SIGNALING_PATHWAY	
	LEUKOCYTE_MIGRATION	
	POSITIVE_REGULATION_OF_TYPE_2_IMMUNE_RESPONSE	
	LYMPHOCYTE_MIGRATION	
	TRANSFORMING_GROWTH_FACTOR_BETA_PRODUCTION	
	COLLAGEN_ACTIVATED_SIGNALING_PATHWAY	
	POSITIVE_REGULATION_OF_INTERLEUKIN_6_PRODUCTION	
	NEGATIVE_REGULATION_OF_CELL_ADHESION	
	POSITIVE_REGULATION_OF_ADAPTIVE_IMMUNE_RESPONSE	
	POSITIVE_REGULATION_OF_ACUTE_INFLAMMATORY_RESPONSE	
	INTERFERON_GAMMA_PRODUCTION	
	FIBROBLAST_PROLIFERATION	

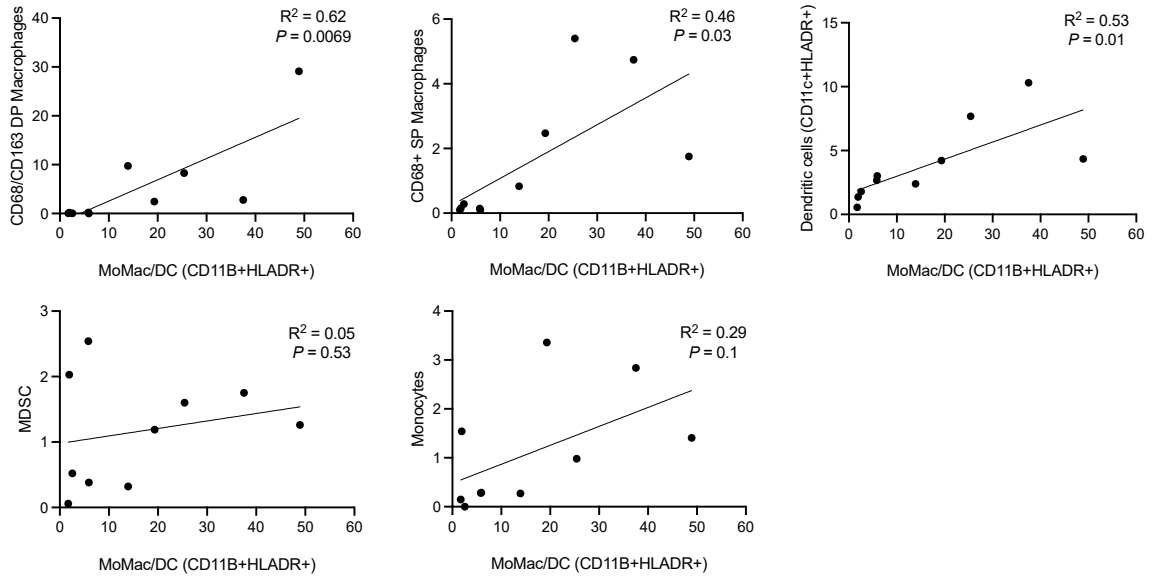
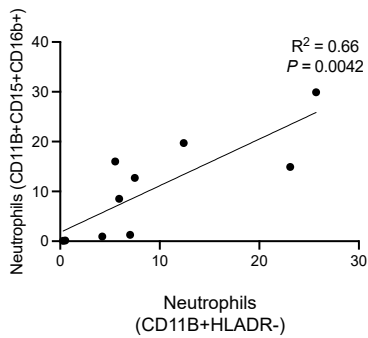
Supplementary Figures



Supplementary Figure 1 Flow Cytometry Panel Gating Strategy for Immune Cells. Depiction of gating strategy for Immune cells panel is depicted and includes the following cell populations in order from 'Among CD45⁺ cells': Monocyte/Macrophage/Dendritic cells (CD11b⁺ HLADR⁺), Neutrophils (CD11b⁺ HLADR⁻); 'Among Lymphocytes': total T cells (CD3⁺CD56⁻), NK cells (CD3⁻CD56⁺), NKT cells (CD3⁺CD56⁺); 'Among CD3⁺ cells': CD8⁺T cells, CD4⁺T cells, and Innate T cells (ILC); 'Among CD4⁺ cells': Tregs (CD25^{high}FOXP3⁺).

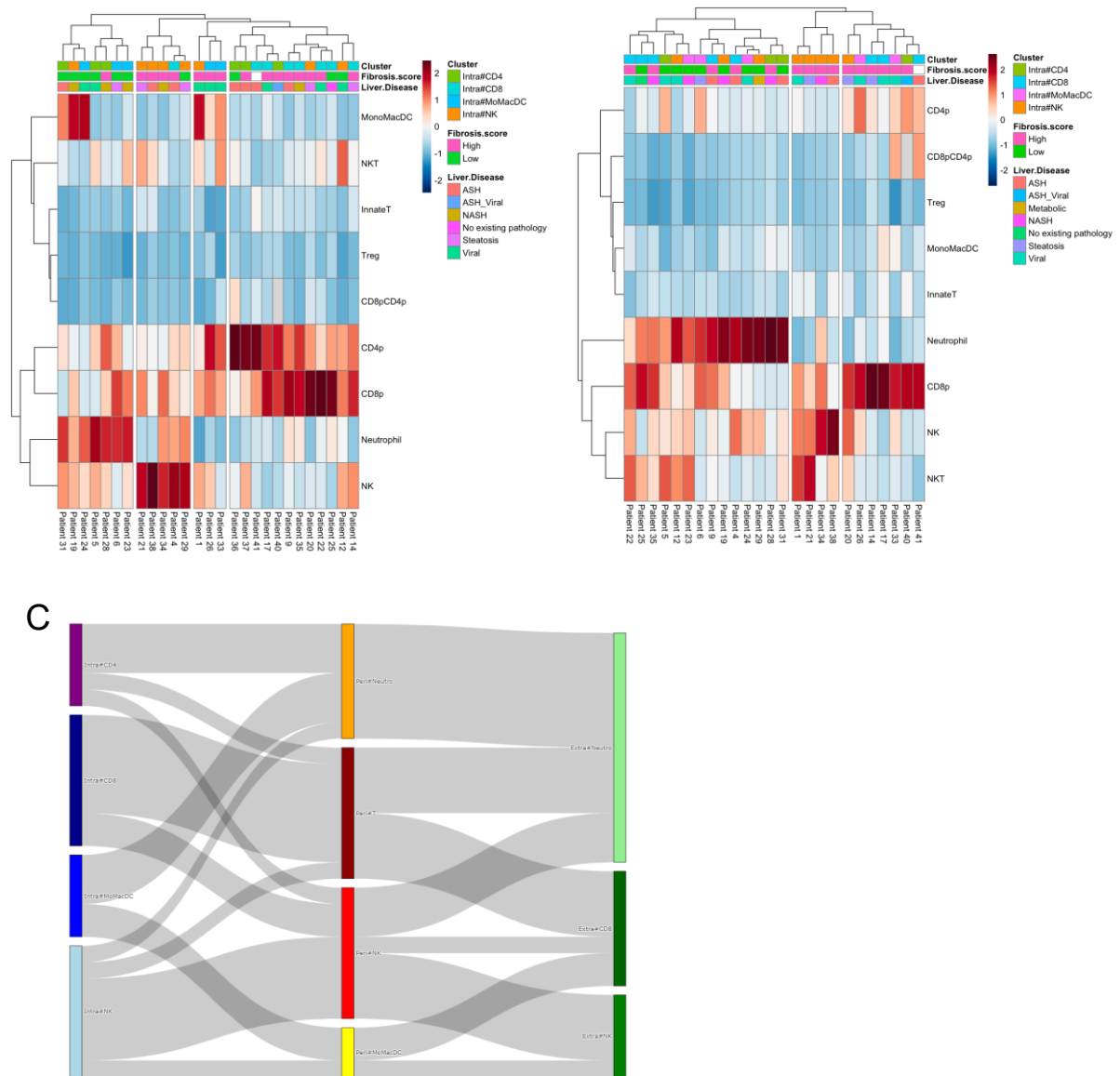


Supplementary Figure 2 Flow Cytometry Panel Gating Strategy for Myeloid and Granulocytic cell subsets. Depiction of gating strategy for Myeloid/Granulocyte panel is depicted and includes the following cell populations in order from 'Among CD45⁺ cells': Total Myeloid cells (CD11b⁺ CD14⁺), Monocyte/Macrophages (CD11b⁺CD14⁺CD33⁺HLADR⁺); MDSC (CD11b⁺CD14⁺CD33⁺HLADR⁻), CD68SP Macrophages (CD68⁺CD163⁻), CD68/CD163DP Macrophages (CD68⁺CD163⁺), Monocytes (CD68⁻CD163⁻), Dendritic cells (CD11c⁺HLADR⁺), Mast cells (CD117⁺FceRI⁺), Neutrophils (CD45^{low}CD15⁺).

A**B**

Supplementary Figure 3. A/ Spearman correlation in paired tumor samples from patients between myeloid cell subsets (CD68⁺CD163⁺ Double-positive macrophages, CD68⁺ Single-positive Macrophages, Dendritic cells, Myeloid-derived Suppressor cells (MDSC) and Monocytes with global cell population CD11B⁺HLADR⁺ (MoMacDC). **B/** Spearman correlation in paired tumor samples from patients between Neutrophils (CD11B⁺CD16b⁺CD15⁺) with global cell population CD11B⁺HLADR⁻ cells.

clusters (wilcox t-test). **B/** Measurement of liver fibrosis (Elastometry) and Steatosis (CAP) by Magnetic Resonance Elastography and compared across resected HCC immune clusters (wilcox t-test). **D/** Blood measurement of liver enzymes (AST, ALT, GGT and LDH), Bilirubin, Albumin, AFP, CRP, NLR, dNLR and compared across resected HCC immune clusters (wilcox t-test).



Supplementary Figure 5. A/ Unsupervised clustering of margin infiltrating immune cell subsets. **B/** Unsupervised clustering of extra-tumor liver tissue infiltrating immune cell subsets **C/** Sankey diagram of patients with paired extra-tumor, margin, and intra-tumor immune phenotyping. The corresponding immune cluster per tissue zone is indicated.

Discussion and Perspectives

General Discussion – Chapters 1 & 2

The liver is a frequent site of metastasis for patients with advanced colorectal cancer and has long been associated with poor prognosis in clinical practice. Significant advancements have been made over the past 20 years, increasing five-year survival rates from less than 5% to near 50%. These improvements can be attributed to advancements in imaging techniques, surgical procedures, and the application of neo-adjuvant and adjuvant therapies. Although the current selection of biomarkers in MSS mCRC relying on *RAS/BRAF* mutational status has led to better outcomes for some subtypes, a considerable number of patients experience disease recurrence and refractory disease following surgical resection and will eventually succumb to liver metastatic disease. Therefore, the identification of reliable biomarkers of prognosis and new avenues for therapy treatment are desperately needed to combat these mechanisms of resistance in patients with mCRC.

The first two chapters of the thesis addressed this question through a comprehensive assessment of tumor immune infiltrate, secreted factor measurement and multiplex immunohistochemistry within prospectively collected surgically resected colorectal cancer liver metastasis tissue from *KRAS/BRAF* mutated and *KRAS/BRAF* wildtype mCRC patients.

Our observations revealed that increased mast cell and T cell infiltration correlated with prolonged RFS **in chapter 1**, while elevated neutrophil infiltration was associated with decreased RFS **in chapter 2**. Intriguingly, both effects were specific to *KRAS/BRAF*-wildtype patients. The high infiltration of mast cells correlated with response to pre-operative chemotherapy, whereas neutrophil infiltration was associated with stable disease or progressive disease in response to treatment. We did not find an impact of mast cells, neutrophils, or T cells on RFS in *KRAS* mutated patients. *KRAS* mutation is a poor prognostic marker in mCRC.¹⁸² *KRAS* mutation in colorectal cancer is associated with immune escape mechanisms including modulation of inflammatory pathways leading to immune escape, T cell dysfunction and activation-induced cell death.^{184,185} However, we did not delineate a specific immune escape mechanism in *KRAS* mutated tumors in this study as none of the patients

included had a prolonged RFS, despite their variable immune infiltration profiles. Also, it is relevant to mention that the comparison of immunologic profiles in KRAS mutated patients to those of KRAS/BRAF wildtype patients with decreased RFS may not be ideal as the patients more commonly receive chemotherapy combination with bevacizumab (anti-VEGF), which has its own immunomodulatory effects in mCRC.³⁵⁷ In KRAS/BRAF wildtype patients, tumor infiltration with mast cells or neutrophils was not impacted by treatment type. However, mast cell infiltration was significantly increased in chemotherapy-treated tumors. This result is in line with a previous retrospective study of the prognostic impact of immune responses in CRC liver metastasis treated by surgery alone or surgery with perioperative FOLFOX.¹⁶⁵ They observed significant increase in mast cell infiltration in tumors, and this was positively correlated with prolonged RFS.¹⁶⁵ The T-cell score in this study based on the numeration of CD3⁺T and CD8⁺T cells in the tumor and at the invasive front (margin) of the tumor was also associated with increased RFS. They found no effects of CD8⁺T cells alone on RFS in the study. This could be because there was no distinction performed between KRASwt and KRASmut tumors, of which we observed KRASmut tumors to all be low in mast cells, but to contain similar levels of CD8⁺T cells as KRASwt tumors, but with poor prognosis. We hypothesize that this may be due to other immune escape mechanisms present in KRASmut tumors despite an elevated CD8⁺ T cell infiltrate.

Immunogenic cell death of cancer cells because of Fluorouracil and Oxaliplatin chemotherapies have been linked to T cell infiltration, clonal expansion, and improved survival in CRC liver metastasis.^{170,171} Other studies have demonstrated their impact on enhanced cross presentation of tumor antigens by myeloid dendritic cells.³⁷⁵ Furthermore, cetuximab can enhance infiltration of T cells and antibody-dependent cellular cytotoxicity in patients who respond to treatment.^{169,375} Oxaliplatin is a platinum-based chemotherapy drug in the same family as cisplatin and carboplatin. It has been previously reported that mast cells are activated by cisplatin in mouse models of kidney injury.³⁷⁶ However, we do not know whether this could be also directly activating mast cells in mCRC in the liver or whether mast cells are responding to secreted factors or immunostimulatory molecules in these tumors as a consequence of immunogenic cell death and T cell infiltration.

A proposed model of the tumor-immune microenvironment in KRAS wt mCRC patients with poor versus good prognosis is proposed in **Figure 1**. In mCRC patients with positive prognosis, higher mast cell infiltration was linked to their activation, as evidenced by increased histamine secretion. This activation positively correlated with CD8⁺T cell infiltration, CD69 expression and T effector memory RA (TemRA) phenotype. Further in vitro experiments using blood-derived mast cells pre-conditioned with tumor storage solution from patients with prolonged RFS increased granzyme B and IFN γ expression in autologous lymphocytes. These results suggest a costimulatory role for mast cells in KRASwt patients with prolonged RFS. However, their precise role and function in vivo remains to be determined. Due to the limited number of cells in each sample, we could only perform one phenotyping panel of immune cells in mCRC which included the surface activation markers Fc ϵ RI and CD203c. The possibility to apply Nanostring GeoMxTM on mast cells in FFPE tissue sections was explored to look for differences in intra-tumor mast cell transcriptome, however due to the low number of mast cells/mm² in patients with high mast infiltration, it would not have been technically possible to obtain a sufficient transcriptomic depth on such low numbers of cells. Furthermore, recent proteomics analysis on human mast cells has demonstrated the disparity between transcriptomic and proteomics assessment on mast cells.

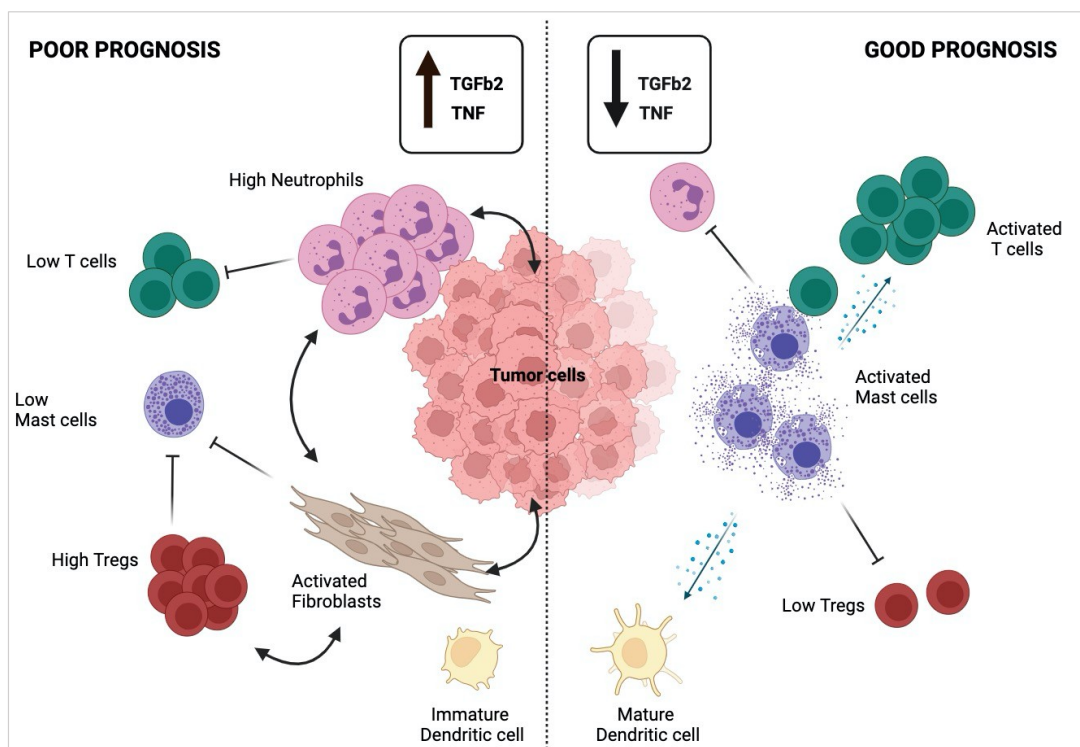


Figure 1 Proposed model of the tumor-immune microenvironment within KRAS wildtype metastatic CRC patients with poor versus good prognosis. In patients with poor prognosis, elevated

TGF β 2 and TNF drive neutrophil infiltration, and T cell and mast cell exclusion. Neutrophils, fibroblasts, and tumor cells likely participate in a cellular crosstalk that fuels their proliferation and pro-tumor functions. Furthermore, activated fibroblasts are likely to be the major source of TGF β that can also drive the proliferation and activation of Tregs, while suppressing dendritic cell maturation. In contrast, in patients with good prognosis, decreased levels of TGF β 2 and TNF are associated with increased prevalence and activation of mast cells, and T cells, and decreased prevalence of Tregs. Degranulated factors from mast cells such as histamine, could influence the activation and maturation of both dendritic cells and T cells and block the suppressive role of Tregs.

Although we measured elevated histamine levels associated with mast cell presence, we do not know which cells are responding specifically to histamine. Histamine has pleiotropic effects on the immune system and depending on the receptor can differentially modulate immune responses.²⁶⁰ Histamine signaling through H1R on Tregs can suppress their function.²⁰² Histamine has also been reported to modulate dendritic cells to enhance their priming of T effector cells in mice.²⁷⁵ Mast cells have also been reported to be in proximity with dendritic cells and to form immunological synapses with them to promote T cell activation.³⁷⁷ It is also possible that mast cells play a direct costimulatory role toward T cells or protect effector T cells from myeloid cell-derived reactive oxygen species, which can restore their function and activation within the tumor microenvironment.^{276,277} To answer these questions, further work is required, notably experiments in mice. Several ideas include a liver metastasis model in OT-1 mice crossed with Mast-cell specific knock-out mice, in which MSS CRC cell line over-expressing OVA can be injected intra-hepatically. The subsequent injection of these mice with Mast cells pre-exposed to OVA peptide could help answer the question of whether mast cells can stimulate an anti-tumor immune response *in vivo* against intra-hepatically injected tumors. The modulation of the mast cells to be histamine deficient (*Hdc*^{-/-}) in this model and the consequences on intrahepatic T cell activation and myeloid or dendritic cell maturation could also help answer our question on whether histamine from mast cells is critical in anti-tumor mediated immunity in liver tumors.

The good impact of mast cells and elevated histamine goes against a recent publication that demonstrated elevated systemic levels of histamine due to allergies in breast and melanoma cancer patients was associated with decreased response to Immunotherapy treatment.²⁷⁹ However, the direct causal link between allergies and cancer are controversial. For example, allergic diseases are associated with a decreased cancer risk in CRC, and inversely correlated with CRC mortality.^{378,379} However, elevated serum IgE concentrations are associated with

decreased survival in Estrogen-Receptor positive breast cancer.³⁸⁰ This demonstrates how the tumor immune microenvironment in different tissues could differentially program mast cells and lead to different patient outcomes. Also, the benefit of histamine may be specific to the liver. Notably, Stage IV melanoma patients treated with subcutaneous histamine and low-dose IL-2 had increased frequency of circulating IFN γ + T cells compared to patients treated with IL2 alone.³⁸¹ Interestingly, patients with liver metastatic melanoma showed greatest improvement in survival rates under the Histamine/IL-2 treatment arm compared to liver metastatic patients treated with IL2 alone, whereas the survival of patients without liver metastasis did not significantly differ between groups.^{382,383}

Although TemRA cells have been reportedly associated with enhanced cytotoxicity,^{257,259} we cannot conclude that these cells are truly tumor-antigen specific and functional cells in our cohort. Ideally, single-cell RNA sequencing in combination with TCR sequencing could help identify which T cell subset is associated with clonal expansion and anti-tumor immunity. We had considered BD RhapsodyTM single cell gene expression profiling, however logistically it required cell sorting CD45⁺ cells and proceeding with freeze-thaw steps, both of which are not possible with neutrophils and mast cells, as they are highly sensitive to cell sorting and cryopreservation.

Due to the small sample sizes and low number of cells, it was not possible to cell sort intra-tumor mast cells and T cells in the cohort for invitro assessment of costimulatory phenotype of the mast cells or the cytotoxic capacity of the T cells. Therefore, the invitro assessment of the costimulatory role of mast cells was performed with blood-derived mast cells preconditioned in tumor storage solution from resected tumors. Although this experiment provided interesting results to support the notion of mast cell costimulatory function in mCRC specifically in patients with prolonged RFS, the exact mechanism remains to be elucidated. Although we were able to identify TGF β 2 as the main factor associated with decreased mast cell activation, we do not know what the driver of mast cell infiltration and activation in tumors is. Contrary to our expectations, soluble SCF and IL3 were not different between the patients. However, it is known that membrane SCF is an important driver of mast cell infiltration and maturation, which could explain this disparity. Given the inverse correlation of secreted TGF β 2 on mast cell activation phenotype, it would be of interest to repeat the in vitro experiment

with TGFβR blocking on mast cells preconditioned in tumor storage solution from patients with poor prognosis to assess whether T cell activation can be restored.

In KRASwt patients with poor prognosis, we observed significantly increased neutrophil infiltration in tumors, which positively correlated with blood absolute neutrophil counts (ANC), indicating systemic mobilization of neutrophils. For the first time, we demonstrate in KRASwt patients that this elevation of ANC is positively associated with enhanced tumor infiltration of neutrophils and that these cells are specifically prognostic for decreased RFS. Furthermore, we showed that the neutrophils appeared to derive from LOX1⁺ PMN-MDSC type neutrophils in the blood that migrated to the tumors. These cells are known to be highly immunosuppressive.³⁰⁸ In the tumors, neutrophils negatively impacted T cell and mast cell infiltration and positively correlated with the secretion of CXCL8, TGFβ2, and TNF. These three molecules negatively correlated with T cells, while TGFβ2 was negatively associated with mast cell activation. The absence of neutrophils in KRASwt patients did not always associate with elevated T cells or mast cell infiltration/activation, as we saw RFS was adversely affected in KRASwt patients with low neutrophils and low T cells or mast cells. This was primarily due to elevated TGFβ2 levels in tumors, which, when decreased, correlated with T cell infiltration, mast cell activation/histamine release and improved RFS. Therefore, in the absence of neutrophils and histamine, T cell infiltration was not rescued, and this may be due to TGFβ2 impact on mast cell activation.

Future Directions – Chapters 1 & 2

Proteomics profiling of tumor tissue storage solution

In collaboration with Proteom'IC platform at Institut Cochin, mass spectrometry assessment of the tumor tissue storage solution and extra-tumor storage solution has been recently performed on N=10 KRASwt and N=5 KRASmut patients with good versus poor prognosis, detecting a total of more than 6500 proteins. A proteomic functional analysis could provide further insight on the biological processes associated with mast cell activation as well as TNF and TGFβ2 secretion in these samples

Testing and validating the secreted factors in liver metastatic biopsies from KRAS wild-type patients to predict RFS

The secreted factors within the tumor microenvironment, termed the 'secretome', refers to all secreted factors ensuing from the crosstalk between the cancer cells, the tumor microenvironment (TME), as well as the tumor-infiltrating lymphocytes and other immune cell components.³⁸⁴ The secretome can provide information on carcinogenesis, neoangiogenesis, tumoral invasion and metastasis as well as chemotherapy resistance.^{385,386} Currently in the laboratory of research in translational immunology (LRTI) at Gustave Roussy directed by Aurélien Marabelle, are testing the measurement of the Tumor Interstitial Fluid (TIF) or "tumor juice" from biopsies of patients enrolled in immunotherapy clinical trials. This non-invasive measurement permits the measurement of proteins secreted or shed by tumor cells, stromal cells as well as TILs. Briefly, core biopsies are sampled from patients before and during treatment and left in 200µl of 0.9% NaCl for a set time before performing secretome measurements using the Mesoscale Discovery platform. Recent results (unpublished data) have demonstrated the utility of this method as a tool for predicting patient response, dynamic monitoring and evaluating the heterogeneity of responses within the same patient at different tissue sites.

Although it would need validation, we could imagine the application of this procedure on liver metastatic biopsies in mCRC patients before the start of chemotherapy treatment and before resection to assess the levels of secreted proteins including Histamine, TNF and TGFβ2 to provide a reflection of the nature of the immune microenvironment in tumors and of possible escape mechanisms for which more personalized and targeted approaches could be applied to prevent recurrence.

Identifying the cellular source and downstream effects of CXCL8, TGFβ and TNF

CXCL8, TGFβ2 and TNF are three molecules involved in colorectal cancer malignancy, chemotherapy resistance and metastatic progression.^{178,314,317} They are also known chemo-attractants of neutrophils, and closely linked to their pro-tumoral function in mCRC.^{287,288,319} Furthermore, TGFβ2 and TNF are known to induce CAF activation in different models of liver pathologies, including liver metastasis.^{325,329,330} In our IHC-stained tissue sections, we observed a trend toward increased FAP-positivity within the tumor stroma of patients with decreased

RFS. A neutrophil-fibroblast crosstalk has been proposed in several pre-clinic models gastrointestinal tumors and liver metastasis mediated by TNF or TGF β .^{178,329,387,388} The blockade of neutrophils and resulting fibrosis reduction in these models suggests a positive feedback loop between the cells in orchestrating tumor promotion and immune escape.

Nanostring GeoMXTM or CosMXTM of the tumor cells, neutrophils as well as fibroblasts could help identify the cellular source of CXCL8, TGF β and TNF as well as the amplified signaling pathways downstream of these factors in FFPE tissue sections of resected tumors. IHC multiplex staining of the downstream signaling pathways and cell subtypes at the protein level could validate and identify the cells responding to these factors. TNF and TGF β are known to have synergistic effects in fibroblast activation, liver fibrosis and in the promotion of cancer cell proliferation, epithelial mesenchymal transition, and apoptosis inhibition.³⁸⁹

The multiple mechanisms through which these factors can orchestrate chronic inflammation and poor prognosis leads us to question whether there is one key driver or if they work in tandem to facilitate immune escape in mCRC. Different drugs targeting TNF and TGF β have been developed, including etanercept, infliximab, and certolizumab for TNF, and galunisertib, fresolimumab, and bintrafusp alfa for TGF β . In a pancreatic cancer liver metastasis model, Etanercept in combination with immunotherapy promoted immune activation.³²⁹ In a mouse CRC liver metastasis model galunisertib in combination with anti-PDL1 significantly increased therapy efficiency.¹⁷⁸ However, in early phase trials TGF β targeted therapy has shown only modest effects in the clinic.³⁹⁰ Importantly, TNF levels are increased in colorectal cancer tumors resistant to oxaliplatin.³⁹¹ Moreover, TNF production by tumors can trigger TNF-R1 dependent activation-induced cell death of CD8⁺T cells, as well as the activation and differentiation of MDSCs.^{326,392} As such, combinatorial treatment targeting both TNF and TGF β may be more effective within liver tumors to boost survival and response rates.

General Discussion – Chapter 3

In the advent of immunotherapy treatment for HCC, our preliminary study addresses the need for a better understanding of the immunopathologic contexture of primary resected HCC with the global aim to improve patient stratification for improved response to immunotherapies. HCC, being a leading cause of cancer-related death globally, has seen recent advances in immunotherapies targeting immune checkpoint molecules like PD-1 and CTLA-4.^{67,69} These therapies have shown promise in a subset of patients, but understanding the immune microenvironment is crucial, as only a limited percentage of patients exhibit objective responses to treatment.

In **Chapter 3** we addressed this question, through a comprehensive assessment of tumor immune infiltrate, secreted factor measurement and transcriptomic analysis within prospectively collected surgically resected intra-tumor, marginal and extra-tumor tissue from HCC patients. Initially, we identified distinct immune subclasses within HCC tumors based on flow cytometry cell phenotyping. These immune clusters, namely #CD8, #CD4, #NK, and #M-DC, are characterized by the dominant immune cell subsets enriched within them. The identified immune clusters present varying different associations with clinical and biological factors. For instance, the #CD4 cluster is predominantly characterized by T2 stage tumors, while the #CD8 cluster shows higher CD45⁺ cell infiltration. In addition, the #CD4 cluster, though it contains high levels of CD4⁺ T cells, may be associated with the presence of largely exhausted CD4⁺ T cells, due to the higher prevalence of activated CD4⁺ Tregs. These findings suggest that immune suppressive mechanisms may be driven by increased Treg activation within the #CD4 cluster.

Furthermore, the lymphoid clusters can be further subdivided into 'cytotoxic' and 'non-cytotoxic' based on their secretome profiles. This division implies that the immune landscape within HCC tumors is not solely determined by the presence of immune cell types but also by the functional state of these cells, which may influence their response to immunotherapies. The 'cytotoxic' subgroup exhibits enhanced expression of specific immune checkpoints and cytotoxic factors, indicating a more active immune response, albeit with signs of exhaustion on the cells and increased activation of Tregs. On the other hand, the 'non-inflammatory' and

'non-cytotoxic' subgroup displays a unique set of enriched cytokines, suggesting different mechanisms driving immune escape. This observation underscores that the identification of specific immunologic subgroups in HCC is more nuanced and comprises both the proportion of immune cell types as well as the ensemble of secreted factors which shape the HCC immune microenvironment.

We conducted gene expression analyses to understand the molecular basis behind these immune clusters. GSEA results demonstrate enriched pathways related to TNF signaling, inflammatory response, IL6-JAK-Stat3, IL2-Stat5 and TGF β signaling in the #CD4 cluster. These pathways collectively indicate complex immune environment characterized by inflammation, and immune regulation.

The 'cytotoxic' subgroup, which is characterized by an elevated secretion of specific cytotoxic factors, presents a distinct transcriptomic signature. The upregulation of genes associated with immune activation, such as GZMA, CD80, CD8A, CD2, and HLA-DOB, in this subgroup aligns with the observed cytotoxic secretome. Furthermore, the increased expression of immune checkpoint molecules like BTLA, CTLA4, and PD1 in this subgroup implies ongoing immune regulation and potential exhaustion, despite the cytotoxic phenotype.

Despite some clear distinctions in the secretome profiles between the 'cytotoxic' and 'non-cytotoxic' subgroups, enrichment pathway analysis on differentially expressed genes did not reveal clear differences between the groups. This suggests that the immunological landscape in HCC is influenced by different interconnected pathways that do not neatly segregate into distinct categories, at least at the transcriptome level when we group patients together. Rather, the dynamic interplay between immune activation and suppression may be a continuous process within these tumors. In summary, our study provides critical insights into the HCC immune microenvironment, where a lymphoid-myeloid dichotomy and a further subdivision into cytotoxic and non-cytotoxic subgroups are evident.

Our research has its limitations, including a relatively small patient cohort. Expanding the cohort and obtaining longitudinal clinical data would strengthen the statistical power of our findings and allow us to draw more robust conclusions regarding the clinical relevance of the immune subtypes we have identified. While we have identified immune clusters, further

research is needed to explore the molecular mechanisms that underlie their immune profiles. Also, while we successfully characterized the main immune cell subsets within HCC tumors, we recognise the need for a more in-depth exploration of myeloid and dendritic cell subtypes as they play important roles in co-stimulation as well as co-inhibition of anti-tumor immune cells within the liver microenvironment. We have yet to characterize patient subgroups based on tissue resident memory markers CXCR6 and CD103. This additional layer of analysis, as well as discrimination on the intensity of PD1 expression on the cells, may help find better correlations between the 'non-inflamed', 'cytotoxic', and 'non-cytotoxic' profiles based on secretome analysis.

Future Directions – Chapter 3

Multi-Omics approaches for Precision Immunotherapy for HCC

Our research holds potential to provide a comprehensive understanding of the immune landscape in HCC, by integrating various data sources, including flow cytometry, cytokine secretion and transcriptomics, along with upcoming Whole Exome Sequencing analysis. The incorporation of these diverse datasets can lead to the identification of very specific subgroups. The identification of distinct intra-tumor immune clusters and the associated immune profiles, as well as the elucidation of the intricate interplay between these clusters, presents a promising perspective for advancing precision immunotherapy in Hepatocellular Carcinoma (HCC). The heterogeneity of immune profiles in primary resected HCC underlines the need for tailored treatment strategies to ensure sensitivity and to prevent primary or acquired resistance. These include: (i) combination strategies that could promote immune cell activation and T cell priming; (ii) relieving tumor-microenvironment-induced immune suppression; and (iii) support the effector functions of anti-tumor immune cells.³⁶⁵

By leveraging this detailed immune profiling, we can work towards developing personalized immunotherapies that target specific immune mechanisms and pathways, optimizing the clinical response and outcomes for HCC patients.

Concluding Remarks

In summary, the research conducted in this thesis has led to advancements in our understanding of the immune microenvironment in mCRC and HCC. For mCRC, the study identified specific immune infiltrates, particularly mast cells and neutrophils that play distinct roles in prognosis and response to treatment in KRAS/BRAF wild-type patients. It also shed light on the potential costimulatory role of mast cells and their activation that may modulate anti-tumor immune responses. Despite limitations in sample size and the need for further mechanistic and validation studies, the research provides valuable information for future investigations, such as the proteomic analysis of secreted factors to predict recurrence and the cellular sources of critical molecules such as TGF β and TNF.

Regarding HCC, the study revealed the existence of immune subclasses and the dichotomy between lymphoid and myeloid cells within the tumor microenvironment. The identification of 'cytotoxic' and 'non-cytotoxic' subgroups based on secretome profiles added depth to the lymphoid subgroup in HCC. While we acknowledge the need for a larger patient cohort and more in-depth investigations into the residential, myeloid, and dendritic cell subtypes, it offers a valuable foundation in classifying HCC patients into immunologic subgroups. The multi-omics approach, integrating flow cytometry, cytokine secretion, transcriptomics, and whole-exome sequencing, could pave the way in the future for tailored treatment strategies targeting specific immune mechanisms and pathways, ultimately improving clinical responses and outcomes for HCC patients.

In conclusion, a comprehensive approach to assess the tumor microenvironment in liver pathologies is crucial for identifying immune escape mechanisms and delivering more effective treatments. This research underscores the need for tailored approaches in addressing the diverse challenges presented by these complex diseases.

Bibliography

1. Sung, H. *et al.* Global Cancer Statistics 2020: GLOBOCAN Estimates of Incidence and Mortality Worldwide for 36 Cancers in 185 Countries. *CA. Cancer J. Clin.* **71**, 209–249 (2021).
2. Dekker, E., Tanis, P. J., Vleugels, J. L. A., Kasi, P. M. & Wallace, M. B. Colorectal cancer. *Lancet* **394**, 1467–1480 (2019).
3. Kasi, P. M. *et al.* Rising Proportion of Young Individuals With Rectal and Colon Cancer. *Clin. Colorectal Cancer* **18**, e87–e95 (2019).
4. Patel, S. G., Karlitz, J. J., Yen, T., Lieu, C. H. & Boland, C. R. The rising tide of early-onset colorectal cancer: a comprehensive review of epidemiology, clinical features, biology, risk factors, prevention, and early detection. *Lancet Gastroenterol. Hepatol.* **7**, 262–274 (2022).
5. Grady, W. M. & Carethers, J. M. Genetic and Epigenetic Instability in Colorectal Cancer Pathogenesis. *Gastroenterology* **135**, 1079–1099 (2008).
6. Koopman, M. *et al.* Deficient mismatch repair system in patients with sporadic advanced colorectal cancer. *Br. J. Cancer* **100**, 266–273 (2009).
7. Jess, T., Rungoe, C. & Peyrin-Biroulet, L. Risk of Colorectal Cancer in Patients With Ulcerative Colitis: A Meta-analysis of Population-Based Cohort Studies. *Clin. Gastroenterol. Hepatol.* **10**, 639–645 (2012).
8. Kerr, J., Anderson, C. & Lippman, S. M. Physical activity, sedentary behaviour, diet, and cancer: an update and emerging new evidence. *Lancet Oncol.* **18**, 457–471 (2017).
9. Liu, P.-H. *et al.* Association of Obesity With Risk of Early-Onset Colorectal Cancer Among Women. *JAMA Oncol.* **5**, 37–44 (2019).
10. van den Berg, I., Coebergh van den Braak, R. R. J., van Vugt, J. L. A., Ijzermans, J. N. M. & Buettner, S. Actual survival after resection of primary colorectal cancer: results from a prospective multicenter study. *World J. Surg. Oncol.* **19**, 1–10 (2021).
11. Robinson, J. R., Newcomb, P. A., Hardikar, S., Cohen, S. A. & Phipps, A. I. Stage IV colorectal cancer primary site and patterns of distant metastasis. *Cancer Epidemiol.* **48**, 92–95 (2017).
12. Riihimäki, M., Hemminki, A., Sundquist, J. & Hemminki, K. Patterns of metastasis in colon and rectal cancer. *Sci. Rep.* **6**, 1–9 (2016).
13. Engstrand, J., Nilsson, H., Strömberg, C., Jonas, E. & Freedman, J. Colorectal cancer liver metastases - a population-based study on incidence, management and survival. *BMC Cancer* **18**, 1–11 (2018).
14. Stewart, C. L. *et al.* Cytoreduction for colorectal metastases: Liver, Lung, Peritoneum, Lymph nodes, Bone, Brain. When does it Palliate, Prolong Survival, and Potentially Cure? *Curr Prob Surg* **55**, 330–379 (2018).
15. Tomlinson, J. S. *et al.* Actual 10-year survival after resection of colorectal liver metastases defines cure. *J. Clin. Oncol.* **25**, 4575–4580 (2007).
16. Viganò, L., Ferrero, A., Lo Tesoriere, R. & Capussotti, L. Liver surgery for colorectal metastases: Results after 10 years of follow-up. Long-term survivors, late recurrences, and prognostic role of morbidity. *Ann. Surg. Oncol.* **15**, 2458–2464 (2008).
17. Abdalla, E. K. *et al.* Recurrence and outcomes following hepatic resection, radiofrequency ablation, and combined resection/ablation for colorectal liver metastases. *Ann. Surg.* **239**, 818–827 (2004).
18. Cucchetti, A. *et al.* Cure Model Survival Analysis After Hepatic Resection for Colorectal Liver Metastases. *Ann. Surg. Oncol.* **22**, 1908–1914 (2015).
19. Nordlinger, B. *et al.* Perioperative chemotherapy with FOLFOX4 and surgery versus surgery alone for resectable liver metastases from colorectal cancer (EORTC

- Intergroup trial 40983): a randomised controlled trial. *Lancet* **371**, 1007–1016 (2008).
20. Van Cutsem, E. *et al.* ESMO consensus guidelines for the management of patients with metastatic colorectal cancer. *Ann. Oncol.* **27**, 1386–1422 (2016).
 21. Viganò, L. *et al.* Evolution of long-term outcome of liver resection for colorectal metastases: Analysis of actual 5-year survival rates over two decades. *Ann. Surg. Oncol.* **19**, 2035–2044 (2012).
 22. André, T. *et al.* Multicenter Phase II Study of Bimonthly High-Dose Leucovorin, Fluorouracil Infusion, and Oxaliplatin for Metastatic Colorectal Cancer Resistant to the Same Leucovorin and Fluorouracil Regimen. *J. Clin. Oncol.* **17**, (1999).
 23. Padman, S. *et al.* Liver only metastatic disease in patients with metastatic colorectal cancer: Impact of surgery and chemotherapy. **52**, 1699–1706 (2013).
 24. Wieser, M., Sauerland, S., Arnold, D., Schmiegel, W. & Reinacher-schick, A. Peri-operative chemotherapy for the treatment of resectable liver metastases from colorectal cancer: A systematic review and meta-analysis of randomized trials. *BMC Cancer* **10**, 1–13 (2010).
 25. Hurwitz, H. *et al.* Bevacizumab plus Irinotecan, Fluorouracil, and Leucovorin for Metastatic Colorectal Cancer. *New Engl. Journal Med.* **350**, 2335–2342 (2004).
 26. Saltz, L. B. *et al.* Bevacizumab in Combination With Oxaliplatin-Based Chemotherapy As First-Line Therapy in Metastatic Colorectal Cancer: A Randomized Phase III Study. *J. Clin. Oncol.* **26**, 2013–2019 (2008).
 27. Van Cutsem, E. *et al.* Cetuximab and Chemotherapy as Initial Treatment for Metastatic Colorectal Cancer. *New Engl. Journal Med.* **360**, 1408–1417 (2009).
 28. Bokemeyer, C. *et al.* Fluorouracil, Leucovorin, and Oxaliplatin With and Without Cetuximab in the First-Line Treatment of Metastatic Colorectal Cancer. *J. Clin. Oncol.* **27**, 663–671 (2009).
 29. Cremolini, C. *et al.* FOLFOXIRI plus bevacizumab versus FOLFIRI plus bevacizumab as first-line treatment of patients with metastatic colorectal cancer: updated overall survival and molecular subgroup analyses of the open-label, phase 3 TRIBE study. *Lancet* **16**, 1306–1315 (2015).
 30. Boland, R. C. & Goel, A. Microsatellite instability in colorectal cancer. *Gastroenterology* **138**, 2073–2087 (2010).
 31. Vogelstein, B. *et al.* Cancer Genome Landscapes. *Science (80-.)*. **339**, 1546–1558 (2013).
 32. Smyrk, T. C., Watson, P., Kaul, K. & Lynch, H. T. Tumor-infiltrating lymphocytes are a marker for microsatellite instability in colorectal carcinoma. *Cancer* **91**, 2417–2422 (2001).
 33. Llosa, N. J. *et al.* The vigorous immune microenvironment of microsatellite instable colon cancer is balanced by multiple counter-inhibitory checkpoints. *Cancer Discov.* **5**, 43–51 (2015).
 34. Mandal, R. *et al.* Genetic diversity of tumors with mismatch repair deficiency influences anti-PD-1 immunotherapy response. *Science (80-.)*. **364**, 485–491 (2019).
 35. André, T. *et al.* Pembrolizumab in Microsatellite-Instability–High Advanced Colorectal Cancer. *N. Engl. J. Med.* **383**, 2207–2218 (2020).
 36. Diaz Jr, L. A. *et al.* Pembrolizumab versus chemotherapy for microsatellite instability-high or mismatch repair-deficient metastatic colorectal cancer (KEYNOTE-177): final analysis of a randomised, open-label, phase 3 study. *Lancet Oncol.* **23**, 659–670 (2022).
 37. Casak, S. J. *et al.* FDA approval summary: Pembrolizumab for the first-line treatment of patients with MSI-H/dMMR advanced unresectable or metastatic colorectal carcinoma. *Clin. Cancer Res.* **27**, 4680–4684 (2021).

38. Overman, M. J. *et al.* Durable clinical benefit with nivolumab plus ipilimumab in DNA mismatch repair-deficient/microsatellite instability-high metastatic colorectal cancer. *J. Clin. Oncol.* **36**, 773–779 (2018).
39. Overman, M. J. *et al.* Nivolumab (NIVO) ± ipilimumab (IPI) in patients (pts) with microsatellite instability-high/mismatch repair-deficient (MSI-H/dMMR) metastatic colorectal cancer (mCRC): Five-year follow-up from CheckMate 142. *J. Clin. Oncol.* **40**, 3510 (2022).
40. André, T. *et al.* Nivolumab plus low-dose ipilimumab in previously treated patients with microsatellite instability-high/mismatch repair-deficient metastatic colorectal cancer: 4-year follow-up from CheckMate 142. *Ann. Oncol.* **33**, 1052–1060 (2022).
41. Le, D. T. *et al.* PD-1 Blockade in Tumors with Mismatch-Repair Deficiency. *N. Engl. J. Med.* **372**, 2509–2520 (2015).
42. Marie, P. K. *et al.* Pilot clinical trial of perioperative durvalumab and tremelimumab in the treatment of resectable colorectal cancer liver metastases. *Clin. Cancer Res.* **27**, 3039–3049 (2021).
43. Wang, C. *et al.* Clinical Response to Immunotherapy Targeting Programmed Cell Death Receptor 1/Programmed Cell Death Ligand 1 in Patients with Treatment-Resistant Microsatellite Stable Colorectal Cancer with and without Liver Metastases. *JAMA Netw. Open* **4**, 1–12 (2021).
44. Venook, A. P. *et al.* Effect of First-line Chemotherapy Combined with Cetuximab or Bevacizumab on Overall Survival in Patients with KRAS Wild-Type Advanced or Metastatic Colorectal Cancer A Randomized Clinical Trial. *JAMA* **317**, 2392–2401 (2017).
45. Van Cutsem, E. *et al.* Cetuximab Plus Irinotecan, Fluorouracil, and Leucovorin As First-Line Treatment for Metastatic Colorectal Cancer : Updated Analysis of Overall Survival According to Tumor KRAS and BRAF Mutation Status. *J. Clin. Oncol.* 1–10 (2011) doi:10.1200/JCO.2010.33.5091.
46. Douillard, J. Y. *et al.* Final results from PRIME: randomized phase III study of panitumumab with FOLFOX4 for first-line treatment of metastatic colorectal cancer. *Ann. Oncol.* **25**, 1346–1355 (2014).
47. Stinzinger, S. *et al.* Impact of BRAF and RAS mutations on first-line efficacy of FOLFIRI plus cetuximab versus FOLFIRI plus bevacizumab: analysis of the FIRE-3 (AIO KKR-0306) study. *Eur. J. Cancer* **79**, 50–60 (2017).
48. Holch, J., Ricard, I., Stinzinger, S., DP, M. & Heinemann, V. The relevance of primary tumour location in patients with metastatic colorectal cancer: A meta-analysis of first-line clinical trials. *Eur. J. Cancer* **70**, 87–98 (2017).
49. Wang, Z. *et al.* Chemotherapy With or Without Anti-EGFR Agents in Left- and Right-Sided Metastatic Colorectal Cancer: An Updated Meta-Analysis. *JNCCN* **17**, 805–811 (2019).
50. Biller, L. & Schrag, D. Diagnosis and Treatment of Metastatic Colorectal Cancer A Review. *JAMA Clin. Rev. Educ.* **325**, 669–685 (2021).
51. Memon, M. & Beekingham, I. Surgical resection of colorectal liver metastases. *Color. Dis.* **3**, 361–372 (2001).
52. de Jong, M. *et al.* Repeat Curative Intent Liver Surgery is Safe and Effective for Recurrent Colorectal Liver Metastasis: Results from an International Multi-institutional Analysis. *J. Gastrointest. Surg.* **13**, 2141–2151 (2009).
53. Grothey, A. *et al.* Regorafenib monotherapy for previously treated metastatic colorectal cancer (CORRECT): An international, multicentre, randomised, placebo-controlled, phase 3 trial. *Lancet* **381**, 303–312 (2013).
54. Mayer, R. J. *et al.* Randomized Trial of TAS-102 for Refractory Metastatic Colorectal

- Cancer. *N. Engl. J. Med.* **372**, 1909–1919 (2015).
55. Runggay, H. *et al.* Global burden of primary liver cancer in 2020 and predictions to 2040. *J. Hepatol.* **77**, 1598–1606 (2022).
 56. Arnold, M. *et al.* Global Burden of 5 Major Types of Gastrointestinal Cancer. *Gastroenterology* **159**, 335-349.e15 (2020).
 57. Forner, A., Reig, M. & Bruix, J. Hepatocellular Carcinoma. *Lancet* **391**, 1301–1314 (2018).
 58. Ganne-Carrié, N. & Nahon, P. Hepatocellular carcinoma in the setting of alcohol-related liver disease. *J. Hepatol.* **70**, 284–293 (2019).
 59. Hassan, M. M. *et al.* Risk factors for hepatocellular carcinoma: Synergism of alcohol with viral hepatitis and diabetes mellitus. *Hepatology* **36**, 1206–1213 (2002).
 60. Anstee, Q. M., Reeves, H. L., Kotsiliti, E., Govaere, O. & Heikenwalder, M. From NASH to HCC: current concepts and future challenges. *Nat. Rev. Gastroenterol. Hepatol.* **16**, 411–428 (2019).
 61. Petrick, J. L. & McGlynn, K. A. The changing epidemiology of primary liver cancer. *Curr Epidemiol Rep.* **6**, 104–111 (2019).
 62. Estes, C., Razavi, H., Loomba, R., Younossi, Z. & Sanyal, A. J. Modeling the epidemic of nonalcoholic fatty liver disease demonstrates an exponential increase in burden of disease. *Hepatology* **67**, 123–133 (2018).
 63. Llovet, J., Brù, C. & Bruix, J. Prognosis of Hepatocellular Carcinoma: The BCLC Staging Classification. *Thieme Semin. Liver Dis.* **19**, 329–338 (1999).
 64. Wang, Y. Y. *et al.* Albumin-bilirubin versus Child-Pugh score as a predictor of outcome after liver resection for hepatocellular carcinoma. *Br. J. Surg.* **103**, 725–734 (2016).
 65. Roayaie, S. *et al.* Resection of hepatocellular cancer ≤ 2 cm: Results from two Western centers. *Hepatology* **57**, 1426–1435 (2013).
 66. Imamura, H. *et al.* Risk factors contributing to early and late phase intrahepatic recurrence of hepatocellular carcinoma after hepatectomy. *J. Hepatol.* **38**, 200–207 (2003).
 67. Finn, R. S. *et al.* Atezolizumab plus Bevacizumab in Unresectable Hepatocellular Carcinoma. *N. Engl. J. Med.* **382**, 1894–1905 (2020).
 68. Llovet, J. M. *et al.* Immunotherapies for hepatocellular carcinoma. *Nat. Rev. Clin. Oncol.* **19**, 151–172 (2022).
 69. Abou-Alfa, G. K. *et al.* Tremelimumab plus Durvalumab in Unresectable Hepatocellular Carcinoma. *NEJM Evid.* **1**, 1–12 (2022).
 70. Yau, T. *et al.* CheckMate 459: A randomized, multi-center phase III study of nivolumab (NIVO) vs sorafenib (SOR) as first-line (1L) treatment in patients (pts) with advanced hepatocellular carcinoma (aHCC). *Ann. Oncol.* **30**, v874–v875 (2019).
 71. Llovet, J. M. *et al.* Hepatocellular carcinoma. *Nat. Rev. Dis. Prim.* **7**, (2021).
 72. Lu, L. C. *et al.* Differential Organ-Specific Tumor Response to Immune Checkpoint Inhibitors in Hepatocellular Carcinoma. *Liver Cancer* **8**, 480–490 (2019).
 73. Kim, H. S. *et al.* The presence and size of intrahepatic tumors determine the therapeutic efficacy of nivolumab in advanced hepatocellular carcinoma. *Ther. Adv. Med. Oncol.* **14**, 1–13 (2022).
 74. Huang, K. W. *et al.* Role of organ-specific response to immune checkpoint inhibitor in survival for advanced hepatocellular carcinoma. *Meet. Abstr. | 2022 ASCO Annu. Meet.* **150**, (2022).
 75. Kaseb, A. O. *et al.* Perioperative nivolumab monotherapy versus nivolumab plus ipilimumab in resectable hepatocellular carcinoma: a randomised, open-label, phase 2 trial. *Lancet Gastroenterol. Hepatol.* **7**, 208–218 (2022).

76. Macparland, S. A. *et al.* Single cell RNA sequencing of human liver reveals distinct intrahepatic macrophage populations. *Nat. Commun.* **9**, 1–21 (2018).
77. Schenk, W. G., McDonald, J. C., McDonald, K. & Drapanas, T. Direct Measurement of Hepatic Blood Flow in Surgical Patients. *Ann. Surg.* **156**, 463–471 (1962).
78. Rappaport, A. M. Hepatic blood flow: morphologic aspects and physiologic regulation. *Int. Rev. Physiol.* **21**, 1–63 (1980).
79. Saxena, R., Theise, N. D. & Crawford, J. M. Microanatomy of the human liver - Exploring the hidden interfaces. *Hepatology* **30**, 1339–1346 (1999).
80. Cantor, H. M. & Dumont, A. E. Hepatic suppression of sensitization to antigen absorbed into the portal system [23]. *Nature* **215**, 744–745 (1967).
81. Callery, M. P., Kamei, T. & Flye, M. W. The effect of portacaval shunt on delayed-hypersensitivity responses following antigen feeding. *J. Surg. Res.* **46**, 391–394 (1989).
82. Yang, R., Liu, Q., Grosfeld, J. L. & Pescovitz, M. D. Intestinal venous drainage through the liver is a prerequisite for oral tolerance induction. *J. Pediatr. Surg.* **29**, 1145–1148 (1994).
83. Limmer, A. *et al.* Cross-presentation of oral antigens by liver sinusoidal endothelial cells leads to CD8 T cell tolerance. *Eur. J. Immunol.* **35**, 2970–2981 (2005).
84. Diehl, L. *et al.* Tolerogenic maturation of liver sinusoidal endothelial cells promotes B7-homolog 1-dependent CD8+ T cell tolerance. *Hepatology* **47**, 296–305 (2008).
85. Schurich, A. *et al.* Dynamic Regulation of CD8 T Cell Tolerance Induction by Liver Sinusoidal Endothelial Cells. *J. Immunol.* **184**, 4107–4114 (2010).
86. Knolle, P. A. *et al.* Induction of cytokine production in naive CD4+ T cells by antigen-presenting murine liver sinusoidal endothelial cells but failure to induce differentiation toward T(h1) cells. *Gastroenterology* **116**, 1428–1440 (1999).
87. Carambia, A. *et al.* Inhibition of inflammatory CD4 T cell activity by murine liver sinusoidal endothelial cells. *J. Hepatol.* **58**, 112–118 (2013).
88. Carambia, A. *et al.* TGF- β -dependent induction of CD4+CD25+Foxp3 + Tregs by liver sinusoidal endothelial cells. *J. Hepatol.* **61**, 594–599 (2014).
89. Sumpter, T. L. *et al.* Hepatic Stellate Cells Undermine the Allostimulatory Function of Liver Myeloid Dendritic Cells via STAT3-Dependent Induction of IDO. *J. Immunol.* **189**, 3848–3858 (2012).
90. Höchst, B. *et al.* Activated human hepatic stellate cells induce myeloid derived suppressor cells from peripheral blood monocytes in a CD44-dependent fashion. *J. Hepatol.* **59**, 528–535 (2013).
91. Bhatt, S. *et al.* All- trans Retinoic Acid Induces Arginase-1 and Inducible Nitric Oxide Synthase–Producing Dendritic Cells with T Cell Inhibitory Function . *J. Immunol.* **192**, 5098–5108 (2014).
92. Ichikawa, S., Mucida, D., Tyznik, A., Kronenberg, M. & Cheroutre, H. Hepatic Stellate Cells Function as Regulatory Bystanders Shintaro. *J Immunol* **186**, 5549–5555 (2011).
93. Dunham, R. M. *et al.* Hepatic Stellate Cells Preferentially Induce Foxp3 + Regulatory T Cells by Production of Retinoic Acid . *J. Immunol.* **190**, 2009–2016 (2013).
94. Jiang, Z. *et al.* Hepatic stellate cells promote immunotolerance following orthotopic liver transplantation in rats via induction of T cell apoptosis and regulation of Th2/Th3-like cell cytokine production. *Exp. Ther. Med.* **5**, 165–169 (2013).
95. Yang, H.-R. *et al.* A Critical Role of TRAIL Expressed on Cotransplanted Hepatic Stellate Cells in Prevention of Islet Allograft Rejection. *Microsurgery* **30**, 332–337 (2009).
96. Dangi, A. *et al.* Selective Expansion of Allogeneic Regulatory T Cells by Hepatic

- Stellate Cells: Role of Endotoxin and Implications for Allograft Tolerance. *J. Immunol.* **188**, 3667–3677 (2012).
97. Kumar, S., Wang, J., Thomson, A. W. & Gandhi, C. R. Hepatic stellate cells increase the immunosuppressive function of natural Foxp3 + regulatory T cells via IDO-induced AhR activation. *J. Leukoc. Biol.* **101**, 429–438 (2017).
 98. De Simone, G. *et al.* Identification of a Kupffer cell subset capable of reverting the T cell dysfunction induced by hepatocellular priming. *Immunity* **54**, 2089–2100.e8 (2021).
 99. Heymann, F. *et al.* Liver Inflammation Abrogates Immunological Tolerance Induced by Kupffer Cells. *Hepatology* **62**, 279–291 (2015).
 100. Breous, E., Somanathan, S., Vandenberghe, L. H. & Wilson, J. M. Hepatic regulatory T cells and Kupffer cells are crucial mediators of systemic T cell tolerance to antigens targeting murine liver. *Hepatology* **50**, 612–621 (2009).
 101. You, Q., Cheng, L., Kedl, R. M. & Ju, C. Mechanism of T Cell Tolerance Induction by Murine Hepatic Kupffer Cells. *Hepatology* **48**, 978–990 (2008).
 102. Knolle, P. *et al.* Human Kupffer cells secrete IL-10 in response to lipopolysaccharide (LPS) challenge. *J. Hepatol.* **22**, 226–229 (1995).
 103. Yan, M. L., Wang, Y. D., Tian, Y. F., Lai, Z. De & Yan, L. N. Inhibition of allogeneic T-cell response by Kupffer cells expressing indoleamine 2,3-dioxygenase. *World J. Gastroenterol.* **16**, 636–640 (2010).
 104. Chen, Y. *et al.* Role of Kupffer Cells in the Induction of Tolerance of Orthotopic Liver Transplantation in Rats. *Liver Transplant.* 823–836 (2008) doi:10.1002/lt.
 105. Tu, Z. *et al.* TLR-dependent cross talk between human Kupffer cells and NK cells. *J. Exp. Med.* **205**, 233–244 (2008).
 106. Bamboat, Z. M. *et al.* Human Liver Dendritic Cells Promote T Cell Hyporesponsiveness. *J. Immunol.* **182**, 1901–1911 (2009).
 107. Goubier, A. *et al.* Plasmacytoid Dendritic Cells Mediate Oral Tolerance. *Immunity* **29**, 464–475 (2008).
 108. Tokita, D. *et al.* Poor allostimulatory function of liver plasmacytoid DC is associated with pro-apoptotic activity, dependent on regulatory T cells. *J. Hepatol.* **49**, 1008–1018 (2008).
 109. Ono, Y. *et al.* Graft-infiltrating PD-L1hi cross-dressed dendritic cells regulate antidonor T cell responses in mouse liver transplant tolerance. *Hepatology* **67**, 1499–1515 (2018).
 110. Steptoe, R. J. *et al.* Augmentation of dendritic cells in murine organ donors by Flt3 ligand alters the balance between transplant tolerance and immunity. *J. Immunol.* **159**, 5483–91 (1997).
 111. Kelly, A. *et al.* CD141+ myeloid dendritic cells are enriched in healthy human liver. *J. Hepatol.* **60**, 135–142 (2014).
 112. Ho, W. W. *et al.* Dendritic cell paucity in mismatch repair – proficient colorectal cancer liver metastases limits immune checkpoint blockade efficacy. *Proc. Natl. Acad. Sci.* **118**, (2021).
 113. Pedroza-Gonzalez, A. *et al.* Tumor-infiltrating plasmacytoid dendritic cells promote immunosuppression by Tr1 cells in human liver tumors. *Oncoimmunology* **4**, 1–9 (2015).
 114. Gurish, M. F. & Austen, K. F. Developmental Origin and Functional Specialization of Mast Cell Subsets. *Immunity* **37**, 25–33 (2012).
 115. Ji, J. *et al.* Hepatic stellate cell and monocyte interaction contributes to poor prognosis in hepatocellular carcinoma. *Hepatology* **62**, 481–495 (2015).
 116. Li, Z. *et al.* Adult Connective Tissue-Resident Mast Cells Originate from Late

- Erythro-Myeloid Progenitors. *Immunity* **49**, 640-653.e5 (2018).
117. Gilfillan, A. M. & Tkaczyk, C. Integrated signalling pathways for mast-cell activation. *Nat. Rev. Immunol.* **6**, 218–230 (2006).
 118. Jarido, V. *et al.* The emerging role of mast cells in liver disease. *Am. J. Physiol. - Gastrointest. Liver Physiol.* **313**, G89–G101 (2017).
 119. Armbrust, T., Batusic, D., Ringe, B. & Ramadori, G. Mast cells distribution in human liver disease and experimental rat liver fibrosis. Indications for mast cell participation in development of liver fibrosis. *J. Hepatol.* **26**, 1042–1054 (1997).
 120. Yamashiro, M. *et al.* Distribution of intrahepatic mast cells in various hepatobiliary disorders. *Virchows Arch.* **433**, 471–479 (1998).
 121. Norris, S. *et al.* Resident human hepatic lymphocytes are phenotypically different from circulating lymphocytes. *J. Hepatol.* **28**, 84–90 (1998).
 122. Bowen, D. G. *et al.* The site of primary T cell activation is a determinant of the balance between intrahepatic tolerance and immunity. *J. Clin. Invest.* **114**, 701–712 (2004).
 123. Böttcher, J. P. *et al.* Liver-primed memory T cells generated under noninflammatory conditions provide anti-infectious immunity. *Cell Rep.* **3**, 779–795 (2013).
 124. Tay, S. S. *et al.* Antigen expression level threshold tunes the fate of CD8 T cells during primary hepatic immune responses. *Proc. Natl. Acad. Sci. U. S. A.* **111**, (2014).
 125. Boni, C. *et al.* Characterization of Hepatitis B Virus (HBV)-Specific T-Cell Dysfunction in Chronic HBV Infection. *J. Virol.* **81**, 4215–4225 (2007).
 126. Ochel, A. *et al.* Effective intrahepatic CD8⁺ T-cell immune responses are induced by low but not high numbers of antigen-expressing hepatocytes. *Cell. Mol. Immunol.* **13**, 805–815 (2016).
 127. Cebula, M. *et al.* TLR9-Mediated Conditioning of Liver Environment Is Essential for Successful Intrahepatic Immunotherapy and Effective Memory Recall. *Mol. Ther.* **25**, 2289–2298 (2017).
 128. Steger, U. *et al.* Exhaustive differentiation of alloreactive CD8⁺ T cells: Critical for determination of graft acceptance or rejection. *Transplantation* **85**, 1339–1347 (2008).
 129. Thai, N. L. *et al.* Interleukin-2 and interleukin-12 mediate distinct effector mechanisms of liver allograft rejection. *Liver Transplant. Surg.* **3**, 118–129 (1997).
 130. Lim, T. Y. *et al.* Low dose interleukin-2 selectively expands circulating regulatory T cells but fails to promote liver allograft tolerance in humans. *J. Hepatol.* 1–12 (2022) doi:10.1016/j.jhep.2022.08.035.
 131. Katz, S. C. *et al.* T cell infiltrate predicts long-term survival following resection of colorectal cancer liver metastases. *Ann. Surg. Oncol.* **16**, 2524–2530 (2009).
 132. Kurebayashi, Y. *et al.* Landscape of immune microenvironment in hepatocellular carcinoma and its additional impact on histological and molecular classification. *Hepatology* **68**, 1025–1041 (2018).
 133. Li, W. *et al.* New insights into mechanisms of spontaneous liver transplant tolerance: The role of Foxp3-expressing CD25⁺CD4⁺ regulatory T cells. *Am. J. Transplant.* **8**, 1639–1651 (2008).
 134. Francis, R. S. *et al.* Induction of transplantation tolerance converts potential effector T cells into graft-protective regulatory T cells. *Eur. J. Immunol.* **41**, 726–738 (2011).
 135. Pu, L.-Y. *et al.* Adoptive transfusion of ex vivo donor alloantigen-stimulated CD4⁺CD25⁺ regulatory T cells ameliorates rejection of DA-to-Lewis rat liver transplantation. *Surgery* **142**, 67–73 (2007).
 136. Taubert, R. *et al.* Hepatic Infiltrates in Operational Tolerant Patients after Liver Transplantation Show Enrichment of Regulatory T Cells before Proinflammatory Genes Are Downregulated. *Am. J. Transplant.* **16**, 1285–1293 (2016).

137. Todo, S. *et al.* A pilot study of operational tolerance with a regulatory T-cell-based cell therapy in living donor liver transplantation. *Hepatology* **64**, 632–643 (2016).
138. Pallett, L. J. *et al.* IL-2high tissue-resident T cells in the human liver: Sentinels for hepatotropic infection. *J. Exp. Med.* **214**, 1567–1580 (2017).
139. Stelma, F. *et al.* Human intrahepatic CD69 + CD8+ T cells have a tissue resident memory T cell phenotype with reduced cytolytic capacity. *Sci. Rep.* **7**, 1–10 (2017).
140. Wiggins, B. G. *et al.* The human liver microenvironment shapes the homing and function of CD4+ T-cell populations. *Gut* **71**, 1399–1411 (2022).
141. Zakeri, N. *et al.* Characterisation and induction of tissue-resident gamma delta T-cells to target hepatocellular carcinoma. *Nat. Commun.* **13**, 1–16 (2022).
142. Christo, S. N. *et al.* Discrete tissue microenvironments instruct diversity in resident memory T cell function and plasticity. *Nat. Immunol.* **22**, 1140–1151 (2021).
143. McNamara, H. A. *et al.* Up-regulation of LFA-1 allows liver-resident memory T cells to patrol and remain in the hepatic sinusoids H. *Sci. Immunol.* **2**, (2017).
144. Doherty, D. G. *et al.* The Human Liver Contains Multiple Populations of NK Cells, T Cells, and CD3 + CD56+ Natural T Cells with Distinct Cytotoxic Activities and Th1, Th2, and Th0 Cytokine Secretion Patterns. *J. Immunol.* **163**, 2314–2321 (1999).
145. Filipovic, I. *et al.* 29-Color Flow Cytometry: Unraveling Human Liver NK Cell Repertoire Diversity. *Front. Immunol.* **10**, 1–14 (2019).
146. Lassen, M. G., Lukens, J. R., Dolina, J. S., Brown, M. G. & Hahn, Y. S. Intrahepatic IL-10 Maintains NKG2A+ Ly49– Liver NK Cells in a Functionally Hyporesponsive State Matthew. *J Immunol* **184**, 2693–2701 (2010).
147. Harmon, C. *et al.* Liver-derived TGF- β maintains the eomesitbetlo phenotype of liver resident natural killer cells. *Front. Immunol.* **10**, 1–9 (2019).
148. Lunemann, S. *et al.* Human liver-derived CXCR6+ NK cells are predominantly educated through NKG2A and show reduced cytokine production. *J. Leukoc. Biol.* **105**, 1331–1340 (2019).
149. Diniz, M. O. *et al.* NK cells limit therapeutic vaccine–induced CD8+T cell immunity in a PD-L1–dependent manner. *Sci. Transl. Med.* **14**, (2022).
150. Spada, F. M., Koezuka, Y. & Porcelli, S. A. CD1d-restricted recognition of synthetic glycolipid antigens by human natural killer T cells. *J. Exp. Med.* **188**, 1529–1534 (1998).
151. Faure, F., Jitsukawa, S., Miossec, C. & Hercend, T. CD1c as a target recognition structure for human T lymphocytes: Analysis with peripheral blood γ/δ cells. *Eur. J. Immunol.* **20**, 703–706 (1990).
152. Huang, W. *et al.* The Role of CD1d and MR1 Restricted T Cells in the Liver. *Front. Immunol.* **9**, 1–11 (2018).
153. Reantragoon, R. *et al.* Antigen-loaded MR1 tetramers define T cell receptor heterogeneity in mucosal-associated invariant T cells. *J. Exp. Med.* **210**, 2305–2320 (2013).
154. Dusseaux, M. *et al.* Human MAIT cells are xenobiotic-resistant, tissue-targeted, CD161 hi IL-17-secreting T cells. *Blood* **117**, 1250–1259 (2011).
155. Tang, X.-Z. *et al.* IL-7 Licenses Activation of Human Liver Intrasinusoidal Mucosal-Associated Invariant T Cells. *J. Immunol.* **190**, 3142–3152 (2013).
156. Vidal-Vanaclocha, F. *Liver Metastasis: Biology and Clinical Management, Cancer Metastasis - Biology and Treatment.* Springer (2011). doi:10.1007/978-94-007-0292-9.
157. Brodt, P. Role of the microenvironment in liver metastasis: From pre- to prometastatic niches. *Clin. Cancer Res.* **22**, 5971–5982 (2016).
158. Izraely, S. & Witz, I. P. Site-specific metastasis: A cooperation between cancer cells and the metastatic microenvironment. *Int. J. Cancer* **148**, 1308–1322 (2021).

159. Kather, J. N. *et al.* Topography of cancer-associated immune cells in human solid tumors. *Elife* **7**, 1–19 (2018).
160. Kwak, Y. *et al.* Immunoscore encompassing CD3+ and CD8+ T cell densities in distant metastasis is a robust prognostic marker for advanced colorectal cancer. *Oncotarget* **7**, 81778–81790 (2016).
161. Zhou, S. N. *et al.* Comparison of Immune Microenvironment Between Colon and Liver Metastatic Tissue in Colon Cancer Patients with Liver Metastasis. *Dig. Dis. Sci.* **66**, 474–482 (2021).
162. Galon, J. *et al.* Type, Density, and Location of Immune Cells Within Human Colorectal Tumors Predict Clinical Outcome. *Science (80-.)*. **313**, 1960–1964 (2006).
163. Mlecnik, B. *et al.* Comprehensive intrametastatic immune quantification and major impact of immunoscore on survival. *J. Natl. Cancer Inst.* **110**, 97–108 (2018).
164. Van den Eynde, M. *et al.* The Link between the Multiverse of Immune Microenvironments in Metastases and the Survival of Colorectal Cancer Patients. *Cancer Cell* **34**, 1012–1026 (2018).
165. Tanis, E. *et al.* Prognostic impact of immune response in resectable colorectal liver metastases treated by surgery alone or surgery with perioperative FOLFOX in the randomised EORTC study 40983. *Eur. J. Cancer* **51**, 2708–2717 (2015).
166. Dosset, M. *et al.* PD-1/PD-L1 pathway: an adaptive immune resistance mechanism to immunogenic chemotherapy in colorectal cancer. *Oncoimmunology* **7**, 1–14 (2018).
167. Vincent, J. *et al.* 5-Fluorouracil selectively kills tumor-associated myeloid-derived suppressor cells resulting in enhanced T cell-dependent antitumor immunity. *Cancer Res.* **70**, 3052–3061 (2010).
168. Pfirschke, C. *et al.* Immunogenic Chemotherapy Sensitizes Tumors to Checkpoint Blockade Therapy. *Immunity* **44**, 343–354 (2016).
169. Inoue, Y. *et al.* Cetuximab strongly enhances immune cell infiltration into liver metastatic sites in colorectal cancer. *Cancer Sci.* **108**, 455–460 (2017).
170. Dagenborg, V. J. *et al.* Neoadjuvant chemotherapy is associated with a transient increase of intratumoral T-cell density in microsatellite stable colorectal liver metastases. *Cancer Biol. Ther.* **21**, 432–440 (2020).
171. Høye, E. *et al.* Abstract 1346: T cell receptor repertoire sequencing reveals chemotherapy-driven clonal expansion in colorectal liver metastases. *Cancer Res.* **82**, 1346 (2022).
172. Angelova, M. *et al.* Evolution of Metastases in Space and Time under Immune Selection. *Cell* **175**, 1–15 (2018).
173. Lee, J. C. *et al.* Regulatory T cell control of systemic immunity and immunotherapy response in liver metastasis. *Sci. Immunol.* **5**, (2020).
174. Yu, J. *et al.* Liver metastasis restrains immunotherapy efficacy via macrophage-mediated T cell elimination. *Nat. Med.* **27**, 152–164 (2021).
175. Katz, S. C. *et al.* Regulatory T cell infiltration predicts outcome following resection of colorectal cancer liver metastases. *Ann. Surg. Oncol.* **20**, 946–955 (2013).
176. Pedroza-Gonzalez, A. *et al.* Activated tumor-infiltrating CD4+ regulatory T cells restrain antitumor immunity in patients with primary or metastatic liver cancer. *Hepatology* **57**, 183–194 (2013).
177. Woolston, A. *et al.* Genomic and Transcriptomic Determinants of Therapy Resistance and Immune Landscape Evolution during Anti-EGFR Treatment in Colorectal Cancer. *Cancer Cell* **36**, 35–50 (2019).
178. Tauriello, F. *et al.* TGF β drives immune evasion in genetically reconstituted colon cancer metastasis. *Nature* **554**, 538–543 (2018).
179. Wu, Y. *et al.* Spatiotemporal Immune Landscape of Colorectal Cancer Liver

- Metastasis at Single-Cell Level. *Cancer Discov.* **12**, 134–153 (2022).
180. Che, L. H. *et al.* A single-cell atlas of liver metastases of colorectal cancer reveals reprogramming of the tumor microenvironment in response to preoperative chemotherapy. *Cell Discov.* **7**, (2021).
 181. Prior, I. a, Lewis, P. D. & Mattos, C. A comprehensive survey of Ras mutations in cancer. *Cancer Res.* **72**, 2457–2467 (2012).
 182. Brudvik, K. W. *et al.* Meta-analysis of KRAS mutations and survival after resection of colorectal liver metastases. *Br. J. Surg.* **102**, 1175–1183 (2015).
 183. Ledys, F. *et al.* RAS status and neoadjuvant chemotherapy impact CD8+ cells and tumor HLA class i expression in liver metastatic colorectal cancer. *J. Immunother. Cancer* **6**, 1–14 (2018).
 184. Liu, H. *et al.* Mutant KRAS Drives Immune Evasion by Sensitizing Cytotoxic T-Cells to Activation-Induced Cell Death in Colorectal Cancer. *Adv. Sci.* **10**, 1–15 (2023).
 185. Liao, W. *et al.* KRAS-IRF2 Axis Drives Immune Suppression and Immune Therapy Resistance in Colorectal Cancer. *Cancer Cell* **35**, 559–572 (2019).
 186. Polidoro, M. A. *et al.* Impact of RAS mutations on the immune infiltrate of colorectal liver metastases: A preliminary study. *J. Leukoc. Biol.* **108**, 715–721 (2020).
 187. Varricchi, G. *et al.* Physiological Roles of Mast Cells: Collegium Internationale Allergologicum Update 2019. *Int. Arch. Allergy Immunol.* **179**, 247–261 (2019).
 188. Varricchi, G., Raap, U., Rivellese, F., Marone, G. & Gibbs, B. Human mast cells and basophils-How are they similar how are they different? *Immunol. Rev.* **282**, 8–34 (2018).
 189. Galli, S. J. *et al.* Mast cells as ‘tunable’ effector and immunoregulatory cells: Recent advances. *Annu. Rev. Immunol.* **23**, 749–786 (2005).
 190. Galli, S. J., Grimaldeston, M. & Tsai, M. Immunomodulatory mast cells: negative, as well as positive, regulators of immunity Stephen. *Nature* **8**, 478–486 (2008).
 191. Gaudenzio, N. *et al.* Different activation signals induce distinct mast cell degranulation strategies. *J. Clin. Invest.* **126**, 3981–3998 (2016).
 192. Karhausen, J. & Abraham, S. N. How mast cells make decisions. *J. Clin. Invest.* **126**, 3735–3738 (2016).
 193. Irani, A. & Schwartz, L. B. Human mast cell heterogeneity. *Allergy Protoc.* **15**, 303–308 (1994).
 194. Plum, T. *et al.* Human Mast Cell Proteome Reveals Unique Lineage, Putative Functions, and Structural Basis for Cell Ablation. *Immunity* **52**, 404–416 (2020).
 195. Hauswirth, A. W. *et al.* CD203c is overexpressed on neoplastic mast cells in systemic mastocytosis and is upregulated upon IgE receptor cross-linking. **21**, 797–806 (2008).
 196. Bouzima, R. *et al.* Marked improvement of the basophil activation test by detecting CD203c instead of CD63. *Clin. Exp. Allergy* **33**, 259–265 (2003).
 197. Varricchi, G. *et al.* Are mast cells MASTers in cancer? *Front. Immunol.* **8**, 1–13 (2017).
 198. Oldford, S. A. & Marshall, J. S. Mast cells as targets for immunotherapy of solid tumors. *Mol. Immunol.* **63**, 113–124 (2015).
 199. Yang, Z. *et al.* Mast cells mobilize myeloid-derived suppressor cells and Treg cells in tumor microenvironment via IL-17 pathway in murine hepatocarcinoma model. *PLoS One* **5**, 1–9 (2010).
 200. De Filippo, K. *et al.* Mast cell and macrophage chemokines CXCL1/CXCL2 control the early stage of neutrophil recruitment during tissue inflammation. *Blood* **121**, 4930–4937 (2013).
 201. Yang, X.-D. *et al.* Histamine deficiency promotes inflammation-associated carcinogenesis through reduced myeloid maturation and accumulation of CD11b+

- Ly6G+ immature myeloid cells Xiang. *Nat. Med.* **17**, 87–95 (2011).
202. Forward, N. A., Furlong, S. J., Yang, Y., Lin, T.-J. & Hoskin, D. W. Mast Cells Down-Regulate CD4+CD25+ T Regulatory Cell Suppressor Function via Histamine H1 Receptor Interaction. *J. Immunol.* **183**, 3014–3022 (2009).
 203. Blatner, N. R. *et al.* In colorectal cancer mast cells contribute to systemic regulatory T-cell dysfunction. *Proc. Natl. Acad. Sci.* **107**, 6430–6435 (2010).
 204. Piconese, S. *et al.* Mast cells counteract regulatory T-cell suppression through interleukin-6 and OX40/OX40L axis toward Th17-cell differentiation. *Blood* **114**, 2639–2648 (2009).
 205. Oldford, S. A. *et al.* A Critical Role for Mast Cells and Mast Cell-Derived IL-6 in TLR2-Mediated Inhibition of Tumor Growth. *J. Immunol.* **185**, 7067–7076 (2010).
 206. Caron, G. *et al.* Histamine Induces CD86 Expression and Chemokine Production by Human Immature Dendritic Cells. *J. Immunol.* **166**, 6000–6006 (2001).
 207. Dawicki, W., Jawdat, D. W., Xu, N. & Marshall, J. S. Mast Cells, Histamine, and IL-6 Regulate the Selective Influx of Dendritic Cell Subsets into an Inflamed Lymph Node. *J. Immunol.* **184**, 2116–2123 (2010).
 208. Gulubova, M. V. Structural examination of tryptase- and chymase-positive mast cells in livers, containing metastases from gastrointestinal cancers. *Clin. Exp. Metastasis* **20**, 611–620 (2003).
 209. Suzuki, S. *et al.* High infiltration of mast cells positive to tryptase predicts worse outcome following resection of colorectal liver metastases. *BMC Cancer* **15**, 1–8 (2015).
 210. Giușcă, S. E. *et al.* Tryptase-positive and CD117 Positive Mast Cells Correlate with Survival in Patients with Liver Metastasis. *Anticancer Res.* **35**, 5325–5331 (2015).
 211. Ringelhan, M., Pfister, D., O’Connor, T., Pikarsky, E. & Heikenwalder, M. The immunology of hepatocellular carcinoma review-article. *Nat. Immunol.* **19**, 222–232 (2018).
 212. Zhang, Q. *et al.* Landscape and Dynamics of Single Immune Cells in Hepatocellular Carcinoma. *Cell* **179**, 829–845 (2019).
 213. Leslie, J. *et al.* CXCR2 inhibition enables NASH-HCC immunotherapy. *Gut* **71**, 2093–2106 (2022).
 214. Pfister, D. *et al.* NASH limits anti-tumour surveillance in immunotherapy-treated HCC. *Nature* **592**, 450–456 (2021).
 215. Han, Y. *et al.* Human CD14+CTLA-4+ regulatory dendritic cells suppress T-cell response by cytotoxic T-lymphocyte antigen-4-dependent IL-10 and indoleamine-2,3-dioxygenase production in hepatocellular carcinoma. *Hepatology* **59**, 567–579 (2014).
 216. Ruf, B. *et al.* Tumor-associated macrophages trigger MAIT cell dysfunction at the HCC invasive margin. *Cell* **186**, 3686–3705 (2023).
 217. Sia, D. *et al.* Identification of an Immune-specific Class of Hepatocellular Carcinoma, Based on Molecular Features. *Gastroenterology* **153**, 812–826 (2017).
 218. Montironi, C. *et al.* Inflamed and non-inflamed classes of HCC: a revised immunogenomic classification. *Gut* **0**, 1–12 (2022).
 219. Pfister, D. *et al.* NASH limits anti-tumour surveillance in immunotherapy-treated HCC. **592**, 450–456 (2021).
 220. Wolf, M. J. *et al.* Metabolic activation of intrahepatic CD8+ T cells and NKT cells causes nonalcoholic steatohepatitis and liver cancer via cross-talk with hepatocytes. *Cancer Cell* **26**, 549–564 (2014).
 221. Dudek, M. *et al.* Auto-aggressive CXCR6+ CD8 T cells cause liver immune pathology in NASH. *Nature* **592**, 444–449 (2021).
 222. Kassel, R. *et al.* Chronically Inflamed Livers Up-regulate Expression of Inhibitory B7

- Family Members. *Hepatology* **50**, 1625–1637 (2009).
223. Haber, P. K. *et al.* Evidence-Based Management of Hepatocellular Carcinoma: Systematic Review and Meta-analysis of Randomized Controlled Trials (2002–2020). *Gastroenterology* **161**, 879–898 (2021).
 224. Lim, C. J. *et al.* Multidimensional analyses reveal distinct immune microenvironment in hepatitis B virus-related hepatocellular carcinoma. *Gut* **68**, 916–927 (2019).
 225. Lu, Y. *et al.* A single-cell atlas of the multicellular ecosystem of primary and metastatic hepatocellular carcinoma. *Nat. Commun.* **13**, 1–18 (2022).
 226. Barsch, M. *et al.* T-cell exhaustion and residency dynamics inform clinical outcomes in hepatocellular carcinoma. *J. Hepatol.* **77**, 397–409 (2022).
 227. Zhu, A. X. *et al.* Molecular correlates of clinical response and resistance to atezolizumab in combination with bevacizumab in advanced hepatocellular carcinoma. *Nat. Med.* **28**, 1599–1611 (2022).
 228. Haber, P. K. *et al.* Molecular Markers of Response to Anti-PD1 Therapy in Advanced Hepatocellular Carcinoma. *Gastroenterology* **164**, 72–88 (2023).
 229. Magen, A. *et al.* Intratumoral dendritic cell–CD4⁺ T helper cell niches enable CD8⁺ T cell differentiation following PD-1 blockade in hepatocellular carcinoma. *Nat. Med.* **29**, 1389–1399 (2023).
 230. Marron, T. U. *et al.* Neoadjuvant cemiplimab for resectable hepatocellular carcinoma: a single-arm, open-label, phase 2 trial. *Lancet Gastroenterol. Hepatol.* **7**, 219–229 (2022).
 231. Hou, M. M. *et al.* Association between Programmed Death-Ligand 1 (PD-L1) expression and gene signatures of Response to Tislelizumab Monotherapy in Hepatocellular Carcinoma. *J. Immunother. Cancer* **A84** (2020).
 232. Funazo, T., Nomizo, T. & Kim, Y. H. Liver Metastasis Is Associated with Poor Progression-Free Survival in Patients with Non–Small Cell Lung Cancer Treated with Nivolumab. *J. Thorac. Oncol.* **12**, 140–141 (2017).
 233. Tumeh, P. C. *et al.* Liver metastasis and treatment outcome with anti-PD-1 monoclonal antibody in patients with melanoma and NSCLC. *Cancer Immunol. Res.* **5**, 417–424 (2017).
 234. Bilen, M. A. *et al.* Sites of metastasis and association with clinical outcome in advanced stage cancer patients treated with immunotherapy. *BMC Cancer* **19**, 1–8 (2019).
 235. Kanas, G. P. *et al.* Survival after liver resection in metastatic colorectal cancer: Review and meta-analysis of prognostic factors. *Clin. Epidemiol.* **4**, 283–301 (2012).
 236. Abbas, S., Lam, V. & Hollands, M. Ten-Year Survival after Liver Resection for Colorectal Metastases: Systematic Review and Meta-Analysis. *ISRN Oncol.* **2011**, 1–11 (2011).
 237. Ye, L. C. *et al.* Randomized controlled trial of cetuximab plus chemotherapy for patients with KRAS wild-type unresectable colorectal liver-limited metastases. *J. Clin. Oncol.* **31**, 1931–1938 (2013).
 238. Gruenberger, T. *et al.* Bevacizumab plus mFOLFOX-6 or FOLFOXIRI in patients with initially unresectable liver metastases from colorectal cancer: The OLIVIA multinational randomised phase II trial. *Ann. Oncol.* **26**, 702–708 (2015).
 239. Spelt, L., Andersson, B., Nilsson, J. & Andersson, R. Prognostic models for outcome following liver resection for colorectal cancer metastases: A systematic review. *Eur. J. Surg. Oncol.* **38**, 16–24 (2012).
 240. Lee, J. C. *et al.* Regulatory T cell control of systemic immunity and immunotherapy response in liver metastasis. *Sci. Immunol.* **5**, (2020).
 241. Mlecnik, B. *et al.* Comprehensive intrametastatic immune quantification and major

- impact of immunoscore on survival. *J. Natl. Cancer Inst.* **110**, 97–108 (2018).
242. Kather, J. N. *et al.* Topography of cancer-associated immune cells in human solid tumors. *Elife* **7**, 1–19 (2018).
 243. Wagner, P. *et al.* Detection and functional analysis of tumor infiltrating T-lymphocytes (TIL) in liver metastases from colorectal cancer. *Ann. Surg. Oncol.* **15**, 2310–2317 (2008).
 244. Duhén, T. *et al.* Co-expression of CD39 and CD103 identifies tumor-reactive CD8 T cells in human solid tumors. *Nat. Commun.* **9**, 1–13 (2018).
 245. Wernersson, S. & Pejler, G. Mast cell secretory granules: Armed for battle. *Nat. Rev. Immunol.* **14**, 478–494 (2014).
 246. Dercle, L. *et al.* High serum LDH and liver metastases are the dominant predictors of primary cancer resistance to anti-PD(L)1 immunotherapy. *Eur. J. Cancer* **177**, 80–93 (2022).
 247. Joulia, R. *et al.* Mast cells form antibody-dependent degranulatory synapse for dedicated secretion and defence. *Nat. Commun.* **6**, 1–12 (2015).
 248. Fereydouni, M. *et al.* Human Tumor Targeted Cytotoxic Mast Cells for Cancer Immunotherapy. *Front. Oncol.* **12**, 1–16 (2022).
 249. Ott, V. L., Cambier, J. C., Kappler, J., Marrack, P. & Swanson, B. J. Mast cell-dependent migration of effector CD8⁺ T cells through production of leukotriene B₄. *Nat. Immunol.* **4**, 974–981 (2003).
 250. Stelekati, E. *et al.* Mast Cell-Mediated Antigen Presentation Regulates CD8⁺ T Cell Effector Functions. *Immunity* **31**, 665–676 (2009).
 251. Hackler, Y., Siebenhaar, F., Löhning, M., Maurer, M. & Muñoz, M. Mast Cells Modulate Antigen-Specific CD8⁺ T Cell Activation During LCMV Infection. *Front. Immunol.* **12**, 1–13 (2021).
 252. Gri, G. *et al.* CD4⁺CD25⁺ Regulatory T Cells Suppress Mast Cell Degranulation and Allergic Responses through OX40-OX40L Interaction. *Immunity* **29**, 771–781 (2008).
 253. Fan, F. *et al.* Elevated Mast Cell Abundance Is Associated with Enrichment of CCR2⁺ Cytotoxic T Cells and Favorable Prognosis in Lung Adenocarcinoma. *Cancer Res.* 2690–2703 (2023).
 254. Gomez, G. *et al.* TGF-β1 Inhibits Mast Cell FcεRI Expression. *J. Immunol.* **174**, 5987–5993 (2005).
 255. Kang, N., Gores, G. J. & Shah, V. H. Hepatic stellate cells: Partners in crime for liver metastases? *Hepatology* **54**, 707–713 (2011).
 256. Tan, H. X. *et al.* CXCR4/TGF-β1 mediated hepatic stellate cells differentiation into carcinoma-associated fibroblasts and promoted liver metastasis of colon cancer. *Cancer Biol. Ther.* **21**, 258–268 (2020).
 257. Hamann, D. *et al.* Phenotypic and functional separation of memory and effector human CD8⁺ T cells. *J. Exp. Med.* **186**, 1407–1418 (1997).
 258. Verma, K. *et al.* Human CD8⁺ CD57⁻ TEMRA cells: Too young to be called ‘old’. *PLoS One* **12**, 1–14 (2017).
 259. Roychoudhuri, R. *et al.* Transcriptional profiles reveal a stepwise developmental program of memory CD8⁺ T cell differentiation. *Vaccine* **33**, 914–923 (2015).
 260. Branco, A. C. C. C., Yoshikawa, F. S. Y., Pietrobon, A. J. & Sato, M. N. Role of Histamine in Modulating the Immune Response and Inflammation. *Mediators Inflamm.* **2018**, (2018).
 261. Martinelli, E. *et al.* Cetuximab rechallenge plus avelumab in pretreated patients with RAS Wild-type Metastatic Colorectal Cancer: The Phase 2 Single-Arm Clinical CAVE Trial. *JAMA Oncol.* **7**, 1529–1535 (2021).
 262. Miholjic, T. B. S. *et al.* Rationale for LDH-targeted cancer immunotherapy. *Eur. J.*

- Cancer* **181**, 166–178 (2023).
263. Caslin, H. L. *et al.* Inhibiting Glycolysis and ATP Production Attenuates IL-33-Mediated Mast Cell Function and Peritonitis. *Front. Immunol.* **9**, 3026 (2018).
 264. Caslin, H. L. *et al.* Lactic Acid Inhibits Lipopolysaccharide-Induced Mast Cell Function by Limiting Glycolysis and ATP Availability. *J. Immunol.* **203**, 453–464 (2019).
 265. Abebayehu, D. *et al.* Lactic acid suppresses IgE-mediated mast cell function in vitro and in vivo. *Cell. Immunol.* **341**, 1–7 (2019).
 266. Kashiwakura, J., Yokoi, H., Saito, H. & Okayama, Y. T Cell Proliferation by Direct Cross-Talk between OX40 Ligand on Human Mast Cells and OX40 on Human T Cells: Comparison of Gene Expression Profiles between Human Tonsillar and Lung-Cultured Mast Cells. *J. Immunol.* **173**, 5247–5257 (2004).
 267. Bhattacharyya, S. P. *et al.* Activated T lymphocytes induce degranulation and cytokine production by human mast cells following cell-to-cell contact. *J. Leukoc. Biol.* **63**, 337–341 (1998).
 268. Tang, L. Y. *et al.* Transforming growth factor- β (TGF- β) directly activates the JAK1-STAT3 axis to induce hepatic fibrosis in coordination with the SMAD pathway. *J. Biol. Chem.* **292**, 4302–4312 (2017).
 269. Tang, J. J. H., Thng, D. K. H., Lim, J. J. & Toh, T. B. JAK/STAT signaling in hepatocellular carcinoma. *Futur. Med.* **7**, (2020).
 270. Bühring, H.-J., Streble, A. & Valent, P. The Basophil-Specific Ectoenzyme E-NPP3 (CD203c) as a Marker for Cell Activation and Allergy Diagnosis. *Int. Arch. Allergy Immunol.* **133**, 317–329 (2004).
 271. Gorelik, A., Randriamihaja, A., Illes, K. & Nagar, B. Structural basis for nucleotide recognition by the ectoenzyme CD203c. *FEBS J.* **285**, 2481–2494 (2018).
 272. Tsai, S. H. *et al.* The Ectoenzyme E-NPP3 Negatively Regulates ATP-Dependent Chronic Allergic Responses by Basophils and Mast Cells. *Immunity* **42**, 279–293 (2015).
 273. Pols, M. S. & Klumperman, J. Trafficking and function of the tetraspanin CD63. *Exp. Cell Res.* **315**, 1584–1592 (2009).
 274. Jutel, M. *et al.* Histamine regulates T-cell and antibody responses by differential expression of H1 and H2 receptors. *Nature* **413**, 420–425 (2001).
 275. Vanbervliet, B. *et al.* Histamine receptor H1 signaling on dendritic cells plays a key role in the IFN- γ /IL-17 balance in T cell-mediated skin inflammation. *J. Allergy Clin. Immunol.* **127**, (2011).
 276. Martner, A. *et al.* Histamine Promotes the Development of Monocyte-Derived Dendritic Cells and Reduces Tumor Growth by Targeting the Myeloid NADPH Oxidase. *J. Immunol.* **194**, 5014–5021 (2015).
 277. Grauers Wiktorin, H. *et al.* Histamine targets myeloid-derived suppressor cells and improves the anti-tumor efficacy of PD-1/PD-L1 checkpoint blockade. *Cancer Immunol. Immunother.* **68**, 163–174 (2019).
 278. Sander, F. E. *et al.* Dynamics of cytotoxic T cell subsets during immunotherapy predicts outcome in acute myeloid leukemia. *Oncotarget* **7**, 7586–7596 (2016).
 279. Li, H. *et al.* The allergy mediator histamine confers resistance to immunotherapy in cancer patients via activation of the macrophage histamine receptor H1. *Cancer Cell* **40**, 36–52 (2022).
 280. Lorentz, A., Bilotta, S. & Civelek, M. Molecular links between allergy and cancer. *Trends Mol. Med.* **28**, 1070–1081 (2022).
 281. Eisenhauer, E. A. *et al.* New response evaluation criteria in solid tumours: Revised RECIST guideline (version 1.1). *Eur. J. Cancer* **45**, 228–247 (2009).

282. Bindea, G. *et al.* Spatiotemporal Dynamics of Intratumoral Immune Cells Reveal the Immune Landscape in Human Cancer. *Immunity* **39**, 782–795 (2008).
283. Bagaev, A. *et al.* Article Conserved pan-cancer microenvironment subtypes predict response to immunotherapy | Article Conserved pan-cancer microenvironment subtypes predict response to immunotherapy. *Cancer Cell* **39**, 845–865 (2021).
284. Colotta, F., Allavena, P., Sica, A., Garlanda, C. & Mantovani, A. Cancer-related inflammation, the seventh hallmark of cancer: Links to genetic instability. *Carcinogenesis* **30**, 1073–1081 (2009).
285. Maiorino, L., Daßler-Plenker, J., Sun, L. & Egeblad, M. Innate Immunity and Cancer Pathophysiology. *Annu. Rev. Pathol. Mech. Dis.* **17**, 425–457 (2021).
286. Garner, H. & de Visser, K. E. Immune crosstalk in cancer progression and metastatic spread: a complex conversation. *Nat. Rev. Immunol.* **20**, 483–497 (2020).
287. Jackstadt, R. *et al.* Epithelial NOTCH Signaling Rewires the Tumor Microenvironment of Colorectal Cancer to Drive Poor-Prognosis Subtypes and Metastasis. *Cancer Cell* **36**, 319–336 (2019).
288. Yang, L. *et al.* IL-8 mediates a positive loop connecting increased neutrophil extracellular traps (NETs) and colorectal cancer liver metastasis. *J. Cancer* **11**, 4384–4396 (2020).
289. Gordon-Weeks, A. N. *et al.* Neutrophils promote hepatic metastasis growth through fibroblast growth factor 2–dependent angiogenesis in mice. *Hepatology* **65**, 1920–1935 (2017).
290. Cools-Lartigue, J. *et al.* Neutrophil extracellular traps sequester circulating tumor cells and promote metastasis. *J. Clin. Invest.* **123**, 3446–3458 (2013).
291. Halazun, K. J. *et al.* Elevated preoperative neutrophil to lymphocyte ratio predicts survival following hepatic resection for colorectal liver metastases. *Eur. J. Surg. Oncol.* **34**, 55–60 (2008).
292. Dell’Aquila, E. *et al.* Prognostic and predictive role of neutrophil/ lymphocytes ratio in metastatic colorectal cancer: A retrospective analysis of the TRIBE study by GONO. *Ann. Oncol.* **29**, 924–930 (2018).
293. Grothey, A. *et al.* Association of baseline absolute neutrophil counts and survival in patients with metastatic colorectal cancer treated with second-line antiangiogenic therapies: Exploratory analyses of the RAISE trial and validation in an electronic medical record data se. *ESMO Open* **3**, 1–9 (2018).
294. Tang, H. *et al.* Prognostic Significance of Neutrophil-to-Lymphocyte Ratio in Colorectal Liver Metastasis: A Systematic Review and Meta-Analysis. *PLoS One* **11**, 1–15 (2016).
295. Wood, G. *et al.* Derived neutrophil to lymphocyte ratio as a prognostic factor in patients with advanced colorectal cancer according to RAS and BRAF status: A post-hoc analysis of the MRC COIN study. *Anticancer. Drugs* **28**, 546–550 (2017).
296. Ciardiello, D. *et al.* Final results of the CAVE trial in RAS wild type metastatic colorectal cancer patients treated with cetuximab plus avelumab as rechallenge therapy: Neutrophil to lymphocyte ratio predicts survival. *Clin. Colorectal Cancer* **21**, 141–148 (2022).
297. Mise, Y. *et al.* RAS Mutations Predict Radiologic and Pathologic Response in Patients Treated with Chemotherapy Before Resection of Colorectal Liver Metastases. *Ann. Surg. Oncol.* **22**, 834–842 (2015).
298. Margonis, G. A. *et al.* KRAS mutational status impacts pathologic response to pre-hepatectomy chemotherapy: a study from the International Genetic Consortium for Liver Metastases. *Int. Hepato-Pancreato-Biliary Assoc.* **21**, 1527–1534 (2019).
299. Schluter, F., Dotzer, K., Prufer, M. & Bazhin, A. Immunophenotyping of Liver and

- Lung Metastases in Colorectal Cancer. *Journal A27* (2020).
300. Laurent-Puig, P. *et al.* Analysis of PTEN, BRAF, and EGFR status in determining benefit from cetuximab therapy in wild-type KRAS metastatic colon cancer. *J. Clin. Oncol.* **27**, 5924–5930 (2009).
 301. Di Nicolantonio, F. *et al.* Wild-type BRAF is required for response to panitumumab or cetuximab in metastatic colorectal cancer. *J. Clin. Oncol.* **26**, 5705–5712 (2008).
 302. Tol, J. *et al.* Markers for EGFR pathway activation as predictor of outcome in metastatic colorectal cancer patients treated with or without cetuximab. *Eur. J. Cancer* **46**, 1997–2009 (2010).
 303. Di Fiore, F., Sesboüé, R., Michel, P., Sabourin, J. C. & Frebourg, T. Molecular determinants of anti-EGFR sensitivity and resistance in metastatic colorectal cancer. *Br. J. Cancer* **103**, 1765–1772 (2010).
 304. Oden-Gangloff, A. *et al.* TP53 mutations predict disease control in metastatic colorectal cancer treated with cetuximab-based chemotherapy. *Br. J. Cancer* **100**, 1330–1335 (2009).
 305. Huemer, F. *et al.* Sidedness and TP53 mutations impact OS in anti-EGFR but not anti-VEGF treated mCRC - An analysis of the KRAS registry of the AGMT (Arbeitsgemeinschaft Medikamentöse Tumortherapie). *BMC Cancer* **18**, 1–11 (2018).
 306. Bronte, V. *et al.* Recommendations for myeloid-derived suppressor cell nomenclature and characterization standards. *Nat. Commun.* **7**, 1–10 (2016).
 307. Lu, Y. *et al.* CD16 expression on neutrophils predicts treatment efficacy of capecitabine in colorectal cancer patients. *BMC Immunol.* **21**, 1–14 (2020).
 308. Condamine, T. *et al.* Lectin-type oxidized LDL receptor-1 distinguishes population of human polymorphonuclear myeloid-derived suppressor cells in cancer patients. *Sci. Immunol.* **1**, 1–32 (2016).
 309. Nan, J. *et al.* Endoplasmic reticulum stress induced LOX-1+CD15+ polymorphonuclear myeloid-derived suppressor cells in hepatocellular carcinoma. *Immunology* **154**, 144–155 (2018).
 310. Perez-Ruiz, E. *et al.* Prophylactic TNF blockade uncouples efficacy and toxicity in dual CTLA-4 and PD-1 immunotherapy. *Nature* **569**, 428–432 (2019).
 311. Watt, D. G., Martin, J. C., Park, J. H., Horgan, P. G. & McMillan, D. C. Neutrophil count is the most important prognostic component of the differential white cell count in patients undergoing elective surgery for colorectal cancer. *Am. J. Surg.* **210**, 24–30 (2015).
 312. Trompet, S. *et al.* High innate production capacity of proinflammatory cytokines increases risk for death from cancer: Results of the PROSPER study. *Clin. Cancer Res.* **15**, 7744–7748 (2009).
 313. Grimm, M. *et al.* Evaluation of immunological escape mechanisms in a mouse model of colorectal liver metastases. *BMC Cancer* **10**, (2010).
 314. Grimm, M. *et al.* Tumor necrosis factor-A is associated with positive lymph node status in patients with recurrence of colorectal cancer-indications for anti-TNF-A agents in cancer treatment. *Cell. Oncol.* **34**, 315–326 (2011).
 315. Schimek, V. *et al.* Tumour cell apoptosis modulates the colorectal cancer immune microenvironment via interleukin-8-dependent neutrophil recruitment. *Cell Death Dis.* **13**, (2022).
 316. Xiao, Y.-C. *et al.* CXCL8, overexpressed in colorectal cancer, enhances the resistance of colorectal cancer cells to anoikis. *Cancer Lett.* **361**, 22–32 (2015).
 317. Cheng, X. S. *et al.* CCL20 and CXCL8 synergize to promote progression and poor survival outcome in patients with colorectal cancer by collaborative induction of the epithelial-mesenchymal transition. *Cancer Lett.* **348**, 77–87 (2014).

318. Asfaha, S. *et al.* Mice that express human interleukin-8 have increased mobilization of immature myeloid cells, which exacerbates inflammation and accelerates colon carcinogenesis. *Gastroenterology* **144**, 155–166 (2013).
319. Wu, P. *et al.* $\gamma\delta$ T17 cells promote the accumulation and expansion of myeloid-derived suppressor cells in human colorectal cancer. *Immunity* **40**, 785–800 (2014).
320. Alfaro, C. *et al.* Tumor-Produced Interleukin-8 Attracts human myeloid-derived suppressor cells and elicits extrusion of Neutrophil Extracellular Traps (NETs). *Clin. Cancer Res.* **22**, 3924–3936 (2016).
321. Teijeira, Á. *et al.* CXCR1 and CXCR2 Chemokine Receptor Agonists Produced by Tumors Induce Neutrophil Extracellular Traps that Interfere with Immune Cytotoxicity. *Immunity* **52**, 856–871 (2020).
322. Fridlender, Z. G. *et al.* Polarization of Tumor-Associated Neutrophil Phenotype by TGF- β : ‘N1’ versus ‘N2’ TAN. *Cancer Cell* **16**, 183–194 (2009).
323. Chung, J. Y. F. *et al.* Smad3 is essential for polarization of tumor-associated neutrophils in non-small cell lung carcinoma. *Nat. Commun.* **14**, (2023).
324. Qin, F. *et al.* Anti-TGF- β attenuates tumor growth via polarization of tumor associated neutrophils towards an anti-tumor phenotype in colorectal cancer. *J. Cancer* **11**, 2580–2592 (2020).
325. Yang, Q., Yan, C. & Gong, Z. Interaction of hepatic stellate cells with neutrophils and macrophages in the liver following oncogenic kras activation in transgenic zebrafish. *Sci. Rep.* **8**, 1–12 (2018).
326. Zhao, X. *et al.* TNF signaling drives myeloid-derived suppressor cell accumulation. *J. Clin. Invest.* **122**, 4094–4104 (2012).
327. Sade-Feldman, M. *et al.* Tumor Necrosis Factor- α Blocks Differentiation and Enhances Suppressive Activity of Immature Myeloid Cells during Chronic Inflammation. *Immunity* **38**, 541–554 (2013).
328. Michaeli, J. *et al.* Tumor-associated neutrophils induce apoptosis of non-activated CD8 T-cells in a TNF α and NO-dependent mechanism, promoting a tumor-supportive environment. *Oncoimmunology* **6**, (2017).
329. Bianchi, A. *et al.* Cell-Autonomous Cxcl1 Sustains Tolerogenic Circuitries and Stromal Inflammation via Neutrophil-Derived TNF in Pancreatic Cancer. *Cancer Discov.* **13**, 1428–1453 (2023).
330. Zhao, X., Lu, Y. & Cui, L. Neutrophil-sourced TNF in cancer: deciphering an intricate orchestrator of immunosuppressive communication in the tumor microenvironment. *Signal Transduct. Target. Ther.* **8**, 2–4 (2023).
331. Galle, P. R. *et al.* EASL Clinical Practice Guidelines: Management of hepatocellular carcinoma. *J. Hepatol.* **69**, 182–236 (2018).
332. Kim, J. *et al.* Substantial risk of recurrence even after 5 recurrence-free years in early-stage hepatocellular carcinoma patients. *Clin. Mol. Hepatol.* **26**, 516–528 (2020).
333. Nguyen, P. H. D. *et al.* Intratumoural immune heterogeneity as a hallmark of tumour evolution and progression in hepatocellular carcinoma. *Nat. Commun.* **12**, 1–13 (2021).
334. Cheng, Y. *et al.* Non-terminally exhausted tumor-resident memory HBV-specific T cell responses correlate with relapse-free survival in hepatocellular carcinoma. *Immunity* **54**, 1825–1840 (2021).
335. Huang, D. Q., El-Serag, H. B. & Loomba, R. Global epidemiology of NAFLD-related HCC: trends, predictions, risk factors and prevention. *Nat. Rev. Gastroenterol. Hepatol.* **18**, 223–238 (2021).
336. El-Serag, H. B. Epidemiology of viral hepatitis and hepatocellular carcinoma. *Gastroenterology* **142**, 1264–1273 (2012).

337. Fisicaro, P. *et al.* Targeting mitochondrial dysfunction can restore antiviral activity of exhausted HBV-specific CD8 T cells in chronic hepatitis B. *Nat. Med.* **23**, 327–336 (2017).
338. Zong, L. *et al.* Breakdown of adaptive immunotolerance induces hepatocellular carcinoma in HBsAg-tg mice. *Nat. Commun.* **10**, (2019).
339. Liu, X. *et al.* PD-1+ TIGIT+ CD8+ T cells are associated with pathogenesis and progression of patients with hepatitis B virus-related hepatocellular carcinoma. *Cancer Immunol. Immunother.* **68**, 2041–2054 (2019).
340. Yan, G. *et al.* Chronic Alcohol Consumption Promotes Diethylnitrosamine-Induced Hepatocarcinogenesis via Immune Disturbances. *Sci. Rep.* **7**, 1–8 (2017).
341. Zhang, Q. *et al.* Integrated multiomic analysis reveals comprehensive tumour heterogeneity and novel immunophenotypic classification in hepatocellular carcinomas. *Gut* **68**, 2019–2031 (2019).
342. Gao, X. *et al.* Tumor Immune Microenvironment Characterization in Hepatocellular Carcinoma Identifies Four Prognostic and Immunotherapeutically Relevant Subclasses. *Front. Oncol.* **10**, 1–11 (2021).
343. Johnson, P. J. *et al.* A nssessment of liver function in patients with hepatocellular carcinoma: A new evidence-based approach - The albi grade. *J. Clin. Oncol.* **33**, 550–558 (2015).
344. Di Blasi, D. *et al.* Unique T-Cell Populations Define Immune-Inflamed Hepatocellular Carcinoma. *Cmgh* **9**, 195–218 (2020).
345. Stegmann, K. A. *et al.* CXCR6 marks a novel subset of T-bet lo Eomes hi natural killer cells residing in human liver. *Sci. Rep.* **6**, 1–10 (2016).
346. Liao, Y., Wu, C., Li, Y., Wen, J. & Zhao, D. MIF is a critical regulator of mononuclear phagocytic infiltration in hepatocellular carcinoma. *iScience* **26**, 107273 (2023).
347. Cao, Z. *et al.* Overexpression of Chemokine (C-X-C) ligand 1 (CXCL1) associated with tumor progression and poor prognosis in hepatocellular carcinoma. *Cancer Cell Int.* **14**, 1–7 (2014).
348. Zhao, W. *et al.* Activated hepatic stellate cells promote hepatocellular carcinoma development in immunocompetent mice. *Int. J. Cancer* **129**, 2651–2661 (2011).
349. Marvin, D. L., Heijboer, R., ten Dijke, P. & Ritsma, L. TGF- β signaling in liver metastasis. *Clin. Transl. Med.* **10**, 1–20 (2020).
350. Hu, Z. Q. *et al.* Overexpression of semaphorin 3A promotes tumor progression and predicts poor prognosis in hepatocellular carcinoma after curative resection. *Oncotarget* **7**, 51733–51746 (2016).
351. Schwinghammer, U. A. *et al.* α 2-Adrenergic Receptor in Liver Fibrosis: Implications for the Adrenoblocker Mesedin. *Cells* **9**, 1–13 (2020).
352. Bartsch, L. M., Damasio, M. P. S., Subudhi, S. & Drescher, H. K. Tissue-Resident Memory T Cells in the Liver-Unique Characteristics of Local Specialists. *Cells* **9**, 1–22 (2020).
353. Wang, B. *et al.* CXCR6 is required for antitumor efficacy of intratumoral CD8 + T cell. *J. Immunother. Cancer* **9**, (2021).
354. Li, X. *et al.* Integrated single cell and bulk sequencing analysis identifies tumor reactive CXCR6+ CD8 T cells as a predictor of immune infiltration and immunotherapy outcomes in hepatocellular carcinoma. *Front. Oncol.* **13**, 1–25 (2023).
355. Ma, J. *et al.* PD1Hi CD8+ T cells correlate with exhausted signature and poor clinical outcome in hepatocellular carcinoma. *J. Immunother. Cancer* **7**, 1–15 (2019).
356. Terme, M., Tartour, E. & Taieb, J. VEGFA/VEGFR2-targeted therapies prevent the VEGFA-induced proliferation of regulatory T cells in cancer. *Oncoimmunology* **2**,

- (2013).
357. Terme, M. *et al.* VEGFA-VEGFR pathway blockade inhibits tumor-induced regulatory T-cell proliferation in colorectal cancer. *Cancer Res.* **73**, 539–549 (2013).
 358. Voron, T. *et al.* VEGF-A modulates expression of inhibitory checkpoints on CD8⁺⁺ T cells in tumors. *J. Exp. Med.* **212**, 139–148 (2015).
 359. Gabrilovich, D. I. *et al.* Production of vascular endothelial growth factor by human tumors inhibits the functional maturation of dendritic cells. *Nat. Med.* **2**, 1096–1103 (1996).
 360. Huang, Y. *et al.* Distinct roles of VEGFR-1 and VEGFR-2 in the aberrant hematopoiesis associated with elevated levels of VEGF. *Blood* **110**, 624–631 (2007).
 361. de Galarreta, M. R. *et al.* β -catenin activation promotes immune escape and resistance to anti-PD-1 therapy in hepatocellular carcinoma. *Cancer Discov.* **9**, 1124–1141 (2019).
 362. Harding, J. J. *et al.* Prospective Genotyping of Hepatocellular Carcinoma: Clinical Implications of Next-Generation Sequencing for Matching Patients to Targeted and Immune Therapies James. *Clin. Cancer Res.* **25**, 6–2126 (2019).
 363. Park, B. V. *et al.* TGF β 1-mediated SMAD3 enhances PD-1 expression on antigen-specific T cells in cancer. *Cancer Discov.* **6**, 1366–1381 (2016).
 364. Mariathasan, S. *et al.* HHS Public Access. **554**, 544–548 (2018).
 365. O'Donnell, J. S., Teng, M. W. L. & Smyth, M. J. Cancer immunoediting and resistance to T cell-based immunotherapy. *Nat. Rev. Clin. Oncol.* **16**, 151–167 (2019).
 366. Schinzari, V. *et al.* Wnt3a/b-Catenin signaling conditions differentiation of partially exhausted T-effector cells in human cancers. *Cancer Immunol. Res.* **6**, 941–952 (2018).
 367. Pacella, I. *et al.* Wnt3a neutralization enhances T-cell responses through indirect mechanisms and restrains tumor growth. *Cancer Immunol. Res.* **6**, 953–964 (2018).
 368. Nishida, N. *et al.* Association between Genetic and Immunological Background of Hepatocellular Carcinoma and Expression of Programmed Cell Death-1. *Liver Cancer* **9**, 426–439 (2020).
 369. Shen, Y. *et al.* TGF- β regulates hepatocellular carcinoma progression by inducing treg cell polarization. *Cell. Physiol. Biochem.* **35**, 1623–1632 (2015).
 370. Yan, W. *et al.* Tim-3 fosters HCC development by enhancing TGF-beta-mediated alternative activation of macrophages. *Gut* **64**, 1502–1503 (2015).
 371. Chiang, D. Y. *et al.* Focal gains of VEGFA and molecular classification of hepatocellular carcinoma. *Cancer Res.* **68**, 6779–6788 (2008).
 372. Hoshida, Y. *et al.* Integrative transcriptome analysis reveals common molecular subclasses of human hepatocellular carcinoma. *Cancer Res.* **69**, 7385–7392 (2009).
 373. Halima, A., Vuong, W. & Chan, T. A. Next-generation sequencing: unraveling genetic mechanisms that shape cancer immunotherapy efficacy. *J. Clin. Invest.* **132**, 1–10 (2022).
 374. Bassaganyas, L. *et al.* Copy-number alteration burden differentially impacts immune profiles and molecular features of hepatocellular carcinoma. *Clin. Cancer Res.* **26**, 6350–6361 (2020).
 375. Pozzi, C. *et al.* The EGFR-specific antibody cetuximab combined with chemotherapy triggers immunogenic cell death. *Nat. Med.* **22**, 624–631 (2016).
 376. Weimershaus, M. *et al.* Mast cell-mediated inflammation relies on insulin-regulated aminopeptidase controlling cytokine export from the Golgi. *J. Allergy Clin. Immunol.* **151**, 1595–1608 (2023).
 377. Carroll-Portillo, A. *et al.* Mast cells and dendritic cells form synapses that facilitate

- antigen transfer for T cell activation. *J. Cell Biol.* **210**, 851–864 (2015).
378. Negri, E. *et al.* Allergy and other selected diseases and risk of colorectal cancer. *Eur. J. Cancer* **35**, 1838–1841 (1999).
379. Ma, W., Yang, J., Li, P., Lu, X. & Cai, J. Association between allergic conditions and colorectal cancer risk/mortality: a meta-analysis of prospective studies. *Sci. Rep.* **7**, 1–7 (2017).
380. Ownby, D. R. *et al.* Presurgical Serum Immunoglobulin Concentrations and the Prognosis of Operable Breast Cancer in Women. *JNCI J. Natl. Cancer Inst.* **75**, 655–663 (1985).
381. Asemisen, A. M. *et al.* Addition of histamine to interleukin 2 treatment augments type 1 T-cell responses in patients with melanoma in vivo: Immunologic results from a randomized clinical trial of interleukin 2 with or without histamine (MP 104). *Clin. Cancer Res.* **11**, 290–297 (2005).
382. Agarwala, S. S. *et al.* Results from a Randomized Phase III Study Comparing Combined Treatment with Histamine Dihydrochloride Plus Interleukin-2 versus Interleukin-2 Alone in Patients with Metastatic Melanoma. *J. Clin. Oncol.* **20**, 125–133 (2002).
383. Agarwala, S. S., Hellstrand, K., Gehlsen, K. & Naredi, P. Immunotherapy with histamine and interleukin 2 in malignant melanoma with liver metastasis. *Cancer Immunol. Immunother.* **53**, 840–841 (2004).
384. Paltridge, J. ., Belle, L. & Khew-Goodall, Y. The secretome in cancer progression. *Biochim. Biophys. Acta - Proteins Proteomics* **1834**, 2233–2241 (2013).
385. Pavlou, M. P. & Diamandis, E. P. The cancer cell secretome: A good source for discovering biomarkers? *J. Proteomics* **73**, 1896–1906 (2010).
386. Ziegler, Y. S., Moresco, J. J., Yates, J. R. & Nardulli, A. M. Integration of breast cancer secretomes with clinical data elucidates potential serum markers for disease detection, diagnosis, and prognosis. *PLoS One* **11**, 1–24 (2016).
387. Zhang, J. *et al.* Tumor-Educated Neutrophils Activate Mesenchymal Stem Cells to Promote Gastric Cancer Growth and Metastasis. *Front. Cell Dev. Biol.* **8**, 1–11 (2020).
388. Nielsen, S. R. *et al.* Suppression of tumor-associated neutrophils by lorlatinib attenuates pancreatic cancer growth and improves treatment with immune checkpoint blockade. *Nat. Commun.* **12**, 1–15 (2021).
389. Liu, Z. W. *et al.* Duality of Interactions Between TGF- β and TNF- α During Tumor Formation. *Front. Immunol.* **12**, 1–14 (2022).
390. Ciardiello, D., Elez, E., Tabernero, J. & Seoane, J. Clinical development of therapies targeting TGF β : current knowledge and future perspectives. *Ann. Oncol.* **31**, 1336–1349 (2020).
391. Huang, D., Xue, J., Li, S. & Yang, D. Oxaliplatin and infliximab synergize to induce regression of colon cancer. *Oncol. Lett.* **15**, 1517–1522 (2018).
392. Bertrand, F. *et al.* Blocking tumor necrosis factor α enhances CD8 T-cell-dependent immunity in experimental melanoma. *Cancer Res.* **75**, 2619–2628 (2015).